Regulation of intra-tumoral T cell immunity in liver cancer

Guoying (Estella) Zhou

周国影

To my family members who are no longer with us

Regulation of Intra-tumoral T Cell Immunity in Liver Cancer

Regulatie van intra-tumorale T cel immuniteit in lever kanker

Thesis

To obtain the degree of Doctor from the

Erasmus University Rotterdam

by command of the

Rector Magnificus

Prof. Dr. R.C.M.E. Engels

and in accordance with the decision of the Doctorate Board

The public defence shall be held on

Wednesday 4th of July 2018 at 13:30 hrs

by

Guoying Zhou

born in Shunde, Guangdong Province, China

Erasmus University Rotterdam

Doctoral committee

Promotor:

      Prof. Dr. M.J. Bruno

Inner committee:

      Prof. Dr. S.H. van der Burg

      Prof. Dr. J.N.M. IJzermans

      Dr. R. Debets

Co-promotor:

      Dr. J. Kwekkeboom

TABLE OF CONTENTS

CHAPTER 1

General introduction and outline of the thesis

Review: Immune suppressor cells and checkpoints in liver cancer

Guoying Zhou[1], Patrick P.C. Boor[1], Marco J. Bruno[1], Dave Sprengers[1] and Jaap Kwekkeboom[1]

[1]Department of Gastroenterology and Hepatology, Erasmus MC-University Medical Center, Rotterdam, the Netherlands.

1 Hepatocellular carcinoma (HCC)

Liver cancer is one of the most prevalent and aggressive cancers,(1) and is the second most common cause of cancer-related mortality worldwide. The most common primary liver cancer is hepatocellular carcinoma (HCC), an aggressive malignancy derived from hepatocytes. The current treatment options for HCC, such as surgical resection, liver transplantation and radiofrequency ablation, are curative only for patients with early stage disease. Unfortunately, the majority of HCC patients are not eligible for curative procedures because of late diagnosis and thus have poor prognosis.(2) HCC patients with intermediate stage can be offered transarterial chemoembolization as palliative therapy, patients with advanced disease can only be offered systemic sorafenib therapy which provides a survival advantage of <3 months. HCC is highly resistant to chemotherapy, but immunotherapy may be an attractive therapeutic option, since an inflammatory tumor microenvironment is associated with improved survival.(3, 4)

Chronic infection with hepatitis B virus (HBV) is the leading cause of HCC worldwide, and chronic infection with hepatitis C virus (HCV) is currently the leading cause of end-stage liver disease and HCC in the western world.(5) In patients with hepatitis B, the incidence of HCC increases with viral load, duration of infection, and severity of the liver disease. Occult HBV infection is also associated with increased risk because of DNA damage induced by virus integration.(6) In chronic viral hepatitis, the natural history and risk for the development of HCC is linked to the degree of liver inflammation. Both HBV and HCV are non-cytopathic, and liver damage is induced mainly by immune responses to the virus. Immune reactions during persistent infection with HBV or HCV are insufficient to clear the virus, which leads to progressive liver damage.(5) HCC-related mortality can be prevented by avoiding the risk factors. Once chronic infection is acquired, elimination of viral replication by antiviral agents should prevent the progression to cirrhosis and probably the development of HCC. However, if cirrhosis is established, the risk of HCC remains.(6)

2 Cholangiocarcinoma (CCA)

Cholangiocarcinoma (CCA) accounts for 10% of primary liver cancers, but its incidence is increasing significantly. CCA is an aggressive hepatobiliary malignancy originating from the biliary tract epithelium with features of cholangiocyte differentiation.(7, 8) It is classified into the following types according to its anatomic location along the biliary tree: intrahepatic (iCCA), perihilar (pCCA) and distal hepatic (dCCA).(8-10) The median overall survival after diagnosis is 24 months and 5-year survival rate is around 10%.(11) Surgical resection is potentially curative, but it can only be achieved in 10% of the CCA patients and is associated

with a high recurrence rate (>50%).(8) Liver transplantation is a curative option for selected patients with pCCA but not with iCCA or dCCA.(10) The therapeutic efficacy of chemotherapy for advanced CCA is disappointing.(8) Therefore, novel therapies for curing HCC and CCA and preventing recurrence are urgently needed.

3 Liver metastasis of colorectal cancer (LM-CRC)

Colorectal cancer (CRC) is the third most common cause of cancer-related mortality worldwide.(1) More than 50% of patients with CRC develop metastatic disease to their liver over the course of their life, and liver metastasis is a leading cause of death from CRC.(12) Liver metastasis of CRC (LM-CRC) is also the most prevalent secondary liver cancer. Unlike most other solid cancers, it is now standard for patients with isolated LM-CRC to be considered for liver resection and/or other focal therapies upon presentation.(13) The other therapeutic approach for LM-CRC is systemic therapy such as chemotherapy. Unfortunately, patients have a high rate of recurrence after both types of treatments.(14, 15) Surgical resection of LM-CRC is curative in only 30% of patients,(16) and systemic therapy provides limited survival benefit.(17) Patients with unresectable LM-CRC have a poor prognosis with a median survival of only two years.(18) Therefore, there is a pressing need for more effective therapeutic strategies for LM-CRC.

4 Cancer immunotherapy

As more effective therapies for curing liver cancers and preventing their recurrence are needed, cancer immunotherapy offers a promising alternative for classic oncological treatments (Figure 1).

Tumors are immunogenic. Both cells of the innate immune system such as NK cells and cells of the adaptive immune system such as CD8$^+$ T cells can kill tumor cells. Compared to the innate immunity, the adaptive immunity is highly specific and induces memory that can prevent tumor recurrence. Tumor-specific CD8$^+$ cytotoxic T cells and CD4$^+$ T helper cells, which are needed for effective anti-tumor T cell immunity, are present in most cancer patients. But these spontaneous T cell responses generally do not eradicate the established tumors, because the responses are too weak and their effects are counteracted by the presence of several immunosuppressive mechanisms in the tumor microenvironment: e.g. 1) Suppressive immune cells, such as regulatory T cells (Treg), myeloid-derived suppressor cells (MDSC), tumor-associated macrophages (TAM) that can inhibit effector T cell functions; 2) Co-inhibitory interactions between T cells which can express co-inhibitory receptors, and tumor cells and intra-tumoral immune cells which can express the ligands for these

receptors; 3) Immune suppressive metabolites generated by enzymes in the tumors, such as kynurenine generated by IDO or TDO; 4) Suppression of migration of immune effector cells into the tumors.

The main purposes of cancer immunotherapy are 1) to strengthen the spontaneous immune responses and/or to induce new anti-tumor immune responses, and 2) to abrogate the immunosuppressive mechanisms in the tumor microenvironment. For aim 1 the options available are therapeutic vaccination with tumor antigens, adoptive cell transfer of T cells transduced with tumor antigen-specific T cell receptor, and chimeric antigen receptor T cell therapy etc. For aim 2 options include antibody blockade of co-inhibitory immune checkpoints, agonistic antibodies against co-stimulatory receptors, depletion of suppressive immune cells such as CD25 antibody-mediated intra-tumoral Treg depletion, and inhibitors of IDO etc.

In the next sections of the introduction, we will provide a detailed description of the recent insights in immune suppressive mechanisms within the tumor microenvironment of HCC, CCA and LM-CRC, summarize the results of recent clinical studies to overcome these immunosuppressive mechanisms, and suggest alternative therapeutic approaches to abrogate them based on the described novel insights. Furthermore, we will indicate the current gaps in our knowledge on immunosuppressive mechanisms in the tumor microenvironment of HCC, CCA and LM-CRC.

5 Immunogenicity of liver cancers

HCC and LM-CRC have been shown to be immunogenic but also to induce different immunosuppressive effects in the tumor microenvironment. Tumor antigen-specific CD4^{+} and CD8^{+} T cells that recognize classic tumor-associated antigens have been detected in the circulation of HCC patients,(19, 20) and are also present in tumor tissues of patients with HCC or LM-CRC.(21, 22) Higher numbers of intra-tumoral CD8^{+} T cells in HCC, LM-CRC and CCA are associated with better survival. Amongst the classic tumor antigens expressed in HCC tumor cells and recognized by T cells in HCC patients are cancer-testis antigens, oncofetal antigens, and over-expressed antigens.(19, 20, 22, 23) However, in the tumors these T cells are partially dysfunctional, possibly through an antigen-driven dynamic differentiation program (due to continuous tumor antigen exposure) already initiated early during tumorigenesis.(21, 22, 24) High-dimensional transcriptomic and proteomic analyses have delineated an immunosuppressive landscape in HCC tumor microenvironment in which regulatory T cells (Treg), exhausted CD8^{+} T cells, resident natural killer cells and tumor-associated macrophages (TAM) are enriched.(25, 26) Whether tumor-specific T cells that

recognize classic tumor antigens exist in CCA patients and whether those cells are dysfunctional are unclear.

With advances in whole-exome sequencing, recent technological innovations have made it possible to identify a new class of patient-specific tumor antigens derived from mutated proteins that are only found in tumor cells but not in normal cells.(27, 28) These so-called neoantigens have been demonstrated to be recognized by tumor-specific T cells in cancer patients, and they are highly specific targets for anti-tumor immunity, because of their exclusive expression in tumor cells and their absence during fetal development. It is now thought that neoantigens considerably add to the immunogenicity of cancers. Recent studies using next generation sequencing have shown that the genomes of liver tumors contain many mutations, including many mutations in protein-encoding sequences,(27, 29, 30) which create amino acid changes in the encoded proteins and in theory can generate neoantigenic short peptides that can be presented in MHC molecules and be recognized by patient T cells as foreign body.(27, 31) For melanoma it has been shown that mutated genes in tumors can indeed generate neoantigenic peptides that bind to MHC class I or II molecules of the patient, which are recognized by tumor-infiltrating lymphocytes (TIL), and induce anti-tumor T cell immune response.(32, 33) In patients with non-small cell lung cancer, higher numbers of mutations in tumors which are related to higher numbers of neoepitopes, are associated with improved objective response rate to PD-1 blockade (pembrolizumab) therapy, durable clinical benefit and progression-free survival.(34) These findings demonstrate that the genetic damage leading to oncogenic outgrowth can be targeted by the immune system to control malignancies. Therefore, it is crucial to develop treatment approaches by which neoantigen-specific T cell reactivity is selectively enhanced. A neoantigen recognized by CD4^{+} TIL was identified in a CCA patient, and these TIL were effective in mediating tumor regression upon in vitro expansion and adoptive transfer.(35) However, neoantigens have not been identified yet in patients with HCC or LM-CRC.

6 Immune suppressive mechanisms in the tumor microenvironment of liver cancers

In order to develop effective immunotherapeutic strategies for the treatment of liver cancer, in depth knowledge of the mechanisms contributing to intra-tumoral immune suppression is needed. Here, we will discuss how immune suppressive immune cell subsets, co-inhibitory pathways, and enzymes generating immune suppressive metabolites contribute to intra-tumoral immune suppression in HCC, CCA and LM-CRC.
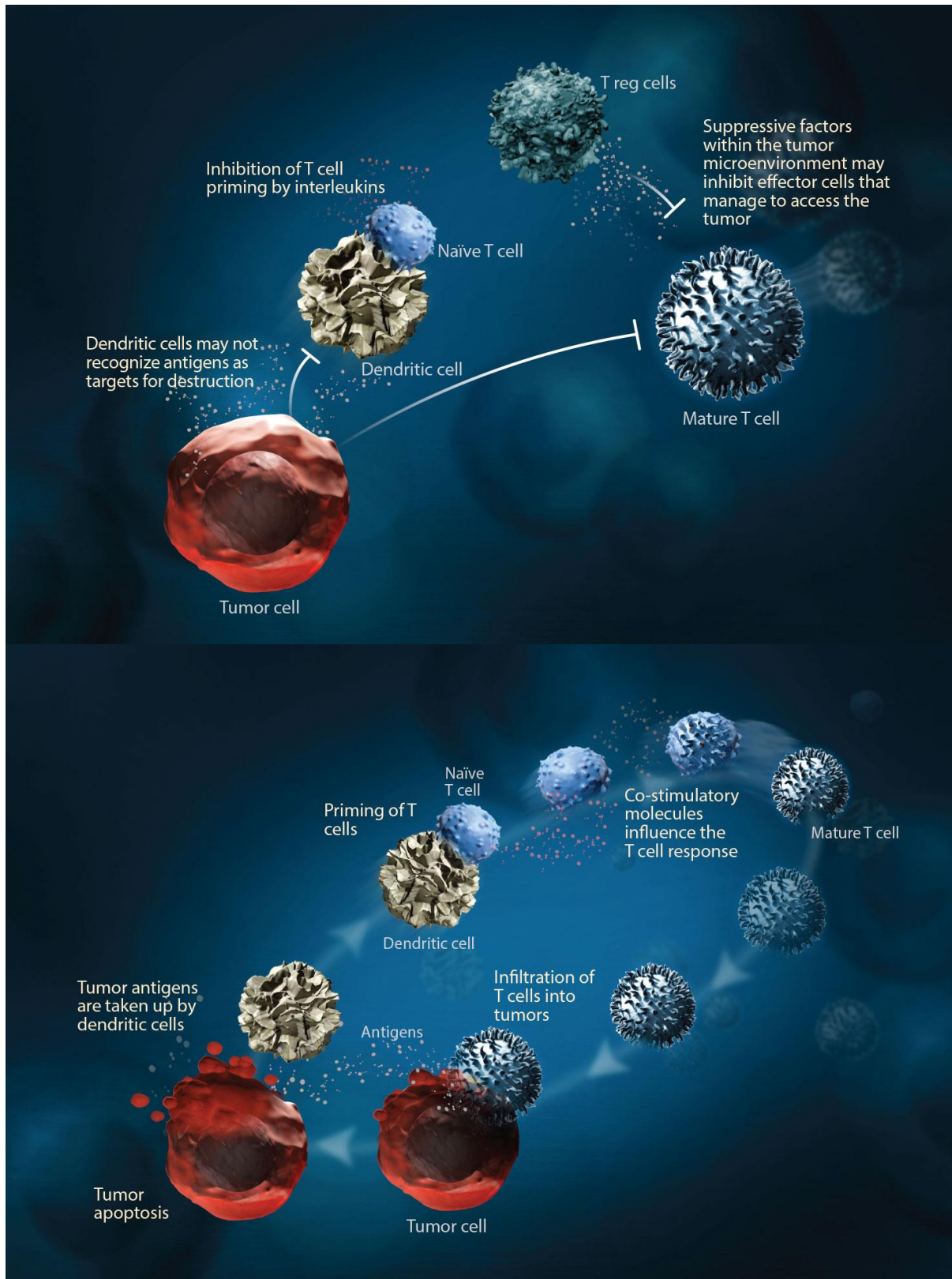
Figure 1. The immune system plays a significant role in the recognition and destruction of cancer cells. 1) Tumors use multiple mechanisms to evade immune destruction. 2) Approaches that modulate the immune system may improve the immune response to cancer. (Reproduced from http://www.amgenoncology.com/science/t-cell-modulation-gitr.html)

6.1 Immune suppressive cells in the tumor microenvironment of liver cancers

6.1.1 Conventional regulatory T cells (Treg)

Regulatory T cells (Treg) are strong immunomodulators in the tumor microenvironment, and play a critical role in tumor immune evasion and tumor development. A number of studies have shown that Treg are increased in the circulation and accumulate in tumors of HCC patients, and that higher numbers of Treg in the tumor are associated with poor survival. Most of these data have been reviewed by F. Zhao et al. a few years ago.(36) We reported that $CD4^+CD25^+Foxp3^+$ regulatory T cells that accumulate in tumors of patients with HCC or LM-CRC are potent suppressors of T cell responses.(21) Strongly activated immunosuppressive Treg accumulating in the LM-CRC are associated with worse survival. The accumulation of Treg in tumors may be driven by selective immigration and/or by local proliferation and/or differentiation. Recent studies demonstrated that in vitro generation of $Foxp3^+$ cells from mouse spleen-derived $CD4^+CD25^-$ T cells can be induced by hepatoma-derived growth factor (HDGF)(37) and that in vivo differentiation of Treg in mouse spleens could be promoted by transforming growth factor-β (TGF-β) in HCC.(38) Whereas immigration of Treg into HCC tumors was previously shown to be driven by CCL20,(39) recently, it has been demonstrated that the migratory activity of Treg and macrophages from patients or mice with HCC is increased by recombinant CCL2 and CCL17 as well as tumor-associated neutrophils which most highly express CCL2 and CCL17. In tumor-bearing mice, the number of tumor-associated neutrophils and levels of CCL2 and CCL17 in tumors are increased by sorafenib treatment, suggesting a pro-tumoral effect of this commonly used drug.(26, 40)

In intrahepatic cholangiocarcinoma, $Foxp3^+$ Treg were shown to be enriched predominantly in the intra-tumoral area, whereas $CD8^+$ lymphocytes were most abundant in the tumor invasive front.(41) However, whether Treg contribute to intra-tumoral immunosuppression in CCA is unknown. No studies have been performed to deplete Treg from liver tumors using antibodies against Treg. Whether and how intra-tumoral Treg can be targeted to reduce their suppressive capacity is unclear. Interestingly, low dose cyclophosphamide was described to decrease the absolute and relative frequency and suppressor function of circulating Treg in HCC patients.(42) However, whether Treg were depleted from the tumors was not studied.

6.1.2 Type 1 regulatory T cells (Tr1)

A more recently discovered inhibitory T cell population in solid tumor is named type 1 regulatory T cells (Tr1), which are functionally characterized as IL-10-producing $CD4^+$ T cells

and are phenotypically defined as CD4$^+$Foxp3$^-$CD49b$^+$LAG3$^+$ T cells.(43) Tr1 have been described to play an important role in promoting and maintaining tolerance in transplantation, autoimmunity and allergy. There is some evidence that this regulatory T cell population is also involved in tumor escape from immune surveillance.(44-48) Kakita et al. identified two types of CD4$^+$CD127$^-$ T cells with comparable regulatory ability which are CD25^{high+}Foxp3$^+$ Treg and CD25$^-$Foxp3$^-$ T cells. The peripheral and tumor-infiltrating frequencies of CD25$^-$Foxp3$^-$ T cells in HCC patients are higher than those in healthy subjects and patients with hepatitis C and liver cirrhosis.(49) Whether Tr1 are present in CCA tumors is as yet unknown. Until recently, the absence of a defined cell surface signature required the reliance on a cytokine profile to distinguish Tr1 cells from other T cell subsets, which complicated the study of these cells. Therefore. direct evidence for a role of Tr1 cells in human solid tumors was lacking. The recent description of co-expression of CD49b and LAG3 as markers that can specifically identify this population,(43) enables more extensive study of these cells.

6.1.3 Myeloid-derived suppressor cells (MDSC)

Myeloid-derived suppressor cells are a heterogeneous population of immature myeloid cells with immunosuppressive properties that can be recruited into the tumor milieu by multiple cytokines and chemokines. Some studies have shown that MDSC are increased in peripheral blood of HCC patients, and inhibit natural killer cells and T cell functions. These data have been reviewed recently by Greten et al.(50) and previously by Zhao et al.(36) Recently MDSC were shown to be able to induce IL-17A-producing gamma-delta T cells via production of IL-1β and IL-23 in HCC mouse models. Interestingly, IL-17A also enhanced production of IL-1β and IL-23 in MDSC as a positive feedback.(51) In another HCC mouse study, monocytic-MDSC (Mo-MDSC) were found to express more chemokines and chemokine-associated genes than polymorphonuclear-MDSC (PMN-MDSC), and the differential profile of chemokines and chemokine-related genes might modulate the presence and activity of Mo-MDSC and PMN-MDSC in the tumor.(52) Recently, there is evidence that hypoxia can prevent the differentiation of MDSC and therefore promote the maintenance of MDSC through stabilization of hypoxia-inducible factor-1 (HIF-1) which induces ectoenzyme ENTPD2/CD39L1 in cancer cells in HCC.(53) However, chemerin has a tumor-inhibitory effect by inducing a shift in tumor-infiltrating immune cells from MDSC to IFN-γ$^+$ T cells and decreased tumor angiogenesis in HCC mouse models.(54)

6.1.4 Tumor-associated macrophages (TAM)

Another cell type with potential immunomodulatory property in HCC is tumor-associated macrophages (TAM). Alternatively activated macrophages (M2), distinct from classically

activated macrophages (M1), shape the tumor microenvironment and dampen anti-cancer immune responses. M2 macrophages have been found to be associated with poor clinical outcome of HCC patients.(55) Shirabe et al. and Capece et al. have reviewed the role of TAM in the initiation and progression of HCC a few years ago.(56, 57) In addition to immunosuppression, emerging evidence indicates that TAM exert tumor-promoting function. Recently TAM were demonstrated to promote cancer stem cell-like properties in a mouse hepatoma cell line via TGF-β1-induced epithelial-mesenchymal transition,(58) and to promote expansion of human HCC stem cells via IL-6 and STAT3 signaling.(59, 60) Moreover, TAM were reported to be associated with programmed cell death ligand 1 (PD-L1) and NF-kB signaling pathway, and to promote the motility of HCC cells.(61, 62) M2 macrophages were proved to enhance tumor migration and venous infiltration through CCL22-induced epithelial-mesenchymal transition, and to be associated with poor prognosis in HCC patients.(63)

Recently, ways to overcome immunosuppression by TAM in HCC have been identified. Sorafenib was shown to induce pro-inflammatory activity of TAM and thereby triggering tumor-directed NK cell response in vitro and in mice with HCC,(64) also to alter macrophage polarization and reduce macrophage-driven growth of hepatoma cells.(65) In addition, it has demonstrated that therapeutic blocking of the CCL2-CCR2 signaling inhibits the recruitment of inflammatory monocytes, infiltration and M2-polarisation of TAM in experimental models, causing the reversal of the immunosuppressive status in the tumor microenvironment and activation of anti-tumor CD8^{+} T cell response.(66) In intrahepatic cholangiocarcinoma, the number of CD163^{+} and CD68^{+} M2 macrophages positively correlates with the numbers of vessels and Foxp3^{+} Treg, and patients with high counts of CD163^{+} macrophages showed poor disease-free survival.(67) However, another study found high levels of CD68^{+} TAM in the tumor invasive front or absence of histologic tumor necrosis were associated with an improved recurrence-free and overall survival.(68)

6.2 Regulation of intra-tumoral T cell immunity in liver cancers by co-inhibitory immune checkpoint pathways (Figure 2)

6.2.1 Cytotoxic T-lymphocyte associated protein 4 (CTLA4) and CD80 (B7-1)/CD86 (B7-2)

B7 superfamily is a type of peripheral membrane protein found on activated antigen-presenting cells that, when paired with a corresponding surface protein on a T cell, can produce a co-inhibitory signal or a co-stimulatory signal to decrease or enhance the activity of a MHC-TCR signal between the antigen-presenting cell and the T cell, respectively. The

members of this family consist of B7-1 (CD80), B7-2 (CD86), B7-DC (PD-L2), B7-H1 (PD-L1), B7-H2 (ICOSL), B7-H3 (CD276), B7-H4 (VTCN1), B7-H5 (VISTA), B7-H6 (NCR3LG1) and B7-H7 (HHLA2).

Cytotoxic T-lymphocyte associated protein 4 (CTLA4) has been described to be expressed on conventional Treg and to be important for the immunosuppressive function of Treg. We and others have shown that CTLA4 is indeed highly expressed on Treg in human HCC and LM-CRC tumors.(21, 69) however whether CTLA4 is involved in the suppressive function of Treg in liver tumors is unknown. CTLA4 expression can also be induced on effector T cells upon activation and interaction with its ligands CD80 (B7-1) or CD86 (B7-2) can inhibit effector T cell function directly. Antibody blockade of CTLA4 unmasked *ex vivo* tumor-associated antigen (TAA)-specific immune responses in peripheral blood leukocytes of HCC patients.(20) However, whether tumor antigen-specific T cells in the tumor microenvironment of HCC can be activated by CTLA-4 blockade is unknown. Interestingly, a novel subset of human CTLA4-expressing CD14+ regulatory dendritic cells was identified in blood and tumor-infiltrating immune cells of HCC patients which suppresses T cells through CTLA4-dependent IL-10 and IDO production,(69) suggesting that anti-CTLA4 blockade might also alleviate immunosuppressing by targeting non-T cells.

A phase 1 clinical trial of anti-CTLA4 antibody tremelimumab showed a manageable safety profile and a confirmed partial response in 3 of 17 HCV-related advanced HCC patients.(70) Another clinical trial revealed that 5 of 19 evaluable advanced HCC patients had a partial response after being treated with tremelimumab in combination with subtotal radiofrequency ablation or chemoablation.(71) Tremelimumab is of IgG2 subclass which has limited capacity for antibody-dependent cell-mediated cytotoxicity, while the efficacy of anti-CTLA4 antibody therapy is at least partly attributed to intra-tumoral depletion of Treg by antibody-dependent cell-mediated cytotoxicity (ADCC).(72-74) Since another anti-CTLA antibody ipilimumab is of IgG1 subclass which can better mediate ADCC, it might be more effective in HCC. In addition, current clinical trials are testing whether combination treatment of ipilimumab with nivolumab in HCC and CCA patients as well as the combination of tremelimumab and anti-PD-L1 antibody durvalumab in HCC patients result in improved clinical efficacy.(75) Knowledge of the role of CTLA4 in anti-tumor immunity in CCA is very limited. In perihilar cholangiocarcinoma, higher intra-tumoral CTLA4 expression was described to associate with higher density of CD8$^+$ and CD4$^+$ TIL, and prolonged overall survival and disease-free interval.(76)
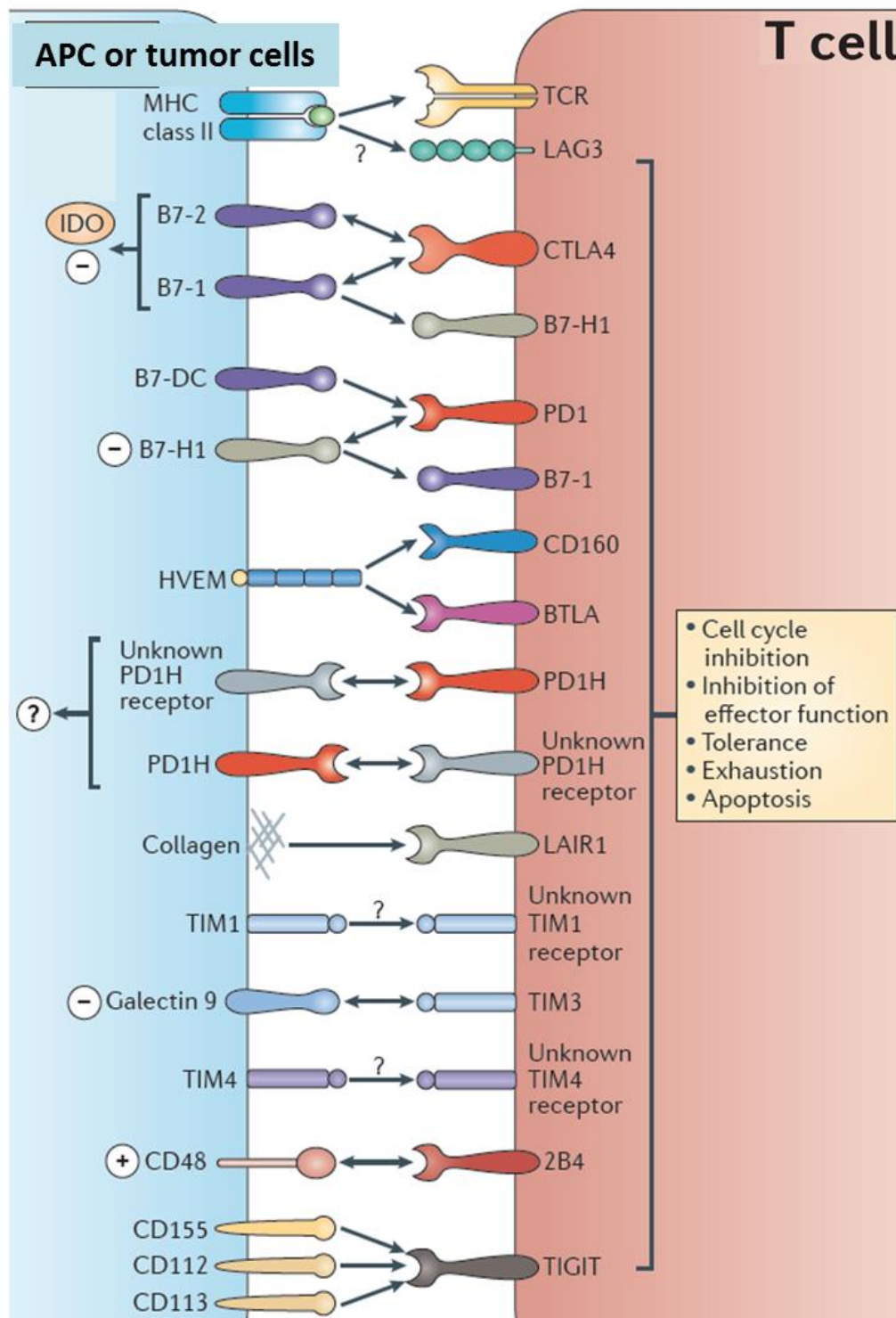
Figure 2. Co-inhibitory interactions in T cells. Co‑inhibitory molecules deliver negative signals into T cells following their engagement by receptors and counter-ligands on antigen-presenting cells (APC) or tumor cells. (Reproduced and modified from Chen & Flies 2013 Nature Reviews(144))

6.2.2 Programmed cell death 1 (PD-1) and programmed cell death ligand 1 (PD-L1, B7-H1)

Antibody blockade of the interaction between the co-inhibitory immune checkpoint receptor PD-1 and its ligand PD-L1 (B7-H1) has shown therapeutic success in melanoma, non-small cell lung cancer and renal cancer, and both anti-PD-1 and anti-PDL1 antibodies have been approved for treatment of several types of cancer in the past few years.(77-79) The PD-1-PD-L1 pathway has been relatively well-studied in HCC. In HCC patients, PD-1 is expressed on intra-tumoral T cells, and PD-L1 is expressed on intra-tumoral monocytes/macrophages and tumor cells.(22, 80, 81) PD-L1 upregulation is mainly induced by IFN-γ produced by activated CD8$^+$ T cells pre-existing in the HCC milieu, and it may represent an adaptive immune resistance mechanism exerted by tumor cells in response to endogenous anti-tumor activity.(82) PD-L1 expression can also be promoted by hypoxia in HCC.(83) PD-1 and PD-L1 have been demonstrated to contribute to local tumor antigen-specific tolerance in experimental animal HCC models, and anti-PD-L1 antibody treatment resulted in a significant delay in HCC progression in these models.(84) In vitro studies have shown that antibody blockade of the interaction between PDL-L1 and PD-1 in co-cultures of monocytes/macrophages and T cells derived from human HCC tumors can restore T cell functions.(85, 86) Research of Kuang and Zheng indicated that PD-L1-expressing monocytes skewed Th22 polarization away from IFN-γ and toward IL-17 via interaction with PD-1, which could create favorable conditions for in vivo aggressive cancer growth and angiogenesis in HCC patients.(87) In addition, a novel pro-tumorigenic PD-1^{hi} regulatory B cell population was recently identified in human HCC, in mouse models the PD-1^{hi} B cells derived from hepatoma acquired regulatory functions that inhibited tumor-specific T cell immunity and fostered disease progression via IL-10-dependent pathways upon interacting with PD-L1-expressing HEK293T cells.(88)

Lately in a phase 1/2 clinical trial, anti-PD-1 antibody nivolumab has resulted in an objective response rate of 20%, disease control with stable disease for ≥6 months in 37%, and encouraging overall survival in 214 patients with advanced HCC regardless of HCC etiology. Moreover, liver toxicity was limited and manageable in the majority of patients.(89) This study is the first to show the promising potential of PD-1/PD-L1 blockade in HCC. However, similar to other cancer types, only a subpopulation of HCC patients respond to anti-PD-1 monotherapy and most of these patients show incomplete response. Therefore, further research should aim to find combinations of anti-PD1 treatment with other therapeutic options to improve its efficacy. In mouse models combined treatment of sorafenib and anti-PD-L1 antibody generated effective natural killer cell responses resulting in remarkable

reduction of HCC tumor growth.(90) Another study demonstrated that anti-PD-1 antibody could boost anti-tumor immune responses in HCC models, but showed additional anti-tumor efficacy only when combined with both sorafenib and an inhibitor of the stromal cell-derived 1 alpha receptor (CXCR4) but not when combined with sorafenib alone because sorafenib increased hypoxia and induced accumulation of Treg and M2 macrophages(83). It is therefore as yet unclear whether combination therapy of anti-PD-1 antibody and sorafenib may be a better treatment option for patients with HCC. However, combining anti-PD-1 antibody with mTOR inhibitor was shown to result in more durable and synergistic tumor regression than either single agent alone in mice with HCC.(91)

In cholangiocarcinoma, the PD-1-PD-L1 pathway has been studied in relation to malignant potential and immune escape mechanism, therefore this pathway may be a potential therapeutic target of CCA.(92-100) All these data are only based on immunohistochemistry staining of CCA tissues. A case report has described that a patient with advanced CCA showed strong and durable response to anti-PD1 antibody pembrolizumab. The patient's tumor displayed DNA mismatch repair deficiency, microsatellite instability and high levels of HLA class I and II antigen expression.(101) Currently a few clinical trials of anti-PD-1 antibodies in CCA patients are ongoing.(75)

In CRC patients, PD-1 and PD-L1 blocking antibodies have shown therapeutic efficacy only in the subgroup of CRC patients with mismatch repair (MMR)-deficient tumors, but not in patients with MMR-proficient tumors.(102, 103) A defective MMR enzyme system occurs in 10%-20% of CRC tumors and results in microsatellite instability, which is used as a molecular marker of MMR-deficiency.(104) It has been hypothesized that the observed difference in responsiveness to PD-1/PD-L1 blockade between MMR-deficient and MMR-proficient CRC is related to the higher numbers of somatic mutations in MMR-deficient tumors, due to the reduced ability to repair DNA damage. The increased mutation rate may result in the presence of more mutation-encoded neo-antigens in the tumors, which elicit stronger anti-tumor T cell responses.(102) Indeed, MMR-deficient CRC tumors are characterized by denser CD8^{+} T cell infiltration.(105) They also have higher expression levels of co-inhibitory checkpoint molecules, probably to resist immune-mediated tumor elimination.(106) Together, enhanced immune cell infiltration and upregulation of co-inhibitory immune checkpoints may render MMR-deficient CRC more sensitive to PD-1/PD-L1 blockade than MMR-proficient CRC. Therefore, there is an urgent need to identify effective immunotherapies for MMR-proficient CRC.

6.2.3 B7-H3 (CD276)

B7-H3 (CD276) is a B7 superfamily member. It has recently been identified as an immune-inhibitory protein expressed on tumor cells or antigen-presenting cells, but its receptor is yet unknown.(107, 108) In mice, B7-H3 is induced on dendritic cells by regulatory T cells in an IL-10 independent fashion.(109) IFN-γ also enhances the expression of B7-H3 on dendritic cells, while B7-H3 upregulation is suppressed by IL-4.(110) When initially discovered, B7-H3 was thought to be co-stimulatory for T cells,(111) but now most publications agree that B7-H3 suppresses the function of T cells.(107, 112) A discrepancy was found between B7-H3 RNA levels and protein levels in human tissue, most likely due to post-transcriptional degradation of B7-H3 RNA molecules by microRNA-29. MicroRNA-29 is downregulated in many solid tumors.(113)

65% of normal livers already have a weak to moderate protein expression of B7-H3, but expression levels increase dramatically on HCC tumors.(114) Expression of B7-H3 on HCC tumor cells is associated with worse survival(115-117) and increased recurrence.(117) B7-H3 expression was significantly associated with the presence of aggressive features, like a higher α-fetoprotein level, advanced TNM stage, poor differentiation, the presence of liver cirrhosis, vascular invasion and metastasis. B7-H3 expression on tumor cells inversely correlated with T cell proliferation, as measured by Ki-67 expression, but showed no association with infiltrating T cell number.(117) All HCC cell lines tested express B7-H3 and this expression was enhanced by IFN-γ. B7-H3 expression on HepG2 cells promoted their proliferation, migration, invasion and adhesion independent of immunity.(116, 118) B7-H3 can be cleaved from the membrane and released in a soluble form. Circulating serum B7-H3 levels are twice as high in patients with HCC compared to healthy individuals and this was related to clinical stage, distant metastasis and the positive expression of B7-H3 in HCC tissues.(119)

Several antibodies against B7-H3 have been developed and are now being tested in clinical trials and are reviewed by Ni et al.(120) They aim to induce antibody-dependent cell-mediated cytotoxicity (ADCC) in B7-H3-expressing tumors rather than to block the interaction between B7-H3 and its unknown receptor on T cells. In extrahepatic cholangiocarcinoma B7-H3 is expressed, however there was no association with prognosis.(121) B7-H3 is a potentially interesting target for immunotherapy of liver cancer.

6.2.4 B7-H4 (VTCN1)

B7-H4 (VTCN1) is another member of the B7 superfamily. Ligation of B7-H4 to its unknown receptor on T cells leads to a reduction in TCR signaling.(122) This results in growth inhibition, lower cytokine production, reduction in cytotoxicity and induction of T cell apoptosis.(123-125) B7-H4 mRNA is widely distributed in a variety of mouse and human tissues, while its protein expression is more restricted.(126) It was reported that B7-H4 was neither expressed on human or mouse dendritic cells, macrophages, monocytes nor on B or T cells regardless of stimulation,(127) while others could induce B7-H4 expression on these cells by LPS, PMA/ionomycin and PHA stimulation.(123) Treg could induce B7-H4 expression on monocytes and macrophages in an indirect way. Treg induces IL-10 production by monocytes or macrophages in a cell-cell contact dependent way. IL-10 binding to the IL-10 receptor on the monocyte or macrophage leads to upregulation of B7-H4.(128, 129) Ectopic B7-H4-immunoglobulin expression could attenuate concanavalin A-induced hepatic injury in mice. B7-H4-immunoglobulin treated mice had lower ALT and AST levels in serum. The IFN-γ, IL-2 and IL-4 levels were also reduced, while IL-10 was enhanced. In spite of soluble B7-H4 that merely acts as a decoy receptor, B7-H4-immunoglobulin was able to cross-link its putative receptor and initiated an inhibitory signal.(130)

Yuan et al. reported that B7-H4 was not expressed in healthy liver, however 45% of HCC tumors expressed B7-H4 and this was positively correlated with TNM stage, differentiation stage and lymph node metastasis. Mice injected with mouse hepatoma H22 cells showed that B7-H4 expression levels increased as tumors increased in size and weight.(131) Another study found that high B7-H4 expression on HCC was associated with shorter survival, vascular invasion, TNM stage and lymph node metastasis. Downregulation of B7-H4 suppressed cell invasion and induced apoptosis in HCC cell lines. In co-culture experiments, knockdown of B7-H4 in HCC cells improved the function of cytotoxic T cells.(132) B7-H4 expression levels were substantially higher in HBV positive HCC tumors than in HBV negative HCC tumors, making HBV-infected livers more prone to hepatocarcinogenesis.(133) Arsenic trioxide, a chemotherapy drug, could downregulate the expression of B7-H4 on MHCC97H cells.(134) Serum levels of soluble B7-H4 were higher in HCC patients compared to healthy controls and were correlated to poor survival, increased tumor size, tumor invasion, differentiation stage, α-fetoprotein levels and lymph node metastasis.(135, 136) Serum levels of soluble B7-H4 in HCC patients correlated negatively with IFN-γ and positively with IL-4 levels.(131) Blocking the B7-H4-B7-H4-ligand interaction could be a promising target for immunotherapy, however clinical trials have not yet been

initiated. Dangaj et al. developed human single chain fragments variable antibodies against B7-H4 that could restore anti-tumor T cell responses in vitro.(137)

B7-H4 is expressed in 49% of cholangiocarcinomas and expression was associated with shorter survival, tumor status, lymph node metastasis and differentiation grade. B7-H4 expression in tumor cells was negatively correlated with the density of CD8$^+$ T cells in the tumor stroma. Knockdown of B7-H4 in cholangiocarcinoma cell lines could restore cytotoxic T cell function in co-culture experiments.(138)

6.2.5 B7-H7 (HHLA2)

B7-H7 (HHLA2) can have both co-inhibitory and co-stimulatory effects on T cells depending on their activation history. It is expressed on monocytes and activated B cells. Addition of B7-H7-immunoglobulin to CD4$^+$ or CD8$^+$ T cells that were stimulated via TCR suppressed their proliferation and cytokine production.(139, 140) However, Zhu et al. identified CD28H (TMIGD2) as a co-stimulatory receptor for HHLA2. CD28H is expressed on CD4$^+$ and CD8$^+$ naïve T cells and its expression is lost after repetitive stimulation.(141) Ligation of B7-H7 to CD28H had a co-stimulatory effect on T cells. Agonistic targeting of CD28H by plate coated B7-H7-immunoglobulin induced proliferation and cytokine production by naïve T cells, which seems to be contradictory to the two former studies. This might be explained by the existence of an additional unknown co-inhibitory receptor which is expressed on activated memory T cells that lost CD28H expression.(142)

HHLA2 protein is widely expressed in human cancers, including HCC. Janakiram et al. reported that 4 out of 10 liver cancers expressed B7-H7.(143) Since most T cells in the tumor microenvironment have a central or effector memory phenotype and probably do not express CD28H, B7-H7 could be a suitable target for checkpoint blockade.

6.2.6 T cell immunoglobulin and mucin domain-containing molecule 3 (TIM3) and galectin 9

T cell immunoglobulin domain and mucin domain-containing molecule 3 (TIM3) has been reported to negatively regulate the immune response against viral infection and play an important role in regulating T cells in cancer.(145-148) Currently several anti-TIM3 monoclonal antibodies as single agent and in combination with anti-PD-1/PD-L1 antibodies are being tested in clinical trials of patients with advanced melanoma, non-small cell lung cancer, renal cell cancer, colorectal cancer, acute myeloid leukemia or myelodysplastic syndromes.(75) High TIM3 expression has been demonstrated on intra-tumoral CD4$^+$ and CD8$^+$ T cells and its ligand galectin 9 is highly expressed on Kupffer cells in hepatitis B virus-

associated HCC patients. Furthermore, blocking the TIM3-galectin 9 interaction improved the ex vivo functionality of tumor-infiltrating CD4$^+$TIM3$^+$ T cells.(149) We demonstrated that galectin 9 is also expressed on tumor cells in most HCC patients,(81) Interestingly, in HCC patients TIM3 is not only expressed on T cells but also on peripheral blood monocytes and tumor-associated macrophages. TIM3 expression on these cells is associated with poor survival. Furthermore, TGF-β fostered TIM3 expression and the alternative activation of macrophages, and down-regulation or antibody blockade of TIM3 on macrophages suppressed HCC cell growth in an experimental mouse model.(150) Together these data suggest that TIM3 may be a promising target for antibody blockade therapy in HCC. Whether TIM3 is involved in suppression of anti-tumor responses in CCA and LM-CRC is unknown. Clinical trials on anti-TIM3 antibody have not been initiated yet in patients with liver cancer.

6.2.7 Lymphocyte activating 3 (LAG3) and MHC class II molecules

Lymphocyte activating 3 (LAG3) is a co-inhibitory molecule that plays an important role in regulation of T cell expansion and function.(151, 152) The interaction between LAG3 and its major ligand MHC class II is implicated in the regulation of dendritic cell function and in maintaining tolerance of CD8$^+$ T cells.(153, 154) In mice, LAG3 and PD-1 are co-expressed on tumor-infiltrating CD8$^+$ and CD4$^+$ T cells in several pre-clinical cancer models and combined blockade of LAG3 and PD-1 was shown to synergize to improve anti-tumor CD8$^+$ T cell responses.(155) CD8$^+$ T cells expressing both LAG3 and PD1 were the dominant TIL population in CT26 colon carcinoma in which LAG3 was shown to control T cell proliferation resulting in hypofunction.(156) In humans, co-expression of LAG3 and PD-1 was indicated to mark dysfunctional CD8$^+$ T cells in ovarian cancer, and combined blockade of LAG3 and PD-1 improved the cytokine production and proliferation of tumor antigen-specific CD8$^+$ T cells.(157) Currently many clinical trials studying blockade of LAG3 as monotherapy or in combination with anti-PD-1 antibodies are ongoing in patients with advanced colorectal cancer, renal cell cancer, melanoma, non-small cell lung cancer, glioblastoma or mesothelioma.(75) In HCC patients LAG3 expression is upregulated on tumor-infiltrating CD8$^+$ T cells compared to peripheral blood T cells, and LAG3 expression associates with functional defects of tumor-infiltrating HBV-specific CD8$^+$ T cells.(158) Tumor-infiltrating Treg and tissue resident memory CD8$^+$ T cells also express LAG3 (together with PD-1) in patient HCC tumors.(26, 159) There is experimental evidence indicating that LSECtin can serve as an alternative ligand for LAG3, and that LAG3-LSECtin interaction can inhibit anti-tumor T cell responses in melanoma.(160) Since LSECtin is highly expressed on liver sinusoidal endothelial cells,(161) , this interaction might be relevant for liver cancer. No data are

available on the expression and functional relevance of LAG3 in CCA and LM-CRC, and clinical trials on LAG3 blockade in patients with liver cancer are still lacking.

6.2.8 B and T lymphocyte associated (BTLA)/CD160 and Herpes virus entry mediator (HVEM), CD244 (2B4) and CD48

Other co-inhibitory receptors expressed on T cells include BTLA, CD160 and CD244. Their ligands are HVEM, HVEM and CD48 respectively. These co-inhibitory interactions may also suppress anti-tumor T cell responses.(152, 162) Herpes virus entry mediator (HVEM) is expressed in tumor cells of almost all HCC patients,(81) and the proportion of HVEM$^+$ tumor cells inversely associates with numbers of tumor-infiltrating CD8$^+$, CD4$^+$ and CD45RO$^+$ lymphocytes as well as expression of granzyme B, perforin and IFN-γ in HCC tissues.(163) Interestingly, a recent paper identified that BTLA$^+$PD-1$^+$CD4$^+$ TIL were highly dysfunctional whereas BTLA$^-$PD-1$^+$CD4$^+$ TIL were activated, and provided evidence that BTLA signals participated in suppressing CD4+ T cell function in HCC.(164)

CD48 is expressed on monocytes/macrophages in HCC tissues, and high infiltration of peri-tumoral stromal monocytes/macrophages associates with impaired functions of NK cells in intra-tumoral areas. Monocyte-induced NK cell dysfunction was markedly attenuated by blocking CD244 (2B4) on NK cells.(165) Whether co-inhibitory receptors CD160 and CD244 are expressed on T cells in HCC is unknown. In addition, no data are available on these co-inhibitory pathways in CCA and LM-CRC.

6.2.9 T cell immunoreceptor with Ig and ITIM domains (TIGIT) and CD112/CD155

T cell immunoreceptor with Ig and ITIM domains (TIGIT) is a co-inhibitory receptor that limits anti-tumor and other CD8$^+$ T cell-dependent chronic immune responses.(166, 167) Two ligands for TIGIT have been identified, CD112 and CD155, of which CD155 seems to be the pre-dominant ligand, while interaction between TIGIT and CD112 is weak.(168) TIGIT shares the ligands with co-stimulatory receptor CD226 and reportedly counterbalances CD226.(169) TIGIT was shown to be highly expressed on tumor-infiltrating T cells in lung squamous cell carcinoma, colon adenocarcinoma, uterine corpus endometroid carcinoma, breast carcinoma and kidney renal clear cell carcinoma. And blockade of both TIGIT and PD-L1 specifically and synergistically enhanced CD8$^+$ T cell function in models of both cancer and chronic viral infection, resulting in tumor and viral clearance.(170) In melanoma patients TIGIT expression was elevated on tumor antigen-specific CD8$^+$ T cells compared with non-specific CD8$^+$ T cells, and was upregulated on CD8$^+$ tumor-infiltrating T cells compared with circulating T cells, and these TIGIT-expressing cells often co-expressed PD-1.(171) Furthermore, blocking

TIGIT and PD-1 enhanced ex vivo proliferation, cytokine production and degranulation of both CD8$^+$ tumor-infiltrating T cells and tumor antigen-specific CD8$^+$ T cells in the presence of TIGIT ligand-expressing cells.(171) In cholangiocarcinoma, mRNA and protein expression of CD155 is increased in tumor tissues compared with corresponding para-cancerous tissues. Up-regulated CD155 associated with aggressive clinicopathologic characteristics, angiogenesis and shorter survival after surgical resection in CCA patients.(172). Interestingly, another co-inhibitory receptor of CD155 is CD96, which is expressed on T cells and NK cells and competes for binding to CD155 with CD226.(173) And another co-inhibitory of CD112 is CD112R, which is preferentially expressed on T cells, inhibits T cell receptor-mediated signals and competes with CD226 for binding to CD112.(168) No data on expression and function of TIGIT or its ligands are available for HCC and LM-CRC, these co-inhibitory pathways need to be investigated in the liver tumor microenvironment.

6.2.10 V-set immunoregulatory receptor (VISTA, B7-H5)

Another immune checkpoint regulator that might be potentially targeted in liver cancer is V-set immunoregulatory receptor (VISTA, B7-H5).(174, 175) It is a newly identified and structurally distinct immunoglobulin superfamily inhibitory molecule, which is homologous to PD-L1 and suppresses T cell activation.(176, 177) VISTA was found to be highly expressed on myeloid cells and regulatory T cells in the tumor microenvironment of murine cancer models.(178) Preclinical studies with VISTA blockade demonstrated promising improvement in anti-tumor T cell response, leading to impeded tumor growth and improved survival.(179) Moreover, combined treatment using monoclonal antibodies specific for VISTA and PD-L1 achieved synergistic therapeutic efficacy in murine tumor models.(180) However, VISTA has not been studied in liver cancer yet.

6.3 Combined targeting of co-inhibitory and co-stimulatory immune checkpoint pathways (Figure3)

Dysfunction of immune cells in cancer patients can be overcome not only by antagonistic antibodies that block co-inhibitory pathways, but also by agonistic antibodies that stimulate immune cells by binding to co-stimulatory receptors. Most immunostimulatory antibodies developed for cancer immunotherapy are directed against co-stimulatory molecules of the tumor necrosis factor receptor superfamily (TNFRSF), such as CD40, CD134 (OX40), CD137 (4-1BB) and glucocorticoid-induced tumor necrosis factor receptor (GITR) (Figure 3).(144, 181) In HCC rat models, treatment with an activating anti-CD40 antibody increased endothelial leucocyte adhesion in tumor vessels, stimulated migration of NK cells and T cells into the tumor, and more importantly, inhibited tumor growth.(182) In addition, treatment with

an agonistic anti-CD137 monoclonal antibody led to anti-tumor immune responses and tumor regression in HCC mice.(183) We have shown that ex vivo agonistic GITR engagement partially reduces the suppression exerted by tumor-infiltrating Treg of patients with HCC or LM-CRC.(21) However, whether agonistic ligation of GITR can invigorate effector responses of tumor-infiltrating T cells of HCC patients remains unknown. No data on expression and functional relevance of co-stimulatory molecules are available for CCA.

A promising new development for cancer immunotherapy is combined treatment with antibodies targeting immunoinhibitory molecules and antibodies targeting immunostimulatory molecules. A triple combination of anti-CD137, anti-CD134 and anti-PD-L1 antibodies increased tumor infiltration of activated and blastic T cells containing cytotoxic granules and prolonged survival in transgenic HCC mouse models, while single treatment of any of the three antibodies didn't have the effects.(184) No data are available on CCA and LM-CRC. Currently, GITR agonistic antibody combined with PD-1 and/or CTLA4 antagonistic antibody, CD134 agonistic antibody combined with PD-1 and/or CTLA4 antagonistic antibody, CD134 agonistic antibody in combination with CD137 agonistic antibody are being tested in clinical trials of HCC patients.(75) Further research on co-expression of immune checkpoints and clinical efficacy of combination therapies in HCC, CCA and LM-CRC is needed to achieve better clinical outcome for patients.

6.4 Regulation of intra-tumoral T cell immunity in liver cancers by enzymatic production of immune suppressive metabolites

Tryptophan catabolism mediated by indoleamine 2,3-dioxygenase (IDO) is an important mechanism of peripheral immune tolerance contributing to tumoral immune resistance. IDO converts tryptophan into kynurenine. While T cells need tryptophan for their functions, kynurenine inhibits T cells.(185, 186) IDO is expressed in HCC tumors cells.(80) Recently a new subset of human $CD14^+CTLA4^+$ regulatory dendritic cells was identified in HCC patients, which suppressed anti-tumor T cell response through IDO and IL-10 production in vitro.(69) IDO can be induced in monocytes by tumor-derived $CD69^+$ T cells isolated from HCC tissues. Medium from IDO^+ macrophages suppressed T cell responses effectively in vitro, which could be reversed by pretreating macrophages with an IDO inhibitor 1-methyl-DL-tryptophan or by adding extrinsic tryptophan.(187) IDO activity in activated HCC-associated fibroblasts triggered the dysfunction of NK cells, and may favor tumor progression.(188) IDO short hairpin RNA inhibited tumor growth in subcutaneous, orthotopic and metastatic liver tumor animal models.(189) Several IDO inhibitors, are currently in clinical trials for solid tumors, but not yet in liver cancer.

Another enzyme that mediates tryptophan catabolism is tryptophan 2,3-dioxygenase (TDO), which is an hepatic enzyme degrading tryptophan along the kynurenine pathway. The tryptophan catabolite kynurenine was identified as an endogenous ligand of human aryl hydrocarbon receptor that was constitutively generated during cancer progression and inflammation. TDO-derived kynurenine suppressed anti-tumor immune responses and promoted tumor cell motility and survival in mouse models.[190] It was described that enzymatically active TDO was expressed in several types of human cancer including hepatocarcinoma, and in a preclinical model TDO expression prevented tumor rejection by immunized mice. Furthermore, treatment with a TDO inhibitor restored the ability of mice to reject TDO-expressing tumors.[191] Whether TDO inhibition may induce effective anti-cancer immune responses in liver cancer is as yet unknown.

6.5 Inhibition of migration of immune effector cells into tumors

We have shown that HCC and LM-CRC tumors contain lower numbers of cytotoxic immune cells such as NK cells and CD8^{+} T cells compared to tumor-free liver tissues of the same patients.[21] This suggests that tumors may inhibit immigration of cytotoxic immune cells, which is another way of immune evasion. For several other cancer types there are now emerging data showing how they prevent infiltration of immune cells, for example by collagen or endothelial barriers.[192, 193] An interesting study indicated that T cells accumulated more efficiently in the stroma than in tumor islets, because the density and orientation of the peri-tumoral extracellular matrix influenced the migration of T cells into tumors. Aligned fibers around tumor epithelial cell regions and in perivascular regions limited T cells from entering tumor islets of lung cancer patients.[194] This should become a field of research that can deliver novel targets to improve immune control of cancer, which may also be effective in liver cancer because the increased number of intra-tumoral CD8^{+} T cells associates with better survival.
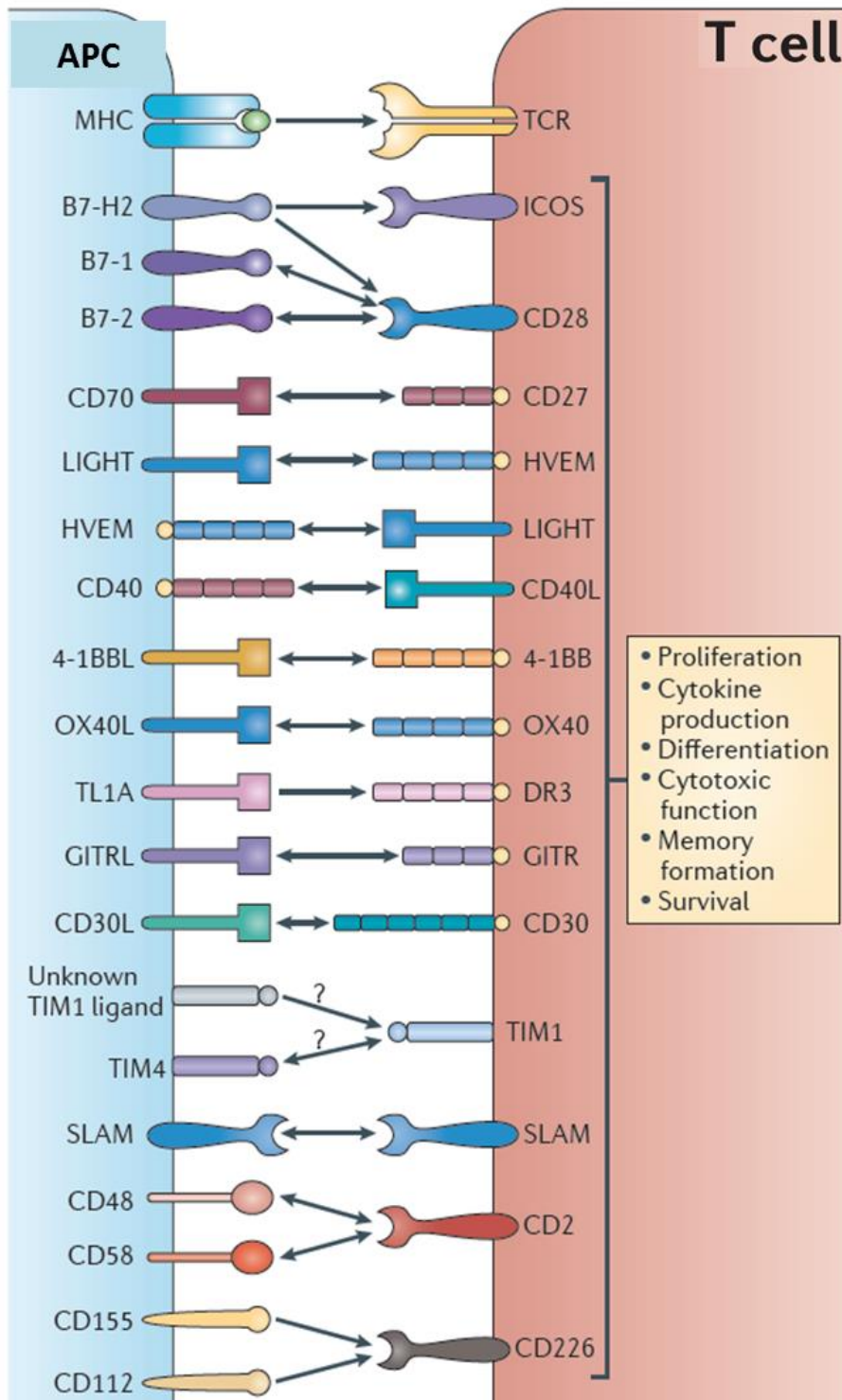
Figure 3. Co-stimulatory interactions in T cells. Co‑stimulatory molecules deliver positive signals to T cells following their engagement by receptors and counter-ligands on antigen-presenting cells (APC). (Reproduced and modified from Chen & Flies 2013 Nature Reviews(144))

7 Aims and outline of this thesis

In the current thesis we investigate some of the abovementioned immune suppressive mechanisms in the tumor microenvironment of liver cancers with the goal to identify new and potentially promising immunotherapeutic targets to overcome the intra-tumoral immune inhibition and enhance anti-tumor reactivity of tumor-infiltrating T cells in patients with liver cancer. We study how to reduce the immunosuppressive capacity of pro-tumor regulatory T cells, and how to activate anti-tumor functions of effector T cells in hepatocellular carcinoma, cholangiocarcinoma and liver metastasis of colorectal cancer by manipulating co-inhibitory and co-stimulatory pathways. For this purpose, we use leukocytes isolated from resected liver tumors, tumor-free liver tissues and peripheral blood collected from patients that undergo liver tumor resection, and perform flow cytometry analyses and *in vitro* immune cell culture assays. The ultimate aim of these studies is to provide new immunotherapeutic approaches to treat patients with primary liver cancer or CRC liver metastasis.

Part I focuses on two types of pro-tumor T cells, immunosuppressive conventional regulatory T cells and type 1 regulatory T cells. We study how to abrogate the immune suppression exerted by these cells in the tumor microenvironment (Figure 4). In **Chapter 2**, we study the phenotype and suppressive capacity of conventional regulatory T cells in hepatocellular carcinoma and liver metastasis of colorectal cancer, and demonstrate that stimulation of these cells via the co-stimulatory molecule GITR in combination with blockade of the co-inhibitory molecule CTLA4 can completely alleviate *ex vivo* inhibition of effector T cell functions by human liver tumor-derived regulatory T cells. In **Chapter 3**, we identify an intra-tumoral population of IL-10-producing Type 1 regulatory T cells in hepatocellular carcinoma and liver metastasis of colorectal cancer, and show in co-cultures that plasmacytoid dendritic cells enhance IL-10 production by these cells through engagement of their co-stimulatory molecule inducible T cell costimulator (ICOS). In **Chapter 4**, we challenge the use of anti-CD25 antibodies to deplete regulatory T cells from human tumors and propose the risk of depleting CD25-expressing non-Treg cells that may be important for anti-tumor immunity.

Part II focuses on two types of anti-tumor T cells, CD4$^+$ T helper cells and CD8$^+$ cytotoxic T cells. We study how to invigorate effector functions of tumor-infiltrating T cells by targeting co-inhibitory and co-stimulatory immune checkpoint pathways (Figure 4). In **Chapter 5**, we investigate which co-inhibitory pathways suppress intra-tumoral helper and cytotoxic T cells in hepatocellular carcinoma, and demonstrate that blocking PD-L1, TIM3, or LAG3 increases anti-tumor antigen responses of tumor-infiltrating CD4$^+$ and CD8$^+$ T cells in *ex vivo* assays. Importantly, combining antibody against PD-L1 with antibodies against TIM3, LAG3, or

CTLA4 further increases *ex vivo* functions of tumor-infiltrating T cells. In **Chapter 6**, we examine co-inhibitory molecules in liver metastasis of colorectal cancer with mismatch repair-proficient type, and compare the immune cell infiltration and expression of co-inhibitory molecules in LM-CRC with those in primary CRC and peritoneal metastasis of colorectal cancer. We show that antibody blockade of LAG3 or PD-L1 enhances *ex vivo* functions of tumor-infiltrating CD4$^+$ and CD8$^+$ T cells from LM-CRC. In **Chapter 7**, we analyze the composition and characteristics of immune infiltrates in cholangiocarcinoma, and test the effect of blocking co-inhibitory and activating co-stimulatory pathways on *ex vivo* effector functions of tumor-infiltrating T cells from cholangiocarcinoma. In **Chapter 8**, we demonstrate that agonistic targeting of the co-stimulatory molecule GITR by GITR ligand or anti-GITR antibody promotes ex vivo functions of T cells isolated from hepatocellular carcinoma.

A summary of the work presented in this thesis, as well as the importance and implications of these studies as a whole are discussed in **Chapter 9**.
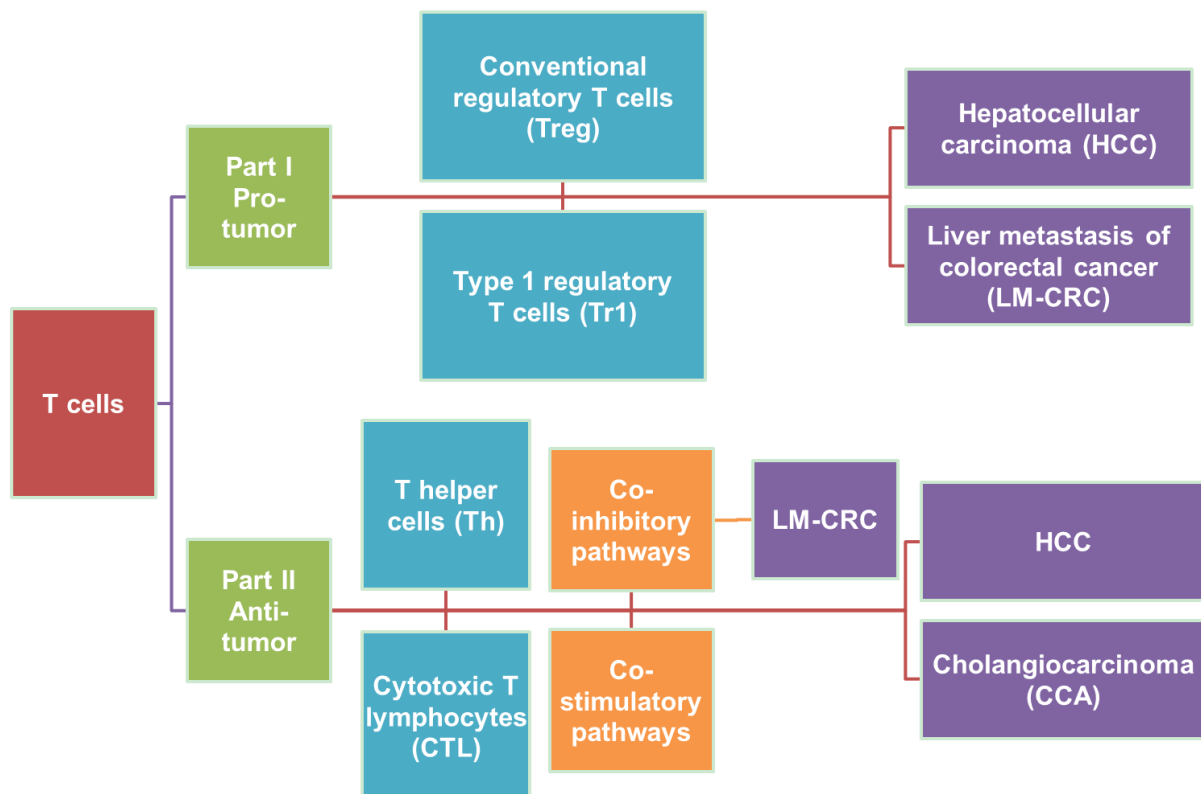

Figure 4. Outline of the thesis

REFERENCES

1.   Torre LA, Bray F, Siegel RL, Ferlay J, Lortet-Tieulent J, Jemal A. Global cancer statistics, 2012. CA Cancer J Clin 2015;65:87-108.
2.   El-Serag HB, Marrero JA, Rudolph L, Reddy KR. Diagnosis and treatment of hepatocellular carcinoma. Gastroenterology 2008;134:1752-1763.
3.   Chew V, Tow C, Teo M, Wong HL, Chan J, Gehring A, Loh M, et al. Inflammatory tumour microenvironment is associated with superior survival in hepatocellular carcinoma patients. J Hepatol 2010;52:370-379.
4.   Gao Q, Qiu SJ, Fan J, Zhou J, Wang XY, Xiao YS, Xu Y, et al. Intratumoral balance of regulatory and cytotoxic T cells is associated with prognosis of hepatocellular carcinoma after resection. J Clin Oncol 2007;25:2586-2593.
5.   Ringelhan M, Pfister D, O'Connor T, Pikarsky E, Heikenwalder M. The immunology of hepatocellular carcinoma. Nat Immunol 2018;19:222-232.
6.   Forner A, Reig M, Bruix J. Hepatocellular carcinoma. Lancet 2018;391:1301-1314.
7.   Patel T. Cholangiocarcinoma--controversies and challenges. Nat Rev Gastroenterol Hepatol 2011;8:189-200.
8.   Rizvi S, Gores GJ. Pathogenesis, diagnosis, and management of cholangiocarcinoma. Gastroenterology 2013;145:1215-1229.
9.   Blechacz B, Komuta M, Roskams T, Gores GJ. Clinical diagnosis and staging of cholangiocarcinoma. Nat Rev Gastroenterol Hepatol 2011;8:512-522.
10.   Razumilava N, Gores GJ. Cholangiocarcinoma. Lancet 2014;383:2168-2179.
11.   Bergquist A, von Seth E. Epidemiology of cholangiocarcinoma. Best Pract Res Clin Gastroenterol 2015;29:221-232.
12.   Kemeny N. The management of resectable and unresectable liver metastases from colorectal cancer. Curr Opin Oncol 2010;22:364-373.
13.   Bartlett EK, Simmons KD, Wachtel H, Roses RE, Fraker DL, Kelz RR, Karakousis GC. The rise in metastasectomy across cancer types over the past decade. Cancer 2015;121:747-757.
14.   Kemeny N. Presurgical chemotherapy in patients being considered for liver resection. Oncologist 2007;12:825-839.
15.   de Jong MC, Pulitano C, Ribero D, Strub J, Mentha G, Schulick RD, Choti MA, et al. Rates and patterns of recurrence following curative intent surgery for colorectal liver metastasis: an international multi-institutional analysis of 1669 patients. Ann Surg 2009;250:440-448.
16.   Tomlinson JS, Jarnagin WR, DeMatteo RP, Fong Y, Kornprat P, Gonen M, Kemeny N, et al. Actual 10-year survival after resection of colorectal liver metastases defines cure. J Clin Oncol 2007;25:4575-4580.
17.   Nordlinger B, Sorbye H, Glimelius B, Poston GJ, Schlag PM, Rougier P, Bechstein WO, et al. Perioperative FOLFOX4 chemotherapy and surgery versus surgery alone for resectable liver metastases from colorectal cancer (EORTC 40983): long-term results of a randomised, controlled, phase 3 trial. Lancet Oncol 2013;14:1208-1215.
18.   Van Cutsem E, Kohne CH, Hitre E, Zaluski J, Chang Chien CR, Makhson A, D'Haens G, et al. Cetuximab and chemotherapy as initial treatment for metastatic colorectal cancer. N Engl J Med 2009;360:1408-1417.
19.   Flecken T, Schmidt N, Hild S, Gostick E, Drognitz O, Zeiser R, Schemmer P, et al. Immunodominance and functional alterations of tumor-associated antigen-specific CD8+ T-cell responses in hepatocellular carcinoma. Hepatology 2014;59:1415-1426.
20.   Mizukoshi E, Nakamoto Y, Arai K, Yamashita T, Sakai A, Sakai Y, Kagaya T, et al. Comparative analysis of various tumor-associated antigen-specific t-cell responses in patients with hepatocellular carcinoma. Hepatology 2011;53:1206-1216.
21.   Pedroza-Gonzalez A, Verhoef C, Ijzermans JN, Peppelenbosch MP, Kwekkeboom J, Verheij J, Janssen HL, et al. Activated tumor-infiltrating CD4+ regulatory T cells restrain antitumor immunity in patients with primary or metastatic liver cancer. Hepatology 2013;57:183-194.
22.   Zhou G, Sprengers D, Boor PPC, Doukas M, Schutz H, Mancham S, Pedroza-Gonzalez A, et al. Antibodies Against Immune Checkpoint Molecules Restore Functions of Tumor-Infiltrating T Cells in Hepatocellular Carcinomas. Gastroenterology 2017;153:1107-1119 e1110.
23.   Sideras K, Bots SJ, Biermann K, Sprengers D, Polak WG, JN IJ, de Man RA, et al. Tumour antigen expression in hepatocellular carcinoma in a low-endemic western area. Br J Cancer 2015;112:1911-1920.
24.   Schietinger A, Philip M, Krisnawan VE, Chiu EY, Delrow JJ, Basom RS, Lauer P, et al. Tumor-Specific T Cell Dysfunction Is a Dynamic Antigen-Driven Differentiation Program Initiated Early during Tumorigenesis. Immunity 2016;45:389-401.
25.   Zheng C, Zheng L, Yoo JK, Guo H, Zhang Y, Guo X, Kang B, et al. Landscape of Infiltrating T Cells in Liver Cancer Revealed by Single-Cell Sequencing. Cell 2017;169:1342-1356 e1316.
26.   Chew V, Lai L, Pan L, Lim CJ, Li J, Ong R, Chua C, et al. Delineation of an immunosuppressive gradient in hepatocellular carcinoma using high-dimensional proteomic and transcriptomic analyses. Proc Natl Acad Sci U S A 2017;114:E5900-E5909.
27.   Schumacher TN, Schreiber RD. Neoantigens in cancer immunotherapy. Science 2015;348:69-74.
28.   Pritchard AL, Burel JG, Neller MA, Hayward NK, Lopez JA, Fatho M, Lennerz V, et al. Exome Sequencing to Predict Neoantigens in Melanoma. Cancer Immunol Res 2015;3:992-998.

29.   Lee JS. The mutational landscape of hepatocellular carcinoma. Clin Mol Hepatol 2015;21:220-229.

30.   Zou S, Li J, Zhou H, Frech C, Jiang X, Chu JS, Zhao X, et al. Mutational landscape of intrahepatic cholangiocarcinoma. Nat Commun 2014;5:5696.

31.   Robbins PF, Lu YC, El-Gamil M, Li YF, Gross C, Gartner J, Lin JC, et al. Mining exomic sequencing data to identify mutated antigens recognized by adoptively transferred tumor-reactive T cells. Nat Med 2013;19:747-752.

32.   Snyder A, Makarov V, Merghoub T, Yuan J, Zaretsky JM, Desrichard A, Walsh LA, et al. Genetic basis for clinical response to CTLA-4 blockade in melanoma. N Engl J Med 2014;371:2189-2199.

33.   van Rooij N, van Buuren MM, Philips D, Velds A, Toebes M, Heemskerk B, van Dijk LJ, et al. Tumor exome analysis reveals neoantigen-specific T-cell reactivity in an ipilimumab-responsive melanoma. J Clin Oncol 2013;31:e439-442.

34.   Rizvi NA, Hellmann MD, Snyder A, Kvistborg P, Makarov V, Havel JJ, Lee W, et al. Cancer immunology. Mutational landscape determines sensitivity to PD-1 blockade in non-small cell lung cancer. Science 2015;348:124-128.

35.   Tran E, Turcotte S, Gros A, Robbins PF, Lu YC, Dudley ME, Wunderlich JR, et al. Cancer immunotherapy based on mutation-specific CD4+ T cells in a patient with epithelial cancer. Science 2014;344:641-645.

36.   Zhao F, Korangy F, Greten TF. Cellular immune suppressor mechanisms in patients with hepatocellular carcinoma. Dig Dis 2012;30:477-482.

37.   Sun AM, Li CG, Zhang YQ, Lin SM, Niu HR, Shi YS. Hepatocarcinoma cell-derived hepatoma-derived growth factor (HDGF) induces regulatory T cells. Cytokine 2015;72:31-35.

38.   Shen Y, Wei Y, Wang Z, Jing Y, He H, Yuan J, Li R, et al. TGF-beta regulates hepatocellular carcinoma progression by inducing Treg cell polarization. Cell Physiol Biochem 2015;35:1623-1632.

39.   Chen KJ, Lin SZ, Zhou L, Xie HY, Zhou WH, Taki-Eldin A, Zheng SS. Selective recruitment of regulatory T cell through CCR6-CCL20 in hepatocellular carcinoma fosters tumor progression and predicts poor prognosis. PLoS One 2011;6:e24671.

40.   Zhou SL, Zhou ZJ, Hu ZQ, Huang XW, Wang Z, Chen EB, Fan J, et al. Tumor-Associated Neutrophils Recruit Macrophages and T-Regulatory Cells to Promote Progression of Hepatocellular Carcinoma and Resistance to Sorafenib. Gastroenterology 2016;150:1646-1658 e1617.

41.   Gu FM, Gao Q, Shi GM, Zhang X, Wang J, Jiang JH, Wang XY, et al. Intratumoral IL-17(+) cells and neutrophils show strong prognostic significance in intrahepatic cholangiocarcinoma. Ann Surg Oncol 2012;19:2506-2514.

42.   Greten TF, Ormandy LA, Fikuart A, Hochst B, Henschen S, Horning M, Manns MP, et al. Low-dose cyclophosphamide treatment impairs regulatory T cells and unmasks AFP-specific CD4+ T-cell responses in patients with advanced HCC. J Immunother 2010;33:211-218.

43.   Gagliani N, Magnani CF, Huber S, Gianolini ME, Pala M, Licona-Limon P, Guo B, et al. Coexpression of CD49b and LAG-3 identifies human and mouse T regulatory type 1 cells. Nat Med 2013;19:739-746.

44.   Bergmann C, Strauss L, Wang Y, Szczepanski MJ, Lang S, Johnson JT, Whiteside TL. T regulatory type 1 cells in squamous cell carcinoma of the head and neck: mechanisms of suppression and expansion in advanced disease. Clin Cancer Res 2008;14:3706-3715.

45.   Bergmann C, Strauss L, Zeidler R, Lang S, Whiteside TL. Expansion and characteristics of human T regulatory type 1 cells in co-cultures simulating tumor microenvironment. Cancer Immunol Immunother 2007;56:1429-1442.

46.   Bergmann C, Strauss L, Zeidler R, Lang S, Whiteside TL. Expansion of human T regulatory type 1 cells in the microenvironment of cyclooxygenase 2 overexpressing head and neck squamous cell carcinoma. Cancer Res 2007;67:8865-8873.

47.   Zhang X, Huang H, Yuan J, Sun D, Hou WS, Gordon J, Xiang J. CD4-8- dendritic cells prime CD4+ T regulatory 1 cells to suppress antitumor immunity. J Immunol 2005;175:2931-2937.

48.   Faget J, Bendriss-Vermare N, Gobert M, Durand I, Olive D, Biota C, Bachelot T, et al. ICOS-ligand expression on plasmacytoid dendritic cells supports breast cancer progression by promoting the accumulation of immunosuppressive CD4+ T cells. Cancer Res 2012;72:6130-6141.

49.   Kakita N, Kanto T, Itose I, Kuroda S, Inoue M, Matsubara T, Higashitani K, et al. Comparative analyses of regulatory T cell subsets in patients with hepatocellular carcinoma: a crucial role of CD25(-) FOXP3(-) T cells. Int J Cancer 2012;131:2573-2583.

50.   Greten TF, Wang XW, Korangy F. Current concepts of immune based treatments for patients with HCC: from basic science to novel treatment approaches. Gut 2015;64:842-848.

51.   Ma S, Cheng Q, Cai Y, Gong H, Wu Y, Yu X, Shi L, et al. IL-17A produced by gammadelta T cells promotes tumor growth in hepatocellular carcinoma. Cancer Res 2014;74:1969-1982.

52.   Zhao W, Xu Y, Xu J, Wu D, Zhao B, Yin Z, Wang X. Subsets of myeloid-derived suppressor cells in hepatocellular carcinoma express chemokines and chemokine receptors differentially. Int Immunopharmacol 2015;26:314-321.

53.   Chiu DK, Tse AP, Xu IM, Di Cui J, Lai RK, Li LL, Koh HY, et al. Hypoxia inducible factor HIF-1 promotes myeloid-derived suppressor cells accumulation through ENTPD2/CD39L1 in hepatocellular carcinoma. Nat Commun 2017;8:517.

54.   Lin Y, Yang X, Liu W, Li B, Yin W, Shi Y, He R. Chemerin has a protective role in hepatocellular carcinoma by inhibiting the expression of IL-6 and GM-CSF and MDSC accumulation. Oncogene 2017;36:3599-3608.

55.   Ding T, Xu J, Wang F, Shi M, Zhang Y, Li SP, Zheng L. High tumor-infiltrating macrophage density predicts poor prognosis in patients with primary hepatocellular carcinoma after resection. Hum Pathol 2009;40:381-389.

56.   Shirabe K, Mano Y, Muto J, Matono R, Motomura T, Toshima T, Takeishi K, et al. Role of tumor-associated macrophages in the progression of hepatocellular carcinoma. Surg Today 2012;42:1-7.

57.   Capece D, Fischietti M, Verzella D, Gaggiano A, Cicciarelli G, Tessitore A, Zazzeroni F, et al. The inflammatory microenvironment in hepatocellular carcinoma: a pivotal role for tumor-associated macrophages. Biomed Res Int 2013;2013:187204.

58.   Fan QM, Jing YY, Yu GF, Kou XR, Ye F, Gao L, Li R, et al. Tumor-associated macrophages promote cancer stem cell-like properties via transforming growth factor-beta1-induced epithelial-mesenchymal transition in hepatocellular carcinoma. Cancer Lett 2014;352:160-168.

59.   Wan S, Zhao E, Kryczek I, Vatan L, Sadovskaya A, Ludema G, Simeone DM, et al. Tumor-associated macrophages produce interleukin 6 and signal via STAT3 to promote expansion of human hepatocellular carcinoma stem cells. Gastroenterology 2014;147:1393-1404.

60.   Mano Y, Aishima S, Fujita N, Tanaka Y, Kubo Y, Motomura T, Taketomi A, et al. Tumor-associated macrophage promotes tumor progression via STAT3 signaling in hepatocellular carcinoma. Pathobiology 2013;80:146-154.

61.   Chen J, Li G, Meng H, Fan Y, Song Y, Wang S, Zhu F, et al. Upregulation of B7-H1 expression is associated with macrophage infiltration in hepatocellular carcinomas. Cancer Immunol Immunother 2012;61:101-108.

62.   Wang H, Wang X, Li X, Fan Y, Li G, Guo C, Zhu F, et al. CD68(+)HLA-DR(+) M1-like macrophages promote motility of HCC cells via NF-kappaB/FAK pathway. Cancer Lett 2014;345:91-99.

63.   Yeung OW, Lo CM, Ling CC, Qi X, Geng W, Li CX, Ng KT, et al. Alternatively activated (M2) macrophages promote tumour growth and invasiveness in hepatocellular carcinoma. J Hepatol 2015;62:607-616.

64.   Sprinzl MF, Reisinger F, Puschnik A, Ringelhan M, Ackermann K, Hartmann D, Schiemann M, et al. Sorafenib perpetuates cellular anticancer effector functions by modulating the crosstalk between macrophages and natural killer cells. Hepatology 2013;57:2358-2368.

65.   Sprinzl MF, Puschnik A, Schlitter AM, Schad A, Ackermann K, Esposito I, Lang H, et al. Sorafenib inhibits macrophage-induced growth of hepatoma cells by interference with insulin-like growth factor-1 secretion. J Hepatol 2015;62:863-870.

66.   Li X, Yao W, Yuan Y, Chen P, Li B, Li J, Chu R, et al. Targeting of tumour-infiltrating macrophages via CCL2/CCR2 signalling as a therapeutic strategy against hepatocellular carcinoma. Gut 2017;66:157-167.

67.   Hasita H, Komohara Y, Okabe H, Masuda T, Ohnishi K, Lei XF, Beppu T, et al. Significance of alternatively activated macrophages in patients with intrahepatic cholangiocarcinoma. Cancer Sci 2010;101:1913-1919.

68.   Atanasov G, Dietel C, Feldbrugge L, Benzing C, Krenzien F, Brandl A, Mann E, et al. Tumor necrosis and infiltrating macrophages predict survival after curative resection for cholangiocarcinoma. Oncoimmunology 2017;6:e1331806.

69.   Han Y, Chen Z, Yang Y, Jiang Z, Gu Y, Liu Y, Lin C, et al. Human CD14+ CTLA-4+ regulatory dendritic cells suppress T-cell response by cytotoxic T-lymphocyte antigen-4-dependent IL-10 and indoleamine-2,3-dioxygenase production in hepatocellular carcinoma. Hepatology 2014;59:567-579.

70.   Sangro B, Gomez-Martin C, de la Mata M, Inarrairaegui M, Garralda E, Barrera P, Riezu-Boj JI, et al. A clinical trial of CTLA-4 blockade with tremelimumab in patients with hepatocellular carcinoma and chronic hepatitis C. J Hepatol 2013;59:81-88.

71.   Duffy AG, Ulahannan SV, Makorova-Rusher O, Rahma O, Wedemeyer H, Pratt D, Davis JL, et al. Tremelimumab in combination with ablation in patients with advanced hepatocellular carcinoma. J Hepatol 2017;66:545-551.

72.   Simpson TR, Li F, Montalvo-Ortiz W, Sepulveda MA, Bergerhoff K, Arce F, Roddie C, et al. Fc-dependent depletion of tumor-infiltrating regulatory T cells co-defines the efficacy of anti-CTLA-4 therapy against melanoma. J Exp Med 2013;210:1695-1710.

73.   Selby MJ, Engelhardt JJ, Quigley M, Henning KA, Chen T, Srinivasan M, Korman AJ. Anti-CTLA-4 antibodies of IgG2a isotype enhance antitumor activity through reduction of intratumoral regulatory T cells. Cancer Immunol Res 2013;1:32-42.

74.   Romano E, Kusio-Kobialka M, Foukas PG, Baumgaertner P, Meyer C, Ballabeni P, Michielin O, et al. Ipilimumab-dependent cell-mediated cytotoxicity of regulatory T cells ex vivo by nonclassical monocytes in melanoma patients. Proc Natl Acad Sci U S A 2015;112:6140-6145.

75.   ClinicalTrials.gov.

76.   Lim YJ, Koh J, Kim K, Chie EK, Kim S, Lee KB, Jang JY, et al. Clinical Implications of Cytotoxic T Lymphocyte Antigen-4 Expression on Tumor Cells and Tumor-Infiltrating Lymphocytes in Extrahepatic Bile Duct Cancer Patients Undergoing Surgery Plus Adjuvant Chemoradiotherapy. Target Oncol 2017;12:211-218.

77.   Wolchok JD, Chiarion-Sileni V, Gonzalez R, Rutkowski P, Grob JJ, Cowey CL, Lao CD, et al. Overall Survival with Combined Nivolumab and Ipilimumab in Advanced Melanoma. N Engl J Med 2017;377:1345-1356.

78.   Ribas A, Hamid O, Daud A, Hodi FS, Wolchok JD, Kefford R, Joshua AM, et al. Association of Pembrolizumab With Tumor Response and Survival Among Patients With Advanced Melanoma. JAMA 2016;315:1600-1609.

79.   Goldberg SB, Gettinger SN, Mahajan A, Chiang AC, Herbst RS, Sznol M, Tsiouris AJ, et al. Pembrolizumab for patients with melanoma or non-small-cell lung cancer and untreated brain metastases: early analysis of a non-randomised, open-label, phase 2 trial. Lancet Oncol 2016;17:976-983.

80.   Calderaro J, Rousseau B, Amaddeo G, Mercey M, Charpy C, Costentin C, Luciani A, et al. Programmed death ligand 1 expression in hepatocellular carcinoma: Relationship With clinical and pathological features. Hepatology 2016;64:2038-2046.

81.   Sideras K, Biermann K, Verheij J, Takkenberg BR, Mancham S, Hansen BE, Schutz HM, et al. PD-L1, Galectin-9 and CD8+ tumor-infiltrating lymphocytes are associated with survival in hepatocellular carcinoma. Oncoimmunology 2017;6:e1273309.

82.   Xie QK, Zhao YJ, Pan T, Lyu N, Mu LW, Li SL, Shi MD, et al. Programmed death ligand 1 as an indicator of pre-existing adaptive immune responses in human hepatocellular carcinoma. Oncoimmunology 2016;5:e1181252.

83.   Chen Y, Ramjiawan RR, Reiberger T, Ng MR, Hato T, Huang Y, Ochiai H, et al. CXCR4 inhibition in tumor microenvironment facilitates anti-programmed death receptor-1 immunotherapy in sorafenib-treated hepatocellular carcinoma in mice. Hepatology 2015;61:1591-1602.

84.   Willimsky G, Schmidt K, Loddenkemper C, Gellermann J, Blankenstein T. Virus-induced hepatocellular carcinomas cause antigen-specific local tolerance. J Clin Invest 2013;123:1032-1043.

85.   Wu K, Kryczek I, Chen L, Zou W, Welling TH. Kupffer cell suppression of CD8+ T cells in human hepatocellular carcinoma is mediated by B7-H1/programmed death-1 interactions. Cancer Res 2009;69:8067-8075.

86.   Kuang DM, Zhao Q, Peng C, Xu J, Zhang JP, Wu C, Zheng L. Activated monocytes in peritumoral stroma of hepatocellular carcinoma foster immune privilege and disease progression through PD-L1. J Exp Med 2009;206:1327-1337.

87.   Kuang DM, Xiao X, Zhao Q, Chen MM, Li XF, Liu RX, Wei Y, et al. B7-H1-expressing antigen-presenting cells mediate polarization of protumorigenic Th22 subsets. J Clin Invest 2014;124:4657-4667.

88.   Xiao X, Lao XM, Chen MM, Liu RX, Wei Y, Ouyang FZ, Chen DP, et al. PD-1hi Identifies a Novel Regulatory B-cell Population in Human Hepatoma That Promotes Disease Progression. Cancer Discov 2016;6:546-559.

89.   El-Khoueiry AB, Sangro B, Yau T, Crocenzi TS, Kudo M, Hsu C, Kim TY, et al. Nivolumab in patients with advanced hepatocellular carcinoma (CheckMate 040): an open-label, non-comparative, phase 1/2 dose escalation and expansion trial. Lancet 2017;389:2492-2502.

90.   Wang Y, Li H, Liang Q, Liu B, Mei X, Ma Y. Combinatorial immunotherapy of sorafenib and blockade of programmed death-ligand 1 induces effective natural killer cell responses against hepatocellular carcinoma. Tumour Biol 2015;36:1561-1566.

91.   Li H, Li X, Liu S, Guo L, Zhang B, Zhang J, Ye Q. PD-1 Checkpoint Blockade in Combination with an mTOR Inhibitor Restrains Hepatocellular Carcinoma Growth Induced by Hepatoma Cell-Intrinsic PD-1. Hepatology 2017.

92.   Gani F, Nagarajan N, Kim Y, Zhu Q, Luan L, Bhaijee F, Anders RA, et al. Program Death 1 Immune Checkpoint and Tumor Microenvironment: Implications for Patients With Intrahepatic Cholangiocarcinoma. Ann Surg Oncol 2016;23:2610-2617.

93.   Ye Y, Zhou L, Xie X, Jiang G, Xie H, Zheng S. Interaction of B7-H1 on intrahepatic cholangiocarcinoma cells with PD-1 on tumor-infiltrating T cells as a mechanism of immune evasion. J Surg Oncol 2009;100:500-504.

94.   Ma K, Wei X, Dong D, Wu Y, Geng Q, Li E. PD-L1 and PD-1 expression correlate with prognosis in extrahepatic cholangiocarcinoma. Oncol Lett 2017;14:250-256.

95.   Wang L, Dong H, Ni S, Huang D, Tan C, Chang B, Sheng W. Programmed death-ligand 1 is upregulated in intrahepatic lymphoepithelioma-like cholangiocarcinoma. Oncotarget 2016;7:69749-69759.

96.   Teuber J, Meier S, Aigner K, Helmke K, Paul F, Federlin K. [Immunohistologic determination of a tumor marker (CEA) in diseases of the gastrointestinal tract] Immunhistologischer Nachweis eines Tumormarkers (CEA) bei Erkrankungen des Gastrointestinaltraktes. Immun Infekt 1983;11:91-98.

97.   Fontugne J, Augustin J, Pujals A, Compagnon P, Rousseau B, Luciani A, Tournigand C, et al. PD-L1 expression in perihilar and intrahepatic cholangiocarcinoma. Oncotarget 2017;8:24644-24651.

98.   Walter D, Herrmann E, Schnitzbauer AA, Zeuzem S, Hansmann ML, Peveling-Oberhag J, Hartmann S. PD-L1 expression in extrahepatic cholangiocarcinoma. Histopathology 2017;71:383-392.

99.   Sato Y, Kinoshita M, Takemura S, Tanaka S, Hamano G, Nakamori S, Fujikawa M, et al. The PD-1/PD-L1 axis may be aberrantly activated in occupational cholangiocarcinoma. Pathol Int 2017;67:163-170.

100.   Sangkhamanon S, Jongpairat P, Sookprasert A, Wirasorn K, Titapun A, Pugkhem A, Ungareevittaya P, et al. Programmed Death-Ligand 1 (PD-L1) Expression Associated with a High Neutrophil/Lymphocyte Ratio in Cholangiocarcinoma. Asian Pac J Cancer Prev 2017;18:1671-1674.

101.   Czink E, Kloor M, Goeppert B, Frohling S, Uhrig S, Weber TF, Meinel J, et al. Successful immune checkpoint blockade in a patient with advanced stage microsatellite-unstable biliary tract cancer. Cold Spring Harb Mol Case Stud 2017;3.

102.   Le DT, Uram JN, Wang H, Bartlett BR, Kemberling H, Eyring AD, Skora AD, et al. PD-1 Blockade in Tumors with Mismatch-Repair Deficiency. N Engl J Med 2015;372:2509-2520.

103.   Le DT, Durham JN, Smith KN, Wang H, Bartlett BR, Aulakh LK, Lu S, et al. Mismatch repair deficiency predicts response of solid tumors to PD-1 blockade. Science 2017;357:409-413.

104.   Grady WM, Carethers JM. Genomic and epigenetic instability in colorectal cancer pathogenesis. Gastroenterology 2008;135:1079-1099.

105.   Mlecnik B, Bindea G, Angell HK, Maby P, Angelova M, Tougeron D, Church SE, et al. Integrative Analyses of Colorectal Cancer Show Immunoscore Is a Stronger Predictor of Patient Survival Than Microsatellite Instability. Immunity 2016;44:698-711.

106.   Llosa NJ, Cruise M, Tam A, Wicks EC, Hechenbleikner EM, Taube JM, Blosser RL, et al. The vigorous immune microenvironment of microsatellite instable colon cancer is balanced by multiple counter-inhibitory checkpoints. Cancer Discov 2015;5:43-51.

107.   Vigdorovich V, Ramagopal UA, Lazar-Molnar E, Sylvestre E, Lee JS, Hofmeyer KA, Zang X, et al. Structure and T cell inhibition properties of B7 family member, B7-H3. Structure 2013;21:707-717.

108.   Leitner J, Klauser C, Pickl WF, Stockl J, Majdic O, Bardet AF, Kreil DP, et al. B7-H3 is a potent inhibitor of human T-cell activation: No evidence for B7-H3 and TREML2 interaction. Eur J Immunol 2009;39:1754-1764.

109.   Mahnke K, Ring S, Johnson TS, Schallenberg S, Schonfeld K, Storn V, Bedke T, et al. Induction of immunosuppressive functions of dendritic cells in vivo by CD4+CD25+ regulatory T cells: role of B7-H3 expression and antigen presentation. Eur J Immunol 2007;37:2117-2126.

110.   Suh WK, Gajewska BU, Okada H, Gronski MA, Bertram EM, Dawicki W, Duncan GS, et al. The B7 family member B7-H3 preferentially down-regulates T helper type 1-mediated immune responses. Nat Immunol 2003;4:899-906.

111.   Chapoval AI, Ni J, Lau JS, Wilcox RA, Flies DB, Liu D, Dong H, et al. B7-H3: a costimulatory molecule for T cell activation and IFN-gamma production. Nat Immunol 2001;2:269-274.

112.   Chen C, Shen Y, Qu QX, Chen XQ, Zhang XG, Huang JA. Induced expression of B7-H3 on the lung cancer cells and macrophages suppresses T-cell mediating anti-tumor immune response. Exp Cell Res 2013;319:96-102.

113.   Xu H, Cheung IY, Guo HF, Cheung NK. MicroRNA miR-29 modulates expression of immunoinhibitory molecule B7-H3: potential implications for immune based therapy of human solid tumors. Cancer Res 2009;69:6275-6281.

114.   Seaman S, Zhu Z, Saha S, Zhang XM, Yang MY, Hilton MB, Morris K, et al. Eradication of Tumors through Simultaneous Ablation of CD276/B7-H3-Positive Tumor Cells and Tumor Vasculature. Cancer Cell 2017;31:501-515 e508.

115.   Kang FB, Wang L, Li D, Zhang YG, Sun DX. Hepatocellular carcinomas promote tumor-associated macrophage M2-polarization via increased B7-H3 expression. Oncol Rep 2015;33:274-282.

116.   Kang FB, Wang L, Jia HC, Li D, Li HJ, Zhang YG, Sun DX. B7-H3 promotes aggression and invasion of hepatocellular carcinoma by targeting epithelial-to-mesenchymal transition via JAK2/STAT3/Slug signaling pathway. Cancer Cell Int 2015;15:45.

117.   Sun TW, Gao Q, Qiu SJ, Zhou J, Wang XY, Yi Y, Shi JY, et al. B7-H3 is expressed in human hepatocellular carcinoma and is associated with tumor aggressiveness and postoperative recurrence. Cancer Immunol Immunother 2012;61:2171-2182.

118.   Wang F, Wang G, Liu T, Yu G, Zhang G, Luan X. B7-H3 was highly expressed in human primary hepatocellular carcinoma and promoted tumor progression. Cancer Invest 2014;32:262-271.

119.   Wang F, Yu G, Liu T, Wang G, Yang J, Zhang G, Luan X. [Expression and clinical significance of soluble B7-H3 in sera of patients with primary hepatocellular carcinoma]. Xi Bao Yu Fen Zi Mian Yi Xue Za Zhi 2013;29:629-632.

120.   Ni L, Dong C. New checkpoints in cancer immunotherapy. Immunol Rev 2017;276:52-65.

121.   Wada ST, M; Watanabe, A; Kubo, N; Araki, K; Suzuki, H; Kuwano, H. Analysis of the immune suppression mechanism in extra-hepatic cholangiocarcinoma. Proceedings of the 106th Annual Meeting of the American Association for Cancer Research 2015;75.

122.   Wang X, Hao J, Metzger DL, Ao Z, Chen L, Ou D, Verchere CB, et al. B7-H4 Treatment of T Cells Inhibits ERK, JNK, p38, and AKT Activation. PLoS One 2012;7:e28232.

123.   Sica GL, Choi IH, Zhu G, Tamada K, Wang SD, Tamura H, Chapoval AI, et al. B7-H4, a molecule of the B7 family, negatively regulates T cell immunity. Immunity 2003;18:849-861.

124.   Mao YX, Chen YJ, Ge Y, Ma HB, Yu JF, Wu HY, Hu YM, et al. Recombinant human B7-H4 expressed in Escherichia coli inhibits T lymphocyte proliferation and IL-2 secretion in vitro. Acta Pharmacol Sin 2006;27:741-746.

125.   Ou D, Wang X, Metzger DL, Ao Z, Pozzilli P, James RF, Chen L, et al. Suppression of human T-cell responses to beta-cells by activation of B7-H4 pathway. Cell Transplant 2006;15:399-410.

126.   Choi IH, Zhu G, Sica GL, Strome SE, Cheville JC, Lau JS, Zhu Y, et al. Genomic organization and expression analysis of B7-H4, an immune inhibitory molecule of the B7 family. J Immunol 2003;171:4650-4654.

127.   Lee JS, Scandiuzzi L, Ray A, Wei J, Hofmeyer KA, Abadi YM, Loke P, et al. B7x in the periphery abrogates pancreas-specific damage mediated by self-reactive CD8 T cells. J Immunol 2012;189:4165-4174.

128.   Kryczek I, Wei S, Zou L, Zhu G, Mottram P, Xu H, Chen L, et al. Cutting edge: induction of B7-H4 on APCs through IL-10: novel suppressive mode for regulatory T cells. J Immunol 2006;177:40-44.

129.   Kryczek I, Wei S, Zhu G, Myers L, Mottram P, Cheng P, Chen L, et al. Relationship between B7-H4, regulatory T cells, and patient outcome in human ovarian carcinoma. Cancer Res 2007;67:8900-8905.

130.   Xu JF, Xiao H, Hu GY, Zheng SH, Liu W, Yuan CL, Yang H, et al. Ectopic B7-H4-Ig expression attenuates concanavalin A-induced hepatic injury. Clin Immunol 2010;136:30-41.

131.   Yuan L, Dong L, Yu G, Fan W, Zhang L, Wang P, Hu X, et al. Aberrant expression of B7H4 may contribute to the development of hepatocellular carcinoma. Mol Med Rep 2016;14:5015-5024.

132.   Kang FB, Wang L, Sun DX, Li HJ, Li D, Wang Y, Kang JW. B7-H4 overexpression is essential for early hepatocellular carcinoma progression and recurrence. Oncotarget 2017;8:80878-80888.

133.   Hong B, Qian Y, Zhang H, Sang YW, Cheng LF, Wang Q, Gao S, et al. Expression of B7-H4 and hepatitis B virus X in hepatitis B virus-related hepatocellular carcinoma. World J Gastroenterol 2016;22:4538-4546.

134.   Cui L, Gao B, Cao Z, Chen X, Zhang S, Zhang W. Downregulation of B7-H4 in the MHCC97-H hepatocellular carcinoma cell line by arsenic trioxide. Mol Med Rep 2016;13:2032-2038.

135.   Zhang C, Li Y, Wang Y. Diagnostic value of serum B7-H4 for hepatocellular carcinoma. J Surg Res 2015;197:301-306.

136.   Zhang SA, Wu ZX, Zhang X, Zeng ZY, Li DL. Circulating B7-H4 in serum predicts prognosis in patients with hepatocellular carcinoma. Genet Mol Res 2015;14:13041-13048.

137.   Dangaj D, Lanitis E, Zhao A, Joshi S, Cheng Y, Sandaltzopoulos R, Ra HJ, et al. Novel recombinant human b7-h4 antibodies overcome tumoral immune escape to potentiate T-cell antitumor responses. Cancer Res 2013;73:4820-4829.

138.   Zhao X, Guo F, Li Z, Jiang P, Deng X, Tian F, Li X, et al. Aberrant expression of B7-H4 correlates with poor prognosis and suppresses tumor-infiltration of CD8+ T lymphocytes in human cholangiocarcinoma. Oncol Rep 2016;36:419-427.

139.   Zhao R, Chinai JM, Buhl S, Scandiuzzi L, Ray A, Jeon H, Ohaegbulam KC, et al. HHLA2 is a member of the B7 family and inhibits human CD4 and CD8 T-cell function. Proc Natl Acad Sci U S A 2013;110:9879-9884.

140.   Wang JH, Manick B, Wu GP, Hao RY. Biofunctions of three new B7 family members. Journal of Immunology 2014;192.

141.   Zhu Y, Yao S, Iliopoulou BP, Han X, Augustine MM, Xu H, Phennicie RT, et al. B7-H5 costimulates human T cells via CD28H. Nat Commun 2013;4:2043.

142.   Xiao Y, Freeman GJ. A New B7:CD28 Family Checkpoint Target for Cancer Immunotherapy: HHLA2. Clin Cancer Res 2015;21:2201-2203.

143.   Janakiram M, Chinai JM, Fineberg S, Fiser A, Montagna C, Medavarapu R, Castano E, et al. Expression, Clinical Significance, and Receptor Identification of the Newest B7 Family Member HHLA2 Protein. Clin Cancer Res 2015;21:2359-2366.

144.   Chen L, Flies DB. Molecular mechanisms of T cell co-stimulation and co-inhibition. Nat Rev Immunol 2013;13:227-242.

145.   Huang YH, Zhu C, Kondo Y, Anderson AC, Gandhi A, Russell A, Dougan SK, et al. CEACAM1 regulates TIM-3-mediated tolerance and exhaustion. Nature 2015;517:386-390.

146.   Yan J, Zhang Y, Zhang JP, Liang J, Li L, Zheng L. Tim-3 expression defines regulatory T cells in human tumors. PLoS One 2013;8:e58006.

147.   Moorman JP, Wang JM, Zhang Y, Ji XJ, Ma CJ, Wu XY, Jia ZS, et al. Tim-3 pathway controls regulatory and effector T cell balance during hepatitis C virus infection. J Immunol 2012;189:755-766.

148.   Barathan M, Gopal K, Mohamed R, Ellegard R, Saeidi A, Vadivelu J, Ansari AW, et al. Chronic hepatitis C virus infection triggers spontaneous differential expression of biosignatures associated with T cell exhaustion and apoptosis signaling in peripheral blood mononucleocytes. Apoptosis 2015;20:466-480.

149.   Li H, Wu K, Tao K, Chen L, Zheng Q, Lu X, Liu J, et al. Tim-3/galectin-9 signaling pathway mediates T-cell dysfunction and predicts poor prognosis in patients with hepatitis B virus-associated hepatocellular carcinoma. Hepatology 2012;56:1342-1351.

150.   Yan W, Liu X, Ma H, Zhang H, Song X, Gao L, Liang X, et al. Tim-3 fosters HCC development by enhancing TGF-beta-mediated alternative activation of macrophages. Gut 2015.

151.   Anderson AC, Joller N, Kuchroo VK. Lag-3, Tim-3, and TIGIT: Co-inhibitory Receptors with Specialized Functions in Immune Regulation. Immunity 2016;44:989-1004.

152.   Nguyen LT, Ohashi PS. Clinical blockade of PD1 and LAG3--potential mechanisms of action. Nat Rev Immunol 2015;15:45-56.

153.   Andrews LP, Marciscano AE, Drake CG, Vignali DA. LAG3 (CD223) as a cancer immunotherapy target. Immunol Rev 2017;276:80-96.

154.   Goldberg MV, Drake CG. LAG-3 in Cancer Immunotherapy. Curr Top Microbiol Immunol 2011;344:269-278.

155.   Woo SR, Turnis ME, Goldberg MV, Bankoti J, Selby M, Nirschl CJ, Bettini ML, et al. Immune inhibitory molecules LAG-3 and PD-1 synergistically regulate T-cell function to promote tumoral immune escape. Cancer Res 2012;72:917-927.

156.   Waugh KA, Leach SM, Moore BL, Bruno TC, Buhrman JD, Slansky JE. Molecular Profile of Tumor-Specific CD8+ T Cell Hypofunction in a Transplantable Murine Cancer Model. J Immunol 2016;197:1477-1488.

157.   Matsuzaki J, Gnjatic S, Mhawech-Fauceglia P, Beck A, Miller A, Tsuji T, Eppolito C, et al. Tumor-infiltrating NY-ESO-1-specific CD8+ T cells are negatively regulated by LAG-3 and PD-1 in human ovarian cancer. Proc Natl Acad Sci U S A 2010;107:7875-7880.

158.   Li FJ, Zhang Y, Jin GX, Yao L, Wu DQ. Expression of LAG-3 is coincident with the impaired effector function of HBV-specific CD8(+) T cell in HCC patients. Immunol Lett 2013;150:116-122.

159.   Yarchoan M, Xing D, Luan L, Xu H, Sharma R, Popovic A, Pawlik TM, et al. Characterization of the Immune Microenvironment in Hepatocellular Carcinoma (HCC). Clin Cancer Res 2017.

160.   Xu F, Liu J, Liu D, Liu B, Wang M, Hu Z, Du X, et al. LSECtin expressed on melanoma cells promotes tumor progression by inhibiting antitumor T-cell responses. Cancer Res 2014;74:3418-3428.

161.   Liu W, Tang L, Zhang G, Wei H, Cui Y, Guo L, Gou Z, et al. Characterization of a novel C-type lectin-like gene, LSECtin: demonstration of carbohydrate binding and expression in sinusoidal endothelial cells of liver and lymph node. J Biol Chem 2004;279:18748-18758.

162.   Le Mercier I, Lines JL, Noelle RJ. Beyond CTLA-4 and PD-1, the Generation Z of Negative Checkpoint Regulators. Front Immunol 2015;6:418.

163.   Hokuto D, Sho M, Yamato I, Yasuda S, Obara S, Nomi T, Nakajima Y. Clinical impact of herpesvirus entry mediator expression in human hepatocellular carcinoma. Eur J Cancer 2015;51:157-165.

164.   Zhao Q, Huang ZL, He M, Gao Z, Kuang DM. BTLA identifies dysfunctional PD-1-expressing CD4(+) T cells in human hepatocellular carcinoma. Oncoimmunology 2016;5:e1254855.

165.   Wu Y, Kuang DM, Pan WD, Wan YL, Lao XM, Wang D, Li XF, et al. Monocyte/macrophage-elicited natural killer cell dysfunction in hepatocellular carcinoma is mediated by CD48/2B4 interactions. Hepatology 2013;57:1107-1116.

166.   Joller N, Lozano E, Burkett PR, Patel B, Xiao S, Zhu C, Xia J, et al. Treg cells expressing the coinhibitory molecule TIGIT selectively inhibit proinflammatory Th1 and Th17 cell responses. Immunity 2014;40:569-581.

167.   Gur C, Ibrahim Y, Isaacson B, Yamin R, Abed J, Gamliel M, Enk J, et al. Binding of the Fap2 protein of Fusobacterium nucleatum to human inhibitory receptor TIGIT protects tumors from immune cell attack. Immunity 2015;42:344-355.

168.   Zhu Y, Paniccia A, Schulick AC, Chen W, Koenig MR, Byers JT, Yao S, et al. Identification of CD112R as a novel checkpoint for human T cells. J Exp Med 2016;213:167-176.

169.   Martinet L, Smyth MJ. Balancing natural killer cell activation through paired receptors. Nat Rev Immunol 2015;15:243-254.

170.   Johnston RJ, Comps-Agrar L, Hackney J, Yu X, Huseni M, Yang Y, Park S, et al. The immunoreceptor TIGIT regulates antitumor and antiviral CD8(+) T cell effector function. Cancer Cell 2014;26:923-937.

171.   Chauvin JM, Pagliano O, Fourcade J, Sun Z, Wang H, Sander C, Kirkwood JM, et al. TIGIT and PD-1 impair tumor antigen-specific CD8(+) T cells in melanoma patients. J Clin Invest 2015;125:2046-2058.

172.   Huang DW, Huang M, Lin XS, Huang Q. CD155 expression and its correlation with clinicopathologic characteristics, angiogenesis, and prognosis in human cholangiocarcinoma. Onco Targets Ther 2017;10:3817-3825.

173.   Chan CJ, Martinet L, Gilfillan S, Souza-Fonseca-Guimaraes F, Chow MT, Town L, Ritchie DS, et al. The receptors CD96 and CD226 oppose each other in the regulation of natural killer cell functions. Nat Immunol 2014;15:431-438.

174.   Lines JL, Pantazi E, Mak J, Sempere LF, Wang L, O'Connell S, Ceeraz S, et al. VISTA is an immune checkpoint molecule for human T cells. Cancer Res 2014;74:1924-1932.

175.   Wang L, Le Mercier I, Putra J, Chen W, Liu J, Schenk AD, Nowak EC, et al. Disruption of the immune-checkpoint VISTA gene imparts a proinflammatory phenotype with predisposition to the development of autoimmunity. Proc Natl Acad Sci U S A 2014;111:14846-14851.

176.   Wang L, Rubinstein R, Lines JL, Wasiuk A, Ahonen C, Guo Y, Lu LF, et al. VISTA, a novel mouse Ig superfamily ligand that negatively regulates T cell responses. J Exp Med 2011;208:577-592.

177.   Flies DB, Han X, Higuchi T, Zheng L, Sun J, Ye JJ, Chen L. Coinhibitory receptor PD-1H preferentially suppresses CD4(+) T cell-mediated immunity. J Clin Invest 2014;124:1966-1975.

178.   Le Mercier I, Chen W, Lines JL, Day M, Li J, Sergent P, Noelle RJ, et al. VISTA Regulates the Development of Protective Antitumor Immunity. Cancer Res 2014;74:1933-1944.

179.   Lines JL, Sempere LF, Broughton T, Wang L, Noelle R. VISTA is a novel broad-spectrum negative checkpoint regulator for cancer immunotherapy. Cancer Immunol Res 2014;2:510-517.

180.   Liu J, Yuan Y, Chen W, Putra J, Suriawinata AA, Schenk AD, Miller HE, et al. Immune-checkpoint proteins VISTA and PD-1 nonredundantly regulate murine T-cell responses. Proc Natl Acad Sci U S A 2015;112:6682-6687.

181.   Sanmamed MF, Pastor F, Rodriguez A, Perez-Gracia JL, Rodriguez-Ruiz ME, Jure-Kunkel M, Melero I. Agonists of Co-stimulation in Cancer Immunotherapy Directed Against CD137, OX40, GITR, CD27, CD28, and ICOS. Semin Oncol 2015;42:640-655.

182.   Ryschich E, Marten A, Schmidt E, Linnebacher M, Wentzensen N, Eisold S, Klar E, et al. Activating anti-CD40 antibodies induce tumour invasion by cytotoxic T-lymphocytes and inhibition of tumour growth in experimental liver cancer. Eur J Cancer 2006;42:981-987.

183.   Gauttier V, Judor JP, Le Guen V, Cany J, Ferry N, Conchon S. Agonistic anti-CD137 antibody treatment leads to antitumor response in mice with liver cancer. Int J Cancer 2014;135:2857-2867.

184.   Morales-Kastresana A, Sanmamed MF, Rodriguez I, Palazon A, Martinez-Forero I, Labiano S, Hervas-Stubbs S, et al. Combined immunostimulatory monoclonal antibodies extend survival in an aggressive transgenic hepatocellular carcinoma mouse model. Clin Cancer Res 2013;19:6151-6162.

185.   Platten M, Wick W, Van den Eynde BJ. Tryptophan catabolism in cancer: beyond IDO and tryptophan depletion. Cancer Res 2012;72:5435-5440.

186.   Zhai L, Spranger S, Binder DC, Gritsina G, Lauing KL, Giles FJ, Wainwright DA. Molecular Pathways: Targeting IDO1 and Other Tryptophan Dioxygenases for Cancer Immunotherapy. Clin Cancer Res 2015;21:5427-5433.

187.   Zhao Q, Kuang DM, Wu Y, Xiao X, Li XF, Li TJ, Zheng L. Activated CD69+ T cells foster immune privilege by regulating IDO expression in tumor-associated macrophages. J Immunol 2012;188:1117-1124.

188.   Li T, Yang Y, Hua X, Wang G, Liu W, Jia C, Tai Y, et al. Hepatocellular carcinoma-associated fibroblasts trigger NK cell dysfunction via PGE2 and IDO. Cancer Lett 2012;318:154-161.

189.   Huang TT, Yen MC, Lin CC, Weng TY, Chen YL, Lin CM, Lai MD. Skin delivery of short hairpin RNA of indoleamine 2,3 dioxygenase induces antitumor immunity against orthotopic and metastatic liver cancer. Cancer Sci 2011;102:2214-2220.

190.   Opitz CA, Litzenburger UM, Sahm F, Ott M, Tritschler I, Trump S, Schumacher T, et al. An endogenous tumour-promoting ligand of the human aryl hydrocarbon receptor. Nature 2011;478:197-203.

191.   Pilotte L, Larrieu P, Stroobant V, Colau D, Dolusic E, Frederick R, De Plaen E, et al. Reversal of tumoral immune resistance by inhibition of tryptophan 2,3-dioxygenase. Proc Natl Acad Sci U S A 2012;109:2497-2502.

192.   Guzman A, Ziperstein MJ, Kaufman LJ. The effect of fibrillar matrix architecture on tumor cell invasion of physically challenging environments. Biomaterials 2014;35:6954-6963.

193.   Baker EL, Srivastava J, Yu D, Bonnecaze RT, Zaman MH. Cancer cell migration: integrated roles of matrix mechanics and transforming potential. PLoS One 2011;6:e20355.

194.   Salmon H, Franciszkiewicz K, Damotte D, Dieu-Nosjean MC, Validire P, Trautmann A, Mami-Chouaib F, et al. Matrix architecture defines the preferential localization and migration of T cells into the stroma of human lung tumors. J Clin Invest 2012;122:899-910.

PART I

Regulation of intra-tumoral suppressor T cells in liver cancers

CHAPTER 2

GITR engagement in combination with CTLA-4 blockade completely abrogates immunosuppression mediated by human liver tumor-derived regulatory T cells *ex vivo*

Alexander Pedroza-Gonzalez[1, 4], **Guoying Zhou[1],** Simar Pal Singh[1], Patrick P.C. Boor[1], Qiuwei Pan[1], Dirk Grunhagen[2], Jeroen de Jonge[2], T C Khe Tran[2], Cornelis Verhoef[2], Jan NM IJzermans[2], Harry L.A. Janssen[1], Katharina Biermann[3], Jaap Kwekkeboom[1] and Dave Sprengers[1]

[1]Department of Gastroenterology and Hepatology, [2]Department of Surgery and [3]Department of Pathology, Erasmus MC-University Medical Center, Rotterdam, the Netherlands. [4]Laboratory of Immunology Research, Medicine, Faculty of Higher Studies Iztacala, National Autonomous University of Mexico (FES-Iztacala, UNAM), Mexico.

ABSTRACT

In liver cancer tumor-infiltrating regulatory T cells (Ti-Treg) are potent suppressors of tumor-specific T-cell responses and express high levels of the Treg-associated molecules cytotoxic T lymphocyte-associated antigen 4 (CTLA-4) and glucocorticoid-induced tumor necrosis factor receptor (GITR). In this study, we have evaluated the capacity of GITR-ligation, CTLA-4-blockade and a combination of both treatments to alleviate immunosuppression mediated by Ti-Treg. Using *ex vivo* isolated cells from individuals with hepatocellular carcinoma (HCC) or liver metastases from colorectal cancer (LM-CRC) we show that treatment with a soluble form of the natural ligand of GITR (GITRL), or with blocking antibodies to CTLA-4, reduces the suppression mediated by human liver tumor-infiltrating CD4+Foxp3+ Treg, thereby restoring proliferation and cytokine production by effector T cells. Importantly, combined treatment with low doses of both molecules exhibited stronger recovery of T cell function compared with either treatment alone. Our data suggest that in patients with primary and secondary liver cancer both GITR-ligation and anti-CTLA-4 mAb can improve the anti-tumor immunity by abrogating tumor-infiltrating Treg mediated suppression.

Keywords: Hepatocellular carcinoma (HCC), liver metastases from colorectal cancer (LM-CRC), regulatory T cells (Treg), cytotoxic T lymphocyte-associated antigen 4 (CTLA-4) and glucocorticoid-induced tumor necrosis factor receptor (GITR).

Introduction

Hepatocellular carcinoma, the sixth most frequent tumor in the world [1] and the third most common cause of cancer-related death, [2] is an aggressive tumor with poor prognosis. HCC accounts for most of primary liver malignancies. However colorectal cancer (CRC), the third most common cancer worldwide, commonly metastasizes to the liver, which is the leading cause of CRC mortality. [3, 4] The current therapeutic options for HCC and liver metastasis from CRC (LM-CRC) include surgery (resection and liver transplantation) and local (ablative) therapy. Unfortunately, less than 20% of HCC patients are eligible for curative procedures [5] because most of them have advanced disease at the time of diagnosis. Furthermore, over 50% of LM-CRC patients that undergo surgery develop recurrence within 2 years. [6, 7] Chemotherapy has showed limited efficacy and provides a survival advantage of only 2.3-2.8 months in advanced HCC. [8, 9] An attractive alternative to these current therapeutic options is immunotherapy, which is based on the sensitivity, specificity and memory of the immune system. However, immune regulation in the liver and tumor environment may contribute to tumor outgrowth and limit the efficacy of immunotherapeutic strategies. [10, 11] In support of this we and others have described the presence of regulatory CD4+Foxp3+ T cells in liver tumors, that suppress local anti-tumor immunity and that are associated with poor patient prognosis. [12-16] Liver Ti-Treg are characterized by high expression of glucocorticoid-induced tumor necrosis factor receptor related gene (GITR), cytotoxic T lymphocyte-associated antigen 4 (CTLA-4) and inducible T cell co-stimulator (ICOS). [12] These molecules are important for the immunosuppressive function of Treg and can be targets for immunotherapeutic interventions. Abrogation of Ti-Treg function may allow the induction of anti-tumor immunity at the tumor site and improve the outcome of immunotherapy aimed to activate anti-tumor responses. In advanced melanoma, CTLA-4-blocking has demonstrated a survival advantage [17, 18] and CTLA-4-blockade was shown to induce antiviral immunity in HCC-patients infected with hepatitis C virus (HCV). [19] However, only limited tumor-responses were reported, emphasizing the need to improve this strategy. Combining several candidate-immunomodulators may achieve synergistic immunoregulatory activity.

In this study we have evaluated *ex vivo* the capacity of GITR-ligation, CTLA-4-blockade and a combination of both to alleviate immunosuppression mediated by Ti-Treg isolated from patients with primary and secondary liver cancer.

Results

GITR⁺CTLA-4⁺ Treg accumulate in liver tumors and have an increased suppressive capacity

In order to confirm our previous finding showing that activated CD4+Foxp3+Treg are sequestered at the liver tumor site, we analyzed Treg in lymphocytes isolated from fresh liver tumors, tumor-free liver (TFL) tissues, and peripheral blood (PB) in a new cohort of HCC and LM-CRC patients by flow cytometry. Treg were present in all the three compartments analyzed, but were significantly more concentrated in the tumor areas compared with TFL (p = 0.0004) and blood (p < 0.0001) (Fig. 1A). We also corroborate in this new cohort that Ti-Treg are more suppressive than circulating Treg by analyzing their impact on T cell proliferation of autologous CD4+CD25- T cells stimulated with CMV-activated dendritic cells (DC). Ti-Treg showed a stronger suppression of T cell proliferation compared with blood Treg (p = 0.0005) (Fig. 1B). In addition, we analyzed the surface expression level of GITR and intracellular expression of CTLA-4 (Figure 1C). GITR expression was significantly higher on tumor Treg than on Treg isolated from TFL (p = 0.0005) and blood (p = 0.0002). Tumor Treg were also distinguishable from blood and TFL Treg by their elevated intracellular expression of CTLA-4, which is a key negative regulator of T-cell activation (p = 0.0004 and 0.0018 respectively). Moreover, we found that a big proportion of Ti-Treg expressed both molecules, in contrast with blood or TFL derived Tregs that have a very low proportion of double positive cells (Figure 1D). Thus, Ti-Treg derived from liver tumors express high levels of GITR and CTLA-4 and have an enhanced suppressive capacity.

GITR engagement reduces suppressive capacity of Ti-Treg

Soluble GITRL (sGITRL) was able to lower T cell suppression by Ti-Treg derived from liver tumors of patients with HCC or LM-CRC (Figure 2). CD4+CD25- effector T cells proliferated robustly in response to autologous DC activated with CMV. This proliferative response, as well as the production of TNFα was not affected by the addition of 10 or 20 µg/ml of sGITRL. However, GITRL induced an increased amount of IFNγ suggesting a limited direct effect on CD4+CD25- T cells. CMV-specific T cell proliferation and cytokine production were inhibited by Ti-Treg derived from both groups of patients (Figure 2A). Importantly, the addition of 10 µg/ml of sGITRL significantly reduced the suppression mediated by Ti-Treg on CMV-specific T cells, recovering both T-cell proliferation (57 ± 17 % vs 69 ± 20 % proliferating CD4+ T cells, p = 0.0005) and cytokine production by proliferating cells (TNFα: 42 ± 25 % vs 63 ± 28 %, p < 0.0001; IFNγ: 44 ± 24 % vs 80 ± 37 %, p = 0.0001) (Figure 2A-B). However, 10 µg/ml of sGITRL did not abrogate suppression of T cell proliferation completely, and a higher dose of sGITRL (20 µg/ml) could not further restore antigen-specific T cell proliferation nor cytokine production (Figure 2 A-B), and induced T cell death instead in most patients investigated (data not shown). Thus, sGITRL is able to partially decrease T cell suppression mediated by Ti-Treg isolated from liver cancer patients.

CTLA-4 blockade prevents T cell suppression mediated by Ti-Treg in a dose-dependent manner

To address the impact of CTLA-4 in the suppression mediated by Ti-Treg we used a neutralizing antibody for CTLA-4 in our in vitro model of T cell proliferation. The anti-CTLA-4 antibody at a concentration of 10 µg/ml did not affect T cell proliferation or TNFα and IFNγ production in the absence of Treg, however treatment with 20 µg/ml of anti-CTLA-4 antibody induced an increase in the production of IFNγ (Figure 3B), suggesting a direct effect of this antibody on CD4+CD25- effector T cells at this concentration. Anti-CTLA-4 treatment reduced the suppression mediated by Ti-Treg in a dose-dependent manner (Figure 3A). Recovery of T cell function was observed in both T-cell proliferation (52.8 ± 22.5 % when Ti-Treg were present vs 69.3 ± 23 % in the presence of Ti-Treg and 10 µg/ml of anti-CTLA-4, p = 0.008, vs 78.6 ± 19.9 % with 20 µg/ml of anti-CTLA-4 antibody, p = 0.008) and cytokine production by proliferating cells (TNFα: 43 ± 23 % in the presence of Ti-Treg vs 67 ± 18 % with Ti-Treg and 10 µg/ml of anti-CTLA-4 antibody, p = 0.025, and 83 ± 42 % with Ti-Treg and 20 µg/ml of anti-CTLA-4 antibody, p = 0.008; IFNγ: 44 ± 26 % vs 59 ± 33 %, p = 0.48, vs 101 ± 69 %, p = 0.014, respectively) (Figure 3 A-B). Because T cell proliferation was not recovered completely with 20 µg/ml of anti-CTLA-4 antibody, as opposed to (near) full recovery of cytokine production, we were interested in investigating the effect of increasing the concentration of anti-CTLA-4 antibody further. Therefore, another set of antibody blocking experiments was performed with 40 and 80 µg/ml of anti-CTLA-4 antibody, which showed that higher concentrations of the neutralizing antibody for CTLA-4 resulted in complete recovery of T cell proliferation (Figure 4).

GITRL and anti-CTLA-4 antibody combination additively abolish T cell suppression mediated by Ti-Treg

We next asked whether a low dose of GITRL combined with a low dose of neutralizing anti-CTLA-4 antibody could fully recover T cell function in the presence of Ti-Treg. Blood derived CFSE-labeled CD4+CD25- stimulated with autologous DC activated with CMV were cultured in the presence of Ti-Treg and treated with 10 µg/ml of GITRL and anti-CTLA-4 antibody, either as monotherapy or in combination. Monotherapy with GITRL or anti CTLA-4 antibody induced partial recovery of T cell proliferation and cytokine production as observed in the experiments mentioned above (Figure 5, 2 and 3). In comparison with the effect of each treatment alone, the combination of low doses of anti-CTLA-4 and GITRL resulted in marked enhancement of T cell proliferation and cytokine production (Figure 5 A-B). Importantly, the combination of low doses of both molecules provided similar effects as those observed with a

high dose of anti-CTLA-4 antibody, restoring T cell proliferation and TNFα production completely.

Combination of GITRL and anti-CTLA-4 antibody restored tumor-specific T cell response.

To investigate whether the combination of GITRL and anti-CTLA-4 antibody is able to reestablish tumor-specific T cell responses, we used blood derived CFSE-labeled CD4+CD25- T cells stimulated with DC cultured with Tumor Lysates (TL-DC). Cells were co-cultured in the presence of Ti-Treg and treated with 10 μg/ml of GITRL and 10 μg/ml of anti-CTLA-4 antibody. All cell types and the TL were autologous. After one week of culture we observed that Ti-Treg suppressed efficiently cell proliferation and cytokine production of T cells against TL (Figure 6). However when the cells were treated with both GITRL and anti-CTLA-4 antibodies the tumor specific response can be completely restored.

Discussion

New treatment modalities are required to prolong survival in patients with liver cancer. Immunotherapy is an attractive option for HCC patients and patients with liver metastasis of CRC because increasing evidence suggests that immune responses play an important role in the control of these types of cancer. It has been reported that the composition of the tumor infiltrating lymphocytes (TILs) is associated with the prognosis of both diseases, for example increased numbers of Treg are correlated with disease progression [20-24] and recurrence. [25] Furthermore Treg frequencies have been associated with increased numbers of intra-tumoral macrophages, [13, 26] circulating myeloid-derived suppressor cells (MDSC), [27] and with a compromised CD8 T cell response. [14, 15] Altogether these observations suggest that depletion or inhibition of Treg and concomitant stimulation of effector cells may be effective to reduce recurrence and prolong survival in patients with liver cancer. Indeed, depletion of CD25+ T cells in patients or animals models can result in induction of tumor-specific responses. [28, 29] Moreover, in a small clinical trial in advanced HCC patients, treatment with low doses of cyclophosphamide resulted in reduced numbers of Treg and unmasking of circulating tumor-specific CD4+ T cell responses. [30]

We previously reported the presence of highly activated CD4+Foxp3+ Treg in liver tumors of individuals with HCC or LM-CRC. [12] These tumor-infiltrating Treg are characterized by the expression of high levels of GITR and CTLA-4, which are important molecules for their regulatory function and which can be targets for immunotherapy. [12, 16] GITR activation by its ligand acts as a co-stimulatory molecule for effector T cells that confers them less

susceptible to Treg mediated suppression, whereas engagement of GITR expressed by Treg transiently inhibits their suppressive capacity (reviewed in [31]). The GITR agonist antibody DTA-1 represents a very effective antitumor therapy in murine tumor models by increasing antitumor CD4+ and CD8+ T-cell effector functions as well as destabilizing and causing apoptosis of Tregs in the tumor microenvironment. [32, 33] Importantly, our findings support a role for GITR engagement as (part of) an immunotherapy for liver cancer patients, since treatment with sGITRL reduced Treg mediated inhibition of T cell functions. However, the observed effect was only partial and could not be enhanced by dose escalation. Indeed, a high dose of sGITRL had a cytotoxic effect on effector T cells in our in vitro system. In preclinical animal models, treatment with agonistic antibodies for GITR has been shown to cause anaphylaxis upon repeated doses. [34] These observations warrant careful design and dosing strategies of drugs engaging GITR to prevent serious side effects during immunotherapy for patients with liver tumors.

On the other hand, CTLA-4 is constitutively expressed at high levels in CD4+Foxp3+ Treg and is a negative regulator of T-cell activation. By binding the B7 molecules CD80 and CD86, CLTA-4 reduces the T-cell stimulatory capacity of antigen-presenting cells such as dendritic cells (DC). [35] Therefore, by using monoclonal antibodies (mAb) which block CTLA-4, it is possible to alleviate inhibition of DC function by Treg and thereby restore conventional T-cell proliferation after activation. [36] Recent studies have demonstrated that anti-CTLA-4 mAb administration augments clinical anti-tumor responses and improves survival in patients with metastatic melanoma [18, 37] resulting in FDA approval of Ipilimumab, an anti-CTLA-4 antibody, for the treatment of unresectable or metastatic melanoma. The promising clinical activity of anti-CTLA-4 mAb in melanoma encourages to explore its therapeutic applicability in other malignancies, especially because it does not require specific targets expressed on tumor cells. However, there is scarce evidence for efficacy in liver cancer. Only one clinical trial using the anti-CTLA-4 mAb tremelimumab in HCC patients infected with HCV has been conducted, but it showed a partial tumor response in merely 17% of patients. [19] Even though the clinical response was limited, the results point to a potential use for anti-CTLA-4 mAb in immunotherapeutic regimens for these patients. In our study 20 µg/ml of anti-CTLA-4 antibody (BNI3) showed a 60% recovery of T cell proliferation, whereas a concentration of 10 µg/ml only provided a recovery of 35% of T cell proliferation. Higher doses were able to recover T cell functions completely. However, therapy with anti-CTLA-4 mAb ipilimumab has induced life-threatening adverse events, [17, 38, 39] which is a major limitation in exploring higher doses for the treatment. The current clinically approved dosing for anti-CTLA-4 antibody (Ipilimumab) is 3 mg/kg which results in a steady state serum concentration (Cmin) of about

10 µg/ml, [18, 40] and an overall response rate of 4% in patients with advanced melanoma with 3% of patients experiencing severe immune-related adverse events. A higher dose of Ipilimumab of 10 mg/kg (Cmin 32 µg/ml) showed a better response rate of 11% but also higher frequency (15%) of severe adverse events. [18]

Based upon results from murine models, it has previously been suggested that GITR stimulation and CTLA-4 inhibition can be combined to enhance the induction of immune responses and might even work synergistically. [41] Importantly, combination of low doses of anti-CTLA-4 antibody and GITRL resulted in a complete recovery of *in vitro* T cell proliferation and TNFα production. Even though the mechanisms by which these molecules exert their immunomodulatory effects is still elusive, it has been suggested that they can act either by abrogating the immunosuppressive function of Treg or by rendering effector T cells resistant to Treg mediated suppression. In our experiments we observed that both molecules had limited direct effects on effector T cells, only inducing an increase in the production of IFNγ, but this effect was not evident for TNFα and T cell proliferation, suggesting that both mechanisms can play a role in abrogation of the suppression mediated by Ti-Treg. It remains to be seen whether combination therapy of anti-CTLA-4 mAb and GITRL has a more beneficial safety profile compared to treatment with a high dose of either compound alone, but our data show that the combination of both treatments at low doses exhibited stronger inhibition of *ex vivo* Treg-mediated suppression compared with either treatment alone, suggesting that this combination may be more effective to induce anti-tumor immunity in patients with liver cancer.

In conclusion our data suggest that in patients with primary and secondary liver cancer both GITR-ligation and anti-CTLA-4 mAb can improve antigen-specific T cell responses in the tumors by protecting against tumor-infiltrating Treg mediated suppression of their function. However, as part of an immunotherapeutic strategy, combining low doses of both drugs may be at least as effective as monotherapy with higher doses of either of the drugs.

Materials and Methods

Patients

Between June 2011 and November 2013 a total of 28 individuals who were eligible for surgical resection of HCC (n=10) or LM-CRC (n=18) were enrolled. Paired samples of fresh liver tumor tissue and tumor-free liver tissue (TFL) obtained at the maximum distance from the tumor (>1cm), were used for isolating tumor-infiltrating lymphocytes (TILs) and intra-hepatic lymphocytes. In addition, peripheral blood was collected. None of the patients was

treated with chemotherapy or radiation prior to resection. The clinical characteristics of the patients are summarized in table 1. The study was approved by the local ethics committee and all patients in the study gave informed consent before tissue donation.

Cell preparation

Peripheral blood mononuclear cells (PBMC) were isolated by Ficoll density gradient centrifugation. Single cell suspensions from TFL and tumor tissue were obtained by tissue digestion. Fresh tissue was cut into small pieces and digested with 0.5 mg/ml of collagenase (Cat. C5138, Sigma-Aldrich) and 0.2 mg/ml of DNase I (Cat. 10104159001, Roche), for 30 minutes at 37 ºC. Cell suspensions were filtered through 100 and 70 µm pore cell-strainers (BD, biosciences) and mononuclear cells (MNC) were obtained by Ficoll density gradient centrifugation. Viability was determined by trypan blue exclusion.

Flow cytometry analysis

PBMC and MNC isolated from TFL or tumor tissue were analyzed for expression of surface and intracellular markers using the following anti-human antibodies: PE-labeled anti-IFNγ (B27, BD Biosciences) and anti-CD25 (BC96) from ebiosciences; APC-labeled anti-FoxP3 (236A/E7) and anti-TNFa (Mab11) from e-biosciences; APC-H7-labeled anti-CD4 (SK3, BD Biosciences); PeCy7-labeled anti-CD3 (UCTH1); eFluor®450-labeled anti-CD127 (eBioRDR5) from e-biosciences. Cells were incubated with the antibodies 10 min at room temperature in the dark, then washed and fixed with 1% paraformaldehyde. For intracellular cytokine staining, cells were permeabilized using the BD Cytofix/cytoperm fixation/permeabilization kit, and for FoxP3, cells were treated with the FoxP3 staining buffer set from e-biosciences. Dead cells were excluded by using the LIVE/DEAD fixable dead cell stain kit with aqua fluorescent reactive dye (Invitrogen). Cells were analyzed using a FACSCanto II system (BD Biosciences).

Suppression assay

Myeloid dendritic cells (mDC) were isolated from PBMC by positive selection (BDCA-1 DC isolation kit, Cat. 130-090-506, Miltenyi Biotec). mDC were cultured overnight with 10 µg/ml of Cytomegalovirus antigens (CMV, Cat. EL-01-02, Microbix biosystems, Canada). Autologous CD4+CD25- cells were isolated from PBMCs that were kept overnight at 4 ºC in medium supplemented with 10% of bovine fetal serum, by magnetic sorting (Cat. 130-091-301, Miltenyi Biotec). CD4+CD25- T cells were labeled with 0.1 µM of carboxyfluorescein diacetate succinimidyl ester (CFSE, C34554, Invitrogen) and co-cultured with the autologous mDC activated with CMV, at a ratio of 1 to 10 for 5 days in round-bottom 96-well plates with

at least 5 x 10^4 CD4+CD25- T cells. Proliferation was measured by dilution of CFSE. CD4+CD25+ Treg were isolated by magnetic sorting as previously described. [12] Treg were added at 1:5 ratio versus CD4+CD25- T cells, and co-cultured for 5 days. Treg were labeled with CellTrace Violet (Invitrogen) in order to be excluded from proliferating T cells. [12] Furthermore, after co-culture T cells were re-stimulated overnight with autologous monocyte-derived DC activated with CMV, in the presence of brefeldin A and monensin (BD Biosciences). Proliferation and cytokine production were analyzed by flow cytometry and reported as relative proliferation or relative cytokine production where the numbers of proliferating and cytokine-producing cells induced by CMV-DCs were considered 100%. In some experiments azide-free and low endotoxin soluble GITRL (R and D systems, Cat. 6987-GL/CF), anti-CTLA-4 neutralizing (BNI3, Beckman Coulter, Cat. IM2070) or isotype control (IgG2a, Biolegend) antibodies were added to the co-cultures. Monocyte-derived DC were obtained by culturing monocytes with 10 ng/ml IL-4 and 50 ng/ml GM-CSF for 5 days, then immature DC were activated with CMV as described previously for mDC.

Tumor-specific T cell proliferation and suppression assay

Tumor lysates (TL) were generated from freshly dissected tumors by five cycles of freezing and thawing in phosphate buffered saline, followed by filtration (0.2 μm). mDC isolated from PBMC were cultured overnight with media or 20 μg/mL of autologous TL in the presence of 10 ng/mL of granulocyte-macrophage colony-stimulating factor (GM-CSF) (Miltenyi Biotec) and 0.5 μg/mL of polyinosinic:polycytidylic acid (InvivoGen, San Diego, CA). CD4+CD25- cells were isolated from PBMC that were kept overnight at 4ºC in medium supplemented with 10% of bovine fetal serum, by magnetic sorting (Miltenyi Biotec). CD4+CD25- T cells were labeled with 0.1 μM of CFSE (Invitrogen) and co-cultured with autologous mDC cultured with media or TL, at a ratio of 1:10 for 5 days in round-bottom 96-well plates with at least 5 x 10^4 CD4+CD25- T cells. Proliferation was measured by dilution of CFSE. CD4+CD25+ Treg were isolated by magnetic sorting as described above. Treg were added at 1:5 ratio versus CD4+CD25- T cells, and co-cultured for 5 days. Treg were labeled with CellTrace Violet (Invitrogen) in order to be excluded from proliferating T cells. Furthermore, after co-culture T cells were re-stimulated by PMA (40ng/mL) and ionomycin (1μg/mL) for 5 hours in the presence of Brefeldin (Sigma, 5μg/mL) during the last 4 hours. Proliferation and cytokine production were analyzed by flow cytometry and reported as fold increase of specific T cell proliferation or cytokine production, calculated by dividing the percentage of proliferation or cytokine production (TNFα or IFNγ) in the TL condition by that in the control condition (media cultured DC). In all three experiments soluble GITRL (R and D systems, 10 μg/mL),

neutralizing anti-CTLA-4 (BNI3, Beckman Coulter, 10 µg/mL) or isotype control (IgG2a, Biolegend, 10 µg/mL) antibodies were added to the co-cultures.

Statistical analysis

All data set distributions were analyzed for normality using the Shapiro-Wilk normality test. The differences between paired groups of data were analyzed according to their distribution by either paired t-test or Wilcoxon matched pairs test using GraphPad Prism Software (version 5.0). P-values less than 0.05 were considered statistically significant (*$P<0.05$; **$P<0.01$; ***$P<0.001$).

Table 1: Patient characteristics

	HCC (n=10)	LM-CRC (n=18)
Sex (male/female)	8 / 2	12 / 6
Age (years)	55.1 ± 6.8	67.4 ± 1.9
Race (Caucasian/Asian/African)	9 / 0 / 1	18 / 0 / 0
ALT (units/L)	48.2 ± 8.6	27.9 ± 3.6
Bilirubin (µmol/L)	14.0 ± 4.5	8.7 ± 3.4
Prothrombin time (INR)	1.2 ± 0.03	1.0 ± 0.01
Liver fibrosis (metavir score) F0-F1 / F2 / F3-F4-cirrhosis	9 / 0 / 1	18 / 0 / 0
Stage of disease (TNM)	St I n=7 St II n=3	St IVa n=18

Etiology of liver disease in HCC patients: 6 no known liver disease, 1 hemochromatosis, 1 porphyria, 1 hepatitis B virus, 1 cirrhosis ECI

INR= international normalized ratio

Where applicable: mean ±SEM

Figure legends

Figure 1. Tumor-infiltrating Treg are potent suppressors of T cell responses, and they are characterized by the expression of higher levels of CTLA-4 and GITR. (A) The proportions of Treg (CD3+CD4+CD25+FoxP3+) among CD4 T cells were analyzed by flow cytometry in tumor, tumor-free liver tissue (TFL) and peripheral blood from patients with HCC or LM-CRC. Differences were analyzed by Wilcoxon matched pairs test. (B) CFSE-labeled CD4+CD25- T cells from PB were stimulated with autologous CMV-activated mDC (CMV-DC) for 5 days. Autologous blood or tumor derived Treg from HCC-patients or LM-CRC patients were added in a ratio 1:5. Inhibition of T cell proliferation by Treg was determined by flow cytometry and reported as percentage of suppression of T cell proliferation. Data analyzed by paired t-test. (C) Differential expression of surface GITR and intracellular CTLA-4 was measured on Treg present in blood, TFL and tumor tissue. Differences were analyzed by Wilcoxon matched pairs test for GITR and by paired t-test for CTLA-4. (D) FACS analysis of the co-expression of CTLA-4 and GITR by Treg from blood, TFL and tumor tissue. One representative patient and the collective data analyzed by Wilcoxon matched pairs test. HCC (closed symbols) or LM-CRC (open symbols). Values are also depicted as means ± SEM. *p < 0.05, **p < 0.01, ***p< 0.001.

Figure 2. GITR engagement partially abrogates suppression mediated by tumor-infiltrating Treg. CD4+CD25- effector T cells were isolated from peripheral blood and labeled with CFSE, and co-cultured during 5 days with autologous mDC activated with CMV antigens. Autologous tumor Treg from HCC-patients (closed symbols) or LM-CRC patients (open symbols) were added in the absence or presence of different concentrations of soluble GITRL (sGITRL). T cell proliferation (A) and cytokine (IFNγ and TNFα) production by proliferating cells (B) were measured by flow cytometry after re-stimulation with CMV-activated Mo-DC. Values are also depicted as means ± SEM, *p < 0.05, **p < 0.01, ***p< 0.001. Differences were analyzed by paired t-test.

Figure 3. CTLA-4 blockage decreases T cell suppression mediated by tumor-infiltrating Treg in a dose dependent manner. CFSE-labeled CD4+CD25- T cells isolated from PB were stimulated with autologous CMV-DC and cultured with autologous tumor derived Tregs from HCC-patients (closed symbols) or LM-CRC (open symbols) in the absence or presence of 10 or 20 ug/ml of blocking anti-CTLA-4 mAb or an irrelevant isotype control antibody. Cell proliferation (A) and cytokine production by proliferating cells (B) were analyzed by flow cytometry after re-stimulation with CMV-activated Mo-DC. Values are also

depicted as means ± SEM, *p < 0.05, **p < 0.01, ***p< 0.001. All data were analyzed by paired t-test.

Figure 4. High doses of anti-CTLA-4 mAb can completely abrogate T cell suppression mediated by tumor-infiltrating Treg. The effect of higher doses of anti-CTLA-4 mAb on Treg-mediated suppression was tested using lymphocytes isolated from three different LM-CRC patients. T cell proliferation analysis revealed that higher doses of the neutralizing anti-CTLA-4 antibody are able to completely abolish the suppression mediated by tumor-infiltrating Treg.

Figure 5. GITRL and CTLA-4 blockage additively abolish T cell suppressive capacity of tumor-infiltrating Treg. Blood-derived CFSE-labeled CD4+CD25- T cells from HCC-patients or LM-CRC patients were co-cultured with autologous CMV-DC for 5 days. Autologous tumor derived Treg were added in a ratio 1:5. Cells were treated with 10 µg/ml of anti-CTLA-4 mAb or GITRL or a combination of both. Cell proliferation and cytokine production were analyzed by flow cytometry after re-stimulation with CMV-activated Mo-DC. (A) Depicts a representative experiment showing T cell proliferation, IFNγ and TNFα production after co-culture and re-stimulation. (B) Collective data of five patients tested (three LM-CRC and two HCC) showing the relative T cell proliferation or cytokine production (IFNγ and TNFα) by proliferating cells. Values are means ± SEM, *p < 0.05, **p < 0.01, ***p< 0.001. Comparison between groups was made by paired t-test.

Figure 6. Treatment with GITRL and anti-CTLA-4 antibody can recover *ex vivo* anti-tumor T-cell immunity. Blood mDC activated with autologous TL were used to stimulate CFSE-labeled autologous peripheral CD4+CD25- T cells for one week. In some cultures autologous Ti-Treg were added and cells were treated with 10 µg/ml of an isotype control antibody or with a mixture of 10 µg/ml of GITRL and 10 µg/ml of anti-CTLA-4 antibody. T cell proliferation and cytokine production were analyzed by flow cytometry after re-stimulation with PMA and ionomycin. Proliferation and cytokine production are reported as fold increase of specific T cell proliferation or cytokine production, calculated by dividing the percentage of proliferation or cytokine production (TNFα or IFNγ) in the mDC + TL condition by that in the control condition without TL (medium DC). (A) A representative analysis from one patient and (B) Collective data from three different patients tested. HCC (closed symbols) or LM-CRC (open symbols).
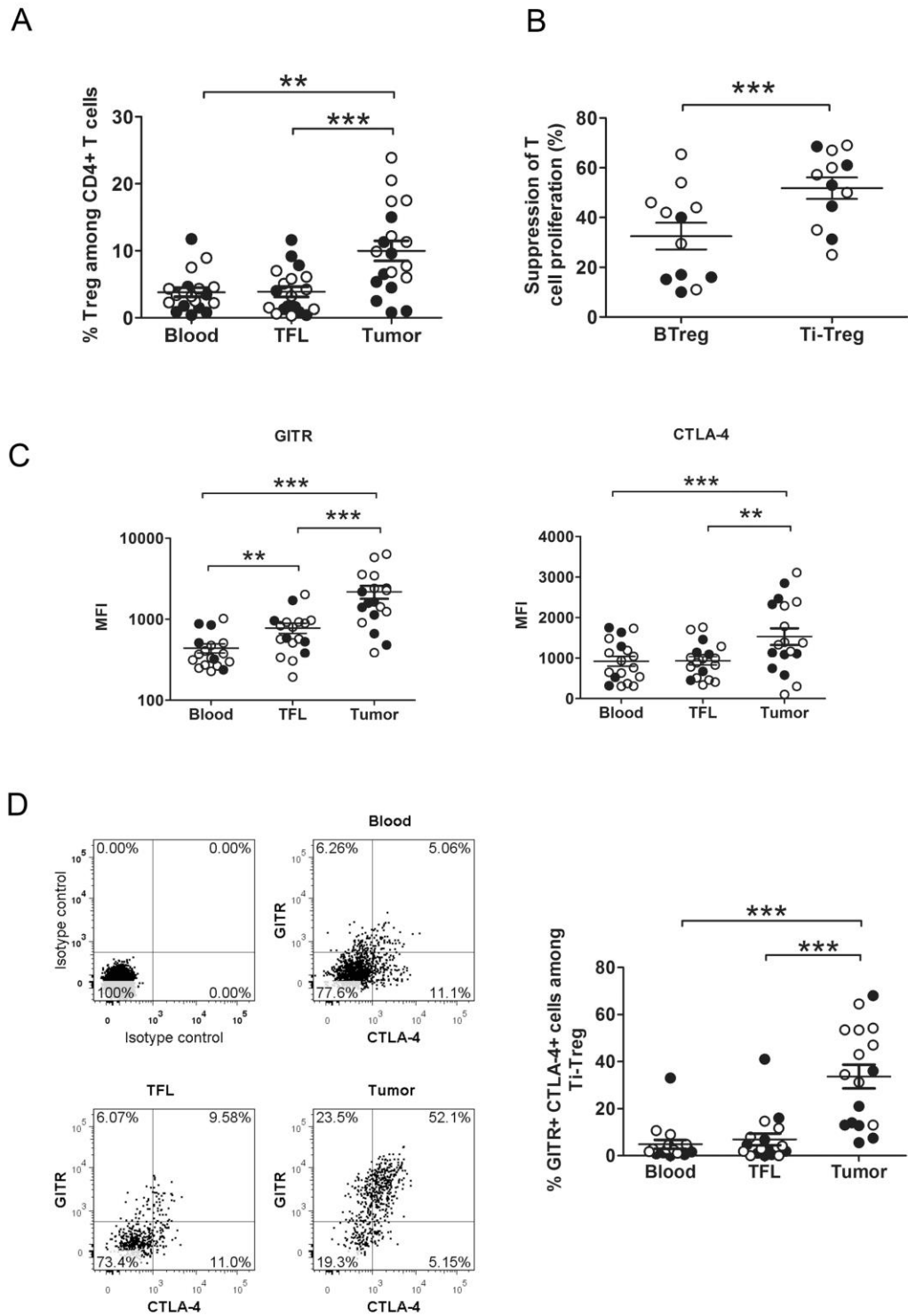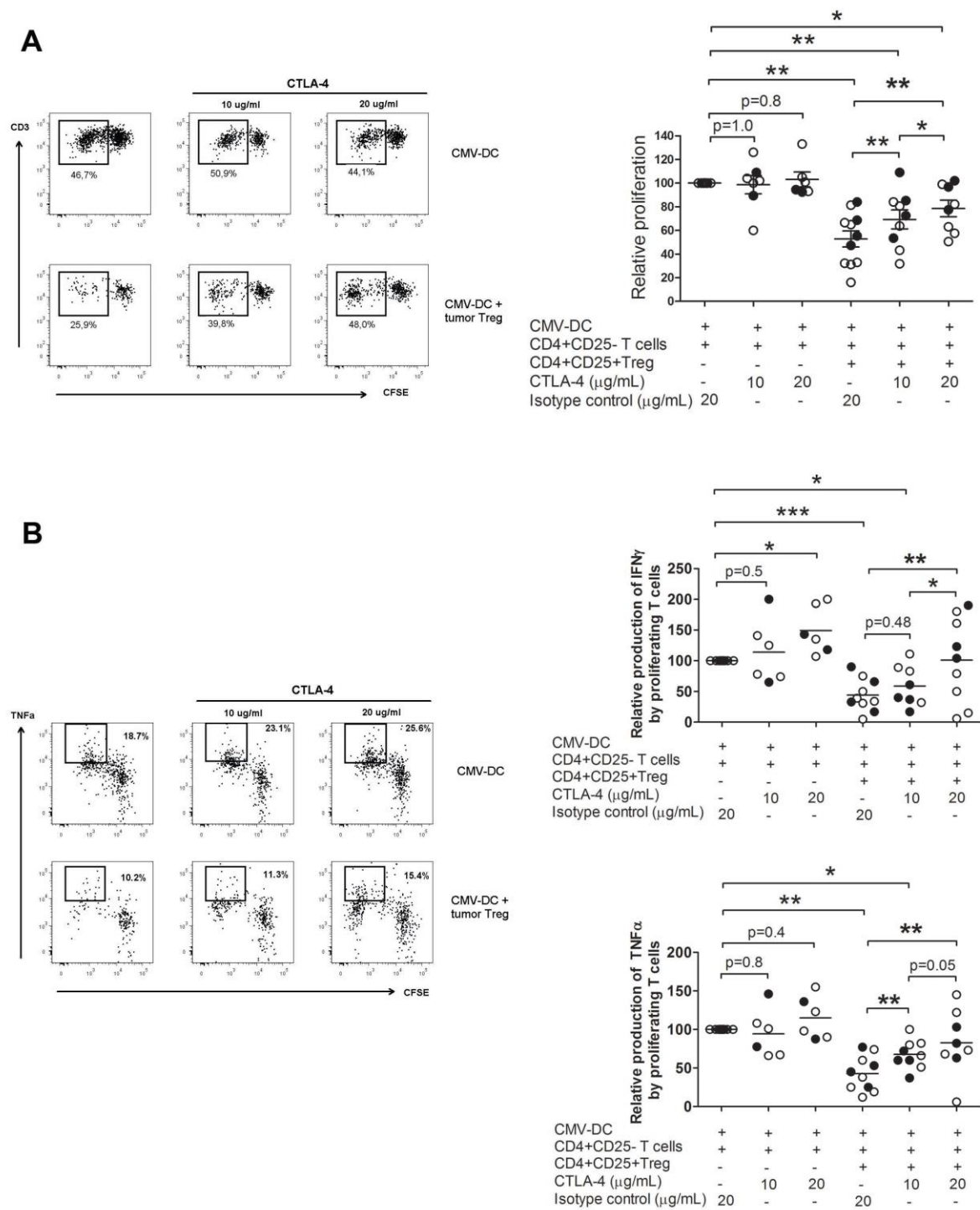
Figure 1.

A

B

C

GITR

CTLA-4

D

Figure 1

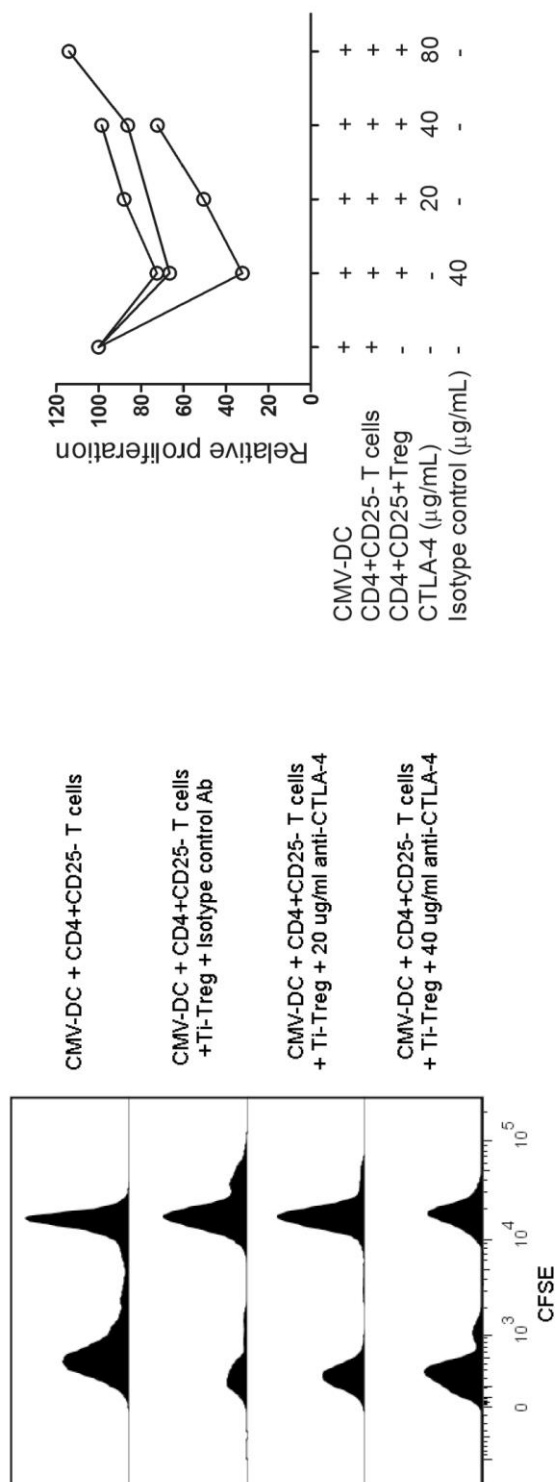**Figure 2.**

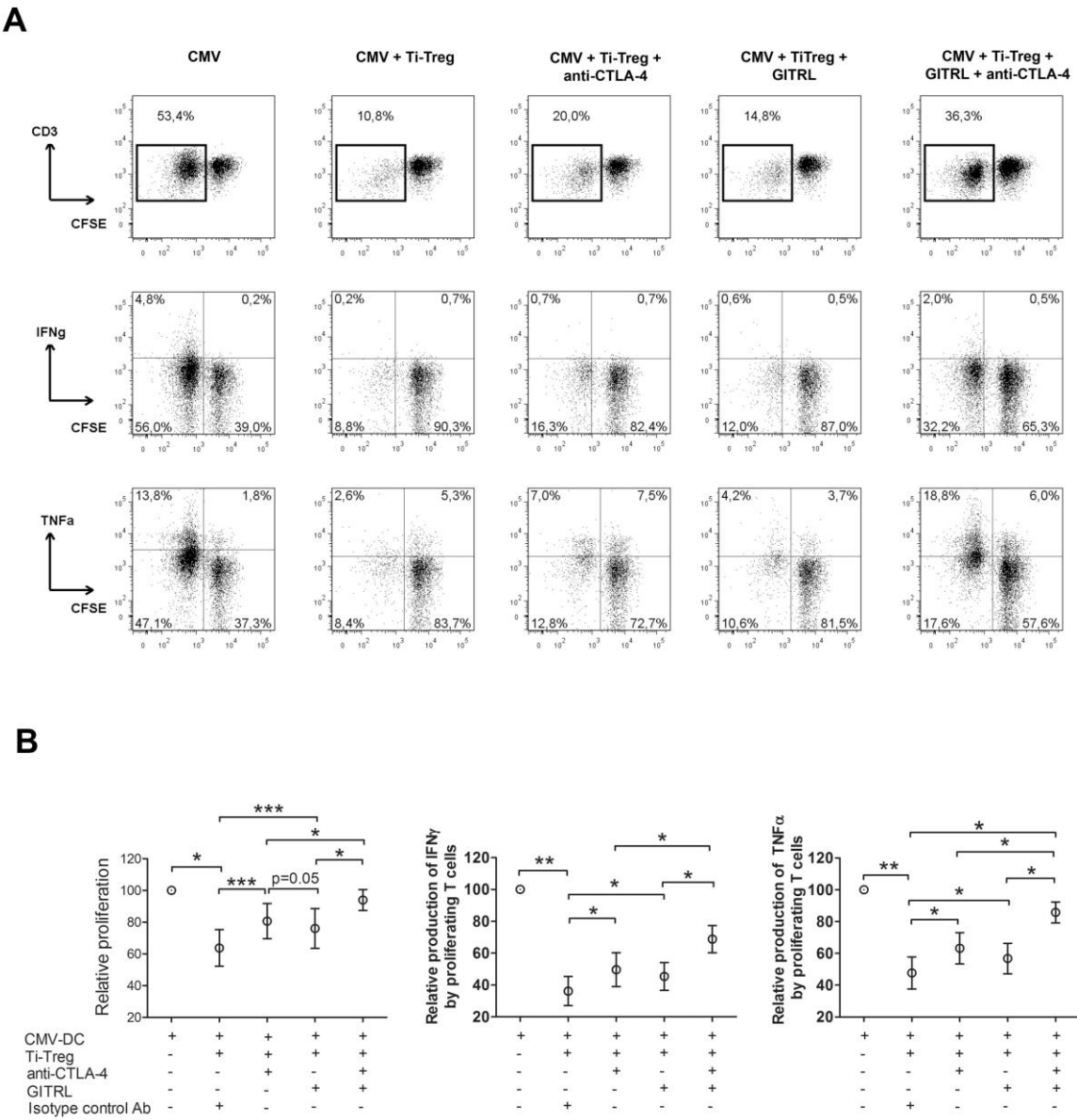**Figure 2**

Figure 3.

Figure 4.

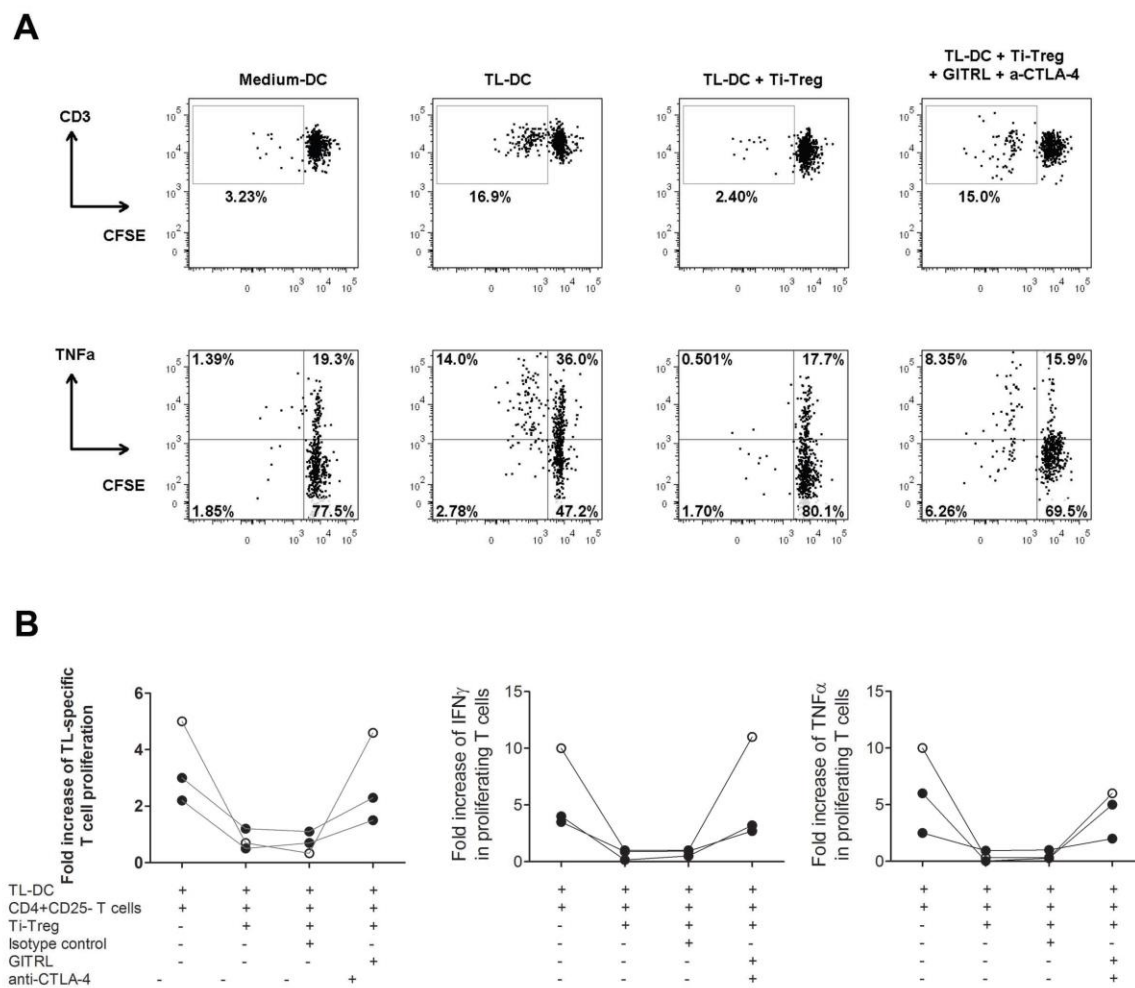

Figure 4

Figure 5.

Figure 6.

REFERENCES

1.	Anthony P. Hepatocellular carcinoma: an overview. Histopathology 2001; 39:109-18.
2.	Parkin DM, Bray F, Ferlay J, Pisani P. Estimating the world cancer burden: Globocan 2000. International journal of cancer 2001; 94:153-6.
3.	de Jong MC, Mayo SC, Pulitano C, Lanella S, Ribero D, Strub J, Hubert C, Gigot JF, Schulick RD, Choti MA. Repeat curative intent liver surgery is safe and effective for recurrent colorectal liver metastasis: results from an international multi-institutional analysis. Journal of Gastrointestinal Surgery 2009; 13:2141-51.
4.	House MG, Ito H, Gönen M, Fong Y, Allen PJ, DeMatteo RP, Brennan MF, Blumgart LH, Jarnagin WR, D'Angelica MI. Survival after hepatic resection for metastatic colorectal cancer: trends in outcomes for 1,600 patients during two decades at a single institution. Journal of the American College of Surgeons 2010; 210:744-52.
5.	El-Serag HB, Marrero JA, Rudolph L, Reddy KR. Diagnosis and treatment of hepatocellular carcinoma. Gastroenterology 2008; 134:1752-63.
6.	Kemeny N. Presurgical chemotherapy in patients being considered for liver resection. The Oncologist 2007; 12:825-39.
7.	de Jong MC, Pulitano C, Ribero D, Strub J, Mentha G, Schulick RD, Choti MA, Aldrighetti L, Capussotti L, Pawlik TM. Rates and patterns of recurrence following curative intent surgery for colorectal liver metastasis: an international multi-institutional analysis of 1669 patients. Annals of surgery 2009; 250:440.
8.	Llovet JM, Ricci S, Mazzaferro V, Hilgard P, Gane E, Blanc JF, de Oliveira AC, Santoro A, Raoul JL, Forner A. Sorafenib in advanced hepatocellular carcinoma. New England Journal of Medicine 2008; 359:378-90.
9.	Siegel AB, Olsen SK, Magun A, Brown RS. Sorafenib: where do we go from here? Hepatology 2010; 52:360-9.
10.	Pedroza-Gonzalez A, Xu K, Wu TC, Aspord C, Tindle S, Marches F, Gallegos M, Burton EC, Savino D, Hori T, et al. Thymic stromal lymphopoietin fosters human breast tumor growth by promoting type 2 inflammation. J Exp Med 2011; 208:479-90.
11.	Pardee AD, Butterfield LH. Immunotherapy of hepatocellular carcinoma: Unique challenges and clinical opportunities. Oncoimmunology 2012; 1:48-55.
12.	Pedroza-Gonzalez A, Verhoef C, Ijzermans JN, Peppelenbosch MP, Kwekkeboom J, Verheij J, Janssen HL, Sprengers D. Activated tumor-infiltrating CD4+ regulatory T cells restrain antitumor immunity in patients with primary or metastatic liver cancer. Hepatology 2013; 57:183-94.
13.	Zhou J, Ding T, Pan W, Zhu LY, Li L, Zheng L. Increased intratumoral regulatory T cells are related to intratumoral macrophages and poor prognosis in hepatocellular carcinoma patients. Int J Cancer 2009; 125:1640-8.
14.	Fu J, Xu D, Liu Z, Shi M, Zhao P, Fu B, Zhang Z, Yang H, Zhang H, Zhou C, et al. Increased regulatory T cells correlate with CD8 T-cell impairment and poor survival in hepatocellular carcinoma patients. Gastroenterology 2007; 132:2328-39.
15.	Unitt E, Rushbrook SM, Marshall A, Davies S, Gibbs P, Morris LS, Coleman N, Alexander GJ. Compromised lymphocytes infiltrate hepatocellular carcinoma: the role of T-regulatory cells. Hepatology 2005; 41:722-30.
16.	Pedroza-Gonzalez A, Kwekkeboom J, Sprengers D. T-cell suppression mediated by regulatory T cells infiltrating hepatic tumors can be overcome by GITRL treatment. Oncoimmunology 2013; 2:e22450.
17.	Hodi FS, O'Day SJ, McDermott DF, Weber RW, Sosman JA, Haanen JB, Gonzalez R, Robert C, Schadendorf D, Hassel JC, et al. Improved survival with ipilimumab in patients with metastatic melanoma. N Engl J Med 2010; 363:711-23.
18.	Wolchok JD, Neyns B, Linette G, Negrier S, Lutzky J, Thomas L, Waterfield W, Schadendorf D, Smylie M, Guthrie T, Jr., et al. Ipilimumab monotherapy in patients with pretreated advanced melanoma: a randomised, double-blind, multicentre, phase 2, dose-ranging study. Lancet Oncol 2010; 11:155-64.
19.	Sangro B, Gomez-Martin C, de la Mata M, Inarrairaegui M, Garralda E, Barrera P, Riezu-Boj JI, Larrea E, Alfaro C, Sarobe P, et al. A clinical trial of CTLA-4 blockade with tremelimumab in patients with hepatocellular carcinoma and chronic hepatitis C. J Hepatol 2013; 59:81-8.
20.	Kobayashi N, Hiraoka N, Yamagami W, Ojima H, Kanai Y, Kosuge T, Nakajima A, Hirohashi S. FOXP3+ regulatory T cells affect the development and progression of hepatocarcinogenesis. Clin Cancer Res 2007; 13:902-11.

21.   Chen KJ, Lin SZ, Zhou L, Xie HY, Zhou WH, Taki-Eldin A, Zheng SS. Selective recruitment of regulatory T cell through CCR6-CCL20 in hepatocellular carcinoma fosters tumor progression and predicts poor prognosis. PLoS One 2011; 6:e24671.

22.   Shen X, Li N, Li H, Zhang T, Wang F, Li Q. Increased prevalence of regulatory T cells in the tumor microenvironment and its correlation with TNM stage of hepatocellular carcinoma. J Cancer Res Clin Oncol 2010; 136:1745-54.

23.   Ling KL, Pratap SE, Bates GJ, Singh B, Mortensen NJ, George BD, Warren BF, Piris J, Roncador G, Fox SB, et al. Increased frequency of regulatory T cells in peripheral blood and tumour infiltrating lymphocytes in colorectal cancer patients. Cancer Immun 2007; 7:7.

24.   Brudvik KW, Henjum K, Aandahl EM, Bjornbeth BA, Tasken K. Regulatory T-cell-mediated inhibition of antitumor immune responses is associated with clinical outcome in patients with liver metastasis from colorectal cancer. Cancer Immunol Immunother 2012; 61:1045-53.

25.   Sasaki A, Tanaka F, Mimori K, Inoue H, Kai S, Shibata K, Ohta M, Kitano S, Mori M. Prognostic value of tumor-infiltrating FOXP3+ regulatory T cells in patients with hepatocellular carcinoma. Eur J Surg Oncol 2008; 34:173-9.

26.   Liu J, Zhang N, Li Q, Zhang W, Ke F, Leng Q, Wang H, Chen J, Wang H. Tumor-associated macrophages recruit CCR6+ regulatory T cells and promote the development of colorectal cancer via enhancing CCL20 production in mice. PLoS One 2011; 6:e19495.

27.   Hoechst B, Ormandy LA, Ballmaier M, Lehner F, Kruger C, Manns MP, Greten TF, Korangy F. A new population of myeloid-derived suppressor cells in hepatocellular carcinoma patients induces CD4(+)CD25(+)Foxp3(+) T cells. Gastroenterology 2008; 135:234-43.

28.   Jones E, Dahm-Vicker M, Simon AK, Green A, Powrie F, Cerundolo V, Gallimore A. Depletion of CD25+ regulatory cells results in suppression of melanoma growth and induction of autoreactivity in mice. Cancer Immun 2002; 2:1.

29.   Dannull J, Su Z, Rizzieri D, Yang BK, Coleman D, Yancey D, Zhang A, Dahm P, Chao N, Gilboa E, et al. Enhancement of vaccine-mediated antitumor immunity in cancer patients after depletion of regulatory T cells. J Clin Invest 2005; 115:3623-33.

30.   Greten TF, Ormandy LA, Fikuart A, Hochst B, Henschen S, Horning M, Manns MP, Korangy F. Low-dose cyclophosphamide treatment impairs regulatory T cells and unmasks AFP-specific CD4+ T-cell responses in patients with advanced HCC. J Immunother 2010; 33:211-8.

31.   Nocentini G, Ronchetti S, Petrillo MG, Riccardi C. Pharmacological modulation of GITRL/GITR system: therapeutic perspectives. Br J Pharmacol 2012; 165:2089-99.

32.   Cohen AD, Diab A, Perales MA, Wolchok JD, Rizzuto G, Merghoub T, Huggins D, Liu C, Turk MJ, Restifo NP, et al. Agonist anti-GITR antibody enhances vaccine-induced CD8(+) T-cell responses and tumor immunity. Cancer research 2006; 66:4904-12.

33.   Cohen AD, Schaer DA, Liu C, Li Y, Hirschhorn-Cymmerman D, Kim SC, Diab A, Rizzuto G, Duan F, Perales MA, et al. Agonist anti-GITR monoclonal antibody induces melanoma tumor immunity in mice by altering regulatory T cell stability and intra-tumor accumulation. PLoS One 2010; 5:e10436.

34.   Murphy JT, Burey AP, Beebe AM, Gu D, Presta LG, Merghoub T, Wolchok JD. Anaphylaxis caused by repetitive doses of a GITR agonist monoclonal antibody in mice. Blood 2014; 123:2172-80.

35.   Wing K, Suri-Payer E, Rudin A. CD4+ CD25+-Regulatory T Cells from Mouse to Man. Scandinavian journal of immunology 2005; 62:1-15.

36.   Wing K, Onishi Y, Prieto-Martin P, Yamaguchi T, Miyara M, Fehervari Z, Nomura T, Sakaguchi S. CTLA-4 control over Foxp3+ regulatory T cell function. Science 2008; 322:271-5.

37.   Hodi FS, O'Day SJ, McDermott DF, Weber RW, Sosman JA, Haanen JB, Gonzalez R, Robert C, Schadendorf D, Hassel JC. Improved survival with ipilimumab in patients with metastatic melanoma. New England Journal of Medicine 2010; 363:711-23.

38.   Phan GQ, Yang JC, Sherry RM, Hwu P, Topalian SL, Schwartzentruber DJ, Restifo NP, Haworth LR, Seipp CA, Freezer LJ, et al. Cancer regression and autoimmunity induced by cytotoxic T lymphocyte-associated antigen 4 blockade in patients with metastatic melanoma. Proc Natl Acad Sci U S A 2003; 100:8372-7.

39.   Beck KE, Blansfield JA, Tran KQ, Feldman AL, Hughes MS, Royal RE, Kammula US, Topalian SL, Sherry RM, Kleiner D, et al. Enterocolitis in patients with cancer after antibody blockade of cytotoxic T-lymphocyte-associated antigen 4. J Clin Oncol 2006; 24:2283-9.

40.   Trinh VA, Hagen B. Ipilimumab for advanced melanoma: a pharmacologic perspective. J Oncol Pharm Pract 2013; 19:195-201.

41.   Pruitt SK, Boczkowski D, de Rosa N, Haley NR, Morse MA, Tyler DS, Dannull J, Nair S. Enhancement of anti-tumor immunity through local modulation of CTLA-4 and GITR by dendritic cells. Eur J Immunol 2011; 41:3553-63.

CHAPTER 3

Tumor-infiltrating plasmacytoid dendritic cells promote immunosuppression by Tr1 cells in human liver tumors

Alexander Pedroza-Gonzalez[1, 6], **Guoying Zhou[1],** Ernesto Vargas-Mendez[1], Patrick P.C. Boor[1], Shanta Mancham[1], Cornelis Verhoef[2], Wojciech G. Polak[2], Dirk Grunhagen[2], Qiuwei Pan[1], Harry L.A. Janssen[1], Gina S. Garcia-Romo[4], , Katharina Biermann[3], Eric T.T.L. Tjwa[1], Jan N.M. IJzermans[2], Jaap Kwekkeboom[1], and Dave Sprengers[1, 5]

[1]Department of Gastroenterology and Hepatology, [2]Department of Surgery and [3]Department of Pathology, Erasmus MC-University Medical Center, Rotterdam, the Netherlands. [4]Department of Nephrology, Leiden University Medical Center, Leiden, the Netherlands. [5]Department of Gastroenterology and Hepatology, Academic Medical Center, University of Amsterdam, the Netherlands. [6]Laboratory of Immunology Research, FES-Iztacala, UNAM, Mexico.

ABSTRACT

CD4+ type 1 T regulatory (Tr1) cells have a crucial role in inducing tolerance. Immune-regulation by these cells is mainly mediated through the secretion of high amounts of IL-10. Several studies have suggested that this regulatory population may be involved in tumor-mediated immune-suppression. However, direct evidence of a role for Tr1 cells in human solid tumors is lacking. Using *ex vivo* isolated cells from individuals with hepatocellular carcinoma (HCC; n=39) or liver metastases from colorectal cancer (LM-CRC; n=60) we identify a CD4+FoxP3-IL-13-IL-10+ T cell population in tumors of individuals with primary or secondary liver cancer that is characterized as Tr1 cells by the expression of CD49b and the lymphocyte activation gene 3 (LAG-3) and strong suppression activity of T cell responses in an IL-10 dependent manner. Importantly, the presence of tumor-infiltrating Tr1 cells is correlated with tumor infiltration of plasmacytoid dendritic cells (pDCs). pDCs exposed to tumor-derived factors enhance IL-10 production by Tr1 cells through up-regulation of the inducible co-stimulatory ligand (ICOS-L). These findings suggest a role for pDCs and ICOS-L in promoting intra-tumoral immunosuppression by Tr1 cells in human liver cancer, which may foster tumor progression and which might interfere with attempts of immunotherapeutic intervention.

Keywords: Hepatocellular carcinoma; colorectal cancer liver metastasis; ICOS-L; IL-10; Immunotherapy, Tr1 cells.

Introduction

The two most common types of cancer affecting the liver are HCC and LM-CRC. [1, 2] For the majority of patients curative treatments are not available and alternative treatments like immunotherapy have so far shown limited efficacy. [3, 4] One of the main obstacles for immunotherapy is the immunosuppressive environment within tumors. [5, 6] In support of this, we recently described the accumulation of CD4+FoxP3+ regulatory T cells (Tregs) that are potent suppressors of anti-tumor immunity at the tumor site of patients with liver cancer. [7, 8] However, other types of inhibitory T cells may also be involved in local immunosuppression inside the tumor.

Tr1 cells were initially described in individuals who developed long-term tolerance after allogenic transplantation. [9] Since then Tr1 cells have proven to be important in promoting and maintaining tolerance in autoimmunity, allergy and transplantation. [10] There is experimental evidence suggesting a putative role for Tr1 cells in tumor escape from immune surveillance. [11, 12] However, the absence of a defined cell surface signature and the reliance on a cytokine profile to distinguish Tr1 cells from other T cell subsets complicated their identification and study. [9] It was shown that exposure of dendritic cells to tumor-derived factors favors the induction of Tr1-like cells from naïve CD4+ T cells. [13] Additionally, tumor-infiltrating lymphocytes (TILs) of patients with head and neck squamous cell carcinoma were shown to contain more Tr1 precursors than peripheral blood. [14] These findings suggest that this regulatory T cell population could be involved in tumor-mediated immune-suppression. However, direct evidence for the presence of Tr1 cells and their role in solid tumor development remained elusive. Now, using recently described surface markers for the identification of Tr1 cells, [15] we report that TILs in patients with liver cancer contain a subset of suppressive CD4+Foxp3- T cells with the phenotypic and functional characteristics of Tr1 cells. In addition, we provide evidence suggesting that intra-tumoral immunosuppression by Tr1 cells is promoted by tumor-infiltrating pDCs.

Results

IL-10 producing CD4$^+$Foxp3$^-$ T cells accumulate in human liver tumors

In order to characterize the CD4+ T cell subsets present in liver tumors we compared pair wise the cytokine profile of CD4+ TILs isolated from individuals with HCC or liver metastasis from CRC (LM-CRC) to the cytokines produced by CD4+ T cells from the tumor-free area of the liver (TFL) and peripheral blood (Figure 1 and Supplementary Figure 1). Freshly isolated single cell suspensions were activated with PMA and Ionomycin in the presence of protein

transporter inhibitors and analyzed by flow cytometry. Compared to TFL and blood, CD4+ TILs contained significantly higher frequencies of IL-10-producing cells in both groups of patients (Figure 1A). In contrast, the frequencies of IFNγ, TNFα and IL-13 producing CD4+ T cells were similar in TFL and tumors.

To further characterize these IL-10-producing CD4+ T cells, we analyzed their expression of IL-13 and FoxP3, and we observed that the majority of IL-10+ cells did not produce IL-13 nor expressed FoxP3 (Figure 1B, C and D). These cells were also negative for IL-4 (Supplementary Figure 1B). Therefore, only a minor proportion of tumor-infiltrating IL-10-producing CD4+ T cells correspond to FoxP3+ Tregs or Th2 cells. Instead, the large majority of IL10-producing CD4+ T cells are FoxP3-negative and IL-13-negative, and these cells are enriched at the tumor site (Figure 1E). Moreover, an important proportion of these cells produced IFNγ without significant differences between blood, TFL and tumor (Supplementary Figure 1C).

Tumor-infiltrating CD4$^+$FoxP3$^-$IL-10$^+$ T cells are potent suppressors of T cell function in an IL-10 dependent mechanism

To investigate the functional properties of tumor-infiltrating CD4+FoxP3-IL-13-IL-4-IL-10+ cells, we isolated CD4+CD25- T cells, which are FoxP3$^-$ (Supplementary Figure 2A), from TILs and activated them with antibodies to CD3 and CD46 [16] or ICOS [17], two co-stimulatory molecules that have been described to stimulate IL-10 production (Supplementary Figure 2B). Importantly, we activated these cells for only 24-48 hours to prevent de novo generation of IL10-producing cells from naïve T cells. Similar to what we had observed upon short-term stimulation with PMA and ionomycin, this stimulation also revealed higher proportions of IL10-producing CD4+ cells in tumor tissue than in TFL or blood, (Supplementary Figures 2C-D). After activation IL-10+ cells were enriched by magnetic sorting (Supplementary figure 3). We investigated the immunosuppressive potential of tumor-infiltrating IL-10 producing CD4+CD25- T cells by assessing their capacity to suppress T-cell proliferation and cytokine production in vitro (Figure 2A, B). CFSE-labeled PBMCs from healthy donors were stimulated with PHA and co-cultured in the presence of the IL-10+ enriched fraction (IL-10^{high}) or the remaining fraction (IL-10^{low}). Notably, both cell fractions suppressed proliferation and cytokine production of responder CD3+ T cells (Figure 2A, B), but the degree of suppression differed considerably. Whereas the IL-10^{low} fraction suppressed moderately (20.4 ± 5.5 %; mean ± SE), the IL-10^{high} fraction strongly suppressed T cell proliferation (60.2 ± 9.2 %, p=0.005). No difference in suppression between cells stimulated with CD46 or anti-ICOS antibodies was observed (Supplementary Figure 3B). Similar findings were observed

in the setting of CMV-specific CD4+ T cell responses (Supplementary Figure 4). To investigate whether the suppression was mediated by IL-10, we administered a neutralizing anti-IL-10R antibody to the co-cultures. As expected, suppression by the high IL10 producing CD4+ T cells was prevented when IL-10R was blocked, in all patients tested (Figure 2C). Thus, these data show that liver tumors are infiltrated by IL-10 producing CD4+FoxP3- T cells which are potent suppressors of T cell responses in an IL-10 dependent manner. The limited suppression observed when the IL-10^low fraction was added to the T-cell culture is likely a consequence of IL-10 producing cells remaining in this fraction after enrichment of the IL-10^high fraction by magnetic sorting (Supplementary Figure 5A), and could also be blocked by neutralizing anti-IL-10R antibodies (data not shown). In support of this explanation, there is a positive correlation (p = 0.023) between the frequencies of IL-10+ cells present in the IL-10 high or low fractions obtained after magnetic sorting and their degree of T cell suppression observed in the co-cultures (Supplementary Figure 5B).

Tumor-infiltrating CD4⁺FoxP3⁻IL-10⁺ T cells display phenotypic characteristics corresponding to Tr1 cells

A recent study has identified that CD49b and LAG-3 are stably and selectively co-expressed on Tr1 cells. [15] Because Tr1 cells are functionally characterized by the production of high levels of IL-10 and T-cell suppressive capacity, we examined the expression of these markers on the tumor-infiltrating IL-10+CD4+ T cells that we described above. Notably, the liver tumor-infiltrating CD4+FoxP3- T cells that produced the highest amounts of IL-10 co-expressed CD49b and Lag-3 (Figure 2D) and we observed that CD4+FoxP3-CD49b+LAG-3+ T cells were selectively enriched in the tumor bed in both types of liver tumors (Figure 2 E and F). Therefore, taken together we conclude that the majority of the CD4+FoxP3-IL-10 producing cells infiltrating liver tumors correspond to Tr1 cells and that they are strongly immunosuppressive in an IL-10-dependent manner.

Tumor-exposed pDCs promote immune suppression through activation of Tr1 cells

Given that pDCs have been reported to prime CD4+IL-10-producing T regulatory cells through ICOSL, [18] and in ovarian [19, 20] and breast cancer [21] expand CD4+FoxP3+ Tregs, as well as stimulate production of IL-10 in these cells, we explored tumor infiltration of pDCs in our patients. We observed that pDCs infiltrate liver tumors (Figure 3A and supplementary figure 6A), and in both groups of patients liver tumors contained higher frequencies compared to TFL. We hypothesized that in liver tumors infiltrating pDCs may promote the differentiation and/or activation of tumor-infiltrating Tr1 cells, as has been observed for CD4+FoxP3+ Tregs. [22] Supporting this hypothesis, the frequencies of tumor-infiltrating pDCs

and those of Tr1 cells as determined by flow cytometry, showed a highly significant positive correlation (Figure 3B). Also, by immunohistochemistry analysis we observed co-localization of CD303+ pDCs and LAG-3+ cells in the tumor milieu of both types of liver tumors (Figure 3C, D) which was substantiated by a significant positive correlation in co-localization (Pearson r = 0.78; p = 0.03) after counting multiple microscopic fields (200x magnifications, 2 independent observers). Such correlation was absent in TFL (r = -0.2; p= 0.49), and moreover less LAG-3+ and CD303+ cells were detected by immunohistochemistry in TFL than in tumors (per microscopic field of 200x magnification: LAG-3+ cells 3.4 ± 1.0 versus 6.6±1.9 (mean ± SEM); and CD303+ cells 1.2 ± 0.4 versus 5.3 ± 1.6). Furthermore, analysis of the expression of ICOS-L in total cell suspensions obtained from tumors of HCC and LM-CRC patients demonstrated that the main cell population expressing this molecule corresponded to CD123+ pDCs (Figure 3E), while Tr1 in tumors express high levels of ICOS (Figure 2D). We therefore hypothesized that pDCs in liver tumors may induce or activate Tr1 cells trough ICOSL in liver tumors.

To test this hypothesis, pDCs isolated from blood of healthy donors were exposed to lysates of tumor or TFL and then used to stimulate autologous naïve CD4+ T cells. pDCs exposed to tumor lysates (TL-pDCS) up-regulated ICOS-L expression (Figure 4A), whereas TFL lysates (TFLL) induced a significant down-regulation of ICOS-L. In contrast, exposure of pDCs to tumor lysate or TFL lysate did not affect expression of the co-stimulatory molecule CD83 and CD86 was up-regulated only in TL-pDCs (supplementary figure 6B). pDCs induced Tr1 from naïve CD4+ T cells and stimulated IL-10 production in these cells (Figures 4B, C). Interestingly, in parallel with their increased expression of ICOS-L, TL-pDCs induced higher numbers of IL-10 producing CD4+FoxP3-CD49+LAG-3+ Tr1 cells from naïve CD4+ T cells compared to pDCs treated with TFL lysate (TFLL-pDCs)(Figure 4B), but their capacity to induce CD49b and LAG-3 expression did not differ significantly (Figure 4C). The ability of TL-pDCs to promote IL-10 production by Tr1 cells was dependent on ICOS-ICOS-L co-stimulation, as it was blocked by addition of a neutralizing antibody against ICOS-L (Figure 4B). Furthermore, there is a positive correlation (r= 0.75, p = 0.006) between the level of expression of ICOS-L on pDCs after exposure to medium, TFLL or tumor lysate, and the frequency of IL-10-producing Tr1 cells induced in the co-culture (Figure 4D). In contrast, the expression of CD49b and LAG-3 was not affected by ICOS-L blocking (Figure 4C). Thus, ICOS-ICOSL signaling seems to be unnecessary for the induction of the Tr1 phenotype by pDCs, but it is critical for the production of IL-10.

Discussion

At the time of diagnosis the majority of HCC patients are not candidates for curative therapy, and in CRC patients with liver metastasis there is a high rate of recurrence after treatment. [1, 2] For these groups of patients immunotherapy aimed at stimulating the local anti-tumor immune response might present an attractive alternative. However, immunotherapeutic attempts have so far shown poor clinical responses and this might be related to the inhibition of tumor-specific immunity by immune regulatory mechanism present in the tumor microenvironment. [3, 8] Detailed insight into the complex nature of intra-tumoral immune regulation is essential for the design of immunotherapeutic strategies, and the findings of this study may contribute to development of such strategies.

TILs in liver tumors are composed mainly of CD4+ T cells that are hypo-responsive to tumor antigens. [7] We previously showed that an important fraction of the CD4+ T cells in these tumors correspond to CD4+FoxP3+ Tregs that are potent suppressors of anti-tumor immunity. [7, 8] There is accumulating evidence for the role of CD4+Foxp3+ Tregs in the development and progression of cancer. [23, 24] Several studies have shown that the presence of increased numbers of these cells in different tumors contributes to the suppression of antitumor immunity and correlates to decreased survival. [23-26] Over the years, several types of Tregs have been identified (reviewed in 9). Whereas CD4+FoxP3+ Tregs are probably the best characterized Treg type, Tr1 cells were until recently a subset of T cells that lacked a defined cell surface signature, and could therefore only be characterized by the production of high levels of IL-10, low levels of IL-2, variable levels of IFNγ and the absence of IL-4 and absence of high and constitutive expression of FoxP3. [9] The reliance on a cytokine profile to distinguish Tr1 cells complicated their identification and study, since these cells are not the only T cell subset that secretes IL-10. Still, experimental evidence suggested that exposure of dendritic cells to tumor derived factors favors the induction of Tr1-like cells from naïve T cells, [13] arguing for a role of Tr1 cells in cancer immunology. Later on, in head and neck carcinoma a suppressive role for in vitro generated CD4$^+$CD25$^-$FoxP3^{low}IL-10$^+$TGFb$^+$ cells was described. [27] Moreover, in Hodgkin lymphoma the presence of CD4+CD25-IL-10+ regulatory T cells has been described [12] and more recently a study described the presence of CD4+FoxP3-CD127- regulatory T cells in blood and tumors from HCC patients. Although they did not show regulatory functionality of the tumor-infiltrating CD4+FoxP3-CD127- cells, the circulating phenotypically counterpart suppressed T cell responses through an IL-10-dependent mechanism, [11] suggesting a Tr1-like cell type.

However, until now direct evidence for a role of Tr1 cells in human solid tumors is lacking. The recent description of co-expression of CD49b and LAG-3 as markers that can specifically identify this population of cells, [15] enabled us to show that the majority of liver

tumor-infiltrating IL-10 producing CD4+ T cells consists of Tr1 cells and only a minor proportion corresponded to Th2 cells or FoxP3+ Tregs. Compared to TFL, higher numbers of these Tr1 cells are present in the liver tumors of both HCC-patients and metastatic CRC-patients, indicating selective accumulation in the tumor tissues. In functional assays the tumor-infiltrating Tr1 cells demonstrated a potent suppressive activity mediated by IL-10. Therefore, these cells represent a suppressive population in the tumor environment potentially contributing to the impaired anti-tumor immunity observed in patients with liver cancer.

Our data suggest that tumor-infiltrating Tr1 cells may be activated by pDCs present in the tumor microenvironment. Using immunohistochemistry analysis pDCs could be identified in the vicinity of Lag3+ cells. Lag3 may also be expressed on CD4+Foxp3+ Tregs [9], but by flow-cytometry we observed that on the average only 6% of HCC or LM-CRC-derived CD4+Foxp3+ Tregs express Lag3 (data not shown). Therefore, this co-localization, together with the correlation between the frequencies of tumor-infiltrating pDCs and Tr1 cells observed in flow cytometric analysis (Figure 3B), suggests a possible interaction between both cell types, but further experiments are needed to confirm this *in situ* interaction. Furthermore, the main population expressing ICOSL in tumor tissues are CD123+ pDCs. In vitro exposure of immature pDCs to tumor lysates, but not lysates of normal liver tissue, conditioned pDCs to up-regulate the expression of ICOS-L and induce the production of IL-10 by Tr1 cells in a mechanism mediated by ICOS-ICOS-L signaling. There is substantial evidence suggesting that pDCs have a specialized role in the induction of peripheral tolerance by inducing IL-10-production by Tregs through ICOS-L-ICOS signaling. [18, 28] Both in breast and in ovarian cancer stimulation of CD4+FoxP3+ Tregs to produce IL-10 by pDCs has been described. [19, 22] Our results are consistent with a role for pDCs to stimulate IL10 production by Tr1 cells in the tumor microenvironment of patients with liver cancer. Altogether these data suggest that ICOS co-stimulation represents a potential target for immunotherapeutic intervention, affecting tumor-specific immunosuppression mediated by both CD4+Foxp3+ Tregs and Tr1 cells.

In summary, in patients with primary and secondary liver cancer we identified a population of tumor-infiltrating Tr1 cells that contributes to local immune suppression in an IL-10 dependent manner. pDCs may drive intra-tumoral immunosuppression by these Tr1 cells by stimulating IL-10 production via ICOS-ICOS-L signaling. Consequently, as has been shown for CD4+FoxP3+ Tregs, [7, 29] Tr1 cells may inhibit anti-tumor immunity at the tumor site in liver cancer and thereby promote tumor development. This knowledge is critical for the design of new immunotherapeutic interventions for patients with liver cancer and other solid cancers in

which IL-10 producing CD4+ T cells are present, and blockade of the engagement of ICOS-ICOS-L may provide alleviation of this intra-tumoral immunosuppressive mechanism.

Patients and Methods

Patients

Between September 2009 and July 2013 a total of 99 individuals who were eligible for surgical resection of HCC (n=39) or LM-CRC (n=60) were enrolled. Paired samples of fresh liver tumor tissue and tumor-free liver tissue (TFL) obtained at the maximum distance (at least 1 cm) from the tumor, were used for isolating TILs and intra-hepatic lymphocytes. In addition, peripheral blood was collected. None of the patients was treated with chemotherapy or radiation prior to resection. The clinical characteristics of the patients are summarized in Table 1. The study was approved by the local ethics committee and all patients in the study gave informed consent before tissue donation.

Cell preparation, flow cytometric analysis, antigen-specific T-cell activation, immunohistochemistry

Detailed descriptions of these methods are provided in the Supplementary Information.

Activation and isolation of IL-10-producing cells

CD4+CD25- T cells were isolated from TILs of patients with liver cancer by magnetic sorting as previously reported.[7] Briefly, the non-CD4+ cells were removed by a magnetically labeled cocktail of antibodies followed by depletion of CD25+ cells (Cat. 130-091-301, Miltenyi Biotec). CD4+CD25- T cells were stimulated with Dynabeads that were coupled to anti-CD3 (OKT-3, Cat. 314304, Biolegend) alone or in combination with anti-CD46 (TRA-2-10, Cat.352404, Biolegend) or anti-ICOS (ISA-3; Cat. 16-9948-82, ebiosciences) antibodies using the Dynabeads antibody coupling kit (Cat. 143.11D, Invitrogen). The bead to cell ratio was 0.5:1. Cells were cultured in the presence of 250 U/mL IL-2 (Cat. 130-097, Miltenyi Biotec) for 24-48 hrs. Then, cells were magnetically sorted into IL-10^{low} and IL-10^{high} fractions using the secretion assay-cell enrichment kit from Miltenyi (Supplementary Figure 2).

Suppression assays

The suppressive effect of IL-10 producing CD4+ T cells was assessed by co-culture with PBMCs from healthy donors that were labeled with 0.1 µM of carboxyfluorescein diacetate succinimidyl ester (CFSE, C34554, Invitrogen), and activated with 6 µg/mL of phytohemagglutinin (PHA, Remel-Thermo Fisher Scientific) for 5 days. The ratio of cells was

1:10 (Tr1:PBMCs) with at least 5×10^4 responder cells. Proliferation and cytokine production were measured by flow cytometry after re-stimulation with PMA/Ionomycin. Inhibition of T cell proliferation or cytokine production was determined by comparison with culture conditions without IL-10 producing CD4+ T cells, and reported as percentage of suppression of T cell proliferation or cytokine production. To analyze the role of IL-10 in the suppressive capacity of Tr1 cells, 30 ug/ml of neutralizing anti-IL-10R antibody (3F9 Cat. 308806) or isotype-matched control antibody (both from Biolegend) were added to some co-cultures.

In vitro activation and co-culture of pDCs and naïve T cells

pDCs were enriched from PBMCs of healthy donors by positive immunomagnetic selection using anti-BDCA-4 antibodies (Cat. 130-090-532, Miltenyi Biotec). Purity of pDCs as determined by CD123 labeling was 92 ± 2.5 %. pDCs were seeded at 10^5 cells/well in 200 µl of sRPMI medium (details can be found in Supplementary Methods) with 10% human AB serum in the presence of 10 ng/ml of IL-3 (Cat. 130-093, Miltenyi Biotec). pDCs were cultured with medium alone or in the presence of liver tissue lysates (200 µg/ml of total protein). After 18 hrs pDCs were harvested and washed. Then pDCs were stained for phenotypic analysis or co-cultured in a ratio 1:5 with autologous naïve CD4+ T cells, which were purified with the naïve CD4 T cell enrichment kit from Stemcell technologies (Cat. 19155). Cells were co-cultured for 7 days. Thereafter the cells were washed and re-stimulated 5 hrs with PMA and Ionomycin. The immunophenotype of CD4+ T cells and their cytokine profile were measured by flow cytometry. Tissue lysates were prepared from freshly dissected paired TFL and tumor tissues by 5 cycles of freezing and thawing in PBS, followed by filtration (0.2 µm). The total protein level was determined by BCA assay (Thermo Scientific), and the lysates were stored at -80° C before use. To determine involvement of ICOS-L in activation of Tr1, 50 µg/ml neutralizing anti-ICOS-L antibody (MIH12, Cat. 16-5889) or isotype-matched control antibody (both from e-Biosciences) were added to the co-cultures.

Statistical analysis

The differences between paired groups of data were analyzed according to their distribution by either t-test or Wilcoxon matched pairs test. Differences between different groups of patients were analyzed by either t-test or Mann Whitney test, using GraphPad Prism Software (version 5.0). P-values less than 0.05 were considered statistically significant (*P<0.05; **P<0.01; ***P<0.001).

Table 1. Patient characteristics

	HCC (*n* = 39)	LM-CRC (*n* = 60)
Sex (male/female)	25/14	37/23
Age (years)	62 ± 2	65 ± 1
Race (Caucasian/Asian/African)	35/3/1	59/0/1
ALT (units/L)	66 ± 16	33 ± 5
Bilirubin (μmol/L)	16 ± 4	8 ± 1.0
Prothrombin time (INR)	1.1 0.01	1.0 ± 0.01
Liver fibrosis (metavir score) F0-F1 / F2 / F3-F4-cirrhosis	19/10/10	60/0/0
Stage of disease (TNM)	St I *n* = 16	St IVa *n* = 55
	St II *n* = 23	St IVb *n* = 5

Etiology of liver disease in HCC patients: 17 no known liver disease, 5 hemochromatosis, 4 NASH, 4 alcohol related liver disease, 1 porphyria, 6 hepatitis B virus, 2 hepatitis C virus.
INR = international normalized ratio.
Where applicable: mean ± SEM.

Figure legends

Figure 1. Accumulation of IL-10-producing CD4$^+$FoxP3$^-$ T cells in liver tumors. PBMCs or MNCs isolated from tissues of HCC (n= 8-9) and LM-CRC (n= 5-14) patients were stimulated in vitro for 5 hours with PMA/Ionomycin in the presence of protein transport inhibitors. IFNγ, TNFα, IL-13 and IL-10 were measured by intracellular staining by flow cytometry. (A) The percentages of cytokine-producing cells among total CD3+CD4+ T cells in blood, tumor-free area of the liver (TFL) and tumor. (B) IL-13 expression in viable tumor-derived CD3$^+$CD4$^+$IL-10$^+$ T cells of HCC and LM-CRC patients stimulated with PMA/Ionomycin. FoxP3 and IL-10 expression in CD3+CD4+ T cells isolated from HCC (C) or LM-CRC tumors (D). (E) Frequencies of CD4$^+$CD3$^+$IL-13$^-$FoxP3$^-$IL-10$^+$ T cells among CD4$^+$ T cells. Red dots correspond to HCC and blue open dots are for LM-CRC (displayed as LMC in graphs). Values are means ± SEM, *p < 0.05, **p < 0.01, ***p< 0.001.

Figure 2. Tumor-infiltrating CD4$^+$FoxP3$^-$IL-10$^+$ T cells are potent suppressors of T cell function and their phenotype corresponds to Tr1 cells. Tumor-infiltrating CD4+CD25- T cells were activated with anti-CD3/CD46 or anti-CD3/ICOS antibodies for 24-48 hrs, then stained for IL-10 and magnetically sorted into IL-10^{low} and IL-10^{high} fractions, which were both co-cultured at a 1:10 ratio with CFSE-labeled PBMCs from healthy donors stimulated with phytohemagglutinin (PHA) for 5 days. (A) T cell proliferation and TNFα production measured by flow cytometry in PHA-stimulated PBMCs cultured alone or in the presence of IL-10^{low} or IL-10^{high} fractions of tumor infiltrating CD4+CD25- T cells. (B) Collective analysis of the percentages of suppression of T cell proliferation and TNFα production from 8 patients. (C) Effect of blocking IL-10R on the suppressive capacity of CD4+IL-10^{high} cells. Cells were cultured as described above in the presence of 30 μg/ml of neutralizing anti-IL-10R antibody or an irrelevant isotype control antibody. (D) Expression of CD49b and LAG-3 on tumor-infiltrating CD4+ T cells activated with antibodies to CD3 and ICOS for 24 hrs. Cells were gated on viable CD3+CD4+ T cells and FoxP3+CD127- Tregs were excluded from the analysis. Histograms show the expression of IL-10 and ICOS in different populations based on the expression of CD49b and LAG-3. (E) CD49b and LAG-3 expression in blood, TFL and TILs isolated from a representative patient with HCC. Cells were gated on viable CD3+CD4+FoxP3- T cells. (F) Collective percentages of CD49b+LAG-3+ cells within CD4+Foxp3- T cells in 21 patients analyzed (HCC n= 8 and LM-CRC n= 13). HCC (red dots) and LM-CRC (blue open dots).

Figure 3. Plasmacytoid DCs are enriched at the tumor site and correlate with the frequencies of Tr1 cells. (A) Percentages of pDCs (CD123+HLA-DR+LIN-) among CD45+ leukocytes from paired samples of TFL and tumor tissue from 78 patients tested (HCC = 27 and LM-CRC = 51). Tumor leukocytes contain significantly higher numbers of pDCs than TFL (on the average 0.74 ± 0.6 % pDCs in HCC tumors and 1.01 ± 0.9 % in LM-CRC tumors, compared to 0.45 % and 0.75 ± 0.6 % in TFL, respectively). (B) Pearson correlation analysis between the frequencies of tumor-infiltrating pDCs and CD4+FoxP3-CD49b+LAG-3+ Tr1 cells in liver tumors (n = 15). Red dots are HCC and blue open dots represent LM-CRC. (C, D) Immunohistochemistry analysis shows co-localization of CD303+ pDCs (red brown) and LAG-3+ cells (blue) in LM-CRC (C) and HCC (D) tumors. Magnification 200x. An insert at higher magnification showing the close localization of CD303+ and Lag-3+ cells in HCC is displayed in D. (E) Expression of ICOSL and CD123 analyzed by flow cytometry in total cell suspensions from liver tumors.

Figure 4. Tumor-derived pDCs induce the production of IL-10 by Tr1 cells through ICOS-ligand-ICOS signaling. (A) Blood pDCs isolated from healthy donors after overnight culture in the presence of lysates from TFL (TFLL-pDCs) or tumor tissue (TL-pDCs) were analyzed for the expression of ICOS-L. pDCs exposed to tissue lysates were used to stimulate autologous naïve CD4+ T cells. The expression of IL-10 (B) and CD49b and Lag-3 (C) were analyzed on CD4+ T cells after co-culture with pDCs and re-stimulation with PMA/Ionomycin. IL-10 production was analyzed in $CD3^+CD4^+FoxP3^-CD49b^+LAG-3^+$ T cells. To evaluate the impact of ICOS-ICOS-L signaling, cells were co-cultured in the presence of 50 ug/ml of control isotype antibody or anti-ICOS-L neutralizing antibody. Values are means ± SEM, *p < 0.05, **p < 0.01. Red dots represent HCC lysates and blue open dots LM-CRC lysates. (D) Pearson correlation analysis of the expression of ICOSL on pDCs cultured with medium, TFLL or TL, and the percentage of IL-10+ Tr1 cells detected after co-culture.
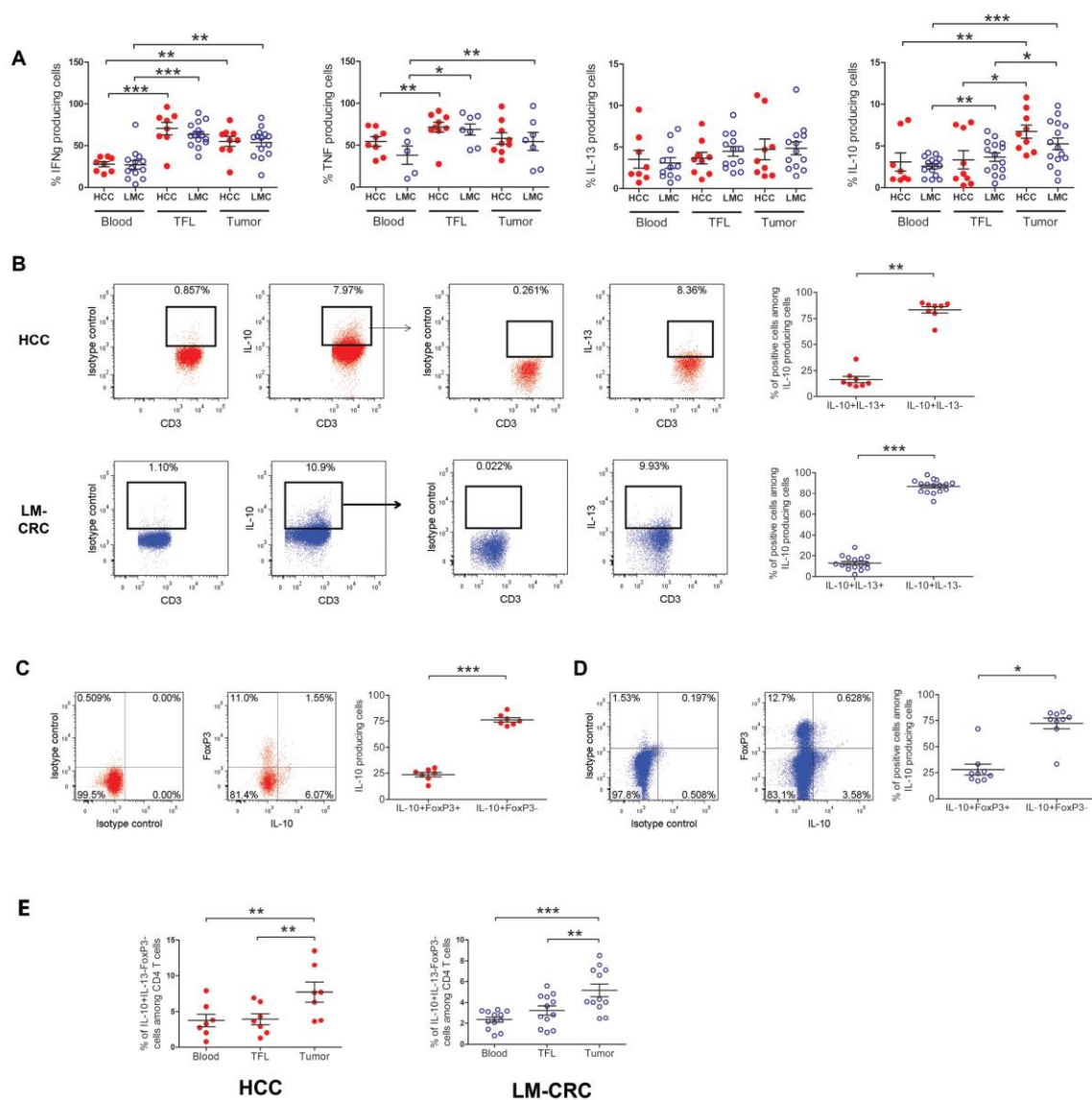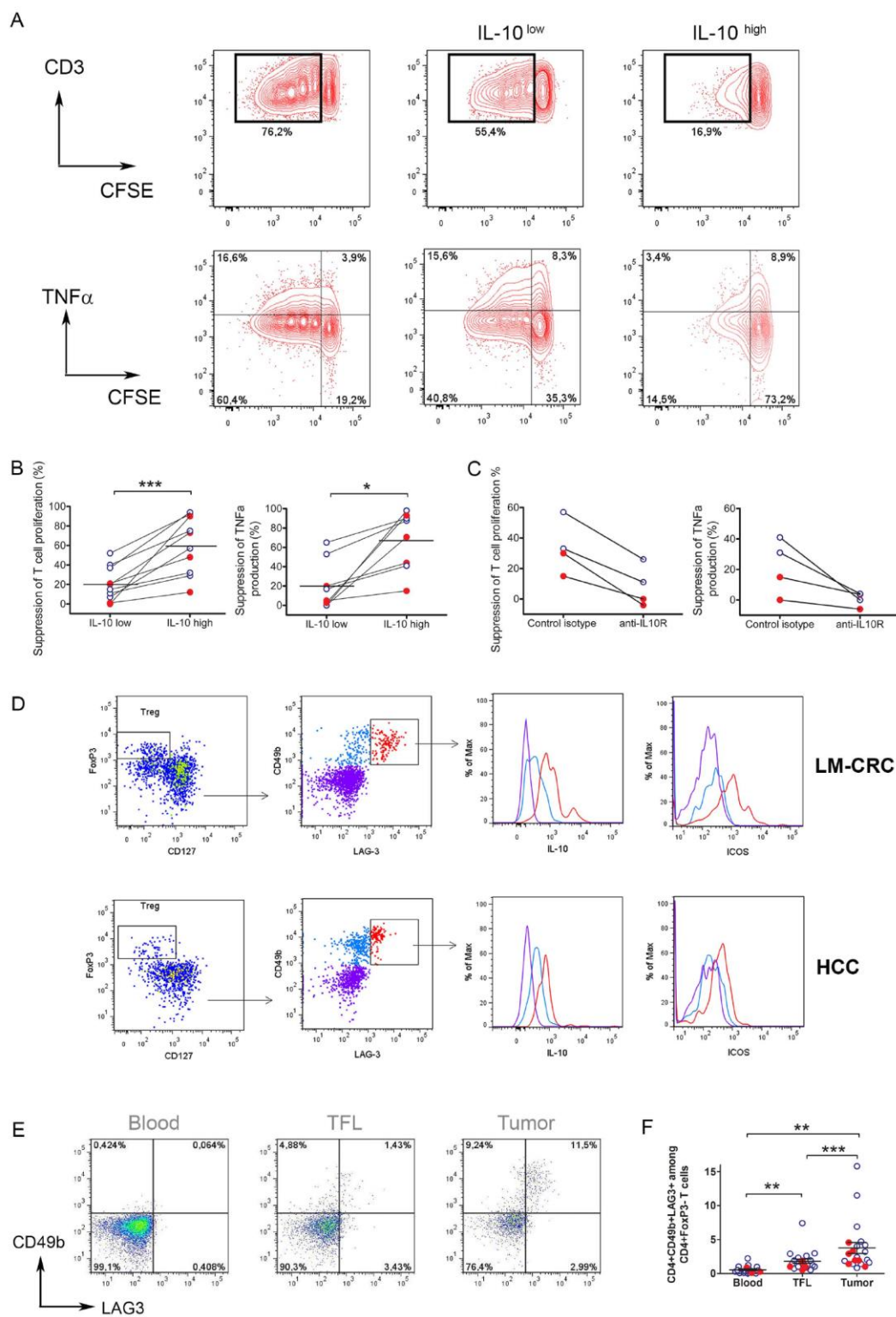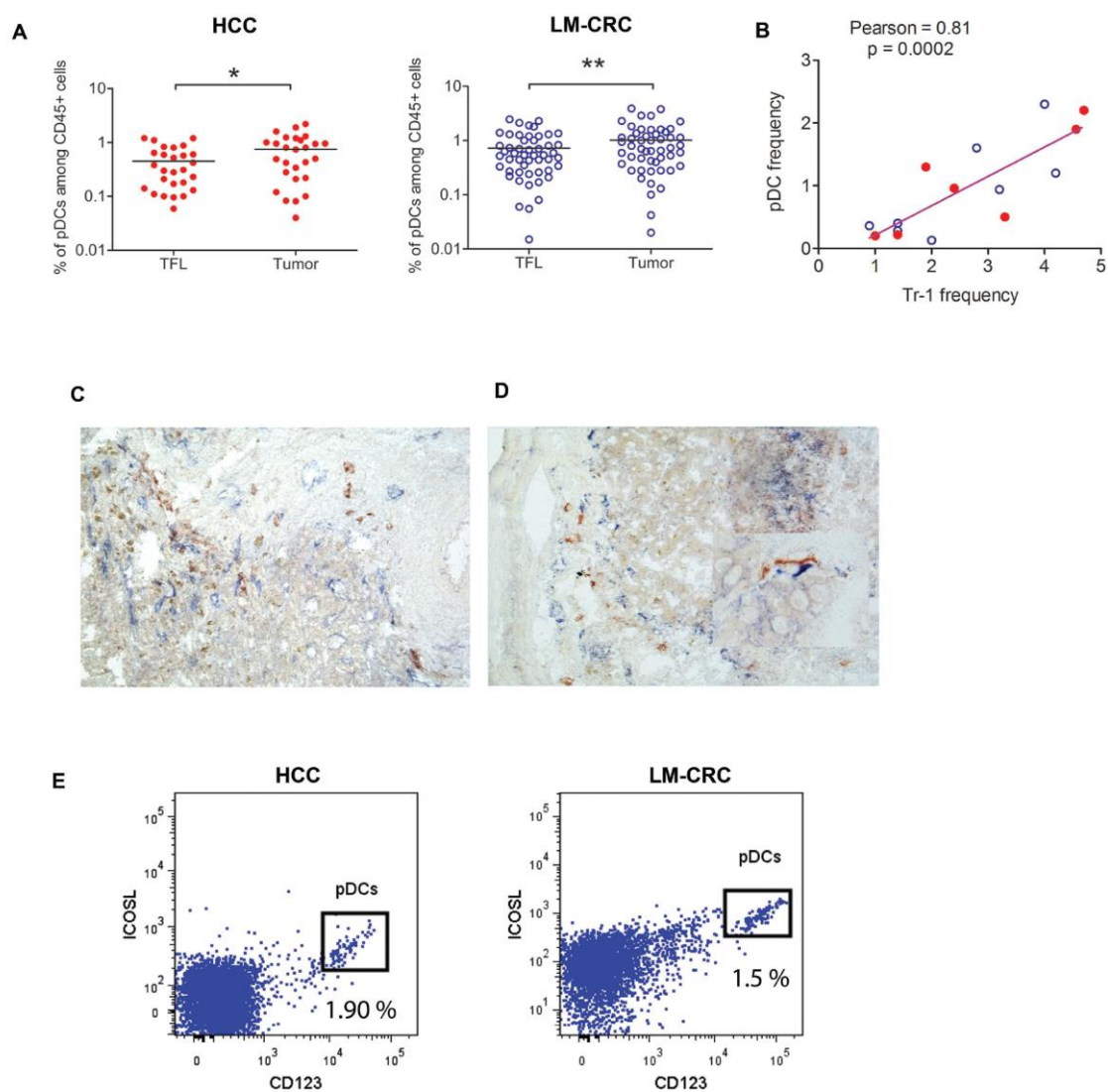
Figure 1.

Figure 2.

Figure 2

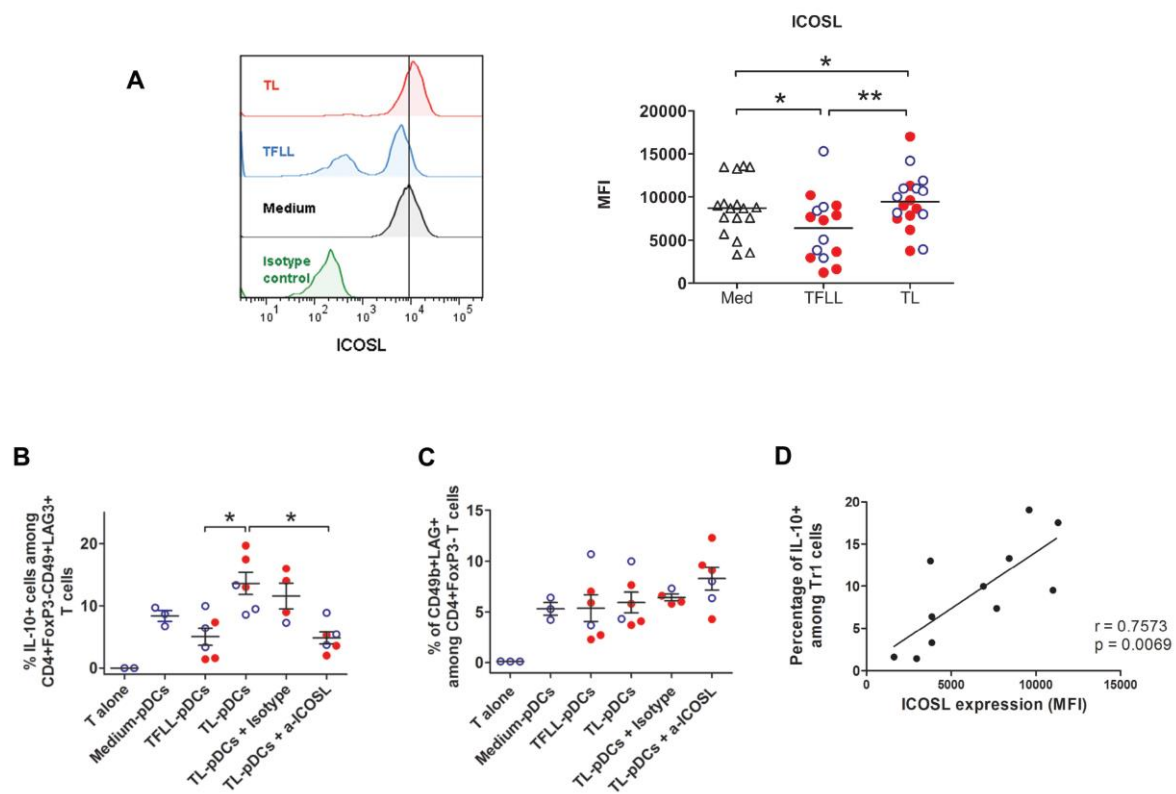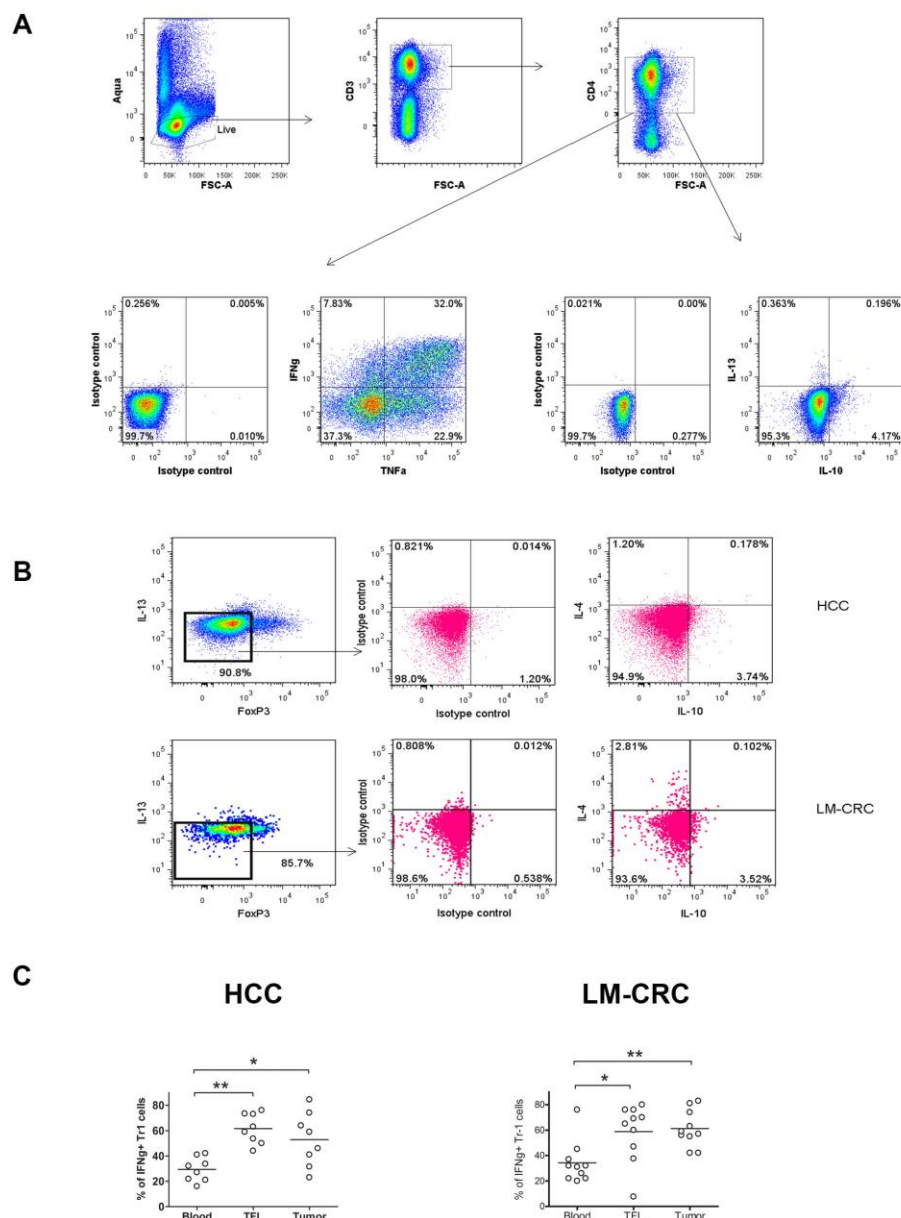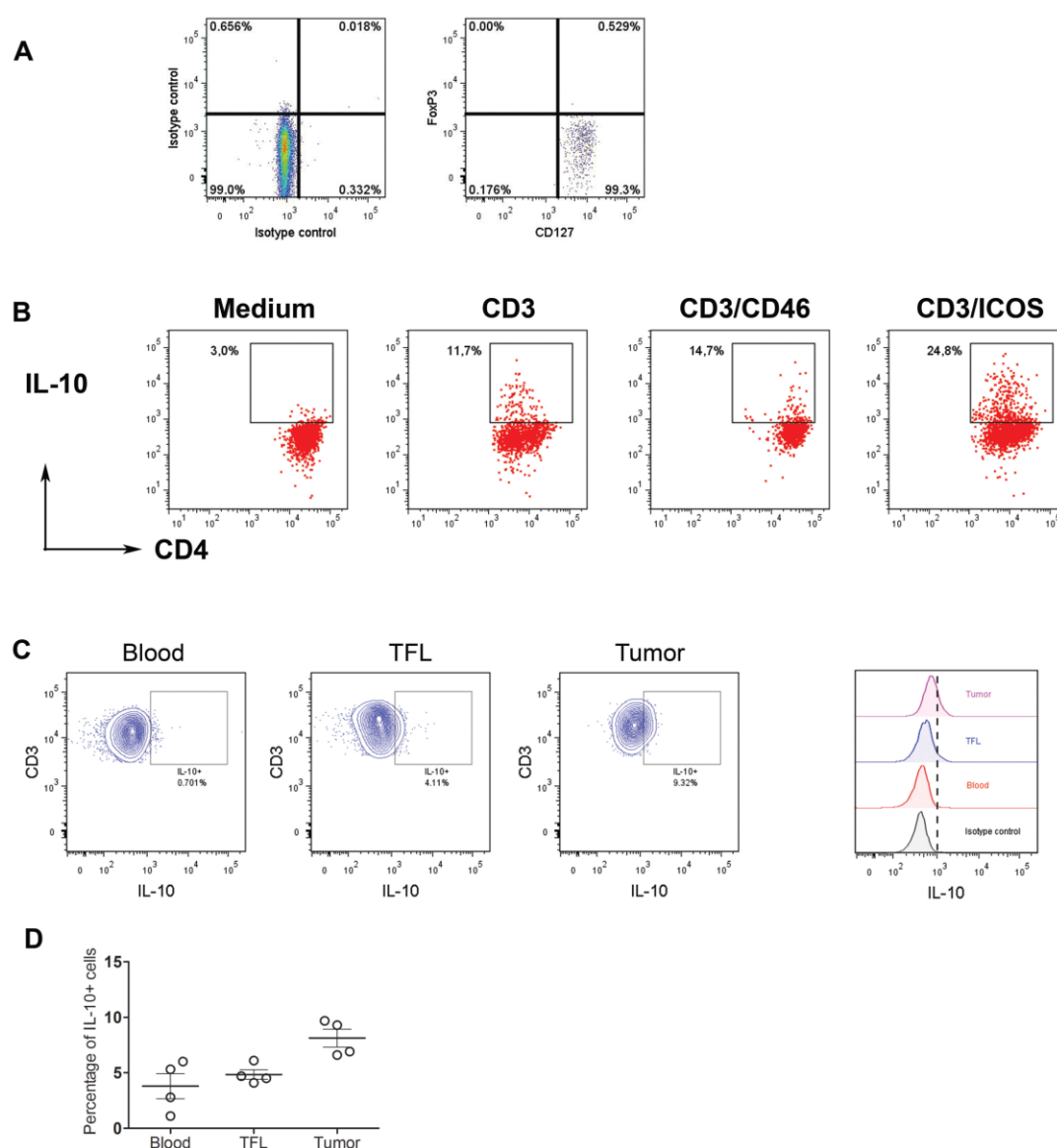**Figure 3.**

Figure 3

Figure 4.
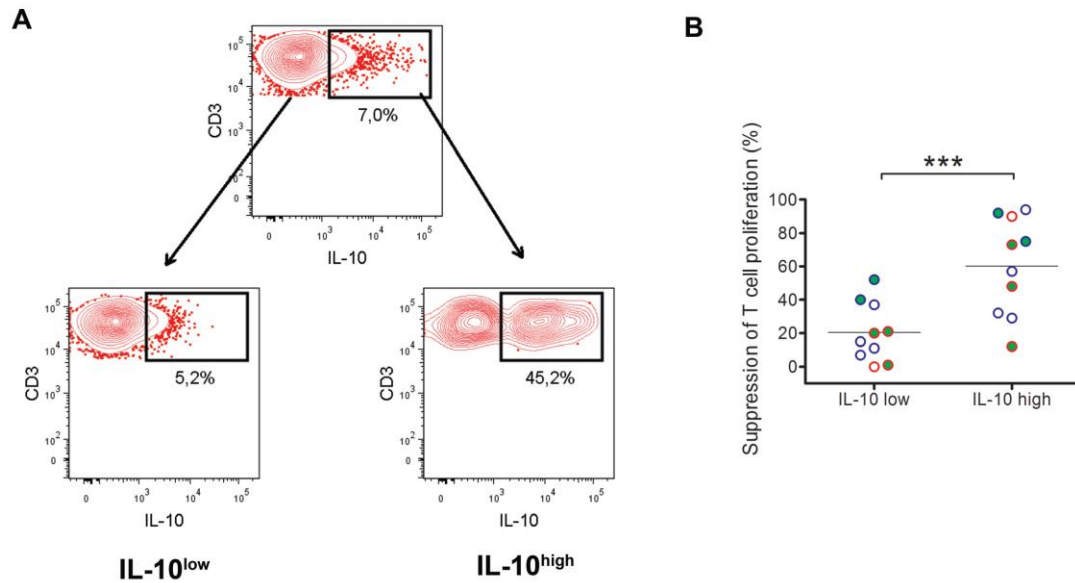

Figure 4

Supplementary Figure 1.

Supplementary figure 1. Cytokine analysis of CD4+ T cells from patients with liver cancer.
(A) Gating strategy for the analysis of intracellular cytokines by flow cytometry in MNCs suspensions isolated from blood, TFL or tumor tissue stimulated by PMA/ionomycin. Viable cells were gated using LIVE/DEAD fixable dead cell stain kit (Aqua). IFNγ, TNFα, IL-13 and IL-10 accumulation was analyzed in CD3+CD4+ T cells. (B) Two of five patients analyzed for the expression of IL-4. Cells were gated on viable CD3+CD4+IL-13-FoxP3- T cells. (C) Expression of IFNγ in Tr1 cells (CD3+CD4+IL-13-FoxP3-).
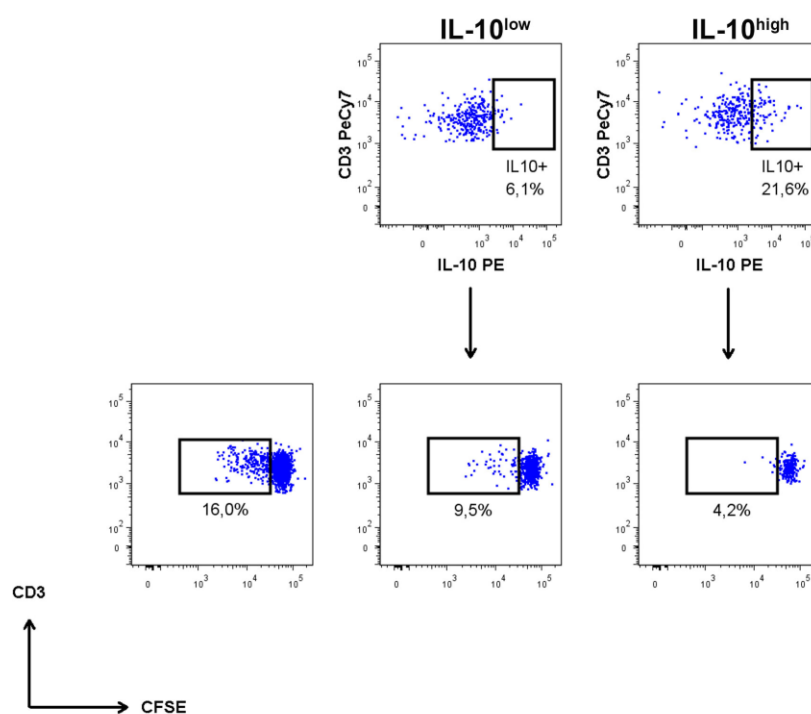
Supplementary Figure 2.

Supplementary figure 2. Stimulation of tumor-infiltrating CD4+CD25- IL-10-producing cells. (A) CD4+CD25- cells isolated from TILs of individuals with HCC or LM-CRC are FoxP3 negative and CD127 positive, and (B) were activated with beads-coupled antibodies to CD3 only, CD3 and CD46, or CD3 and ICOS in the presence of 250 U/ml of IL-2 for 24 hrs. Then cells were stained for IL-10 using a secretion assay and measured by flow cytometry. (C) CD4+CD25- T cells isolated from blood, TFL and tumor were activated with beads-coupled antiodies to CD3 and CD46 in the presence of IL-2 during 48 hrs and the frequency of IL-10+ cells was analyzed by flow cytometry. D) Analysis of the frecuency of IL-10+ cells among CD4+CD25- T cells activated with anti-CD3 and anti-CD46 antibodies (as described in C) in four patients.
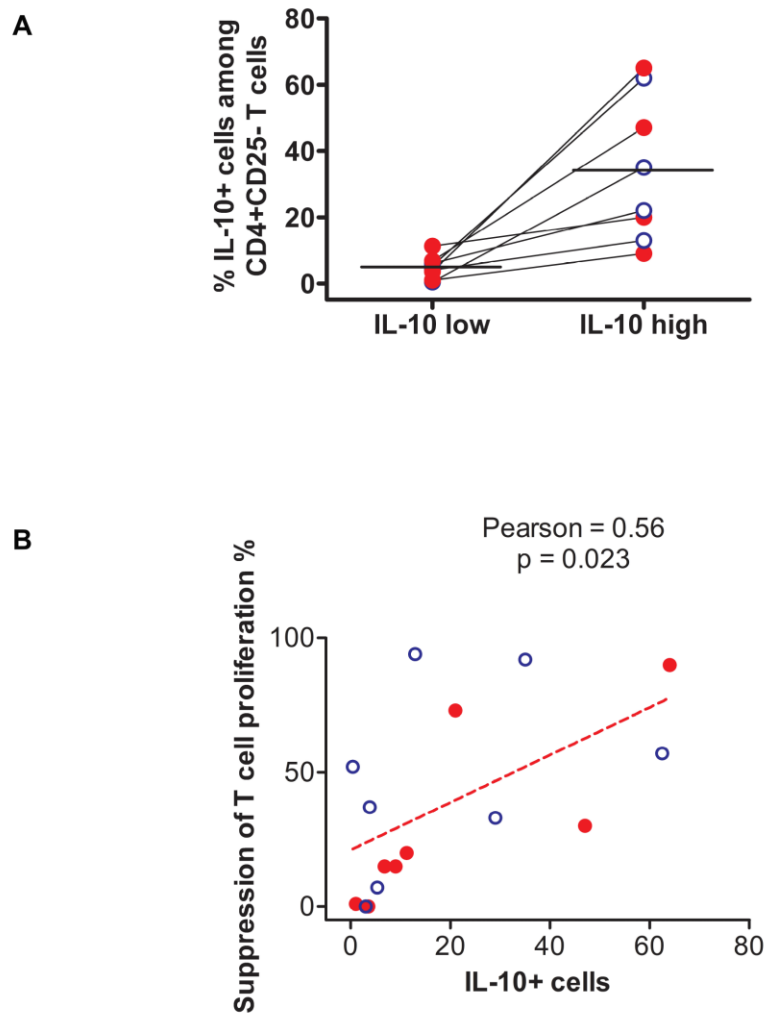
Supplementary Figure 3.

Supplementary figure 3. Isolation and functionality of tumor-infiltrating CD4+CD25- IL-10-producing cells. (A) CD4+CD25- cells isolated from TILs of individuals with HCC or LM-CRC were activated with beads-coupled antibodies to CD3 only, CD3 and CD46, or CD3 and ICOS in the presence of 250 U/ml of IL-2 for 24 hrs. Then cells were stained for IL-10 using a secretion assay and measured by flow cytometry. After activation and staining, cells were magnetically sorted based on the expression of IL-10. (B) Comparison of T cell suppression by tumor-infiltrating CD4+CD25- T cells stimulated with either CD3/ICOS (white dots) versus stimulation with CD3/CD46 (green dots). Red circles: CD4+CD25- T cells from HCC, blue circles: CD4+CD25- T cells from LM-CRC. No difference in suppressive activity was observed between the two protocols for IL-10 enrichment.
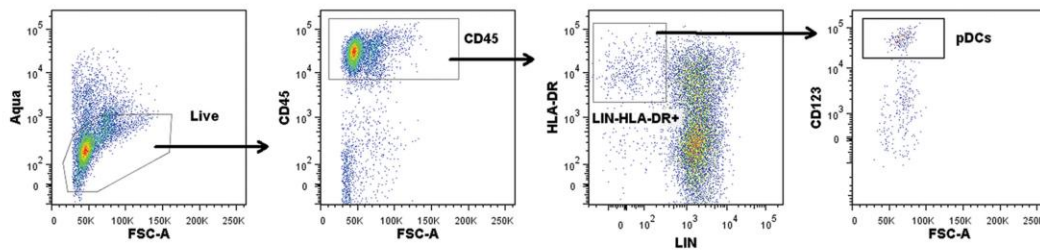
Supplementary Figure 4.

Supplementary figure 4. Tumor-infiltrating Tr1 cells efficiently suppress antigen-specific T cells. CFSE-labeled CD4+CD25- T cells from peripheral blood were stimulated with autologous mDCs that were activated with CMV antigens. Cells were co-cultured for 5 days in the absence or presence of autologous IL-10 low or IL-10 high CD4+ T cells isolated from tumor tissue. The Tr1:CD4+CD25- T cell ratio was 1:10. Proliferation was measured by flow cytometry. A representative analysis of one patient is showed.
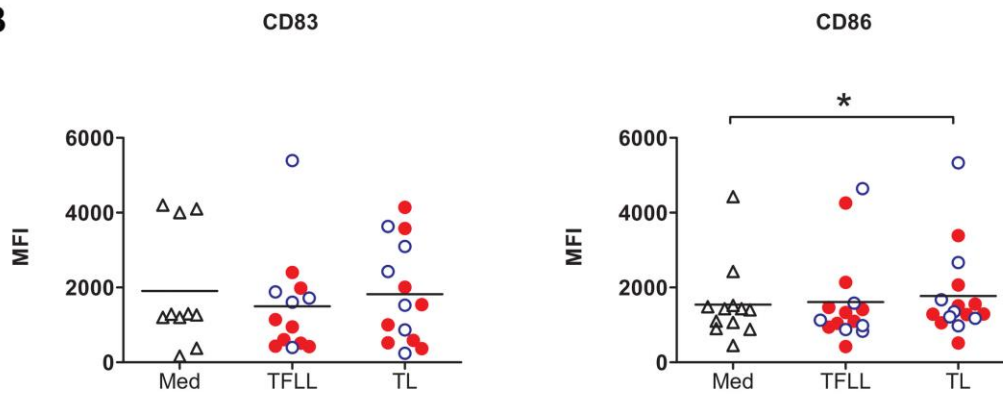
Supplementary Figure 5.

Supplementary figure 5. The suppressive capacity of tumor-infiltrating CD4+CD25- T cells depends on the numbers of IL10-producing cells. (A) Tumor-infiltrating CD4+CD25- T cells activated with beads-coupled antibodies to CD3 and ICOS or CD46 were stained and magnetically sorted as described in supplementary figure 3. The percentage of IL-10+ cells in each fraction was measured by flow cytometry. (B) Correlation analysis between the frequencies of IL-10+ cells detected in each fraction and the amount of suppression of PHA-stimulated CD3+ T cell proliferation observed. Red dots HCC samples and blue open dots LM-CRC samples.

Supplementary Figure 6.

A

B

Supplementary figure 6. Analysis of plasmacytoid DCs by flow cytometry. A) Flow cytometric staining for pDCs in freshly isolated cells from tumor tissue. Cells first were gated on viable cells that were HLA-DR+ and Lineage-, then pDCs were identified by the expression of CD123. B) Expression of CD83 and CD86 measured by flow cytometry on pDCs exposed to tissue lysates from HCC (red dots) or LM-CRC (blue open dots) or medium (trinangles).

Supplementary Material and Methods

Cell preparation

Peripheral blood mononuclear cells (PBMCs) were isolated by Ficoll density gradient centrifugation. Single cell suspensions from TFL and tumor tissue were obtained by tissue digestion. Fresh tissue was cut into small pieces and digested with 0.5 mg/ml of collagenase (Cat. C5138, Sigma-Aldrich) and 0.2 mg/ml of DNase I (Cat. 10104159001, Roche), for 30 minutes at 37 ºC. Cell suspensions were filtered through 100 and 70 µm pore cell-strainers (BD Biosciences) and mononuclear cells (MNCs) were obtained by Ficoll density gradient centrifugation. Viability was determined by trypan blue exclusion.

Cytokine analysis

Single cell MNCs isolated from blood, TFL or tumor were resuspended at 1 million per mL in sRPMI medium (RPMI 1640 medium supplemented with 2mM glutamine, 50 U/mL of penicillin, 50 ug/mL of streptomycin, 0.1 mM MEM nonessential amino acids, 10 mM Hepes buffer and 0.1 mM sodium pyruvate) with 10% fetal calf serum (FCS). Cells were stimulated with 50 ng/mL of PMA and 1 ug/mL of ionomycin (both from Sigma-Aldrich) for 5 hrs in the presence of brefeldin A (GolgiPlug, BD) and monensin (GolgiStop, BD) during the last 3 hrs. Then intracellular cytokine accumulation was analyzed by flow cytometry.

Flow cytometry antibodies

Anti-human antibodies used for flow cytometry: FITC-labeled anti-Lineage (CD3, CD14, CD16, CD19, CD20, CD56) cocktail-1 (Cat. 340546, BD Biosciences); Alexa Fluor 488-labeled anti-CD49b (AK-7, Cat. 314308, Biolegend), PE-labeled anti-IL-10 (JES3-9D7, Cat. 501404, Biolegend), anti-ICOS-L (MIH12, Cat.12-5889, e-biosciences), anti-IFNγ (B27, Cat. 559327, BD Biosciences) and anti-IL-13 (JES10-5A2, Cat. 559328, BD Biosciences); PerCP-labeled anti-HLA-DR (L243 Cat.347402, BD Biosciences) and anti-LAG-3 (FAB2319C, R & D Systems); PerCP-Cy5.5-labeled anti-IL-4 (8D4-8, Cat. 561234, BD Biosciences); APC-labeled anti-FoxP3 (236A/E7 Cat. 17-4777) and anti-TNFa (Mab11, Cat. 17-7349) from e-biosciences and anti-CD83 (HB15e, Cat. 305312, Biolegend); APC-H7-labeled anti-CD4 (SK3, Cat. 641398, BD Biosciences); PeCy7-labeled anti-CD3 (UCTH1, Cat. 25-0038), anti-CD123 (6H6, Cat. 25-1239), and anti-ICOS (ISA-3, Cat. 25-9948) form e-biosciences; eFluor®450-labeled anti-CD45 (HI30, Cat. 48-0459), anti-CD127 (eBioRDR5, Cat. 48-1278) and anti-CD25 (BC96, Cat.48-0259) from e-biosciences, and V450-labeled anti-CD86 (FUN-1, Cat. 560357) and anti-IL-13 (JES10-5A2, Cat. 561158) from BD biosciences.

Suppression of antigen-specific T cells by Tr1 cells

Myeloid DCs (mDCs) were isolated from PBMCs by positive selection (BDCA-1 DC isolation kit, Cat. 130-090-506, Miltenyi Biotec). Dendritic cells were suspended in sRPMI 1640 medium supplemented with 10% of human AB serum and cultured overnight at 37 °C in the presence of 10 µg/ml of Cytomegalovirus antigens (CMV, Cat. EL-01-02, Microbix biosystems, Canada). The CMV antigens is a preparation that contains proteins from all the virus cycle including early and late proteins, nuclear, cytoplasmic, structural and non-structural proteins. CMV-activated

DCs were co-cultured with autologous CFSE-labeled CD4+CD25- T cells isolated from PMBCs at a ratio of 1:10 for 5 days in the presence or absence of IL-10 producing CD4+ T cells. Co-cultures were performed in round-bottom 96-well plates with at least 5×10^4 responder T cells. Proliferation and cytokine production were measured by flow cytometry after re-stimulation with autologous monocyte-derived DC, which were <u>activated</u> with CMV antigens, in the presence of brefeldin A and monensin. Inhibition of T cell proliferation was determined by comparison with culture conditions without suppressive T cells and reported as percentage of suppression of T cell proliferation. Monocyte-derived DCs were obtained by culturing autologous monocytes with 10 ng/ml IL-4 and 50 ng/ml GM-CSF for 5 days, then immature DCs were activated with CMV antigens as described previously for mDCs.

Immunohistochemistry

Frozen sections (6 μm) from liver tissues were fixed with cold acetone for 5 minutes. Unspecific binding was quenched by pre-incubation with PBS containing 10 % goat serum and 5 % of bovine serum albumin for 30 minutes. Endogenous peroxidase blockage and the secondary reagents used to detect the primary antibodies were from the EnVision+ System (Dako). The sections were labelled with 10 μg/ml of anti-CD303 antibody (clone 104C12.08, Dendritics) followed by incubation with anti-mouse IgG antibodies conjugated to HRP- labelled polymer (Cat. K4005). The enzyme-linked secondary reagent was visualized with 3-amino-9-ethylcarbazole (AEC). Thereafter the sections were incubated with 10 μg/ml of anti-LAG-3 antibody (clone 17B4, Enzo Life Sciences) followed by an anti-mouse IgG antibodies conjugated with AP (Cat. D0314, Dako) and visualized with Fast blue. Positive cell were counted in different microscopic fields of 200 times magnification of several tumors by two investigators.

REFERENCES

1. Mazzanti R, Gramantieri L, Bolondi L. Hepatocellular carcinoma: epidemiology and clinical aspects. Mol Aspects Med 2008; 29:130-43.
2. Kemeny N. The management of resectable and unresectable liver metastases from colorectal cancer. Curr Opin Oncol 2010; 22:364-73.
3. Pardee AD, Butterfield LH. Immunotherapy of hepatocellular carcinoma: Unique challenges and clinical opportunities. Oncoimmunology 2012; 1:48-55.
4. Mazzolini G, Ochoa MC, Morales-Kastresana A, Sanmamed MF, Melero I. The liver, liver metastasis and liver cancer: a special case for immunotherapy with cytokines and immunostimulatory monoclonal antibodies. Immunotherapy 2012; 4:1081-5.
5. Pedroza-Gonzalez A, Xu K, Wu TC, Aspord C, Tindle S, Marches F, Gallegos M, Burton EC, Savino D, Hori T, et al. Thymic stromal lymphopoietin fosters human breast tumor growth by promoting type 2 inflammation. J Exp Med 2011; 208:479-90.
6. Palucka K, Banchereau J. Cancer immunotherapy via dendritic cells. Nat Rev Cancer 2012; 12:265-77.
7. Pedroza-Gonzalez A, Verhoef C, Ijzermans JN, Peppelenbosch MP, Kwekkeboom J, Verheij J, Janssen HL, Sprengers D. Activated tumor-infiltrating CD4+ regulatory T cells restrain antitumor immunity in patients with primary or metastatic liver cancer. Hepatology 2013; 57:183-94.
8. Pedroza-Gonzalez A, Kwekkeboom J, Sprengers D. T-cell suppression mediated by regulatory T cells infiltrating hepatic tumors can be overcome by GITRL treatment. Oncoimmunology 2013; 2:e22450.
9. Gregori S, Goudy KS, Roncarolo MG. The cellular and molecular mechanisms of immuno-suppression by human type 1 regulatory T cells. Front Immunol 2012; 3:30.
10. Roncarolo MG, Gregori S, Lucarelli B, Ciceri F, Bacchetta R. Clinical tolerance in allogeneic hematopoietic stem cell transplantation. Immunol Rev 2011; 241:145-63.
11. Kakita N, Kanto T, Itose I, Kuroda S, Inoue M, Matsubara T, Higashitani K, Miyazaki M, Sakakibara M, Hiramatsu N, et al. Comparative analyses of regulatory T cell subsets in patients with hepatocellular carcinoma: a crucial role of CD25(-) FOXP3(-) T cells. Int J Cancer 2012; 131:2573-83.
12. Marshall NA, Christie LE, Munro LR, Culligan DJ, Johnston PW, Barker RN, Vickers MA. Immunosuppressive regulatory T cells are abundant in the reactive lymphocytes of Hodgkin lymphoma. Blood 2004; 103:1755-62.
13. Lundqvist A, Palmborg A, Pavlenko M, Levitskaya J, Pisa P. Mature dendritic cells induce tumor-specific type 1 regulatory T cells. J Immunother 2005; 28:229-35.
14. Bergmann C, Strauss L, Zeidler R, Lang S, Whiteside TL. Expansion of human T regulatory type 1 cells in the microenvironment of cyclooxygenase 2 overexpressing head and neck squamous cell carcinoma. Cancer Res 2007; 67:8865-73.
15. Gagliani N, Magnani CF, Huber S, Gianolini ME, Pala M, Licona-Limon P, Guo B, Herbert DR, Bulfone A, Trentini F, et al. Coexpression of CD49b and LAG-3 identifies human and mouse T regulatory type 1 cells. Nat Med 2013; 19:739-46.
16. Kemper C, Chan AC, Green JM, Brett KA, Murphy KM, Atkinson JP. Activation of human CD4+ cells with CD3 and CD46 induces a T-regulatory cell 1 phenotype. Nature 2003; 421:388-92.
17. Hutloff A, Dittrich AM, Beier KC, Eljaschewitsch B, Kraft R, Anagnostopoulos I, Kroczek RA. ICOS is an inducible T-cell co-stimulator structurally and functionally related to CD28. Nature 1999; 397:263-6.
18. Ito T, Yang M, Wang YH, Lande R, Gregorio J, Perng OA, Qin XF, Liu YJ, Gilliet M. Plasmacytoid dendritic cells prime IL-10-producing T regulatory cells by inducible costimulator ligand. J Exp Med 2007; 204:105-15.
19. Conrad C, Gregorio J, Wang YH, Ito T, Meller S, Hanabuchi S, Anderson S, Atkinson N, Ramirez PT, Liu YJ, et al. Plasmacytoid dendritic cells promote immunosuppression in ovarian cancer via ICOS costimulation of Foxp3(+) T-regulatory cells. Cancer Res 2012; 72:5240-9.
20. Labidi-Galy SI, Sisirak V, Meeus P, Gobert M, Treilleux I, Bajard A, Combes JD, Faget J, Mithieux F, Cassignol A, et al. Quantitative and functional alterations of plasmacytoid dendritic cells contribute to immune tolerance in ovarian cancer. Cancer Res 2011; 71:5423-34.
21. Faget J, Bendriss-Vermare N, Gobert M, Durand I, Olive D, Biota C, Bachelot T, Treilleux I, Goddard-Leon S, Lavergne E, et al. ICOS-ligand expression on plasmacytoid dendritic cells supports breast cancer progression by promoting the accumulation of immunosuppressive CD4+ T cells. Cancer Res 2012; 72:6130-41.

22. Sisirak V, Faget J, Gobert M, Goutagny N, Vey N, Treilleux I, Renaudineau S, Poyet G, Labidi-Galy SI, Goddard-Leon S, et al. Impaired IFN-alpha production by plasmacytoid dendritic cells favors regulatory T-cell expansion that may contribute to breast cancer progression. Cancer Res 2012; 72:5188-97.

23. Chen KJ, Lin SZ, Zhou L, Xie HY, Zhou WH, Taki-Eldin A, Zheng SS. Selective recruitment of regulatory T cell through CCR6-CCL20 in hepatocellular carcinoma fosters tumor progression and predicts poor prognosis. PLoS One 2011; 6:e24671.

24. Nishikawa H, Sakaguchi S. Regulatory T cells in tumor immunity. Int J Cancer 2010; 127:759-67.

25. Yang XH, Yamagiwa S, Ichida T, Matsuda Y, Sugahara S, Watanabe H, Sato Y, Abo T, Horwitz DA, Aoyagi Y. Increase of CD4+ CD25+ regulatory T-cells in the liver of patients with hepatocellular carcinoma. J Hepatol 2006; 45:254-62.

26. Salama P, Phillips M, Grieu F, Morris M, Zeps N, Joseph D, Platell C, Iacopetta B. Tumor-infiltrating FOXP3+ T regulatory cells show strong prognostic significance in colorectal cancer. J Clin Oncol 2009; 27:186-92.

27. Bergmann C, Strauss L, Wang Y, Szczepanski MJ, Lang S, Johnson JT, Whiteside TL. T regulatory type 1 cells in squamous cell carcinoma of the head and neck: mechanisms of suppression and expansion in advanced disease. Clin Cancer Res 2008; 14:3706-15.

28. Akbari O, Freeman GJ, Meyer EH, Greenfield EA, Chang TT, Sharpe AH, Berry G, DeKruyff RH, Umetsu DT. Antigen-specific regulatory T cells develop via the ICOS-ICOS-ligand pathway and inhibit allergen-induced airway hyperreactivity. Nat Med 2002; 8:1024-32.

29. Le Mercier I, Poujol D, Sanlaville A, Sisirak V, Gobert M, Durand I, Dubois B, Treilleux I, Marvel J, Vlach J, et al. Tumor promotion by intratumoral plasmacytoid dendritic cells is reversed by TLR7 ligand treatment. Cancer Res 2013; 73:4629-40.

CHAPTER 4

Concerns regarding targeting tumor-infiltrating regulatory T cells with Fc-optimized anti-CD25 antibodies in humans

Adriaan A. van Beek[1], **Guoying Zhou**[1,6], Lisanne Noordam[1,6], Patrick P.C. Boor[1], Samantha Bucktrout[2], Susan ter Borg[3], Pascal G. Doornebosch[4], Michael Doukas[5], Dave Sprengers[1], Jaap Kwekkeboom[1]

[1]Department of Gastroenterology and Hepatology, Erasmus University Medical Center, Wytemaweg 80, 3015 CN, Rotterdam, The Netherlands.
[2]Rinat Laboratories, Pfizer Inc., 230 E. Grand Ave, South San Francisco, CA 94080, USA.
[3]Pathan B.V., Kleiweg 500, 3045 PM, Rotterdam, The Netherlands.
[4]Department of Surgery, IJsselland Ziekenhuis, Prins Constantijnweg 2, 2906 ZC, Capelle aan den IJssel, The Netherlands.
[5]Department of Pathology, Erasmus University Medical Center, Wytemaweg 80, 3015 CN, Rotterdam, The Netherlands.
[6]These authors contributed equally.

ABSTRACT

A recent paper suggested the use of Fc-modified anti-CD25 antibody for enhancing anti-tumor immunity by intratumoral regulatory T cell (Treg) depletion, because of selectively enhanced expression of the inhibitory CD32b (FcγRIIb) on myeloid cells in mouse tumors. We interrogated hepatocellular carcinoma (HCC) and colorectal carcinoma (CRC) tumor, tumor-free tissue, lymph node, and peripheral blood immune subsets for CD25 expression on effector T cell and Treg subsets, and FcγR expression on cytotoxic innate immune cells.

We show that CD25 is not solely expressed on bona fide Treg, but also on CD4$^+$FoxP3^{lo}CD45RA$^-$ non-Treg in all studied tissues and peripheral blood from HCC and CRC patients. Furthermore, CD32b is not selectively upregulated in human tumors, but instead inhibitory as well as activatory FcγR are differentially expressed on myeloid cells in human tumors, tumor-free tissues and blood. Intratumoral NK cells have a strongly reduced expression of CD16 (FcγRIII).

Treatment with anti-CD25 mAb (daclizumab) did not show any clinical benefit in two studies in cancer patients. Both studies indicated that CD25-expressing non-Treg were affected.

We conclude that CD25-depleting antibodies in its current antibody configuration and dosing would not be appropriate for intratumoral Treg depletion in humans. We discuss possible improvements of CD25-depleting antibodies, as well as alternative targets to deplete human Treg.

Keywords: CD25, Regulatory T cell, Effector T cell, Daclizumab, FcγR, Cancer Immunotherapy

Précis: Expression of CD25 on non-Treg challenges the clinical use of anti-CD25 mAb in cancer patients. Fc optimization of anti-CD25 mAb may improve ADCC activity of intratumoral CD14$^+$ cells, but could also result in depletion of non-Treg in patients.

INTRODUCTION

In a recent paper in Immunity, Arce Vargas et al. demonstrated superior depletion of intratumoral CD4$^+$FoxP3$^+$ regulatory T cells (Treg) in mouse tumor models, including two models for colorectal carcinoma (CRC), using an anti-CD25 mAb with mouse IgG2a constant regions. As opposed to the original rat IgG1 mAb which only binds to a single activatory FcγR, CD16 (FcγRIII), and to the inhibitory CD32b (FcγRIIb), the mouse IgG2a mAb binds to all mouse Fcγ receptor (FcγR) types [1]. In contrast to the rat IgG1 mAb, the mIgG2a CD25 mAb synergized with anti-PD1 mAb treatment to eradicate established tumors in multiple mouse tumor models. Moreover, based on increased CD25 expression on human CD4$^+$FoxP3$^+$ Treg in blood and TIL of melanoma, non-small cell lung carcinoma, and renal cell carcinoma patients, the authors concluded that CD25 is an attractive target for Treg depletion in human tumors [1].

However, FoxP3 alone has been shown to be insufficient for characterizing human Treg [2]. Moreover, recent work has characterized that human CD4$^+$FoxP3^{lo} cells comprise of non-Treg cells which produce pro-inflammatory cytokines and are non-suppressive [3]. Saito et al. highlighted that FoxP3 as a single marker to define Treg cells contributed to contradictory outcomes on the prognostic value of intratumoral Treg numbers in previous CRC studies. Furthermore, they reported that high frequencies of intratumoral CD4$^+$FoxP3^{lo}CD45RA$^-$ non-Treg cells were associated with better prognosis of CRC patients [4], suggesting a critical contribution of this non-Treg subset to anti-tumor immunity.

In addition, although we appreciate the work performed by the authors to demonstrate the requirement for a high activatory to inhibitory FcγR ratio (A/I) of anti-CD25 mAb to efficiently deplete intratumoral Treg in mouse tumor models, we would like to recall that anti-CD25 mAb treatment in human cancer patients has already been performed in combination with therapeutic vaccinations, but without any clinical benefit [5, 6]. In these studies, anti-CD25 mAb daclizumab was used, which is a humanized IgG1 mAb. Importantly, human IgG1 can bind well to all types of activating human FcγR [7]. Arce Vargas et al. show that rat IgG1 CD25 mAb depletes mouse Treg from blood and lymph nodes, but not from MCA205 sarcoma tumors due to high intratumoral expression of the inhibitory CD32b. They show increased CD32b expression on innate immune cell subsets in MCA205 tumors compared to secondary lymphoid tissues of mice, and demonstrate that intratumoral Treg depletion is restored in mice lacking expression of CD32b [1]. Based on these data, they suggest that the absence of beneficial effects of daclizumab in cancer patients may also be explained by increased CD32b expression in the tumor microenvironment. This suggestion is, however,

not corroborated by data from human tumors, which is critically important considering the substantial differences between FcγR repertoires and expression patterns between mice and men (8). In particular, mice express the activatory FcγRIV, which binds mIgG2a with high affinity (9), also shown by Arce Vargas et al. for the mIgG2a CD25 mAb (1). FcγRIV is highly enriched on mouse tumor myeloid cells, and is crucial for efficacy of anti-CTLA4 mAb therapy in a mouse melanoma model (10). This FcγR is not found in humans, and over-represents therefore ADCC activity compared to human.

To evaluate CD25 expression on T helper cell subsets in human cancer, we compared the use of FoxP3 alone versus the use of FoxP3 and CD45RA together, as recommended by Miyara et al. (3) and Saito et al. (4), to discriminate Treg and non-Treg in tumors, tumor-free adjacent tissues, lymph nodes, and blood of patients with hepatocellular carcinoma (HCC) and CRC. Furthermore, we compared FcγR expression on NK cells, and monocytes and macrophages in tumors, non-malignant tissues, and blood of HCC and CRC patients.

PATIENTS AND METHODS

Patients

Seventeen patients who received surgical tumor resection or liver transplantation for hepatocellular carcinoma (HCC) and sixteen patients who received surgical resection of colorectal carcinoma (CRC) were enrolled in the study from August 2016 to November 2017. Fresh tumor-free liver or tumor-free colorectal tissue (≥1cm from tumor), and fresh tumor tissue were obtained from the patients. Liver lymph nodes were obtained from explanted livers of three HCC patients undergoing liver transplantation. Peripheral blood was obtained from all HCC patients and seven CRC patients, just before resection. The clinical characteristics of the patients are summarized in Table 1 (HCC) and Table 2 (CRC).

Tissue digestion and cell preparation

Peripheral blood mononuclear cells (PBMC) were isolated by Ficoll density gradient centrifugation. Single cell suspensions from HCC tumor and tumor-free liver were obtained by digesting cut tissue fragments with 0.125 mg/mL collagenase IV (C5138, Sigma-Aldrich, St. Louis, MO), 500 U/mL hyaluronidase V (H6254, Sigma-Aldrich), 0.2 mg/mL DNAse I (DN25, Sigma-Aldrich), in Hanks' Balanced Salt Solution (H8264, Sigma, Zwijndrecht, The Netherlands) supplemented with 5% fetal calf serum (FCS) under continuous stirring for 30 minutes at 37°C. Tumor-draining lymph nodes were digested under similar conditions for 15 minutes at 37°C. To release epithelial cells, small parts of tumor-free colorectal tissue were first incubated at 37°C in PBS supplemented with 1 mM EDTA, 2.6 mg/mL HEPES and 10%

FCS, for four times 15 minutes. Then, small fragments of tumor-free colorectal tissue and CRC tumor were digested with 400 U/mL collagenase VIII (C2139, Sigma-Aldrich, St. Louis, MO), 500 U/mL hyaluronidase V (H6254, Sigma-Aldrich), 0.2 mg/mL DNAse I (DN25, Sigma-Aldrich) in Hanks' Balanced Salt Solution (H8264, Sigma, Zwijndrecht, The Netherlands) supplemented with 5% FCS under continuous stirring for 45 minutes at 37°C, followed by a second incubation with fresh digestion medium for 20-45 minutes. Cell suspensions from tumor tissue, tumor-free tissue, and lymph node were filtered through 100 µm pore cell strainers (BD Biosciences, Erembodegem, Belgium) and mononuclear immune cells were obtained by Ficoll density gradient centrifugation. Viability was determined by trypan blue exclusion.

Flow cytometry

Flow cytometry was performed using standard procedures. In brief, cells were incubated with live/dead eFluor506 stain (eBioscience, Vienna, Austria) for 20 minutes at 4°C, after which cells were stained with specific antibodies for surface markers (Table 3) for 20 minutes at 4°C. Cells were fixed and permeabilized with the FoxP3 staining buffer set (eBioscience) for 30-45 minutes at room temperature. Intracellular FoxP3 staining was performed for 20 minutes at 4°C, after which cells were acquired using a FACSAria SORP II (BD Biosciences, San Diego, USA). Analysis was performed using FlowJo software vX.07 (Tree Star, San Carlos, USA). Isotype controls were used to set gatings.

Statistical analysis

Kruskal-Wallis test with Dunn's Multiple Comparison Test was used for testing significance for data sets with missing values. Repeated Measures ANOVA Test with Tukey's Multiple Comparison Test (if distribution parametric) or Friedman test with Dunn's Multiple Comparison Test (if distribution non-parametric) was used for testing significant differences in complete paired data sets. Statistical analyses were performed with GraphPad Prism Software (version 5.0). Significant differences are indicated with asterisks: *=$p<0.05$; **=$p<0.01$; ***=$p<0.001$.

RESULTS AND DISCUSSION

Substantial CD25 expression on CD4$^+$FoxP3^{lo}CD45RA$^-$ non-Treg cells

We analyzed CD25 expression on T cell subsets isolated from blood, tumor tissue, adjacent tumor-free tissue, and tumor-draining lymph nodes from 12 patients with hepatocellular carcinoma (HCC) and 10 patients with colorectal carcinoma (CRC). First, similar to Arce

Vargas et al., we analyzed CD25 expression on CD4$^+$FoxP3$^-$ T cells, CD4$^+$FoxP3$^+$ T cells, and CD4$^-$ T cells (Figure 1a). Based on these subset definitions, our data confirmed the findings of Arce Vargas et al. demonstrating that CD25 expression is mainly restricted to CD4$^+$FoxP3$^+$ T cells in PBMC, tumor-free tissues, tumors, and lymph nodes (Figure 1b-e). Subsequently, we included CD45RA in the analysis to distinguish CD4$^+$FoxP3^{lo}CD45RA$^-$ non-Treg cells from CD4$^+$FoxP3^{lo}CD45RA$^+$ resting Treg and CD4$^+$FoxP3^{hi}CD45RA$^-$ activated Treg (Figure 1f). Importantly, CD4$^+$FoxP3^{lo}CD45RA$^-$ non-Treg cells also expressed substantial levels of CD25 in all tissues, on the average at similar levels as resting Treg and in some individual patients at similar levels as activated Treg (Figure 1g-j). Although the mean proportion of CD25-expressing CD4$^+$FoxP3^{hi}CD45RA$^-$ activated Treg was higher than in any other T cell subset, we also observed CD25 expression in up to 80% of CD4$^+$FoxP3^{lo}CD45RA$^-$ non-Treg cells in HCC patients, and up to 60% in CRC patients. Finally, we found that these cells are significantly more present in tumors than in blood or tumor-free tissues, representing up to 25% of total intratumoral CD4$^+$ T cells (Figure 1k).

These data show that CD25 expression in humans is not restricted to Treg, but that CD4$^+$FoxP3^{lo}CD45RA$^-$ non-Treg cells, which critically contribute to anti-tumor immunity (7), also express CD25. This observation is further corroborated by recent data on CD25 expression on circulating T cells from head and neck squamous cell carcinoma patients (11). In addition to CD25 expression on T cells, Simoni et al. recently showed high CD25 expression on human innate lymphoid cells type 2 and 3 (12).

Lack of clinical efficacy of daclizumab

Since CD4$^+$FoxP3^{lo}CD45RA$^-$CD25$^+$ non-Treg cells are probably antigen-experienced T helper cells, which are critical in the anti-tumor immune response (13), anti-CD25 mAb therapy in cancer patients might cause unwanted adverse effects. Although administration of daclizumab to metastatic melanoma patients resulted in significant reduction of circulating CD4$^+$FoxP3$^+$ Treg, daclizumab did not enhance clinical efficacy of dendritic cell (DC) vaccination and prevented the generation of functional vaccine-specific antibodies (5). Jacobs et al. discuss several possible reasons, which they could not investigate in their study, for the absence of clinical benefit. For instance, lack of depletion of CD25-expressing cells at the site of tumor-draining lymph nodes or tumor. Also, timing and dosing of daclizumab infusion may be crucial. They suggest that targeting a better Treg-specific marker to specifically deplete or inactivate Treg could overcome the daclizumab-related problems encountered in their clinical trial (5). Interestingly, recent novel data of Arce Vargas et al. (2018) show that targets like GITR, OX40, and CTLA4 are more highly expressed on

human CD4$^+$FoxP3$^+$ cells than CD25 is (14). These targets may be better candidates for depletion of Treg. However, the expression of GITR, OX40, and CTLA4 on human CD4$^+$FoxP3^{lo}CD45RA$^-$ non-Treg cells is unclear as yet.

A second study in metastatic breast cancer patients demonstrated similar decreases of circulating CD4$^+$FoxP3$^+$CD25$^+$ T cells after combined peptide vaccination and daclizumab infusion (6). However, the vaccine-specific T cell responses after vaccination and daclizumab were not significantly different compared with those in an earlier study that evaluated the effect of peptide vaccination only. Together, these data indicate that daclizumab has no clinical benefit in treating cancer patients. Jacobs et al. reported that daclizumab binds to small fractions of NK cells, CD4$^+$ T cells, and CD8$^+$ T cells, and that daclizumab in patient serum disarms effector T cells *in vitro* (5). Importantly, Rech et al. showed that daclizumab infusion resulted in significantly decreased frequencies of circulating CD4$^+$FoxP3$^-$CD25$^+$ T cells and CD8$^+$CD25$^+$ T cells (6), showing that CD25 antibody targeting in humans, even by a single dose treatment, really affects non-Treg cells.

Two mechanisms by which daclizumab inhibits CD25-expressing T cells have been described. It blocks IL-2 binding to the high-affinity IL-2R (15, 16). Rech et al. have shown that daclizumab, at least *in vitro*, can reprogram Treg to non-suppressive IFN-γ-producing T cells (6). Therefore, the reduction of non-Treg by daclizumab that they observed may be due to reprogramming of Treg and not due to ADCC. Nevertheless, daclizumab also induces antibody-dependent cell-mediated cytotoxicity (ADCC) (17), although the ADCC activity of daclizumab seems low compared with the ADCC activity of rituximab (6). Fc-optimization of therapeutic anti-CD25 mAb by increasing their A/I ratio (as suggested by Arce Vargas et al.) to enhance their ADCC-inducing capacity, has the risk of enhanced depletion of CD25-expressing non-Treg subsets in humans, and may be counter to enhance anti-tumor immunity. On the other hand, it has been reported that target molecule density and median fluorescence intensity (MFI) is important in the context of ADCC of TIL. If target molecules like GITR, OX40, or CTLA4 are expressed by multiple cell subsets, preferential depletion of those with highest relative expression is observed in mouse tumor models (10, 18-20). As yet, it is unknown whether the difference in CD25 expression level between Treg and non-Treg is sufficient to enable selective Treg depletion from human tumors, and therefore it is unclear whether CD25 antibody targeting can be used to selectively deplete Treg from human tumors. It also remains to be demonstrated whether an anti-CD25 antibody optimized for ADCC leads to preferential depletion of Treg from human tumors. If so, Fc optimization of anti-CD25 antibody, or combining anti-CD25 treatment with antagonistic anti-CD32b antibody may be beneficial, as observed with anti-CD20 antibody treatment (21). However, caution is

warranted. While the data of Rech et al. indicate that low dose anti-CD25 antibody therapy already can reduce numbers of circulating effector T cells (6), it is beyond doubt that high doses of anti-CD25 antibodies daclizumab and basiliximab severely target effector T cells in humans, and are for this reason widely used to prevent acute graft rejection after solid organ transplantation (15). We propose therefore to study the potential of depleting anti-CD25 antibodies which do not block binding of IL-2 to CD25, thereby preventing the risk of IL-2 deprivation and subsequent depletion of effector T cells.

In this respect, it is remarkable to note the differences in CD25 expression on intratumoral effector T cells and Treg in relation to the differences in efficacy of anti-CD25 mIgG2a and anti-PD1 mAb combination treatment between tumor models reported by Arce Vargas et al. (1). Lower CD25 expression on CD4$^+$FoxP3$^+$ TIL was observed in MC38 CRC than in MCA205 sarcoma and CT26 CRC, and MC38 tumors also responded less well to anti-CD25 mIgG2a and anti-PD1 mAb combination treatment than MCA205 and CT26 tumors. Interestingly, their data show that in MC38 mice the expression levels of CD25 on intratumoral Treg are about 2.5 times higher than on CD4$^+$FoxP3$^-$ T cells, while in the MCA205 and CT26 models CD25 expression levels on intratumoral Treg are about 5.5 times higher than those on CD4$^+$Foxp3$^-$ TIL. It raises the question whether smaller difference in CD25 expression between Treg and CD4$^+$Foxp3$^-$ TIL may have led to inferior Treg depletion from the tumors in the MC38 model, or may have led to increased depletion of CD4$^+$FoxP3$^-$ TIL, thereby counteracting the therapeutic effect of intratumoral Treg depletion. Data on intratumoral Treg or effector T cell depletion from the MC38 model are not shown, and the lack of these data hampers firm conclusions. Our data show that CD25 expression on FoxP3^{hi}CD45RA$^-$ activated Treg in human HCC and CRC tumors is only ~3 times higher than CD25 expression on FoxP3^{lo}CD45RA$^-$ non-Treg in the same tumors (HCC: MFI FoxP3^{hi}CD45RA$^-$ activated Treg 1887 versus FoxP3^{lo}CD45RA$^-$ non-Treg 708; CRC: mean MFI FoxP3^{hi}CD45RA$^-$ activated Treg 1549 versus FoxP3^{lo}CD45RA$^-$ non-Treg 476). As target molecule density and MFI are important in the context of ADCC, this relatively small difference, as compared with mouse models, may warrant further study.

FcγR expression in human tumors does not correspond to FcγR expression in mouse tumors

While in mouse tumor models Fc-optimization of CD25 mAb was required to efficiently deplete Treg from tumors because of enhanced expression of the inhibitory CD32b in the tumor microenvironment (1), it is unknown whether CD32b is also upregulated in human tumors. Therefore, we investigated FcγR expression in the human tumor setting. We focused

on CD3⁻CD56⁺ NK cells and CD14⁺ monocytes/macrophages as the major cell types involved in ADCC, which are also abundantly present in several tumor types.

First, we confirmed staining patterns expected for CD32b on B cells. Most B cells indeed bound the anti-CD32b, but not the anti-CD32a antibody (Figure 2a). Using the same antibodies, we observed that a major part of tissue-derived CD14⁺ cells expressed both CD32a and CD32b, but also distinguishable fractions of CD14⁺ cells expressed CD32a or CD32b alone (Figure 2b).

The expression of the activatory FcγR CD16 was reduced on NK cells from HCC and CRC tumors, as well as on tumor-free tissue NK cells compared with circulating NK cells (Figure 3a-b). However, in CRC, more tumor NK cells expressed CD16 than tumor-free tissue NK cells (Figure 3b). Only low frequencies of NK cells expressing activatory FcγR CD32a and CD64 were observed (data not shown). Compared with blood, the inhibitory CD32b expression was increased on NK cells in tumor-free tissues, but not in HCC and CRC tumors (Figure 3a-b). Compared with blood, not only the inhibitory CD32b, but also the activatory CD64 was upregulated on CD14⁺ cells in tumor-free and HCC and CRC tumor tissues (Figure 3c-d). In HCC patients, frequencies of CD16⁺CD14⁺ cells were highest in tumors, lowest in blood and intermediate in tumor-free liver tissues (Figure 3c), with a similar trend in CRC patients (Kruskal-Wallis p=0.083, Figure 3d).

While immune cells in HCC and CRC tumors were largely similar in terms of FcγR expression, the frequencies of NK cells and CD14⁺ cells were very different between HCC and CRC. In HCC patients frequencies of NK cells and CD14⁺ cells were similar between blood, liver, and tumor tissues (Figure 3a, 3c), whereas these cell frequencies were significantly lower in colorectal and tumor tissues of CRC patients (Figure 3b, 3d).

Together, these data show that upregulation of the inhibitory CD32b on CD14⁺ monocytes/macrophages is not unique for human tumors but is also found in tumor-free tissues. In addition, compared with blood, the activatory FcγR CD16 and CD64 are upregulated on CD14⁺ cells in both tumors and tumor-free tissues. Since CD16 on human CD14⁺ cells is indispensable for human IgG1 to mediate ADCC (22, 23) and CD16⁺CD14⁺ monocytes have a unique capacity to lyse Treg by ADCC (24), these data suggest that inhibition of ADCC capacity of intratumoral CD14⁺ cells by enhanced CD32b expression may be compensated by higher CD16 expression. However, we observed that nearly all CD14⁺ cells in tumor and tumor-free tissues that express CD16 co-express CD32b (Figure 4). This observation suggests a potential barrier for ADCC induction by IgG1 and supports that Fc

optimization may be needed to increase intratumoral ADCC activity of depleting antibodies in humans.

In contrast to the data on mouse tumors presented by Arce Vargas et al. (1), NK cells in human tumors (and tumor-free tissues) have reduced expression of their sole activatory FcγR CD16, potentially reducing the capacity for ADCC. Interestingly, our data match with the recent data on FcγR expression on NK cells and myeloid cells in human melanoma, published by Arce Vargas et al. (14). Our data may suggest that in humans intratumoral NK cells, but not monocytes and macrophages, have reduced ADCC capacity. In addition, human CRC tumors contain very few NK cells. Therefore, intratumoral depletion of Treg by endogenous NK cells in humans may more be challenging than suspected on basis of mouse tumor models, and design of Treg-depleting antibodies should focus on optimizing ADCC by intratumoral macrophages.

CONCLUSIONS

We conclude that CD25 is, until now, a less attractive target for cancer immunotherapy in humans than suggested by Arce Vargas et al. (1), for two reasons:

1) Substantial expression of CD25 on CD4$^+$FoxP3^{lo}CD45RA$^-$ non-Treg cells and innate lymphoid cells type 2 and 3; anti-CD25-mediated depletion of these cells may counteract enhancement of anti-tumor immunity by Treg depletion.

2) Anti-CD25 mAb daclizumab did not show any clinical benefit in cancer patients. Two clinical studies indicate that CD25-expressing non-Treg cells are affected and this may disrupt anticipated results.

With regard to Fc optimization, we show that FcγR expression on intratumoral immune cells differs between mice and humans. Based on the observed reduction of CD16 expression on intratumoral NK cells in human cancer patients, ADCC capacity of NK cells in human tumors may be more limited than previously expected. On the other hand, Fc optimization of Treg-depleting antibodies may result in enhanced ADCC activity by intratumoral monocytes/macrophages. We propose that anti-CD25 antibodies designed to deplete Treg from tumors should not block binding of IL-2 to CD25, in order to prevent depletion of effector T cells.

In sum, monitoring of activity of daclizumab or next-generation anti-CD25 antibodies on human TIL seems crucial to identify the role of human FcγR. Future research to develop or optimize Treg-depleting mAb therapies should focus on activity of anti-CD25 antibodies in

human tumors, or use of more Treg-selective targets than CD25. Finally, timing and dosing of anti-CD25 treatment should be carefully considered in future trials to improve clinical benefit for cancer patients.

COMPLIANCE WITH ETHICAL STANDARDS

Ethical approval: All procedures performed in studies involving human participants were in accordance with the ethical standards of the institutional research committee and with the 1964 Helsinki declaration and its later amendments or comparable ethical standards. The study was approved by the local ethics committee of the Erasmus University Medical Center. Informed consent was obtained from all individual participants included in the study.

Figure legends

Figure 1. FoxP3^{lo}CD45RA$^-$ non-Treg cells express substantial levels of CD25. (a) Representative example of flow cytometry analysis dividing live CD45$^+$CD3$^+$ cells into CD4$^-$ T cells, CD4$^+$FoxP3$^-$ T cells, and CD4$^+$FoxP3$^+$ regulatory T cells (Treg). **(b)-(e)** Bars show mean values of CD25 median fluorescence intensity (MFI) on, or of CD25$^+$ frequencies within the defined subsets shown in (a), measured in blood, tumor-free (TF) tissue, tumor tissue, and tumor-draining lymph nodes (tdLN) from HCC and CRC patients. **(f)** Representative example of flow cytometry analysis dividing live CD45$^+$CD3$^+$CD4$^+$ cells into five fractions: FoxP3$^-$CD45RA$^+$ cells (fraction V), FoxP3$^-$CD45RA$^-$ cells (fraction IV), FoxP3^{lo}CD45RA$^-$ cells (fraction III, non-Treg), FoxP3^{hi}CD45RA$^-$ cells (fraction II, activated Treg), and FoxP3^{lo}CD45RA$^+$ cells (fraction I, resting Treg), and corresponding CD25 histograms. **(g-j)** Bars show mean values of CD25 median fluorescence intensity (MFI) on, or of CD25$^+$ frequencies within the defined subsets shown in (f). **(k)** Bars show mean percentage of FoxP3^{lo}CD45RA$^-$ non-Treg cells in indicated tissues of HCC and CRC patients. Kruskal-Wallis test with Dunn's Multiple Comparison Test was used for testing significant differences. Each symbol represents one tissue per patient.. *=p<0.05; **=p<0.01; ***=p<0.001.

Figure 2. Distinction between CD32a and CD32b. (a) Representative examples of flow cytometry analysis of CD32a and CD32b expression on live CD19$^+$ B cells in blood, tumor-free colon (TFC), and CRC tumor. Gates based on isotype staining. **(b)** Representative examples of flow cytometry analysis of CD32a and CD32b expression on live CD14$^+$ cells in blood, TFC, and CRC tumor. Gates based on isotype staining.

Figure 3. FcγR expression on CD3⁻CD56⁺ NK cells and CD14⁺ monocytes and macrophages in human tumors. (a) Lines shown mean frequencies (+SEM) of CD3⁻CD56⁺ NK cells, and CD16⁺ and CD32b⁺ frequencies within NK cells in blood, tumor-free (TF) tissue, and tumor of HCC patients. **(b)** As in (a), for blood and tissues of CRC patients. **(c)** Lines show mean (+SEM) frequencies of CD14⁺ monocytes and macrophages, and CD16⁺, CD32a⁺, CD32b⁺, and CD64⁺ frequencies within monocytes/macrophages in blood, tumor-free (TF) tissue, and tumor of HCC patients. **(d)** As in (c), for blood and tissues of CRC patients. Repeated Measures ANOVA Test with Tukey's Multiple Comparison Test or Friedman Test with Dunn's Multiple Comparison Test used for testing significance in HCC patients. Kruskal-Wallis test with Dunn's Multiple Comparison Test was used for testing significance in CRC patients. Each symbol represents one tissue per patient. *=$p<0.05$; **=$p<0.01$; ***=$p<0.001$.

Figure 4. Co-expression of CD32b and CD16 on CD14⁺ monocytes and macrophages in human tumors. Representative examples of flow cytometry analysis of CD16 and CD32b on live CD14⁺ cells in blood, TFC, and CRC tumor. Gates based on isotype staining.
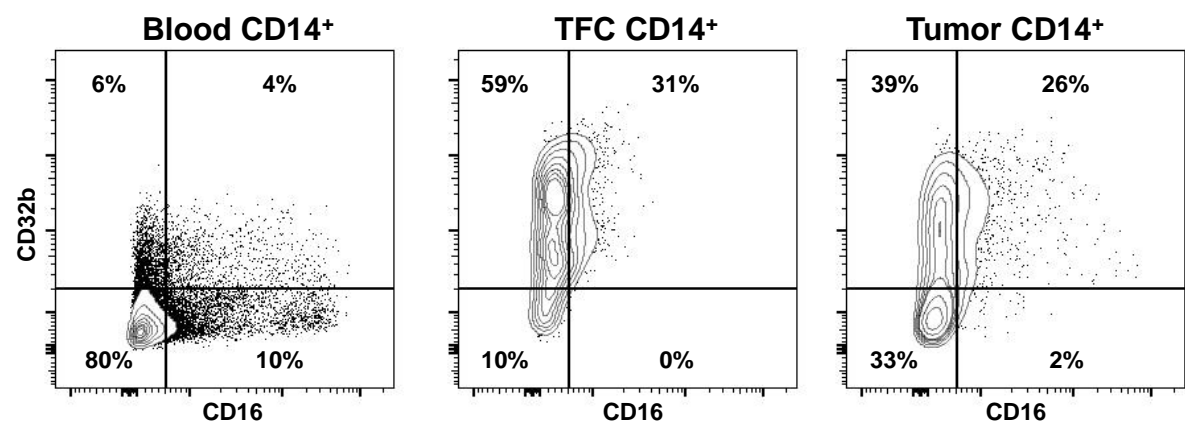
Figure 1.
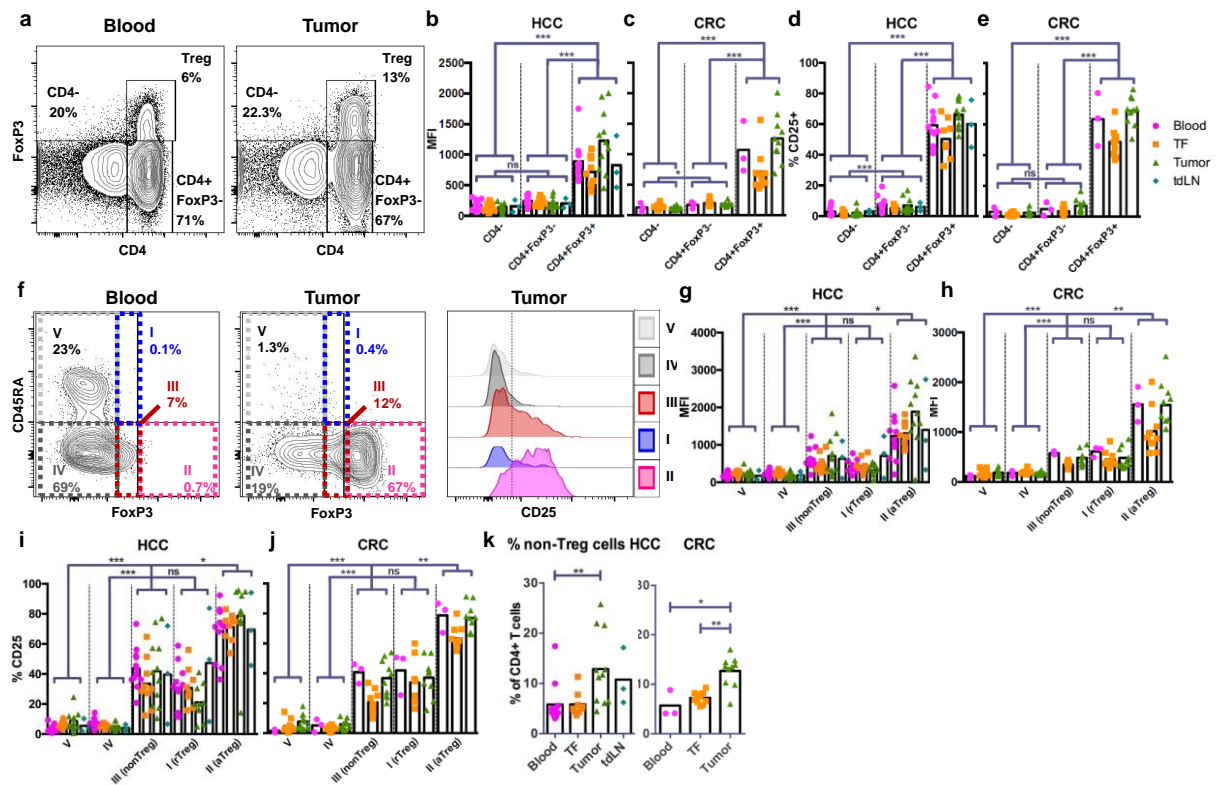
Figure 2.
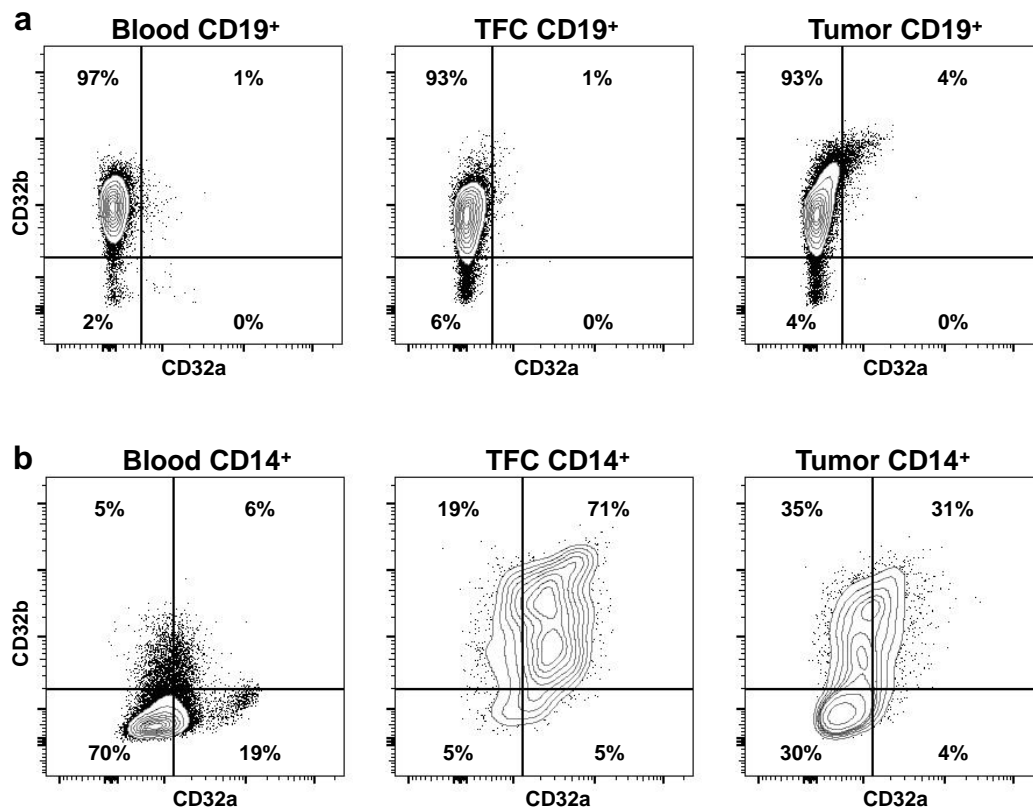
Figure 3.
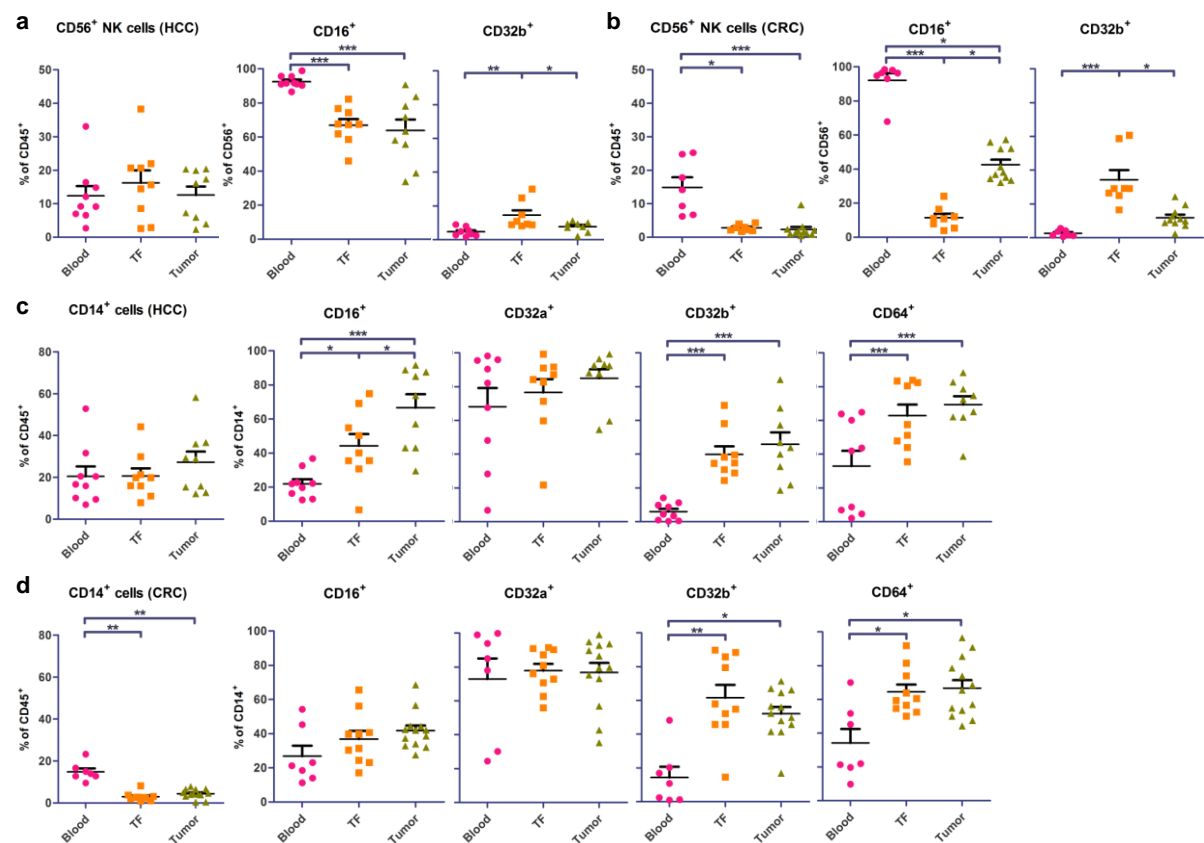
Figure 4.

Table 1. Demographics and clinical characteristics of patients with hepatocellular carcinoma.

	Patient characteristics
Age (range)	57 (38-75)
Sex (F/M)	3/14
Etiology	No underlying liver disease: 6
	Alcoholic: 3
	Alcoholic/HCV: 1
	HBV: 2
	HBV+HDV: 1
	HCV: 4
Histology grade	G1: 2
	G1-G2: 3
	G1-G3: 1
	G2: 6
	G2-G3: 1
	Unclassified: 4
Stage	T2: 9
	T3a: 8
Resection/LTx	12/5
Previous therapy	NA: 12
	VPE: 2
	TACE: 3

F, female; M, male; HDV, hepatitis D virus; LTx, liver transplantation; NA, not applicable; VPE, vena porta embolization; TACE, transarterial chemoembolization.

Table 2. Demographics and clinical characteristics of patients with colorectal carcinoma.

	Age
Age (range)	66 (54-78)
Sex (F/M)	2/14
Stage	T1N0: 2
	T2N0: 3
	T3N0: 5
	T4N0: 1
	T3N1: 3
	ypT1N0: 2
Tumor site	Cecum: 3
	Transversum: 2
	Sigmoid: 6
	Rectum: 5
Previous therapy	NA: 14
	Radiation: 2

F, female; M, male; NA, not applicable.

Table 3. Used antibodies for flow cytometry.

Target	Format	Clone	Company
CD3	APC-R700	UCHT1	BD Biosciences
CD3	PE-Cy7	UCHT1	eBioscience
CD4	eVolve605	SK3	eBioscience
CD14	APC-eFluor780	61D3	eBioscience
CD16	BV421	3G8	BD Biosciences
CD19	eVolve605	SJ25C1	eBioscience
CD25	PE-Cy7	M-A251	BD Biosciences
CD32a	PE	6C4	eBioscience
CD32b	FITC	ch2B6N297Q	MacroGenics*
CD45	APC-Cy7	HI30	eBioscience
CD45	PE-CF594	HI30	BD Biosciences
CD45RA	PE-CF594	HI100	BD Biosciences
CD56	APC-R700	NCAM16.2	BD Biosciences
CD64	PerCP-Cy5.5	10.1	BD Biosciences
FoxP3	PE	236A/E7	eBioscience
Human Fc block	Purified	N/A	BD Biosciences

*This mAb was kindly provided by MacroGenics (Rockville, MD), and recognizes specifically CD32b (25).

REFERENCES

1.   Arce Vargas F, Furness AJS, Solomon I et al. (2017) Fc-Optimized Anti-CD25 Depletes Tumor-Infiltrating Regulatory T Cells and Synergizes with PD-1 Blockade to Eradicate Established Tumors. Immunity. 46: 577-86.

2.   Liu W, Putnam AL, Xu-Yu Z et al. (2006) CD127 expression inversely correlates with FoxP3 and suppressive function of human CD4+ T reg cells. J Exp Med. 203: 1701-11.

3.   Miyara M, Yoshioka Y, Kitoh A et al. (2009) Functional Delineation and Differentiation Dynamics of Human CD4+ T Cells Expressing the FoxP3 Transcription Factor. Immunity. 30: 899-911.

4.   Saito T, Nishikawa H, Wada H et al. (2016) Two FOXP3+ CD4+ T cell subpopulations distinctly control the prognosis of colorectal cancers. Nat Med. 22: 679-84.

5.   Jacobs JFM, Punt CJA, Lesterhuis WJ et al. (2010) Dendritic Cell Vaccination in Combination with Anti-CD25 Monoclonal Antibody Treatment: a Phase I/II Study in Metastatic Melanoma Patients. Clin Cancer Res. 16: 5067-78.

6.   Rech AJ, Mick R, Martin S et al. (2012) CD25 Blockade Depletes and Selectively Reprograms Regulatory T Cells in Concert with Immunotherapy in Cancer Patients. Sci Transl Med. 4: 134ra62.

7.   Smith KGC, Clatworthy MR (2010) FcγRIIB in autoimmunity and infection: evolutionary and therapeutic implications. Nat Rev Immunol. 10: 328-43.

8.   Nimmerjahn F, Ravetch JV (2008) Fcγ receptors as regulators of immune responses. Nat Rev Immunol. 8: 34-47.

9.   Vonderheide RH, Glennie MJ (2013) Agonistic CD40 antibodies and cancer therapy. Clin Cancer Res. 19: 1035-43.

10.   Simpson TR, Li F, Montalvo-Ortiz W et al. (2013) Fc-dependent depletion of tumor-infiltrating regulatory T cells co-defines the efficacy of anti–CTLA-4 therapy against melanoma. J Exp Med. 210: 1695-710.

11.   Ihara F, Sakurai D, Horinaka A et al. (2017) CD45RA− Foxp3high regulatory T cells have a negative impact on the clinical outcome of head and neck squamous cell carcinoma. Cancer Immunol Immunother. 66: 1275-85.

12.   Simoni Y, Fehlings M, Kløverpris HN et al. (2017) Human Innate Lymphoid Cell Subsets Possess Tissue-Type Based Heterogeneity in Phenotype and Frequency. Immunity. 46: 148-61.

13.   Aarntzen EHJG, De Vries IJM, Lesterhuis WJ et al. (2013) Targeting CD4+ T-Helper Cells Improves the Induction of Antitumor Responses in Dendritic Cell–Based Vaccination. Cancer Res. 73: 19-29.

14.   Arce Vargas F, Furness AJS, Litchfield K et al. (2018) Fc Effector Function Contributes to the Activity of Human Anti-CTLA-4 Antibodies. Cancer Cell. 33: 1-15.

15.   Vincenti F, Kirkman R, Light S et al. (1998) Interleukin-2–receptor blockade with daclizumab to prevent acute rejection in renal transplantation. N Engl J Med. 338: 161-5.

16.   Waldmann TA (2007) Daclizumab (anti-Tac, Zenapax) in the treatment of leukemia/lymphoma. Oncogene. 26: 3699-703.

17.   Junghans RP, Waldmann TA, Landolfi NF, Avdalovic NM, Schneider WP, Queen C (1990) Anti-Tac-H, a humanized antibody to the interleukin 2 receptor with new features for immunotherapy in malignant and immune disorders. Cancer Res. 50: 1495-502.

18.   Bulliard Y, Jolicoeur R, Zhang J, Dranoff G, Wilson NS, Brogdon JL (2014) OX40 engagement depletes intratumoral Tregs via activating FcγRs, leading to antitumor efficacy. Immunol Cell Biol. 92: 475-80.

19.   Bulliard Y, Jolicoeur R, Windman M, Rue SM, Ettenberg S, Knee DA, Wilson NS, Dranoff G, Brogdon JL (2013) Activating Fc γ receptors contribute to the antitumor activities of immunoregulatory receptor-targeting antibodies. J Exp Med. 210: 1685-93.

20.   Selby MJ, Engelhardt JJ, Quigley M, Henning KA, Chen T, Srinivasan M, Korman AJ (2013) Anti-CTLA-4 antibodies of IgG2a isotype enhance antitumor activity through reduction of intratumoral regulatory T cells. Cancer Immunol Res. 1: 32-42.

21.   Marshall MJE, Stopforth RJ, Cragg MS (2017) Therapeutic Antibodies: What Have We Learnt from Targeting CD20 and Where Are We Going? Front Immunol. 8: 1245.

22.   Yeap WH, Wong KL, Shimasaki N et al. (2016) CD16 is indispensable for antibody-dependent cellular cytotoxicity by human monocytes. Sci Rep. 6: 34310.

23.   DiLillo DJ, Ravetch JV (2015) Differential Fc-Receptor Engagement Drives an Anti-tumor Vaccinal Effect. Cell. 161: 1035-45.

24.	Romano E, Kusio-Kobialka M, Foukas PG et al. (2015) Ipilimumab-dependent cell-mediated cytotoxicity of regulatory T cells ex vivo by nonclassical monocytes in melanoma patients. Proc Natl Acad Sci U S A. 112: 6140-5.
25.	Boruchov AM, Heller G, Veri M-C, Bonvini E, Ravetch JV, Young JW (2005) Activating and inhibitory IgG Fc receptors on human DCs mediate opposing functions. J Clin Invest. 115: 2914-23.

PART II

Regulation of intra-tumoral effector T cells in liver cancers

CHAPTER 5

Antibodies against immune checkpoint molecules restore functions of tumor-infiltrating T cells in hepatocellular carcinomas

Guoying Zhou[1], Dave Sprengers[1], Patrick P.C. Boor[1], Michail Doukas[2], Hannah Schutz[1], Shanta Mancham[1], Alexander Pedroza-Gonzalez[4], Wojciech G. Polak[3], Jeroen de Jonge[3], Marcia Gaspersz[3], Haidong Dong[5], Kris Thielemans[6], Qiuwei Pan[1], Jan N.M. IJzermans[3], Marco J. Bruno[1], Jaap Kwekkeboom[1]

Departments of [1]Gastroenterology and Hepatology, [2]Pathology, and [3]Surgery, Erasmus MC-University Medical Center, Rotterdam, the Netherlands; [4]Laboratory of Immunology Research, FES-Iztacala, UNAM, Mexico; [5]Department of Urology and Immunology, Mayo Clinic College of Medicine, Rochester, MN, USA; and [6]Laboratory of Molecular and Cellular Therapy, Department of Immunology-Physiology, Vrije Universiteit, Brussels, and eTheRNA immunotherapies NV, Niel, Belgium.

ABSTRACT

Background & Aims: Ligand binding to inhibitory receptors on immune cells, such as programmed cell death 1 (PD-1) and cytotoxic T-lymphocyte associated protein 4 (CTLA4), downregulates the T-cell–mediated immune response (called immune checkpoints). Antibodies that block these receptors increase anti-tumor immunity in patients with melanoma, non-small cell lung cancer, and renal cell cancer. Tumor-infiltrating CD4^{+} and CD8^{+} T cells in patients with hepatocellular carcinoma (HCC) have been found to be functionally compromised. We analyzed HCC samples from patients to determine if these inhibitory pathways prevent T-cell responses in HCCs and to find ways to restore their anti-tumor functions.

Methods: We collected HCC samples from 59 patients who underwent surgical resection from November 2013 through May 2017, along with tumor-free liver tissues (control tissues) and peripheral blood samples. We isolated tumor-infiltrating lymphocytes (TIL) and intra-hepatic lymphocytes. We used flow cytometry to quantify expression of the inhibitory receptors PD-1, hepatitis A virus cellular receptor 2 (TIM3), lymphocyte activating 3 (LAG3), and CTLA4 on CD8^{+} and CD4^{+} T cells from tumor, control tissue, and blood; we studied the effects of antibodies that block these pathways in T-cell activation assays.

Results: Expression of PD-1, TIM3, LAG3, and CTLA4 was significantly higher on CD8^{+} and CD4^{+} T cells isolated from HCC tissue than control tissue or blood. Dendritic cells, monocytes, and B cells in HCC tumors expressed ligands for these receptors. Expression of PD-1, TIM3, and LAG3 was higher on tumor-associated antigen (TAA)-specific CD8^{+} TIL, compared with other CD8+ TIL. Compared to TIL that did not express these inhibitory receptors, CD8^{+} and CD4^{+} TIL that did express these receptors had higher levels of markers of activation, but similar or decreased levels of granzyme B and effector cytokines. Antibodies against CD274 (PD-L1), TIM3, or LAG3 increased proliferation of CD8^{+} and CD4^{+} TIL and cytokine production in response to stimulation with polyclonal antigens or TAA. Importantly, combining antibody against PD-L1 with antibodies against TIM3, LAG3, or CTLA4 further increased TIL functions.

Conclusions: The immune checkpoint inhibitory molecules PD-1, TIM3, and LAG3 are up-regulated on TAA-specific T cells isolated from human HCC tissues, compared to T cells from tumor-free liver tissues or blood. Antibodies against PD-L1, TIM3, or LAG3 restore responses of HCC-derived T cells to tumor antigens, and combinations of the antibodies have additive effects. Strategies to block PD-L1, TIM3, and LAG3 might be developed for treatment of primary liver cancer.

Keywords: immunotherapy; GPC3; MAGEC2; galectin 9

Introduction

Liver cancer represents the second most common cause of cancer-related mortality worldwide, and hepatocellular carcinoma (HCC) is the most prevalent primary liver cancer.[1, 2] The current treatment options for HCC, such as surgical resection, liver transplantation and radiofrequency ablation, are curative only for patients with early stage disease. Unfortunately, the majority of HCC patients are not eligible for curative procedures because of late diagnosis and thus have poor prognosis.[3] HCC is highly resistant to chemotherapy, but immunotherapy may be an attractive therapeutic option for HCC, since an inflammatory tumor microenvironment is associated with improved survival.[4, 5] As reported in our earlier studies, intra-tumoral accumulation of activated regulatory T cells (Treg) is one of the suppressive mechanisms that contribute to HCC immune evasion.[6-8] However, inhibitory receptor-ligand pathways (called immune checkpoints) may additionally contribute to suppression of anti-tumor immunity in the tumor microenvironment.

There is evidence that tumor-infiltrating T cells upon chronic stimulation by tumor antigens lose their effector functions and their ability to kill tumor cells, which is accompanied by a progressive increase in the diversity and amount of inhibitory receptors expressed on them, including PD-1, TIM3, LAG3, CD244, CD160, CTLA4 and BTLA.[9-12] Upon interaction with their respective ligands expressed on tumor cells and tumor-infiltrating antigen-presenting cells (APC), these receptors suppress T cell responses to tumor antigens. Blocking the interactions of PD-1 and CTLA4 with their respective ligands has been shown to be a promising novel therapeutic approach for several types of human malignancies such as advanced melanoma, non-small cell lung cancer and renal cell cancer, which improved anti-tumor T cell responses and provided unprecedented clinical benefits for patients.[13-18]

We and others have observed that tumor-infiltrating CD4$^+$ T helper cells (Th) and CD8$^+$ cytotoxic T cells (CTL) of HCC patients are functionally compromised.[6, 19] Recent studies have shown that the PD-1/PD-L1 inhibitory interaction mediates suppression of CD8$^+$ tumor-infiltrating lymphocytes (TIL),[20-22] while the TIM3/galectin-9 (GAL-9) interaction mediates CD4$^+$ TIL dysfunction[23] in HCC patients. Nevertheless, the expression of these and other inhibitory receptors on tumor-infiltrating T cells, and their functional relevance to both helper and cytotoxic T cell responses to tumor antigens in the HCC microenvironment have not been studied thoroughly. It is also unclear whether combined blockade of inhibitory pathways can additively increase the effector function of HCC-specific T cells.

In this study, we aimed to systematically determine which inhibitory pathways participate in the suppression of T cell responses in the HCC microenvironment. We used paired samples

of leukocytes isolated from resected tumors, tumor-free liver tissues (TFL) and peripheral blood of HCC patients, to measure the expression of five inhibitory receptors on CD4$^+$ Th and CD8$^+$ CTL. We also performed *ex vivo* functional assays to determine whether blockade of inhibitory interactions can invigorate the functionality of tumor-infiltrating T cells. We found that inhibitory receptors PD-1, TIM3, LAG3 and CTLA4 were up-regulated on tumor-infiltrating T cells; and interestingly, PD-1, TIM3 and LAG3 were selectively increased on tumor-associated antigen (TAA)-specific CD8$^+$ TIL. Blocking PD-L1, TIM3 or LAG3 enhanced *ex vivo* proliferation of CD4$^+$ and CD8$^+$ TIL and effector cytokine production, and combined blockade of PD-L1 with TIM3, LAG3 or CTLA4 further enhanced *ex vivo* TIL responses to polyclonal stimuli and TAA.

Patients and Methods

Patients

Fifty-nine patients who were eligible for surgical resection of HCC were enrolled in the study from November 2013 to May 2017. Paired fresh tissue samples from tumors and surrounding (minimum 1cm distance from the tumor) TFL were obtained, and tumor-infiltrating leukocytes and intra-hepatic leukocytes were isolated respectively. Peripheral blood from the same patients was also collected on the day of resection. None of the patients received chemotherapy or immunosuppressive treatment at least three months before surgery. The clinical characteristics of the patients are summarized in Supplementary Table 1. Eighty-five percent of patients included in the study are Caucasians. The study was approved by the local ethics committee, and all the patients signed the informed consent before tissue and blood donation.

Cell preparation

Peripheral blood mononuclear cells (PBMC) were isolated by Ficoll density gradient centrifugation. Single cell suspensions from tumors and TFL were obtained by tissue digestion as described previously.[6-8] Briefly, fresh tissues were cut into small pieces and digested with 0.5 mg/mL of collagenase IV (Sigma-Aldrich, St. Louis, MO) and 0.2 mg/mL of DNAse I (Roche, Indianapolis, IN) for 20-30 minutes at 37 °C. Cell suspensions were filtered through 100 μm pore cell strainers (BD Biosciences, Erembodegem, Belgium) and mononuclear leukocytes were obtained by Ficoll density gradient centrifugation. Viability was determined by trypan blue exclusion.

Ex vivo mRNA-encoded full-length tumor antigen-specific T cell stimulation assay

PBMC or TIL of HCC patients were labeled with 0.1 µM carboxyfluorescein diacetate succinimidyl ester (CFSE, Invitrogen), after which 100,000 cells in RPMI medium supplemented with 10% human AB serum, 2mM L-glutamine, 50 mM Hepes Buffer, 1% penicillin-streptomycin, 5mM Sodium Pyruvate and 1% minimum essential medium non-essential amino acids (MEM NEAA) were transferred to each well of 96-well round-bottom culture plate. Glypican-3 (GPC3) mRNA-, MAGEC2 mRNA- or (as negative controls) eGFP mRNA-transfected or mock-electroporated autologous CD40-activated B cells (B cell blasts) in the same medium were added at a PBMC/TIL : B cell ratio of 1:1. TIL were co-cultured with B cell blasts (200 µl/ well) in the presence or absence of 10 µg/ml neutralizing monoclonal antibodies against human PD-L1, TIM3, LAG3 or CTLA4, or combinations of these antibodies, or isotype control antibodies. After seven days, CFSE-labeled cells were harvested, and stained with CD8, CD4, CD3 antibodies. Dead cells were excluded by using the LIVE/DEAD fixable dead cell stain kit with aqua fluorescent reactive dye, and T cell proliferation was determined based on CFSE dilution by flow cytometry analysis.

Detailed description of other methods is provided in the Supplementary Information.

Results

Increased expression of inhibitory receptors on tumor-infiltrating CD4$^+$ T helper cells and CD8$^+$ cytotoxic T cells from HCC patients.

We first compared the expression levels of five inhibitory receptors (PD-1, TIM3, LAG3, CTLA4 and BTLA) on CD4$^+$ Th and CD8$^+$ CTL, in paired samples of leukocytes freshly isolated from surgically resected tumors, TFL and peripheral blood from HCC patients. We excluded Foxp3$^+$ Treg from CD4$^+$ T cells because we focused on anti-tumor effector T cell populations. PD-1, TIM3 and CTLA4 were expressed on significantly higher proportions of Th and CTL in tumors than in TFL and blood, whereas LAG3 was expressed on significantly higher proportions of CTL in tumors than in TFL and blood (Fig. 1A-C). Compared to the other investigated inhibitory receptors PD-1 was expressed by most tumor-infiltrating Th and CTL and with highest median fluorescence intensity (MFI) (Supplementary Fig. 1). BTLA was expressed at negligible levels, and we did not observe any significant difference between its expression in the tumor and that in TFL. Therefore, we focused on the other four receptors in the rest of our study.

Since PD-1 was the highest expressed receptor on TIL, we analyzed co-expression of PD-1 and the other three receptors on TIL. Interestingly, we observed co-expression of TIM3,

LAG3 or CTLA4 with PD-1 on tumor-infiltrating Th and CTL, but there were also tumor-infiltrating Th and CTL expressing only TIM3, LAG3 or CTLA4 but not PD-1 (Fig. 1D, E). In addition, Supplementary Fig. 2 illustrates that there were significant, although weak, positive correlations between the percentages of PD-1, TIM3, LAG3 or CTLA4 positive Th in tumors and those in blood, and between the percentages of LAG3 or CTLA4 positive CTL in tumors and those in blood. These data indicate that the expression of inhibitory receptors on TIL is partially reflected by their expression on circulating T cells in HCC patients.

Increased expression of PD-1, TIM3 and LAG3 on TAA-specific CD8+ TIL.

To study the expression of these inhibitory receptors on TAA-specific CTL, we used HLA-A*0201 dextramers loaded with GPC3 and MAGEC2 peptides (Fig. 2A). These TAA are among the most frequently expressed TAA in HCC tumors in the Western-European area.[24] TAA dextramer-binding CTL were detectable in tumors from seven out of thirteen HLA-A2+ patients, and in blood from three out of twelve patients (Supplementary Table 3). The resected tumors of the patients with TAA dextramer-binding CTL expressed the corresponding TAA (confirmed by immunohistochemistry staining, data not shown). Fig. 2B presents the percentages of CTL binding to the dominant epitope-HLA-A*0201-dextramer complex of these patients, which ranged from 0.11%–8.0% in tumors and from 0.23%-0.87% in blood. Representative histograms of the expression of inhibitory receptors on TAA dextramer-binding versus TAA dextramer negative CD8+ TIL are presented in Fig. 2C; and Fig. 2D summarizes the comparison of the expression of inhibitory receptors between CTL that did and did not recognize the dominant TAA epitope in each patient. Interestingly, expression of PD-1, TIM3 and LAG3, but not CTLA4, was significantly increased on TAA-specific CD8+ TIL, compared to TAA dextramer negative CD8+ TIL (MFI data are shown in Supplementary Fig. 3). Likewise, CD8+ TIL that recognized non-dominant peptides demonstrated enhanced expression of inhibitory receptors in the same patients (data not shown).

Tumor-infiltrating antigen-presenting cells from HCC patients express inhibitory ligands.

We further analyzed the expression levels of inhibitory ligands PD-L1 (for PD-1), GAL-9 (for TIM3), MHC-II (for LAG3), CD86 and CD80 (for CTLA4) on APC subsets within tumor tissues by flow cytometry. The major human APC subsets, CD45+BDCA1+CD19- myeloid dendritic cells (mDC), CD45+CD14+ monocytes and CD45+CD19+ B cells, were all found in HCC tumors. The percentages of mDC and B cells were higher in tumor-infiltrating CD45+ leukocytes than in TFL-infiltrating CD45+ leukocytes, but cell numbers isolated per gram of

tissue did not differ (Fig. 3A, B). All five ligands were found to be expressed on tumor-infiltrating APC (Fig. 3C, D). The MFI of PD-L1 and GAL-9 on mDC and monocytes, and MHC-II on monocytes were significantly higher in the tumor than in TFL (Supplementary Fig. 4). In a separate study using immunohistochemistry, we found that PD-L1 and GAL-9 were also expressed on tumor cells in HCC tissues.[25] Together, these data suggest the suppression of tumor-infiltrating T cells by these inhibitory interactions in tumors of HCC patients.

Tumor-infiltrating T cells expressing inhibitory receptors display an activated status.

Given the increased expression of inhibitory receptors, tumor-infiltrating T cells in human HCC may be dysfunctional. Alternatively, expression of inhibitory receptors can be the consequence of local T cell activation. To study these two possibilities, we examined the activation status, cytotoxic effector molecule expression and cytokine production profile of tumor-infiltrating T cells expressing inhibitory receptors. We first compared the *ex vivo* activation status of tumor-infiltrating Th and CTL that do or do not express inhibitory receptors, using the activation markers HLA-DR and CD69. PD-1$^+$ cells were significantly more activated than PD-1$^-$ cells in both T cell populations (Fig. 4A). So were TIM3$^+$, LAG3$^+$ and CTLA4$^+$ cells compared with TIM3$^-$, LAG3$^-$ or CTLA4$^-$ cells, respectively. Despite their activated status, the expression of cytotoxic effector molecule granzyme B was comparable or reduced in inhibitory receptor positive CD8$^+$ TIL compared with respective receptor negative cells (Fig. 4B).

Furthermore, we stimulated TIL with PMA and ionomycin in order to assess effector cytokine production. After exposure to PMA and ionomycin for five hours, PD-1, TIM3, LAG3 and CTLA4 were not distinctly up-regulated on TIL (data not shown). The percentages of IFN-γ and TNF-α producing cells in inhibitory receptor positive cells were comparable or reduced compared with those in respective receptor negative cells, in both CD4$^+$ Th and CD8$^+$ CTL (Fig. 4C). Together, these data indicate that tumor-infiltrating T cells that express inhibitory receptors are activated but do not have enhanced functionality.

PD-L1, TIM3 or LAG3 blockade increases ex vivo proliferation and effector cytokine production of tumor-infiltrating T cells.

Given that the inhibitory receptors PD-1, TIM3, LAG3 and CTLA4 are up-regulated on HCC tumor-infiltrating T cells and their respective ligands are expressed on tumor-infiltrating APC subsets, we tested whether blocking the PD-1/PD-L1, TIM3/GAL-9, LAG3/MHC-II or CTLA4/CD80/CD86 pathways can enhance the functionality of tumor-infiltrating T cells. We first stimulated CFSE-labeled total tumor-infiltrating mononuclear leukocytes with CD3/CD28

beads, in the presence or absence of 10 µg/ml neutralizing antibodies against human PD-L1, TIM3, LAG3, CTLA4, or combinations of these neutralizing antibodies, or isotype control antibodies (mIgG1 and mIgG2a). After four days, T cell proliferation was measured by flow cytometry (Fig. 5A), and IFN-γ secretion in culture supernatant was quantified by ELISA. Compared with the control condition without neutralizing antibody, treatment with anti-PD-L1, anti-TIM3 or anti-LAG3 significantly enhanced the proliferation of CD4+ and CD8+ TIL (Fig. 5B); these three antibodies also significantly increased IFN-γ secretion (Fig. 5C). Treatment with anti-CTLA4 significantly enhanced CD4+ TIL proliferation. Interestingly, combined blockade of PD-L1 with CTLA4 further enhanced the proliferation of CD4+ and CD8+ TIL, while PD-L1 blockade together with LAG3 blockade further enhanced CD8+ TIL proliferation and IFN-γ secretion, and combining PD-L1 blockade with TIM3 blockade further enhanced all three types of function compared to single PD-L1 blockade (Fig. 5D, E).

Combining PD-L1 blockade with TIM3, LAG3 or CTLA4 blockade additively increases ex vivo responses of tumor-infiltrating T cells to HCC tumor antigens.

To test the effects of blocking these four inhibitory pathways on tumor-specific T cell immunity, we used two tumor antigen-specific T cell stimulation assays.

In the first assay, we stimulated TIL with pooled HLA-A*0201-restricted GPC3 and MAGEC2 peptides, in the presence or absence of antibody blocking inhibitory pathway or combinations of blocking antibodies. After seven days, expression levels of intracellular IFN-γ, TNF-α, activation-induced CD137 (an accepted marker for detection of antigen-specific T cell responses[26]) and surface CD107a (as a measure for cytotoxic degranulation) in CD8+ TIL were analyzed after re-stimulation with pooled GPC3 and MAGEC2 peptides (Fig. 6A). Compared to the stimulation with control peptide, seven HLA-A2+ patients showed specific CD8+ TIL responses to pooled GPC3 and MAGEC2 peptides. A summary of data (Fig. 6B) illustrates that blocking PD-L1, TIM3, LAG3 or CTLA4 increased tumor-specific CD137, CD107a expression, IFN-γ and/or TNF-α production of CD8+ TIL, but large variations between individual patients were observed, ranging from no effect to higher than two-fold increases of CD8+ TIL responses. Interestingly, PD-L1 blockade in combination with TIM3, LAG3 or CTLA4 blockade further enhanced tumor-specific CD8+ TIL responses compared to single PD-L1 blockade in part of the patients.

In the second assay, autologous B cell blasts expanded from patient PBMC by three-week culture in the presence of trimeric CD40 ligand and rhIL-4 and then transfected with mRNA encoding GPC3 or MAGEC2 by electroporation, served as APC. B cell blasts expressed MHC-II, CD80, CD86,[27] PD-L1 and GAL-9 (data not shown). To enable antigen presentation

to CD4^{+} T cells, the mRNA constructs we used encode these TAA fused to the transmembrane and luminal regions of dendritic cell lysosome-associated membrane protein (DCLamp), which is a targeting signal for the endo-lysosomal compartment, resulting in peptide loading in MHC-II in addition to MHC-I.[28] To validate this assay, we first co-cultured an HLA-A*0201-restricted GPC3-specific CD8^{+} T cell clone[29] or human T cells transfected with a human T cell receptor (TCR) recognizing MAGEC2 presented by HLA-A*0201,[30] with GPC3 mRNA- or MAGEC2 mRNA-transfected B cell blasts expanded from PBMC of an HLA-A2[+] healthy donor. B cell blasts pulsed with the GPC3 FVGEFFTDV peptide or the MAGEC2 ALKVDVEERV peptide served as positive controls. Fig. 7A reveals clear IFN-γ response of the GPC3-specific CD8^{+} T cell clone to GPC3 mRNA-transfected B cell blasts and GPC3 peptide, and clear IFN-γ response of MAGEC2-specific human T cells to MAGEC2 mRNA-transfected B cell blasts and MAGEC2 peptide, but the T cells did not respond to eGFP mRNA-transfected or mock-electroporated B cell blasts (negative controls) or to non-cognate antigens.

Next, we co-cultured CFSE-labeled PBMC from an HCC patient whose resected tumor expressed GPC3 strongly and MAGEC2 weakly (confirmed by immunohistochemistry staining), with GPC3 mRNA-, MAGEC2 mRNA-, eGFP mRNA-transfected or mock-electroporated autologous B cell blasts, and measured T cell proliferation after seven days. Fig. 7B reveals evident specific responses of CD4^{+} and CD8^{+} T cells to GPC3, and weaker responses to MAGEC2, but not to eGFP. These results confirm that TAA-specific CD4^{+} and CD8^{+} T cell responses can be accurately detected and quantified using this T cell stimulation assay.

We co-cultured CFSE-labeled TIL with GPC3 mRNA-, MAGEC2 mRNA-, eGFP mRNA-transfected or mock-electroporated autologous B cell blasts, in the presence or absence of antibody blocking inhibitory pathway or combinations of blocking antibodies, and measured T cell proliferation after seven days. Representative proliferation data of CD4^{+} and CD8^{+} TIL from one patient whose resected tumor expressed MAGEC2 (confirmed by immunohistochemistry staining) are presented in Fig. 7C. In six patients both GPC3- and MAGEC2-specific TIL proliferative responses were observed, and in three patients either GPC3- or MAGEC2-specific responses were observed. In these nine patients, 6.6% ± 3.8% (mean ± SEM) of CD4^{+} and 3.9% ± 1.5% (mean ± SEM) of CD8^{+} proliferating TIL were observed in response to these TAA. A summary of data from these nine patients (Fig. 7D) demonstrates that blocking PD-L1, TIM3, LAG3 or CTLA4 increased tumor-specific proliferation of CD4^{+} and CD8^{+} TIL in most but not all patients. Furthermore, PD-L1 blockade in combination with TIM3, LAG3 or CTLA4 blockade enhanced proliferation of both CD8^{+} and

CD4^{+} TIL in more patients and further enhanced TIL proliferation compared to single PD-L1 blockade.

Discussion

The purpose of this study was to determine whether inhibitory pathways lead to suppression of T cell responses in the HCC microenvironment, and to examine whether blocking these inhibitory pathways can restore the functions of tumor-infiltrating T cells. Overall, the results of our study demonstrate that inhibitory pathways involving the receptors PD-1, TIM3, LAG3 and CTLA4 participate in intra-tumoral suppression of CD4^{+} Th and CD8^{+} CTL in HCC. Single blockade of PD-L1, TIM3, LAG3, or CTLA4 could recover TIL responses to tumor antigens, but large differences in effects were observed between individual patients. Importantly, combining PD-L1 blockade with TIM3, LAG3 or CTLA4 blockade further enhanced the responsiveness of TIL and was effective in more patients.

Previous studies have revealed increased expression of PD-1,[20, 21, 31] TIM3[23] and LAG3[32] on either CD4^{+} or CD8^{+} TIL in HCC patients, but to our knowledge expression of CTLA4 and BTLA as well as co-expression of all these inhibitory receptors on both CD4^{+} and CD8^{+} TIL in HCC patients have not been studied before. Here, we demonstrate that tumor-infiltrating Th have significantly increased PD-1, TIM3 and CTLA4 expression; whereas CTL have significantly increased PD-1, TIM3, LAG3 and CTLA4 expression, compared with their counterparts in TFL and blood (Fig. 1C). Similar to melanoma,[33] BTLA was not up-regulated on tumor-infiltrating T cells. A previous study suggested that HBV positive HCC patients had more intra-tumoral TIM3^{+} T cells compared to HBV negative HCC patients,[23] but we did not find any difference in the expression of inhibitory receptors between HCC patients with HBV or HCV infection or other etiologies for HCC (e.g. alcoholic liver disease). There was also no difference between patients with cirrhotic or non-cirrhotic liver (data not shown). Using HLA-A*0201 dextramers loaded with GPC3 or MAGEC2 peptides, we are the first to demonstrate that PD-1, TIM3 and LAG3 are selectively up-regulated on tumor-infiltrating TAA-specific CD8^{+} T cells from HCC patients (Fig. 2D, supplementary Fig. 3). Similarly, we observed that circulating TAA-specific CD8^{+} T cells express relatively high levels of the same inhibitory receptors, which extends previous observation showing high PD-1 expression on circulating TAA-specific CD8^{+} T cells in HCC patients.[34, 35] The selectively increased expression of these inhibitory receptors on TAA-specific TIL together with the expression of their respective ligands on tumor-infiltrating APC suggests that they may be involved in the regulation of tumor antigen-specific responsiveness of tumor-infiltrating T cells.

Given that expression of individual inhibitory receptor on T cells can be induced by T cell activation,[36, 37] but expression of increasing numbers of inhibitory receptors often coincides with gradual loss of T cell functions,[9, 38, 39] we investigated the activation status, cytotoxic effector molecule expression and cytokine production profile of tumor-infiltrating T cells in relation to the expression inhibitory receptors. Interestingly, CD4^{+} Th and CD8^{+} CTL expressing either inhibitory receptor displayed a more activated status (Fig. 4A); however, they displayed comparable or reduced levels of granzyme B, IFN-γ and TNF-α (Fig. 4B,C). Together with our data showing selectively enhanced expression of inhibitory receptors on TAA-specific TIL, these findings indicate that, in accordance with recent studies in other human cancers,[11, 33, 39] HCC tumor-infiltrating T cells that express inhibitory receptors are probably tumor-reactive T cells, which may continue to up-regulate the expression of inhibitory receptors in response to chronic stimulation by tumor antigens to prevent further over activation. Of note, PD1^{+}TIM3^{+} T cells displayed the lowest level of granzyme B, IFN-γ and TNF-α, which suggests that PD-1 and TIM3 play an important role in T cell suppression in HCC microenvironment.

We performed polyclonal and tumor-specific functional assays to test the effect of blocking these inhibitory pathways on the functions of tumor-infiltrating T cells *ex vivo*. Because we were interested in and measured the net effect of blocking antibody intervention on CD4^{+} and CD8^{+} TIL function in a context that reflected the tumor microenvironment as much as possible, we used total tumor-infiltrating mononuclear leukocytes in all our functional assays which contained both T cells expressing inhibitory receptors and APC subsets expressing inhibitory ligands. As a consequence, tumor-infiltrating Treg and probably other types of suppressor cells were also present. Our data indicate that the *ex vivo* proliferative function of both CD4^{+} and CD8^{+} TIL and IFN-γ secretion in response to polyclonal stimuli were enhanced significantly by blocking PD-L1, TIM3 or LAG3, while blocking CTLA4 only significantly enhanced CD4^{+} TIL proliferation (Fig. 5B,C). Similar effects of blocking the PD-1/PD-L1 pathway on CD8^{+} TIL and blocking the TIM3/GAL-9 pathway on CD4^{+} TIL in HCC patients have been shown before,[20, 21, 23, 31] but we are the first to demonstrate that blocking PD-L1, LAG3 or TIM3 can enhance the functional responsiveness of both CD4^{+} and CD8^{+} TIL in HCC patients. Even more importantly, we found that combining anti-PD-L1 antibody with anti-TIM-3, anti-LAG-3 or anti-CTLA-4 antibody further enhanced the functionality of CD4^{+} or CD8^{+} TIL compared to single PD-L1 blockade (Fig. 5D,E).

The effects of inhibitory receptor-ligand blockade on responses of tumor-infiltrating T cells to tumor antigens were studied in two different assays. In the first TAA peptide assay, activation-induced CD137, cytotoxic degranulation marker CD107a, and effector cytokine

IFN-γ and TNF-α levels were variably increased in CD8^{+} TIL in the presence of single anti-PD-L1, anti-TIM3, anti-LAG3 or anti-CTLA4 antibody (Fig. 6B). Importantly, combined blocking treatments further enhanced these effects in part of the patients compared to single anti-PD-L1 antibody. In the second assay, we used autologous CD40-activated B cell blasts transfected with mRNA encoding full-length GPC3 or MAGEC2 to measure responses of CD4^{+} and CD8^{+} TIL to the natural repertoire of TAA-derived peptides irrespective of patient HLA typing.[40] Tumor antigen-specific proliferation of CD8^{+} and CD4^{+} TIL was increased up to four-fold in the presence of single anti-PD-L1, anti-TIM3, anti-LAG3 or anti-CTLA4 antibody, but the responses to single blockade were also variable between individual patients (Fig. 7D). Combined treatments of anti-PD-L1 with either anti-TIM3, anti-LAG3 or anti-CTLA4 antibody enhanced proliferation of both CD8^{+} and CD4^{+} TIL in more patients compared to single PD-L1 blockade. A recent phase 1 clinical trial of tremelimumab (CTLA4 blockade) has reported a manageable safety profile and a response rate of 17.6% in 17 HCV-related advanced HCC patients.[41] Very recently in a phase 1/2 clinical trial, nivolumab (PD-1 blockade) has demonstrated an objective response rate of 20%, disease control with stable disease for ≥6 months in 37%, and encouraging overall survival in 214 advanced HCC patients in the dose-expansion phase regardless of HCC etiology. In addition, liver toxicity was limited and manageable in the majority of patients, while symptomatic treatment-related adverse events were comparable in patients with and without HCV or HBV infection.[42] These studies are the first to show safety and efficacy of immune checkpoint blockade in HCC patients. Further clinical trials should be performed to verify whether blockade of TIM3 and LAG3 has clinical efficacy in HCC patients, and whether combined targeting of inhibitory pathways improves clinical responses.

In some of the patients we could isolate sufficient TIL to determine the expression of inhibitory receptors directly *ex vivo* in addition to performing the *ex vivo* polyclonal or mRNA-encoded TAA-specific functional assays. In both assays, the high-responding tumor-infiltrating T cells (those with > median % increase of TIL responses in the presence of PD-L1, TIM3, LAG3 or CTLA4 blockade) displayed higher frequencies of PD-1, TIM3 or LAG3-expressing cells than low or non-responding tumor-infiltrating T cells (those with < median % increase of TIL responses), respectively (Supplementary Fig. 5 & 6), suggesting that the inter-individual variations in TIL responses to single immune checkpoint blockade may be related to the differences in the expression levels of the corresponding inhibitory receptor on TIL. Interestingly, the expression levels of several investigated inhibitory receptors on tumor-infiltrating T cells correlated with those on circulating T cells (Supplementary Fig. 2). Although correlations were weak, these findings support the idea that the expression of

inhibitory receptor on circulating T cells may become useful as biomarkers to predict clinical response of individual HCC patient to checkpoint blockade therapy.

Our study has several limitations: 1) the effects of immune checkpoint blockade on tumor antigen-specific responses have been studied in limited numbers of patients, because patient samples are limited and these assays comparing many conditions require large numbers of TIL; 2) in some types of experiments, not all the conditions could be performed in every patient sample, due to limited numbers of isolated cells; 3) we included only two TAA (GPC3 and MAGEC2) in our study, but these antigens are among the most prevalent HCC-specific antigens,[24] they are selectively expressed on tumor cells and have been proven to be immunogenic;[29, 43] 4) our patients all underwent liver resection, and therefore are not representative for the whole HCC patient population; 5) in our patient cohort, there are more non-viral hepatitis patients than viral hepatitis patients, which is different from Asian HCC patient cohorts.

In summary, we conclude that PD-1, TIM3 and LAG3 are up-regulated on TAA-specific TIL in HCC patients. While blocking individual inhibitory pathway has variable effects, combining PD-L1 blockade with TIM3, LAG3 or CTLA4 blockade revitalizes *ex vivo* tumor-specific TIL responses in most patients and additively enhances the effects compared to single PD-L1 blockade. Therefore, our study provides evidence that PD-1/PD-L1, TIM3 and LAG3 are promising immunotherapeutic targets for the most common primary liver cancer, and suggests that the aforementioned combined targeting of immune checkpoints may result in superior clinical responses in more patients than targeting a single checkpoint.

Figure legends

Figure 1. Expression of inhibitory receptors on CD4$^+$ Th and CD8$^+$ CTL in tumors, TFL, and blood. PBMC and mononuclear leukocytes isolated from tumors and TFL were stained with antibodies against PD-1, TIM3, LAG3, CTLA4 and BTLA. (A) Representative dot plots of inhibitory receptor expression and appropriate isotype controls on CD3$^+$CD4$^+$Foxp3$^-$ TIL and (B) CD3$^+$CD8$^+$ TIL. (C) The percentages of inhibitory receptor positive cells among CD4$^+$ Th or CD8$^+$ CTL in tumors, TFL and blood. Values of individual patients are depicted, and lines show medians; * $p < 0.05$, ** $p < 0.01$, *** $p < 0.001$. (D) Representative dot plots of co-expression of inhibitory receptors on CD4$^+$Foxp3$^-$ TIL and CD8$^+$ TIL. (E) The mean percentages of co-expression of inhibitory receptors among CD4$^+$Foxp3$^-$ TIL (n=12) or CD8$^+$ TIL (n=22).

Figure 2. Expression of PD-1, TIM3 and LAG3 is increased on TAA-specific CD8$^+$ TIL. PBMC and TIL of HLA-A2$^+$ patients were stained with HLA-A*0201 dextramers loaded with GPC3 FVGEFFTDV, GPC3 FLAELAYDL, MAGEC2 ALKVDVEERV, or MAGEC2 LLFGLALIEV peptides. (A) Representative dot plots of TAA dextramer staining compared to negative control. CD8$^+$ and CD8$^-$CD4$^+$ TIL were gated within CD56$^-$CD14$^-$CD19$^-$ viable cells. (B) The percentages of dextramer-binding CD8$^+$ T cells in tumors of seven patients and in blood of three patients with detectable dextramer-binding CD8$^+$ T cells. Lines show medians. For each patient, the value of either the only or the dominant dextramer-binding population is depicted. (C) Representative histograms of inhibitory receptor expression on GPC3 FVGEFFTDV dextramer positive (blue line) versus dextramer negative (red line) CD8$^+$ TIL. (D) The percentages of PD-1, TIM3, LAG3 or CTLA4 positive cells in TAA dextramer positive versus TAA dextramer negative CD8$^+$ T cells in tumors and blood. For each patient, the value of either the only or the dominant dextramer-binding population is depicted. * $p < 0.05$, ** $p < 0.01$. (B)(D) Blue symbols: GPC3 FVGEFFTDV positive; green symbol: GPC3 FLAELAYDL positive; red symbols: MAGEC2 LLFGLALIEV positive.

Figure 3. Tumor-infiltrating antigen-presenting cells express inhibitory ligands. Expression of inhibitory ligands PD-L1, GAL-9, MHC-II, CD86 and CD80 was measured by flow cytometry. (A) The percentages of B cells, mDC and monocytes within CD45$^+$ cells gated from tumors, TFL and blood. Lines depict medians; * $p < 0.05$, ** $p < 0.01$, *** $p < 0.001$. (B) The absolute numbers of B cells, mDC and monocytes isolated per gram of tumor and TFL tissues. Values of individual patients are presented, lines depict medians. (C) Representative histograms of inhibitory ligand expression on tumor-infiltrating B cells, mDC and monocytes. Upper panel: ligand staining, lower panel: isotype control. (D) The

percentages of inhibitory ligand positive cells within tumor-infiltrating B cells, mDC or monocytes in individual patients are presented; lines depict medians.

Figure 4. Tumor-infiltrating T cells expressing inhibitory receptors display a more activated status. TIL were stained *ex vivo* with antibodies against surface activation markers HLA-DR and CD69 and stained with an antibody against the cytotoxic effector molecule Granzyme B intracellularly. (A) The percentages of HLA-DR$^+$ or CD69$^+$ cells in CD3$^+$CD4$^+$Foxp3$^-$ TIL or CD3$^+$CD8$^+$ TIL which do or do not express PD-1, TIM3, LAG3 or CTLA4 are presented. (B) The percentages of Granzyme B$^+$ cells in CD8$^+$ TIL which do or do not express inhibitory receptors. (C) TIL were exposed to PMA and ionomycin at 37°C for five hours, in the presence of protein transport inhibitor brefeldin during the last four hours, followed by intracellular cytokine staining. The percentages of cytokine-producing cells in TIL which do or do not express inhibitory receptors are presented. Values of individual patients are depicted, and lines show means. * $p < 0.05$, ** $p < 0.01$, *** $p < 0.001$.

Figure 5. PD-L1, TIM3 or LAG3 blockade increases *ex vivo* proliferation and cytokine production of CD4$^+$ and CD8$^+$ TIL in response to polyclonal stimuli. CFSE-labeled TIL were stimulated with CD3/CD28 beads, in the presence or absence of 10 µg/ml neutralizing antibodies. (A) Dot plots show the proliferation (CFSE-low) of CD3$^+$CD4$^+$ and CD3$^+$CD8$^+$ TIL after stimulation with CD3/CD28 beads, without addition of neutralizing antibody. Scatter plot shows the percentages of the proliferating (CFSE-low) CD4$^+$ and CD8$^+$ TIL of individual patients, without addition of neutralizing antibody. (B) (D) Effects of blocking inhibitory interactions on CD4$^+$ and CD8$^+$ TIL proliferation (n=10). Since the proliferation differed between patients, the results are reported as relative proliferation percentages calculated by dividing the percentages of proliferating (CFSE-low) T cells in the conditions with neutralizing antibody or with combinations of antibodies or with isotype controls, by the percentages in the condition with only CD3/CD28 beads. Values are depicted as means with SEM, * $p < 0.05$, ** $p < 0.01$. (C) (E) IFN-γ accumulation in culture supernatant was quantified by ELISA. Values are depicted as medians with interquartile range (n=10).

Figure 6. Combining PD-L1 blockade with TIM3, LAG3 or CTLA4 blockade additively increases *ex vivo* responses of CD8$^+$ TIL to TAA peptide stimulation. TIL of HLA-A2$^+$ patients were stimulated with pooled GPC3 FVGEFFTDV, GPC3 FLAELAYDL, MAGEC2 ALKVDVEERV and MAGEC2 LLFGLALIEV peptides (1 µg/ml of each), in the presence or absence of 10 µg/ml neutralizing antibodies. Intracellular cytokine production, CD137 and surface CD107a expression were analyzed after restimulation with pooled HCC peptides. Restimulation with HCV antigen peptide served as negative control for HCV negative

patients (including patients negative for both HCV and HBV), while restimulation with HBV antigen peptide served as negative control for HBV negative patients. (A) Representative dot plots of CD137, CD107a, IFN-γ and TNF-α expression in CD3$^+$CD8$^+$ TIL. (B) CD8$^+$ TIL responses to TAA peptides of seven patients, which are reported as fold increase calculated by dividing the percentages of CD137$^+$, CD107a$^+$, IFN-γ$^+$ or TNF-α$^+$ cells in the conditions with neutralizing antibody or with combinations of antibodies, by the percentages in the condition with only pooled HCC peptides. Not all four read-outs were detectable in every patient, therefore results of four to seven patients are presented for each type of response. Each line and each color represent one patient.

Figure 7. Combining PD-L1 blockade with TIM3, LAG3 or CTLA4 blockade additively increases *ex vivo* proliferation of CD4$^+$ and CD8$^+$ TIL in response to TAA presented by mRNA-transfected autologous B cell blasts. (A) HLA-A*0201-restricted GPC3 FVGEFFTDV-specific CD8$^+$ T cell clone or human T cells transfected with a TCR recognizing MAGEC2 ALKVDVEERV were co-cultured with HLA-A2$^+$ B cell blasts transfected with GPC3 mRNA or MAGEC2 mRNA. EGFP mRNA- or mock- (without mRNA) electroporated B cell blasts served as negative controls, while HLA-A2$^+$ B cell blasts pulsed with 1 µg/ml FVGEFFTDV peptide or ALKVDVEERV peptide served as positive controls. IFN-γ accumulation in culture supernatant was quantified by ELISA after 24 hours. (B) CFSE-labeled PBMC from an HCC patient were co-cultured with GPC3 mRNA-, MAGEC2 mRNA-, eGFP mRNA- or mock-electroporated autologous B cell blasts. CD4$^+$ and CD8$^+$ T cell proliferation was measured by flow cytometry. (C) (D) CFSE-labeled TIL were co-cultured with GPC3 mRNA-, MAGEC2 mRNA-, eGFP mRNA- or mock-electroporated autologous B cell blasts, in the presence or absence of 10 µg/ml neutralizing antibodies. (C) Representative dot plots of CD4$^+$ and CD8$^+$ T cell proliferation in response to eGFP mRNA-transfected (negative control) and MAGEC2 mRNA-transfected autologous B cell blasts in the absence or presence of neutralizing antibody. (D) Proliferation of CD4$^+$ and CD8$^+$ TIL of nine patients in response to GPC3 and/or MAGEC2. For each patient, the data of either the only or the average antigen-induced TIL response are presented. Since the proliferative responses to TAA differed between patients, the results are reported as fold increase of antigen-specific T cell proliferation calculated by dividing the percentages of proliferating (CFSE-low) T cells in response to GPC3 or MAGEC2 in the conditions with neutralizing antibody or with combinations of antibodies, by the percentages in the condition without neutralizing antibody.
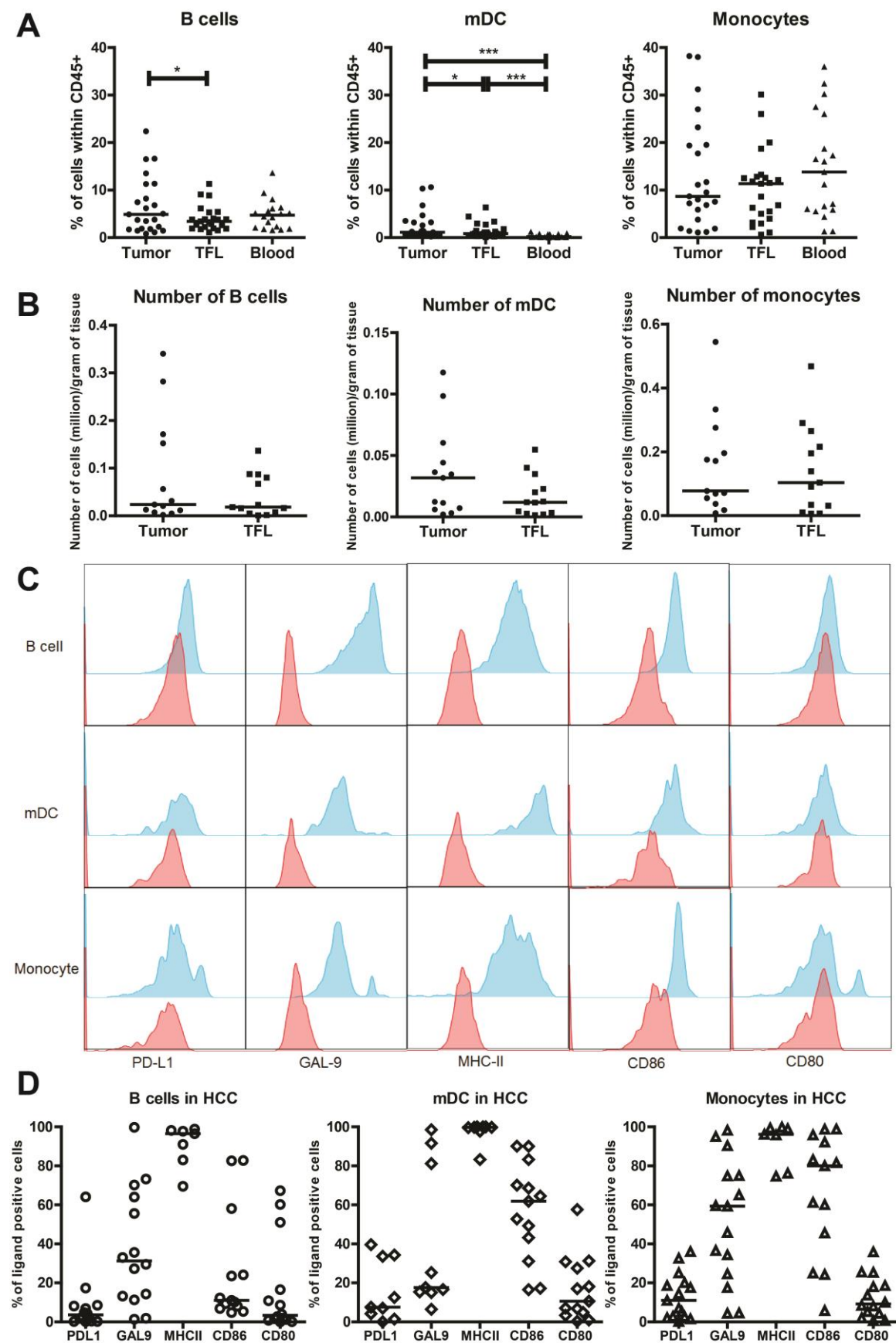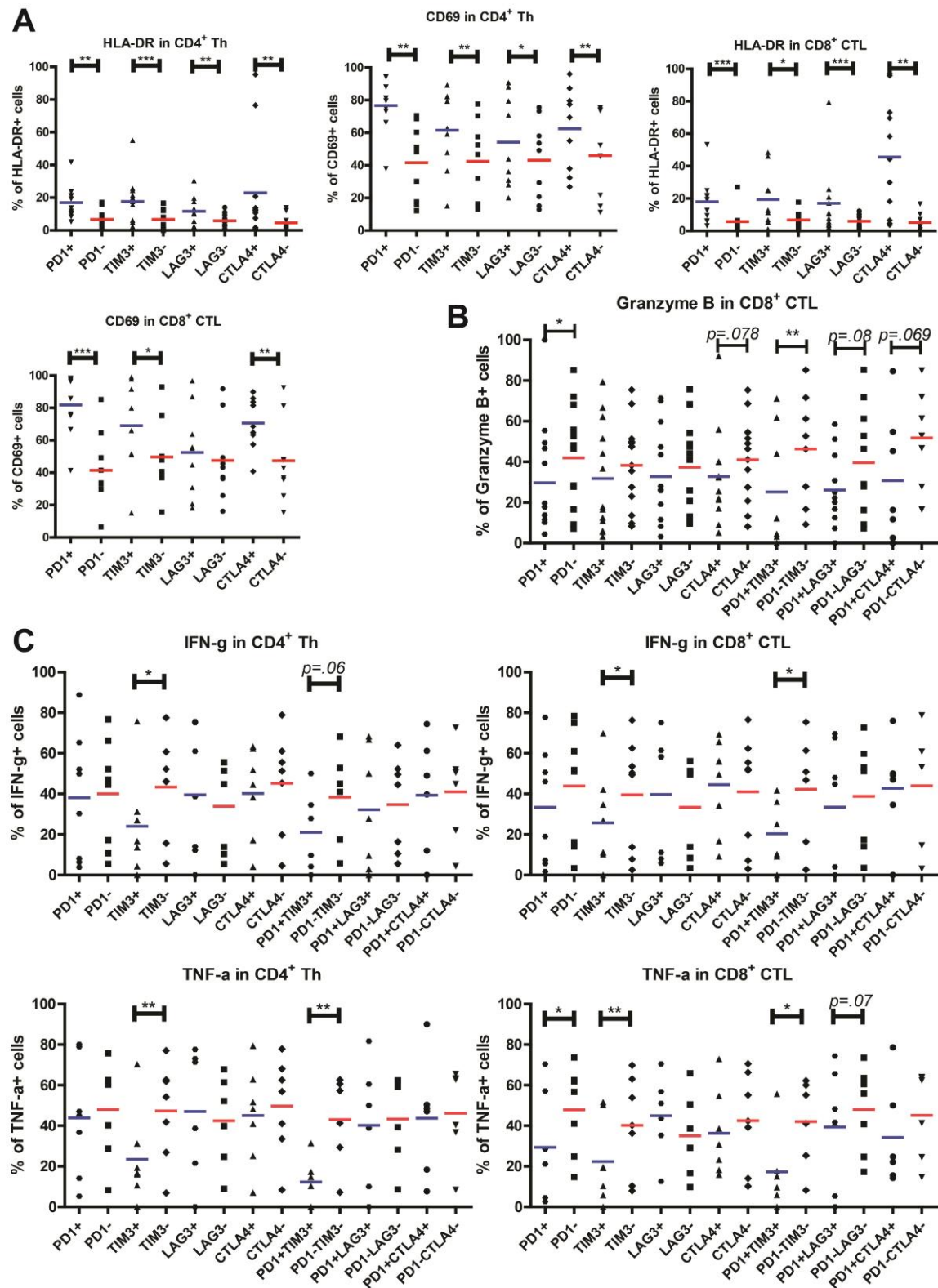
Figure 1.

Figure 2.

Figure 3.

Figure 4.

A

HLA-DR in CD4+ Th

CD69 in CD4+ Th

HLA-DR in CD8+ CTL

CD69 in CD8+ CTL

B Granzyme B in CD8+ CTL

C

IFN-g in CD4+ Th

IFN-g in CD8+ CTL

TNF-a in CD4+ Th
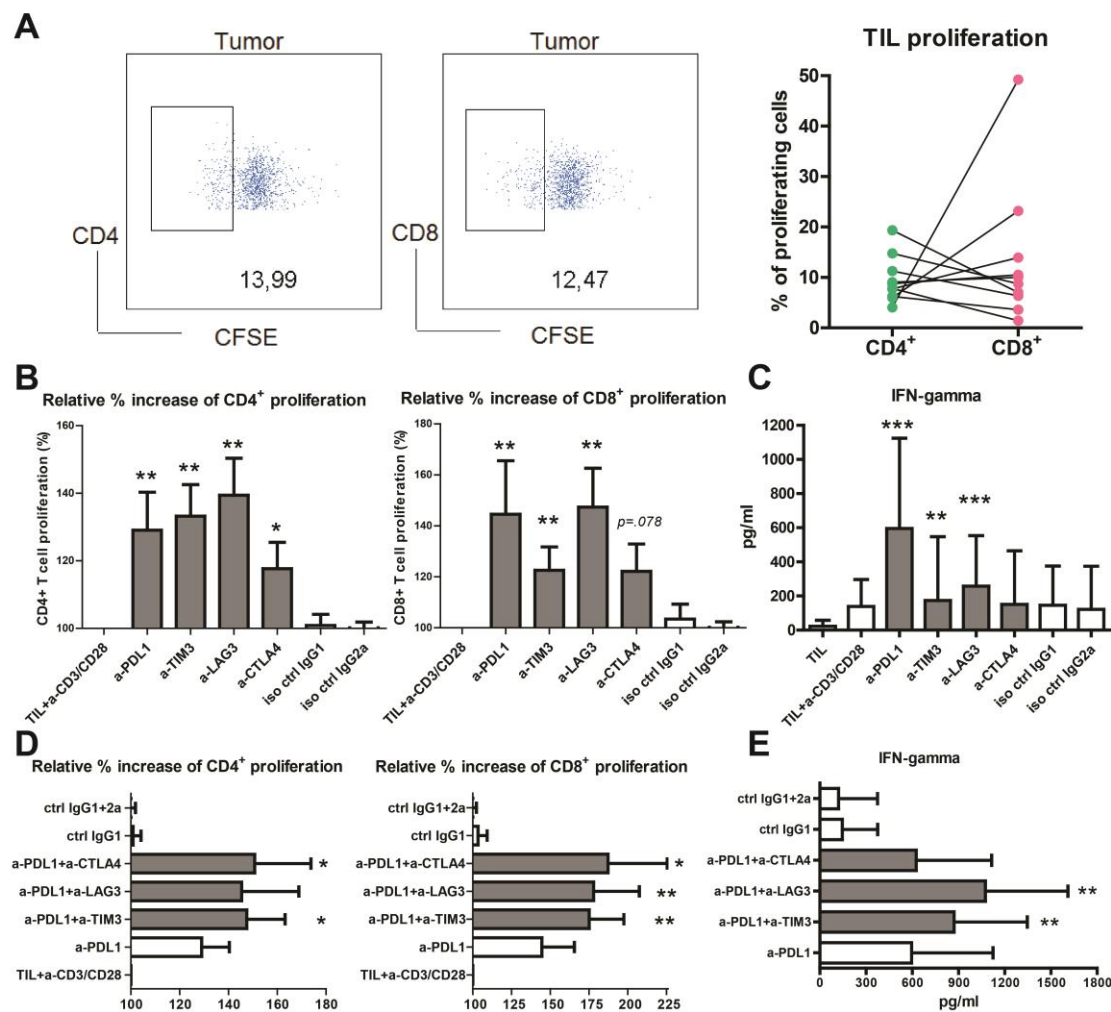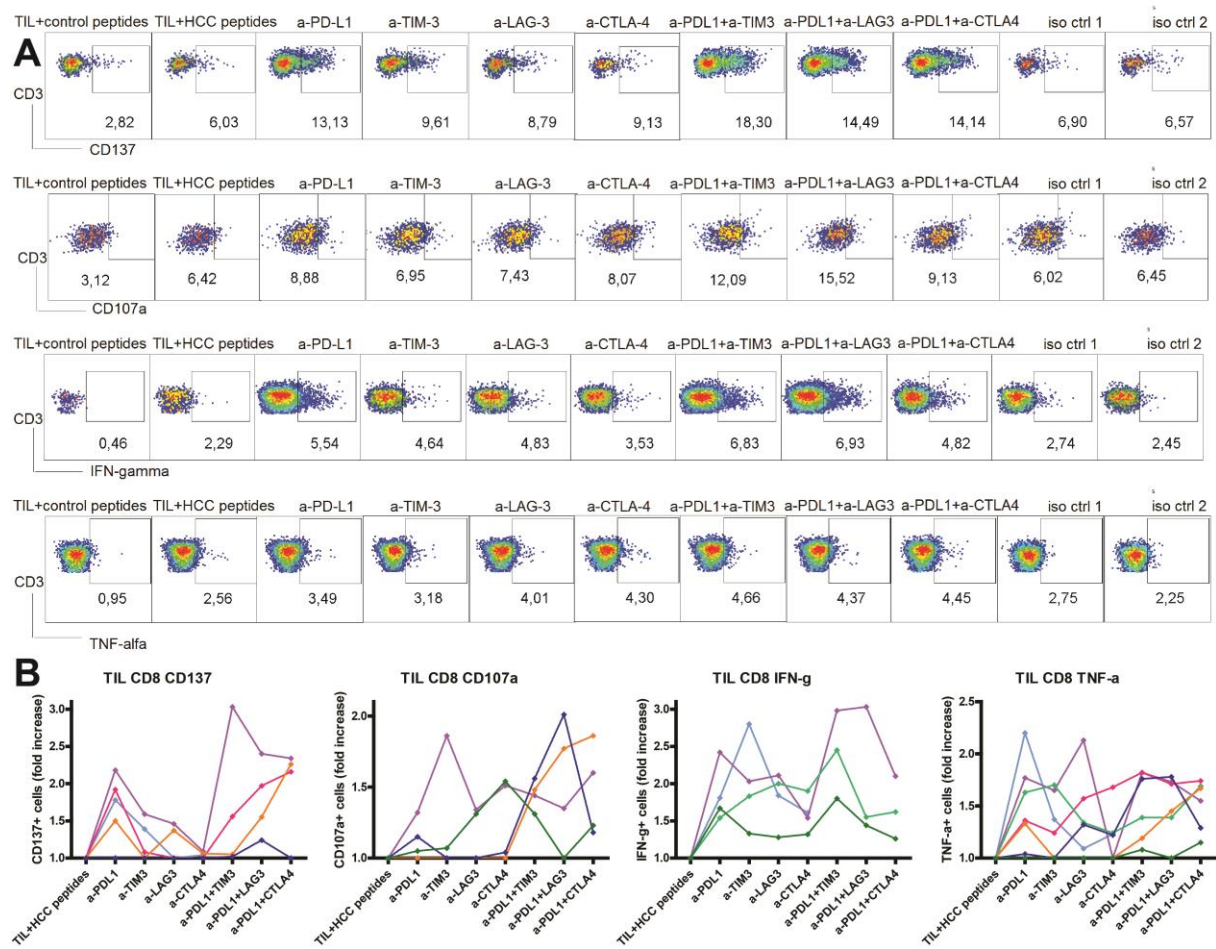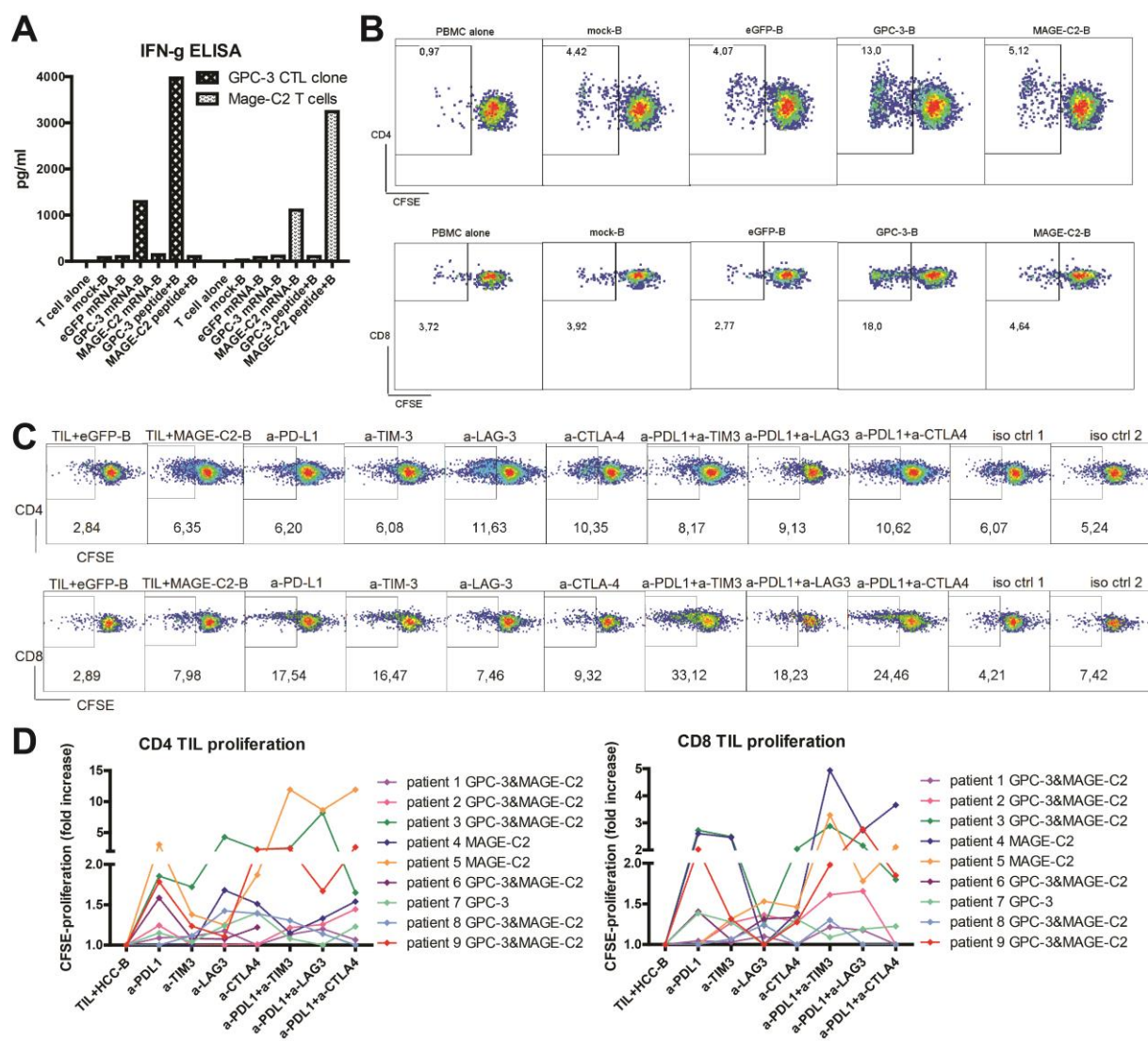
TNF-a in CD8+ CTL
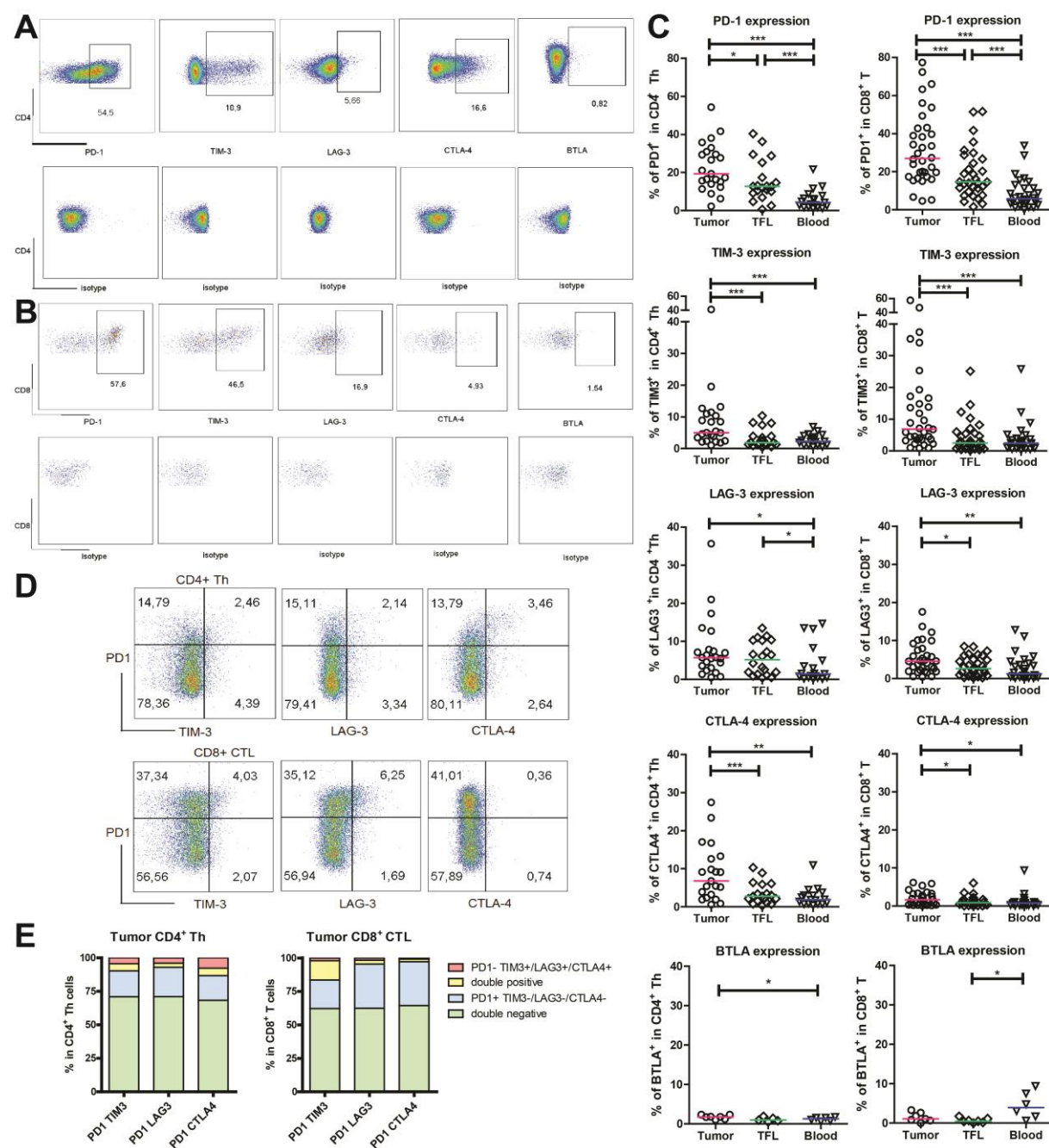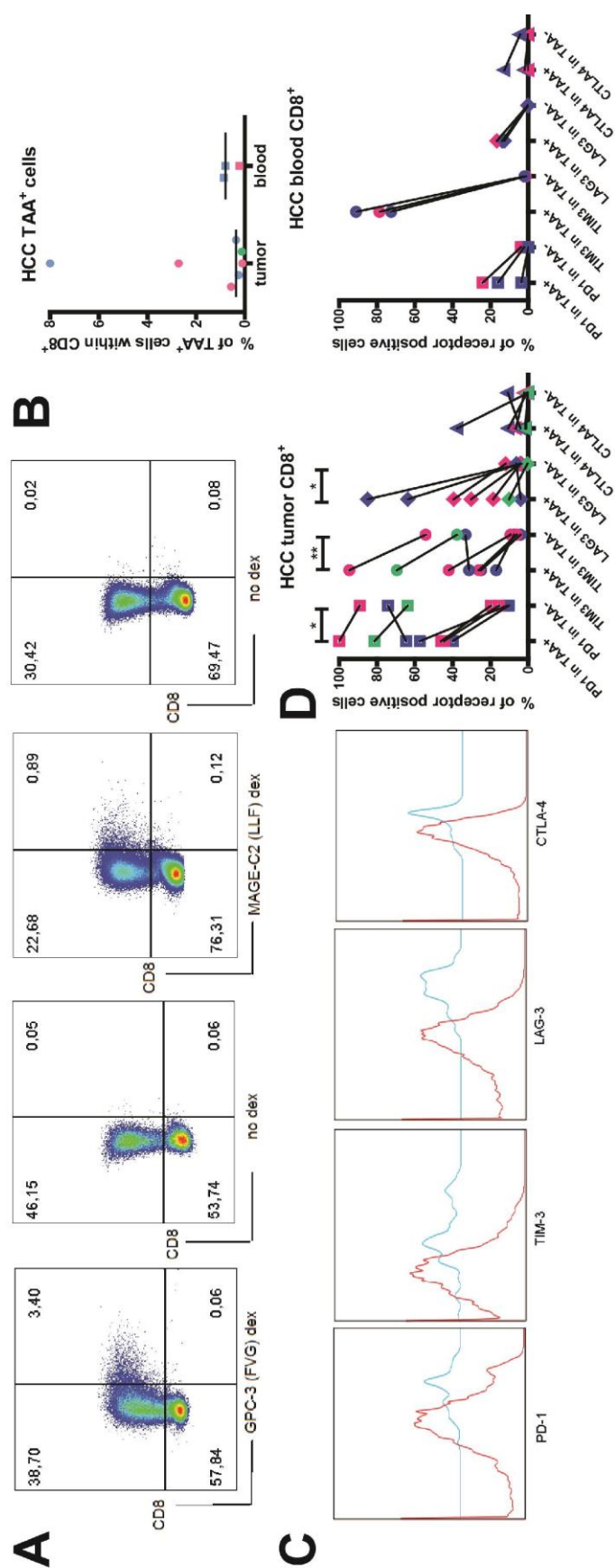
Figure 5.

Figure 6.

Figure 7.

Supplementary figure legends

Supplementary Figure 1. Expression of inhibitory receptors on CD4$^+$ Th and CD8$^+$ CTL in the tumor, TFL, and blood. Median fluorescence intensity of inhibitory receptors PD-1, TIM3, LAG3, CTLA4 and BTLA within (A) CD4$^+$ Th and (B) CD8$^+$ CTL from the tumor, TFL and blood. Values of individual patients are depicted, and lines show medians; * $p < 0.05$, ** $p < 0.01$, *** $p < 0.001$.

Supplementary Figure 2. Correlation of the expression of inhibitory receptors on T cells between the tumor and the blood. Spearman correlation analysis demonstrates (A) positive correlations of the percentages of PD-1, TIM3, LAG3 or CTLA4 positive cells in CD4$^+$ Th between the tumor and the blood, and (B) positive correlations of the percentages of LAG3 or CTLA4 positive cells in CD8$^+$ CTL between the tumor and the blood.

Supplementary Figure 3. Expression of PD-1, TIM3 and LAG3 is increased on HCC TAA-specific CD8$^+$ TIL. Median fluorescence intensity of PD-1, TIM3, LAG3 and CTLA4 in TAA dextramer positive versus TAA dextramer negative CD8$^+$ T cells in the tumor and the blood. For each patient, the value of either the only or the dominant dextramer-binding population is depicted; * $p < 0.05$. Blue symbols: GPC-3 FVGEFFTDV positive; green symbols: GPC-3 FLAELAYDL positive; red symbols: MAGE-C2 LLFGLALIEV positive.

Supplementary Figure 4. Expression of inhibitory ligands on antigen-presenting cells in the tumor, TFL and blood. (A) Median fluorescence intensity of inhibitory ligands PD-L1, MHC-II, GAL-9, CD80 and CD86 and (B) the percentages of cells expressing inhibitory ligands within B cells, myeloid dendritic cells (mDC) and monocytes from the tumor, TFL and blood. Values of individual patients are shown; lines depict (A) means or (B) medians; * $p < 0.05$, ** $p < 0.01$.

Supplementary Figure 5. Association between the expression of inhibitory receptor and the effect of blocking antibody on TIL proliferation in polyclonal T cell activation assay. The percentages of inhibitory receptor positive CD3$^+$CD4$^+$Foxp3$^-$ TIL or CD3$^+$CD8$^+$ TIL are shown, comparing high-responding TIL (n=4) and low or non-responding TIL (n=4) in the four conditions with neutralizing antibody. High-responding TIL are those whose relative % increase of TIL proliferation in the presence of a neutralizing antibody is above the median % increase of all the patients, and low or non-responding TIL are those whose relative % increase of TIL proliferation is below the median level. Values are depicted as means with SEM, * $p < 0.05$.

Supplementary Figure 6. Association between the expression of inhibitory receptor and the effect of blocking antibody on TIL proliferation in mRNA-encoded full-length tumor antigen-specific T cell stimulation assay. The percentages of inhibitory receptor positive CD3$^+$CD4$^+$Foxp3$^-$ TIL or CD3$^+$CD8$^+$ TIL are shown, comparing high-responding TIL (n=3) and low or non-responding TIL (n=4) in the four conditions with neutralizing antibody. High-responding TIL are those whose fold increase of TIL proliferation in the presence of a neutralizing antibody is above the median fold increase of all the patients, and low or non-responding TIL are those whose fold increase of TIL proliferation is below the median level. Values are depicted as means with SEM.

Supplementary Figure 1.
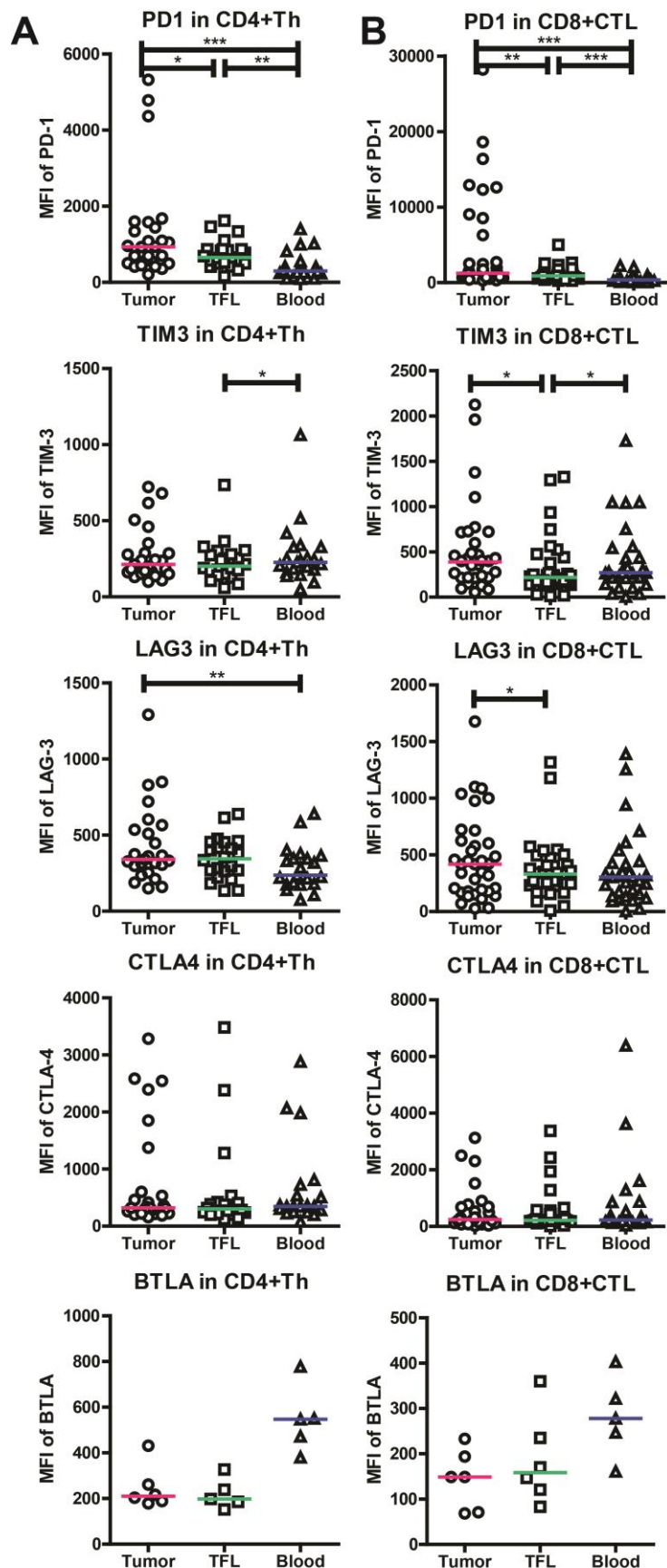
Supplementary Figure 2.
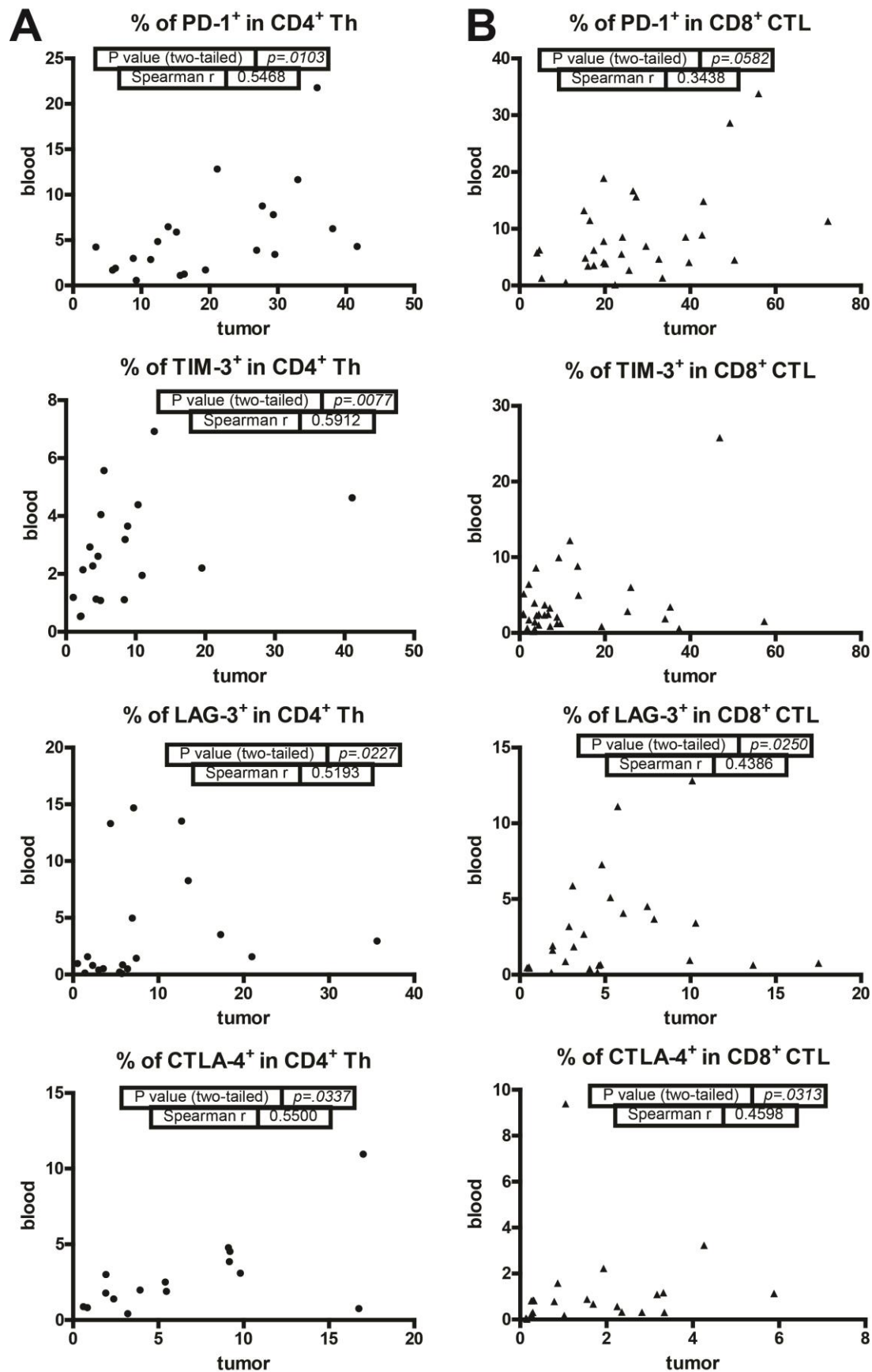
Supplementary Figure 3.
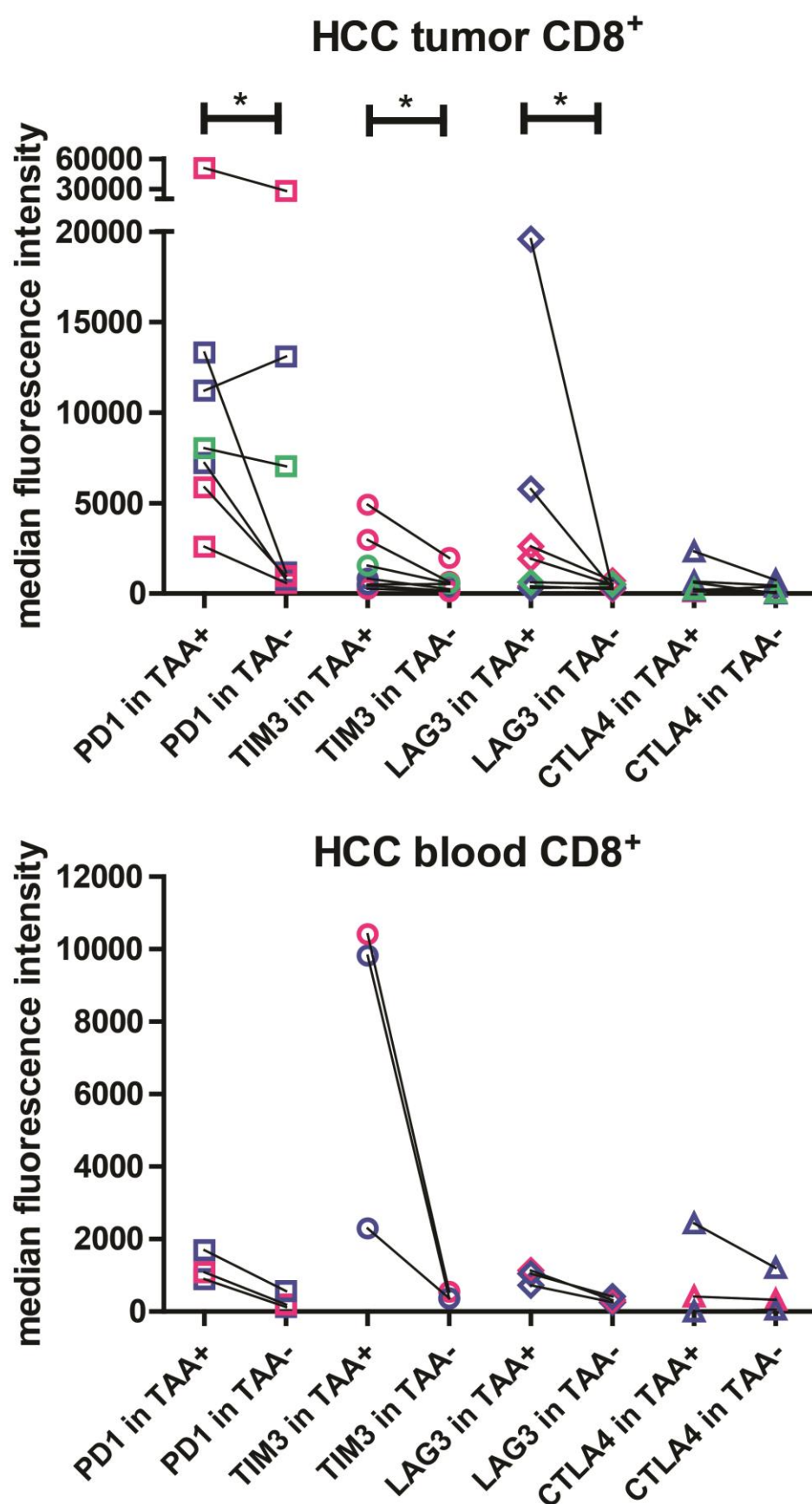
Supplementary Figure 4.
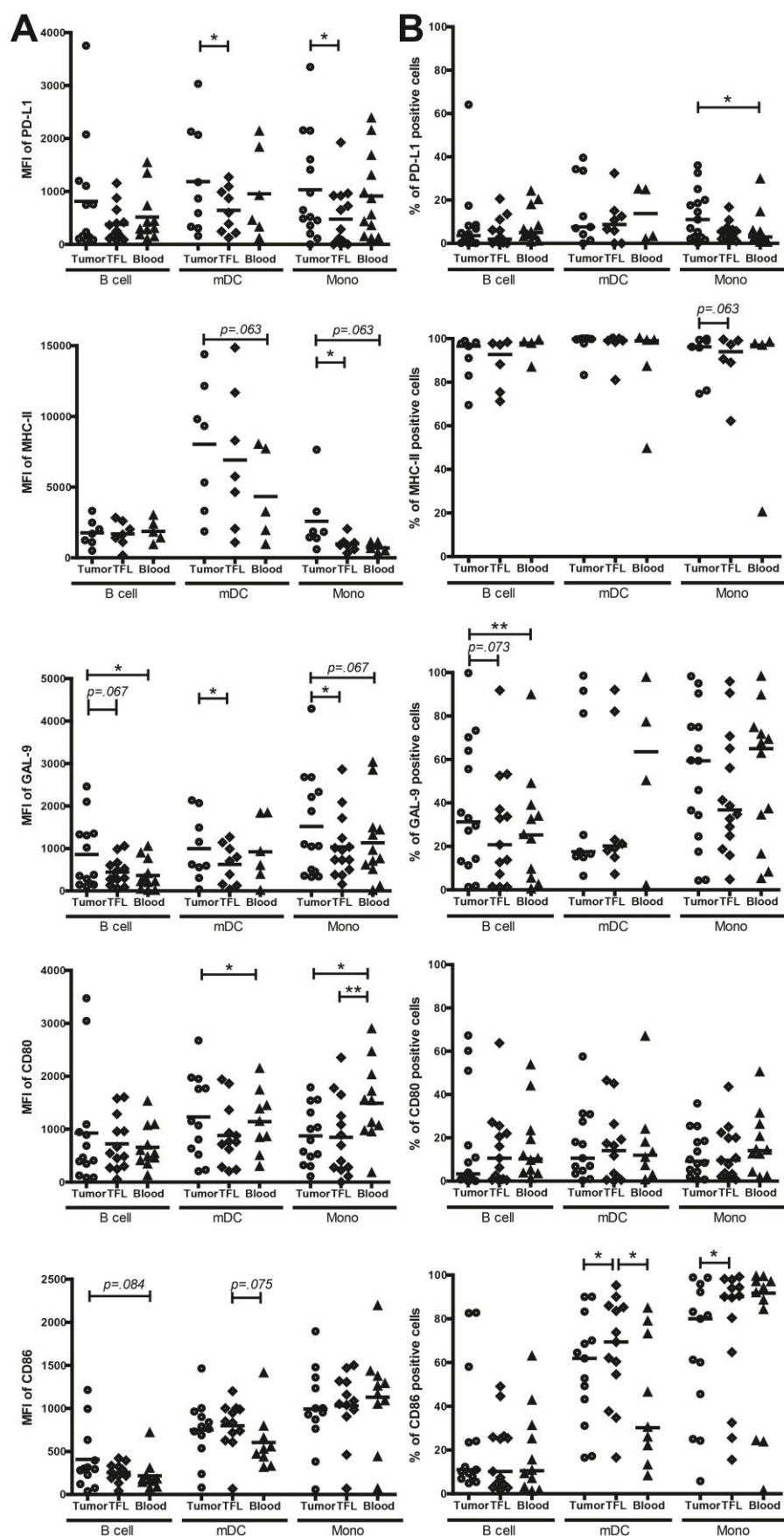
Supplementary Figure 5.

CD4⁺ TIL proliferation in response to checkpoint blockade
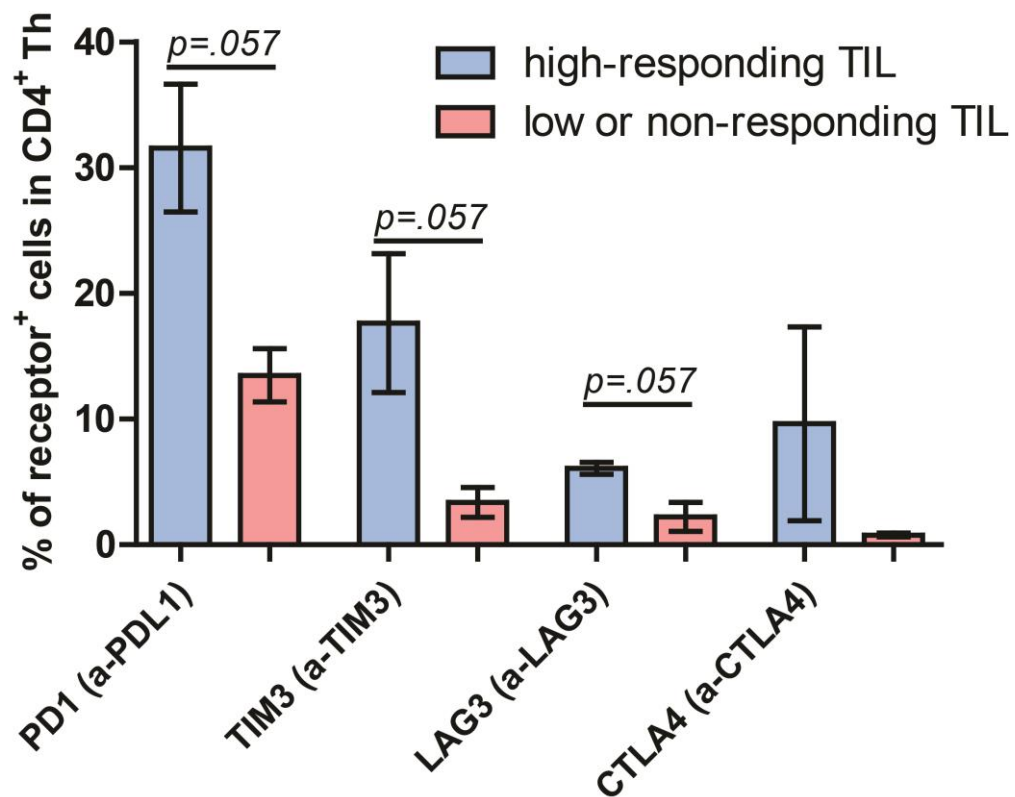
CD8⁺ TIL proliferation in response to checkpoint blockade
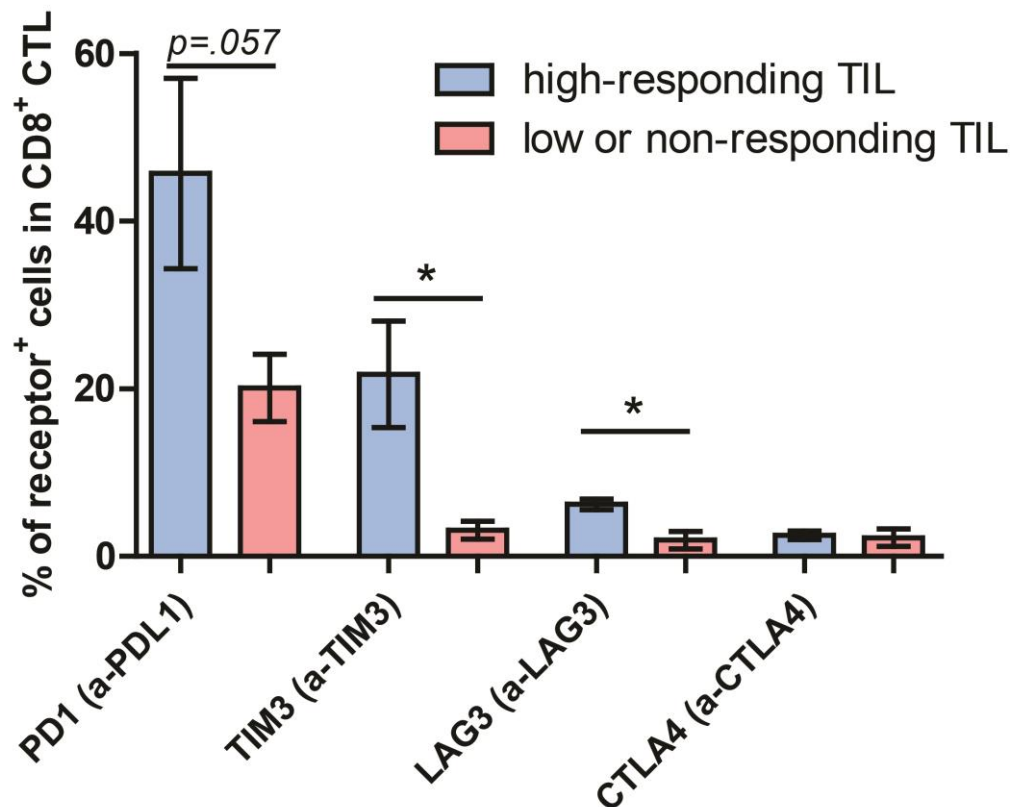
Supplementary Figure 6.

CD4+ TIL proliferation in response to checkpoint blockade
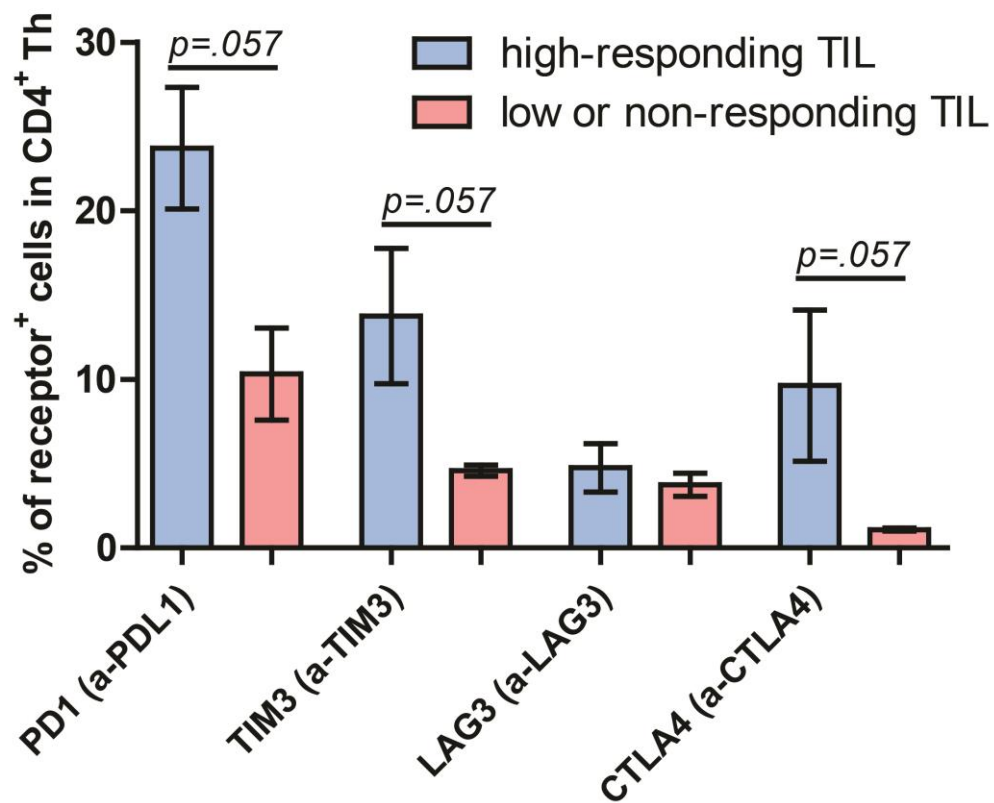
CD8+ TIL proliferation in response to checkpoint blockade
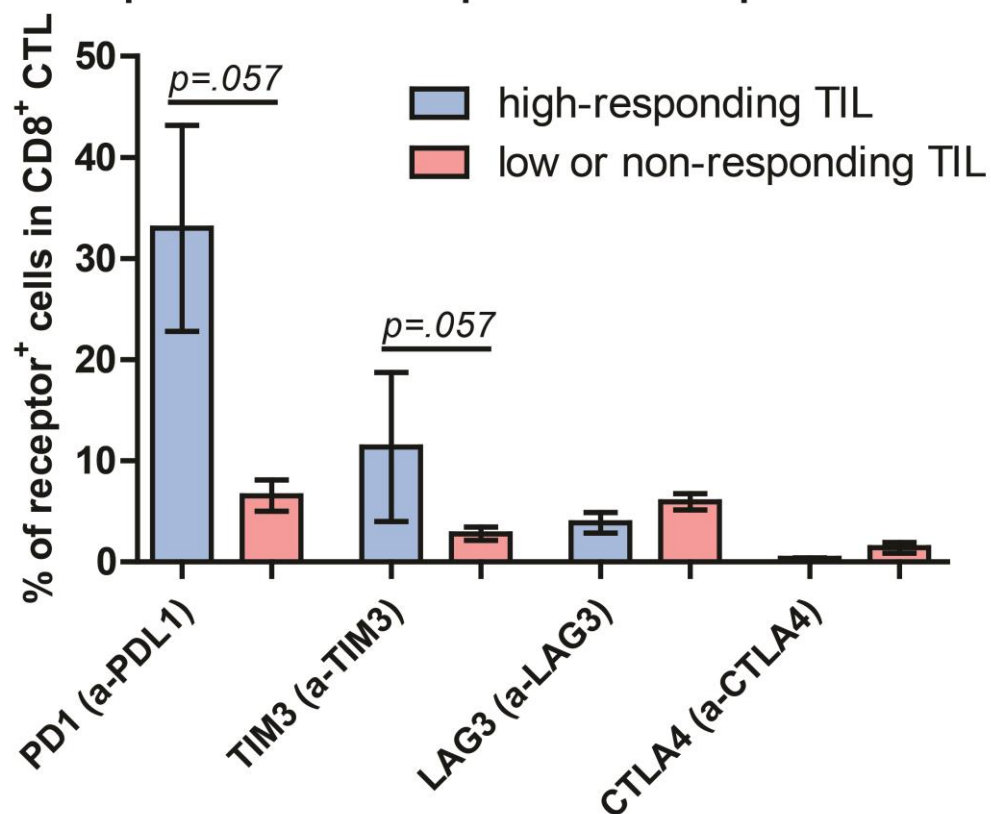
Supplementary Table 1. Patient characteristics

	HCC (n=59)
Sex (male/female)	46 / 13
Age (years)**	64.8 ± 1.8
Race (Caucasian/Asian/African)	50 / 5 / 4
ALT (units/L)**	58.7 ± 6.4
Bilirubin (µmol/L)**	16.4 ± 5.7
Protrombin time (INR)**	1.1 ± 0.02
Liver fibrosis (metavir score) F0-F1 / F2 / F3-F4-cirrhosis	28 / 4 / 27
AFP (µg/L)** <20/ 20-400/ >400/ unknown	45 / 1 / 10 / 3
Stage of disease (TNM)	St I n=28, St II n=26, St IIIa n=4, unknown n=1

Abbreviations: INR, international normalized ratio; AFP, alpha fetoprotein; TNM, tumor-node-metastasis.

Etiology of liver disease: no known liver disease (n = 23), HBV/HCV (n =10/6), alcohol-related liver disease (n = 6), HBV/HCV + alcohol (n = 3), non-alcoholic steatohepatitis (NASH)/non-alcoholic fatty liver disease (NAFLD) (n = 4/4), HBV + NASH (n = 1), porphyria (n = 1), abernathy (n=1).

**Mean ± SEM.

Supplementary Table 2. Anti-human antibodies used in flow cytometry (FACS)

Antibody	Clone	Supplier	Antibody	Clone	Supplier
CD69 APC	L78	BD Biosciences	mIgG1-PE	P3.6.2.8.1	eBioscience
IFN-gamma-FITC	25723.11	BD Biosciences	HLA-DR-APC	LN3	eBioscience
HLA-A2-APC	BB7.2	BD Biosciences	HLA-DR-PE		eBioscience
CD19-HorizonV500	HIB19	BD Biosciences	HLA-DR-PerCP-Cy5.5	LN3	eBioscience
mIgG2a-PerCP	X39	BD Biosciences	CD14 PE-Cy7	61D3	eBioscience
CD3 PerCP-Cy5.5	UCHT1	BD Biosciences	CD3 PE-Cy7	UCHT1	eBioscience
HLA-A2-FITC	BB7.2	BD Biosciences	CD8-APC	okt-08	eBioscience
mIgG2b-FITC	27-35	BD Biosciences	CD14-eFlour450	61D3	eBioscience
mIgG1-PB	MOPC-21	BD Biosciences	IFN-gamma-Pe-Cy7	4S.B3	eBioscience
mIgG2b-PE	27-35	BD Biosciences	HLA-DR-APC-eFluor780	LN3	eBioscience
mIgG1-PerCP	X40	BD Biosciences	CD14-FITC	61D3	eBioscience
mIgG1-FITC	MOPC-21	BD Biosciences	CD279 (PD1)-PE-Cy7	J105	eBioscience
mIgG1-pacific blue	MOPC-21	BD Biosciences	CD8-efluor450	RPA-T8	eBioscience
GranzymeB-V450	GB11	BD Biosciences	CD274(B7-H1)-PE-Cy7	MIH1	eBioscience
CD137 (4-1BB)-APC	4B4-1	BD Biosciences	CD270 (HVEM)-PE	eBioHVEM-122	eBioscience
CD19 PE	J4.119	Beckman	CD4-APC-eFluor780	OKT4	eBioscience
CD69-PE	TP1.55.3	Beckman	CD3-APC-eFluor780	SK7	eBioscience
CD3 FITC	UCHT1	Beckman	FoxP3-eFluor450	236A/E7	eBioscience
mIgG2a-PE	U7.27	Beckman	CD45 efluor 450	HI30	eBioscience
CD152 (CTLA4)-APC	L3D10	Biolegend	CD19-APC-eFluor780	HIB19	eBioscience
CD272 (BTLA)-APC	MIH26	Biolegend	CD8a-PerCp-Cy5.5	RPA-T8	eBioscience
CD3 PE	UCHT1	Biolegend	TNFα APC	MAb11	eBioscience
CD86-PB	IT2.2	Biolegend	CD223(LAG3)-PE	3DS223H	eBioscience
anti-TNF-α-PerCP-Cy5.5	Mab11	Biolegend	CD223(LAG3)-PerCP-eF710	3DS223H	eBioscience
TIM3-Brilliant-Vio421	F38-2E2	Biolegend	CD8-FITC	SK1	eBioscience
Galectin-9 PE	9M1-3	Biolegend	rat IgG2a-APC	eBR2a	eBioscience
CD80-PE-Cy7	2D10	Biolegend	mIgG1-FITC	P3	eBioscience
CD14-BV510	M5E2	Biolegend	mIgG2a-APC	eBM2a	eBioscience
CD56-BV510	HCD56	Biolegend	rat IgG2b-APC	eB149/10H5	eBioscience
HLA-DR, DP, DQ-FITC	Tü39	Biolegend	CD8-PE	RPA-T8	eBioscience
mIgG1-Pe-Cy7	MOPC-21	Biolegend	CD107a PE	H4A3	eBioscience

rat IgG2a-PE	RTK2758	Biolegend	TIM3-PE	344823	R&D systems
mIgG2a-FITC	MOPC-173	Biolegend	BDCA1-APC	AD5-8E7	Miltenyi
mIgG1-APC	MOPC-21	Biolegend			

Supplementary Table 3. The percentages of CD8^{+} T cells binding to different TAA-peptide-HLA-A*0201-dextramer complexes in tumors of 13 HLA-A2^{+} HCC patients and in blood of 12 HLA-A2^{+} HCC patients

Epitope	FVG	FLA	ALK	LLF	FVG	FLA	ALK	LLF
TAA	GPC-3	GPC-3	MAGE-C2	MAGE-C2	GPC-3	GPC-3	MAGE-C2	MAGE-C2
Patient	TIL	TIL	TIL	TIL	PBMC	PBMC	PBMC	PBMC
1	0.36%	0.32%		0.35%				
2					0.8%	0.61%		0.64%
3				0.56%				0.23%
4					0.87%			
5	0.26%	0.15%						
6								
7				0.11%				
8				2.72%				
9					NT	NT	NT	NT
10	8.00%							
11								
12								
13		0.13%						

Abbreviations: TAA, tumor-associated antigen; NT, not tested; FVG, GPC3 peptide FVGEFFTDV; FLA, GPC3 peptide FLAELAYDL; ALK, MAGEC2 peptide ALKVDVEERV; LLF, MAGEC2 peptide LLFGLALIEV; TIL, tumor-infiltrating lymphocytes; PBMC, peripheral blood mononuclear cells.

REFERENCES

1.   Ferlay J, Soerjomataram I, Dikshit R, et al. Cancer incidence and mortality worldwide: sources, methods and major patterns in GLOBOCAN 2012. Int J Cancer 2015;136:E359-86.
2.   Mazzanti R, Gramantieri L, Bolondi L. Hepatocellular carcinoma: epidemiology and clinical aspects. Mol Aspects Med 2008;29:130-43.
3.   El-Serag HB, Marrero JA, Rudolph L, et al. Diagnosis and treatment of hepatocellular carcinoma. Gastroenterology 2008;134:1752-63.
4.   Gao Q, Qiu SJ, Fan J, et al. Intratumoral balance of regulatory and cytotoxic T cells is associated with prognosis of hepatocellular carcinoma after resection. J Clin Oncol 2007;25:2586-93.
5.   Chew V, Tow C, Teo M, et al. Inflammatory tumour microenvironment is associated with superior survival in hepatocellular carcinoma patients. J Hepatol 2010;52:370-9.
6.   Pedroza-Gonzalez A, Verhoef C, Ijzermans JN, et al. Activated tumor-infiltrating CD4+ regulatory T cells restrain antitumor immunity in patients with primary or metastatic liver cancer. Hepatology 2013;57:183-94.
7.   Pedroza-Gonzalez A, Zhou G, Singh SP, et al. GITR engagement in combination with CTLA-4 blockade completely abrogates immunosuppression mediated by human liver tumor-derived regulatory T cells ex vivo. Oncoimmunology 2015;4:e1051297.
8.   Pedroza-Gonzalez A, Zhou G, Vargas-Mendez E, et al. Tumor-infiltrating plasmacytoid dendritic cells promote immunosuppression by Tr1 cells in human liver tumors. Oncoimmunology 2015;4:e1008355.
9.   Fourcade J, Sun Z, Pagliano O, et al. CD8(+) T cells specific for tumor antigens can be rendered dysfunctional by the tumor microenvironment through upregulation of the inhibitory receptors BTLA and PD-1. Cancer Res 2012;72:887-96.
10.   Wherry EJ. T cell exhaustion. Nat Immunol 2011;12:492-9.
11.   Baitsch L, Baumgaertner P, Devevre E, et al. Exhaustion of tumor-specific CD8(+) T cells in metastases from melanoma patients. J Clin Invest 2011;121:2350-60.
12.   Nguyen LT, Ohashi PS. Clinical blockade of PD1 and LAG3--potential mechanisms of action. Nat Rev Immunol 2015;15:45-56.
13.   Brahmer JR, Tykodi SS, Chow LQ, et al. Safety and activity of anti-PD-L1 antibody in patients with advanced cancer. N Engl J Med 2012;366:2455-65.
14.   Topalian SL, Hodi FS, Brahmer JR, et al. Safety, activity, and immune correlates of anti-PD-1 antibody in cancer. N Engl J Med 2012;366:2443-54.
15.   Borghaei H, Paz-Ares L, Horn L, et al. Nivolumab versus Docetaxel in Advanced Nonsquamous Non-Small-Cell Lung Cancer. N Engl J Med 2015;373:1627-39.
16.   Hamid O, Robert C, Daud A, et al. Safety and tumor responses with lambrolizumab (anti-PD-1) in melanoma. N Engl J Med 2013;369:134-44.
17.   Topalian SL, Sznol M, McDermott DF, et al. Survival, durable tumor remission, and long-term safety in patients with advanced melanoma receiving nivolumab. J Clin Oncol 2014;32:1020-30.
18.   Wolchok JD, Kluger H, Callahan MK, et al. Nivolumab plus ipilimumab in advanced melanoma. N Engl J Med 2013;369:122-33.
19.   Flecken T, Schmidt N, Hild S, et al. Immunodominance and functional alterations of tumor-associated antigen-specific CD8+ T-cell responses in hepatocellular carcinoma. Hepatology 2014;59:1415-26.
20.   Kuang DM, Zhao Q, Peng C, et al. Activated monocytes in peritumoral stroma of hepatocellular carcinoma foster immune privilege and disease progression through PD-L1. J Exp Med 2009;206:1327-37.
21.   Wu K, Kryczek I, Chen L, et al. Kupffer cell suppression of CD8+ T cells in human hepatocellular carcinoma is mediated by B7-H1/programmed death-1 interactions. Cancer Res 2009;69:8067-75.
22.   Zhao Q, Xiao X, Wu Y, et al. Interleukin-17-educated monocytes suppress cytotoxic T-cell function through B7-H1 in hepatocellular carcinoma patients. Eur J Immunol 2011;41:2314-22.
23.   Li H, Wu K, Tao K, et al. Tim-3/galectin-9 signaling pathway mediates T-cell dysfunction and predicts poor prognosis in patients with hepatitis B virus-associated hepatocellular carcinoma. Hepatology 2012;56:1342-51.
24.   Sideras K, Bots SJ, Biermann K, et al. Tumour antigen expression in hepatocellular carcinoma in a low-endemic western area. Br J Cancer 2015;112:1911-20.
25.   Sideras K, Biermann K, Verheij J, et al. PD-L1, Galectin-9 and CD8+ tumor-infiltrating lymphocytes are associated with survival in hepatocellular carcinoma. Oncoimmunology 2017;6:e1273309.

26. Shi XL, de Mare-Bredemeijer EL, Tapirdamaz O, et al. CMV Primary Infection Is Associated With Donor-Specific T Cell Hyporesponsiveness and Fewer Late Acute Rejections After Liver Transplantation. Am J Transplant 2015;15:2431-42.

27. Tapirdamaz O, Mancham S, van der Laan LJ, et al. Detailed kinetics of the direct allo-response in human liver transplant recipients: new insights from an optimized assay. PLoS One 2010;5:e14452.

28. Bonehill A, Heirman C, Tuyaerts S, et al. Messenger RNA-electroporated dendritic cells presenting MAGE-A3 simultaneously in HLA class I and class II molecules. J Immunol 2004;172:6649-57.

29. Yoshikawa T, Nakatsugawa M, Suzuki S, et al. HLA-A2-restricted glypican-3 peptide-specific CTL clones induced by peptide vaccine show high avidity and antigen-specific killing activity against tumor cells. Cancer Sci 2011;102:918-25.

30. Straetemans T, van Brakel M, van Steenbergen S, et al. TCR gene transfer: MAGE-C2/HLA-A2 and MAGE-A3/HLA-DP4 epitopes as melanoma-specific immune targets. Clin Dev Immunol 2012;2012:586314.

31. Shi F, Shi M, Zeng Z, et al. PD-1 and PD-L1 upregulation promotes CD8(+) T-cell apoptosis and postoperative recurrence in hepatocellular carcinoma patients. Int J Cancer 2011;128:887-96.

32. Li FJ, Zhang Y, Jin GX, et al. Expression of LAG-3 is coincident with the impaired effector function of HBV-specific CD8(+) T cell in HCC patients. Immunol Lett 2013;150:116-22.

33. Gros A, Robbins PF, Yao X, et al. PD-1 identifies the patient-specific CD8(+) tumor-reactive repertoire infiltrating human tumors. J Clin Invest 2014;124:2246-59.

34. Xu Y, Li H, Gao RL, et al. Expansion of interferon-gamma-producing multifunctional CD4+ T-cells and dysfunctional CD8+ T-cells by glypican-3 peptide library in hepatocellular carcinoma patients. Clin Immunol 2011;139:302-13.

35. Sawada Y, Yoshikawa T, Shimomura M, et al. Programmed death-1 blockade enhances the antitumor effects of peptide vaccine-induced peptide-specific cytotoxic T lymphocytes. Int J Oncol 2015;46:28-36.

36. Baitsch L, Legat A, Barba L, et al. Extended co-expression of inhibitory receptors by human CD8 T-cells depending on differentiation, antigen-specificity and anatomical localization. PLoS One 2012;7:e30852.

37. Legat A, Speiser DE, Pircher H, et al. Inhibitory Receptor Expression Depends More Dominantly on Differentiation and Activation than "Exhaustion" of Human CD8 T Cells. Front Immunol 2013;4:455.

38. Fourcade J, Sun Z, Benallaoua M, et al. Upregulation of Tim-3 and PD-1 expression is associated with tumor antigen-specific CD8+ T cell dysfunction in melanoma patients. J Exp Med 2010;207:2175-86.

39. Matsuzaki J, Gnjatic S, Mhawech-Fauceglia P, et al. Tumor-infiltrating NY-ESO-1-specific CD8+ T cells are negatively regulated by LAG-3 and PD-1 in human ovarian cancer. Proc Natl Acad Sci U S A 2010;107:7875-80.

40. Van Nuffel AM, Tuyaerts S, Benteyn D, et al. Epitope and HLA-type independent monitoring of antigen-specific T-cells after treatment with dendritic cells presenting full-length tumor antigens. J Immunol Methods 2012;377:23-36.

41. Sangro B, Gomez-Martin C, de la Mata M, et al. A clinical trial of CTLA-4 blockade with tremelimumab in patients with hepatocellular carcinoma and chronic hepatitis C. J Hepatol 2013;59:81-8.

42. El-Khoueiry AB, Sangro B, Yau T, et al. Nivolumab in patients with advanced hepatocellular carcinoma (CheckMate 040): an open-label, non-comparative, phase 1/2 dose escalation and expansion trial. Lancet 2017.

43. Germeau C, Ma W, Schiavetti F, et al. High frequency of antitumor T cells in the blood of melanoma patients before and after vaccination with tumor antigens. J Exp Med 2005;201:241-8.

Supplementary Materials and Methods

Flow cytometric analysis

Fresh PBMC and mononuclear leukocytes isolated from tumor and TFL were analyzed for expression of surface and intracellular markers using specific antibodies (Supplementary Table 2). Cell surface staining with fluorochrome-conjugated antibodies was *performed* in the dark at 4°C for 30 minutes, then cells were washed and resuspended in PBS with 0.2 mM EDTA and 0.5% human serum. For Foxp3, Granzyme B and CTLA4 staining, cells were fixed and permeabilized using the Foxp3 staining buffer set from eBioscience (Vienna, Austria). For intracellular cytokine staining, cells were exposed to 40 ng/mL PMA (Sigma, Zwijndrecht, The Netherlands) and 1 µg/mL ionomycin (Sigma) at 37°C for five hours in the presence of 5 µg/mL brefeldin (Sigma) during the last four hours, followed by staining of IFN-γ and TNF-α upon fixation and permeabilization using the Foxp3 staining buffer set. To identify TAA-specific T cells, PBMC and TIL of HLA-A2[+] HCC patients (as determined by flow cytometric analysis of binding to anti-HLA-A2 antibody) were pre-treated with protein tyrosine kinase inhibitor (PKI) dasatinib at a final concentration of 50 nM in PBS at 37°C for 30 minutes.[1-3] Cells were then stained with PE-labeled HLA-A*0201/GPC3 144-152 (FVGEFFTDV), HLA-A*0201/GPC3 522-530 (FLAELAYDL), HLA-A*0201/MAGEC2 336-344 (ALKVDVEERV), HLA-A*0201/MAGEC2 191-200 (LLFGLALIEV) (Immudex, Copenhagen, Denmark) or no dextramer (as a negative control) at room temperature for 10 minutes. Subsequently, cells were stained with CD8 (clone SK1), CD4, PD-1, TIM3, LAG3, CD56, CD19, CD14 antibodies at 4°C for 20 minutes and then CTLA4 antibody intracellularly using the Foxp3 staining buffer set. Dead cells were excluded by using a LIVE/DEAD fixable dead cell stain kit with aqua fluorescent reactive dye (Invitrogen, Paisley, UK). Cells were measured by a FACSCanto II flow cytometer (BD Biosciences, San Diego, USA) and analyzed using FlowJo software. Appropriate isotype control antibodies (Supplementary Table 2) were used for gating purposes.

Ex vivo polyclonal T cell activation assay

All TIL cultures were performed in RPMI 1640 (Lonza, Breda, The Netherlands) supplemented with 10% human AB serum (Invitrogen), 2mM L-glutamine (Invitrogen), 50 mM Hepes Buffer (Lonza), 1% penicillin-streptomycin (Life Technologies), 5mM Sodium Pyruvate (Gibco) and 1% MEM NEAA at 37°C. TIL were labeled with 0.1 µM CFSE (Invitrogen); afterwards 100,000 cells in 200 µl medium were cultured in each well of a 96-well round-bottom culture plate and stimulated with anti-human CD3/CD28 dynabeads (Gibco-Life Technologies AS, Norway) at a cell : bead ratio of 10:1, in the presence or absence of 10

μg/ml neutralizing monoclonal antibodies against human PD-L1 (clone 5H1[4]), TIM3 (clone F38-2E2, Biolegend, San Diego, USA[5, 6]), LAG3 (clone 17B4, AdipoGen, Liestal, Switzerland[7]) or CTLA4 (clone BNI3, Beckman Coulter, Marseille, France[8]), or combinations of these antibodies, or isotype-matched control antibodies (mIgG1 and mIgG2a, Biolegend, London, UK). In preliminary experiments a cell : CD3/CD28 bead ratio of 10:1 was established to provide sub-optimal stimulation of T cell proliferation. After four days, culture supernatant was collected and secretion of IFN-γ was quantified by ELISA (Ready-SET-Go!, eBioscience). CFSE-labeled cells were harvested and stained with CD8, CD4, CD3 antibodies. Dead cells were excluded by using the LIVE/DEAD fixable dead cell stain kit with aqua fluorescent reactive dye, and T cell proliferation was determined based on CFSE dilution by flow cytometry analysis.

Ex vivo tumor antigen peptide stimulation assay

TIL of HLA-A2[+] HCC patients were stimulated with pooled HCC TAA peptides (GPC3 peptide FVGEFFTDV,[9] GPC3 peptide FLAELAYDL,[10, 11] MAGEC2 peptide ALKVDVEERV and MAGEC2 peptide LLFGLALIEV,[12] which are published immunogenic epitopes restricted by HLA-A*0201 (1 μg/ml of each peptide), in the presence or absence of 10 μg/ml neutralizing monoclonal antibodies against human PD-L1, TIM3, LAG3 or CTLA4, or combinations of these antibodies, or isotype control antibodies. 100,000 cells in 200 μl RPMI medium supplemented with 10% human AB serum, 2mM L-glutamine, 50 mM Hepes Buffer, 1% penicillin-streptomycin, 5mM Sodium Pyruvate and 1% MEM NEAA were cultured in each well of a 96-well round-bottom culture plate. Fresh medium containing 20 IU/ml recombinant human interleukin-2 (rhIL-2, Roche) was added after two days. After seven days, cells were re-stimulated with pooled HCC TAA peptides or (as negative controls) HCV nonstructural protein 5B peptide 2594-2602 (ALYDVVTKL) or HBV core protein peptide 18-27 (FLPSDFFPSV) kindly provided by Gertine W. van Oord and Yingying Dou in our laboratory for six hours in the presence of CD107a antibody, and brefeldin (5 μg/mL, Sigma) was present during the final five hours. Re-stimulation with HCV antigen peptide served as negative control for HCV negative patients (including patients negative for both HCV and HBV), HBV antigen peptide served as negative control for HBV negative patients. Cells were then stained with CD8, CD4, CD3 antibodies, followed by staining of IFN-γ, TNF-α and CD137 upon fixation and permeabilization according to the manufacturer's instructions (eBioscience A&B fixation/permeabilization kit). Dead cells were excluded by using the LIVE/DEAD fixable dead cell stain kit with aqua fluorescent reactive dye.

Expansion of human B cells by stimulation with trimeric CD40 ligand and IL-4

Blood from HLA-A2[+] healthy blood bank donors or HCC patients was collected (1-2 months before surgery for HCC patients) for isolating PBMC and expanding B cells. PBMC were seeded in 6-well plates (Costar, Cambridge, USA) at a concentration of $2\text{-}3\times10^6$ cells/ml in IMDM (Lonza, Breda, The Netherlands) with 10% heat inactivated human AB serum, 1% penicillin-streptomycin, 1% insulin-transferrin-selenium solution (Gibco-Invitrogen, Breda, the Netherlands), 40 IU/ml recombinant human interleukin-4 (rhIL-4, Strathmann Bioscience, Germany) and 1 µg/ml soluble human trimeric CD40 ligand (sCD40L, kindly provided by Celldex Therapeutics, Hampton, NJ, USA). During the first seven days of culture, 1 ng/ml cyclosporine A (CsA, Novartis, Basel, Switzerland) was added to prevent T cell expansion. Residual CD3^{+} cells were depleted by magnetic cell sorting using CD3 microbeads (Miltenyi Biotec, Bergisch Gladbach, Germany) after seven days. Since then cells were passed every 3-4 days at a concentration of 0.5×10^6 CD19^{+} cells/ml in the presence of rhIL-4 and sCD40L but without CsA, and after three weeks expanded B cells were cryopreserved. B cells expanded using rhIL-4 and sCD40L become B cell blasts with efficient antigen-presenting capacity[13, 14] and are well-suited for presentation of antigens encoded by transfected mRNA to T cells.[15] The purity of CD40-activated B cells (B cell blasts) was checked after staining with CD19 and CD3 antibodies and was at least 95% before freezing.[13]

In vitro generation of eGFP, GPC3 and MAGEC2 messenger RNA

Messenger RNA (mRNA) encoding for GPC3, MAGEC2 or eGFP were synthesized by *in vitro* transcription. The back bone vector pEtheRNA was constructed in order to maximize the level and duration of protein expression. The plasmid contains a 5' translation enhancer, a 3' RNA stabilizing sequence and a 124 residue long poly A tail. GPC3 and MAGEC2 genes were ligated into this construct and are directly followed by a sequence encoding the transmembrane and luminal regions of DCLamp, which is a targeting signal for the endolysosomal compartment, resulting in peptide loading in MHC-II. The eGFP gene was ligated into the vector without additional targeting sequences. Prior to *in vitro* transcription, the DNA plasmids were linearized with *BfuAI*. RNA synthesis was performed by eTheRNA immunotherapies NV, Niel, Belgium. During transcription a cap analog was incorporated in the mRNA. The quality of the *in vitro* transcribed mRNA was confirmed by capillary gel electrophoresis and the mRNA concentration was measured by spectrophotometry. The obtained mRNA were stored in small aliquots at -80°C till use.

Messenger RNA electroporation

B cell blasts were thawed and washed twice, first with serum-free IMDM and subsequently with Opti-MEM (Life technologies, Bleiswijk, The Netherlands). $5-10 \times 10^6$ B cell blasts were resuspended in a final volume of 200 µL of Opti-MEM containing 20 µg of mRNA. Electroporation was performed in a 4 mm gap cuvette using a Gene Pulser Xcell™ electroporation system (Bio-Rad Laboratories, Hercules, CA). We used a square wave pulse of 600 V in a pulse time of 0.6 ms in all experiments, which we found optimal for antigen presentation to T cells. Immediately after electroporation, B cell blasts were transferred into IMDM without phenol red (Life Technologies) with 10% heat-inactivated human AB serum, 1% penicillin-streptomycin and 1% insulin-transferrin-selenium solution and incubated at 37°C. Two hours after electroporation, cells were harvested for further experiments.

GPC3-specific CD8+ T cell clone and MAGEC2-specific human T cells

A previously described HLA-A*0201-restricted GPC3 (FVGEFFTDV) specific CD8^{+} T cell clone was kindly provided by Dr. Tetsuya Nakatsura, Kashiwa, Japan.[9] Human T cells retrovirally transduced with a TCR that specifically recognizes MAGEC2 peptide (ALKVDVEERV) in HLA-A*0201 as described by Straetemans T *et al.,*[16] were kindly provided by Dr. Reno Debets, Department of Internal Oncology, Erasmus MC. These T cells were used as responder cells for testing presentation of GPC3 and MAGEC2 by mRNA-transfected B cell blasts. GPC3-specific T cells were expanded by non-specific stimulation with 5 µg/ml PHA and irradiated allogeneic PBMC as feeder cells, in AIM-V medium (Gibco) supplemented with 10% human AB serum, 100 IU/ml rhIL-2 and 10 ng/ml recombinant human interleukin-15. Every 3-4 days T cells were further expanded by splitting the cultures and replenishing fresh culture medium without feeder cells or PHA. After14 days, cells were harvested for experiments or cryopreserved till further use.

Statistical analysis

All data set distributions were analyzed for normality by the Shapiro-Wilk normality test. Differences between paired groups of data were analyzed according to their distribution by either paired t test or Wilcoxon matched pairs test. Differences between different groups of patients were analyzed according to their distribution by either unpaired t test or Mann-Whitney test. Correlation was analyzed according to the distribution by either Pearson or Spearman correlation test. The statistical analysis was performed using GraphPad Prism Software (version 5.0). P values less than 0.05 were considered statistically significant (* $P<0.05$; ** $P<0.01$; *** $P<0.001$).

REFERENCES

1.   Dolton G, Lissina A, Skowera A, et al. Comparison of peptide-major histocompatibility complex tetramers and dextramers for the identification of antigen-specific T cells. Clin Exp Immunol 2014;177:47-63.

2.   Lissina A, Ladell K, Skowera A, et al. Protein kinase inhibitors substantially improve the physical detection of T-cells with peptide-MHC tetramers. J Immunol Methods 2009;340:11-24.

3.   Wooldridge L, Lissina A, Cole DK, et al. Tricks with tetramers: how to get the most from multimeric peptide-MHC. Immunology 2009;126:147-64.

4.   Dong H, Strome SE, Salomao DR, et al. Tumor-associated B7-H1 promotes T-cell apoptosis: a potential mechanism of immune evasion. Nat Med 2002;8:793-800.

5.   da Silva IP, Gallois A, Jimenez-Baranda S, et al. Reversal of NK-cell exhaustion in advanced melanoma by Tim-3 blockade. Cancer Immunol Res 2014;2:410-22.

6.   Fourcade J, Sun Z, Benallaoua M, et al. Upregulation of Tim-3 and PD-1 expression is associated with tumor antigen-specific CD8+ T cell dysfunction in melanoma patients. J Exp Med 2010;207:2175-86.

7.   Matsuzaki J, Gnjatic S, Mhawech-Fauceglia P, et al. Tumor-infiltrating NY-ESO-1-specific CD8+ T cells are negatively regulated by LAG-3 and PD-1 in human ovarian cancer. Proc Natl Acad Sci U S A 2010;107:7875-80.

8.   Boor PP, Metselaar HJ, Jonge S, et al. Human plasmacytoid dendritic cells induce CD8(+) LAG-3(+) Foxp3(+) CTLA-4(+) regulatory T cells that suppress allo-reactive memory T cells. Eur J Immunol 2011;41:1663-74.

9.   Yoshikawa T, Nakatsugawa M, Suzuki S, et al. HLA-A2-restricted glypican-3 peptide-specific CTL clones induced by peptide vaccine show high avidity and antigen-specific killing activity against tumor cells. Cancer Sci 2011;102:918-25.

10.   Flecken T, Schmidt N, Hild S, et al. Immunodominance and functional alterations of tumor-associated antigen-specific CD8+ T-cell responses in hepatocellular carcinoma. Hepatology 2014;59:1415-26.

11.   O'Beirne J, Farzaneh F, Harrison PM. Generation of functional CD8+ T cells by human dendritic cells expressing glypican-3 epitopes. J Exp Clin Cancer Res 2010;29:48.

12.   Germeau C, Ma W, Schiavetti F, et al. High frequency of antitumor T cells in the blood of melanoma patients before and after vaccination with tumor antigens. J Exp Med 2005;201:241-8.

13.   Tapirdamaz O, Mancham S, van der Laan LJ, et al. Detailed kinetics of the direct allo-response in human liver transplant recipients: new insights from an optimized assay. PLoS One 2010;5:e14452.

14.   von Bergwelt-Baildon MS, Vonderheide RH, Maecker B, et al. Human primary and memory cytotoxic T lymphocyte responses are efficiently induced by means of CD40-activated B cells as antigen-presenting cells: potential for clinical application. Blood 2002;99:3319-25.

15.   Coughlin CM, Vance BA, Grupp SA, et al. RNA-transfected CD40-activated B cells induce functional T-cell responses against viral and tumor antigen targets: implications for pediatric immunotherapy. Blood 2004;103:2046-54.

16.   Straetemans T, van Brakel M, van Steenbergen S, et al. TCR gene transfer: MAGE-C2/HLA-A2 and MAGE-A3/HLA-DP4 epitopes as melanoma-specific immune targets. Clin Dev Immunol 2012;2012:586314.

CHAPTER 6

Blockade of LAG3 enhances responses of tumor-infiltrating T cells in mismatch repair-proficient liver metastasis of colorectal cancer

Guoying Zhou[1], Lisanne Noordam[1], Dave Sprengers[1], Michail Doukas[2], Patrick P. C. Boor[1], Adriaan A. van Beek[1], Remco Erkens[1], Shanta Mancham[1], Dirk Grünhagen[3], Anand G. Menon[4], Johan F. Lange[3], Pim J. W. A. Burger[3], Alexandra Brandt[3], Boris Galjart[3], Cornelis Verhoef[3], Jaap Kwekkeboom[1], Marco J. Bruno[1]

Departments of [1]Gastroenterology and Hepatology, [2]Pathology, and [3]Surgery, Erasmus MC-University Medical Center, Rotterdam, the Netherlands; [4]Department of Surgery, Havenziekenhuis, Rotterdam, the Netherlands.

ABSTRACT

Purpose: Liver metastasis develops in >50% of patients with colorectal cancer (CRC), and is a leading cause of CRC-related mortality. We aimed to identify which inhibitory immune checkpoint pathways can be targeted to enhance functionality of intra-tumoral T-cells in mismatch repair-proficient liver metastases of colorectal cancer (LM-CRC).

Methodology: Intra-tumoral expression of multiple inhibitory molecules was compared among mismatch repair-proficient LM-CRC, peritoneal metastases of colorectal cancer (PM-CRC) and primary CRC. Expression of inhibitory molecules was also analyzed on leukocytes isolated from paired resected metastatic liver tumors, tumor-free liver tissues, and blood of patients with mismatch repair-proficient LM-CRC. The effects of blocking inhibitory pathways on tumor-infiltrating T-cell responses were studied in *ex vivo* functional assays.

Results: Mismatch repair-proficient LM-CRC showed higher expression of inhibitory receptors on intra-tumoral T-cells and contained higher proportions of CD8$^+$ T-cells, dendritic cells and monocytes than mismatch repair-proficient primary CRC and/or PM-CRC. Inhibitory receptors LAG3, PD-1, TIM3 and CTLA4 were higher expressed on CD8$^+$ T-cells, CD4$^+$ T-helper and/or regulatory T-cells in LM-CRC tumors compared with tumor-free liver and blood. Antibody blockade of LAG3 or PD-L1 increased proliferation and effector cytokine production of intra-tumoral T-cells isolated from LM-CRC in response to both polyclonal and autologous tumor-specific stimulations. Higher LAG3 expression on intra-tumoral CD8$^+$ T-cells associated with longer progression-free survival of LM-CRC patients.

Conclusion: Mismatch repair-proficient LM-CRC may be more sensitive to immune checkpoint inhibitors than mismatch repair-proficient primary CRC. Blocking LAG3 enhances tumor-infiltrating T-cell responses of mismatch repair-proficient LM-CRC, and therefore may be a new promising immunotherapeutic target for LM-CRC.

Keywords: immunotherapy; immune checkpoint inhibitor; tumor-infiltrating lymphocyte; liver metastasis; colorectal cancer; peritoneal metastasis; LAG3; PD-1; T cell; mismatch repair

INTRODUCTION

Colorectal cancer (CRC) is the third most common cause of cancer-related mortality worldwide.(1-3) More than 50% of CRC patients develop metastatic disease to their liver over the course of their life,(4) and liver metastasis is a leading cause of death from CRC.(5-7) Unfortunately, surgical resection of isolated liver metastases of CRC (LM-CRC) is curative in only 20%-30% of patients,(8, 9) and systemic therapy provides limited survival benefit.(10) Patients with unresectable LM-CRC have a poor prognosis with a median survival of only two years.(11) Therefore, there is a pressing need for more effective therapeutic strategies for LM-CRC.

The immune system plays a crucial role in cancer surveillance and elimination, and antibody blockade of inhibitory immune checkpoint pathways that suppress anti-tumor T-cell immunity and assist tumor immune evasion,(12-16) has recently emerged as an attractive treatment option for multiple types of malignancies.(17-21) Targeting the PD-1/PD-L1 inhibitory pathway has resulted in objective responses in 17%-28% of advanced melanoma patients, 12%-27% of renal cell cancer patients, 10%-18% of non-small cell lung cancer patients and 20% of advanced hepatocellular carcinoma patients.(22-25) In contrast, CRC patients hardly respond to PD-1 and PD-L1 blocking antibodies(23-26), except for the minority of patients who are with mismatch repair (MMR)-deficient CRC.(27, 28) A defective MMR enzyme system occurs in 10%-20% of CRC tumors and results in microsatellite instability, which is used as a molecular marker of MMR-deficiency.(29) It has been hypothesized that the observed difference in responsiveness to PD-1/PD-L1 blockade between MMR-deficient and MMR-proficient CRC is related to the higher numbers of somatic mutations in MMR-deficient tumors, due to the reduced ability to repair DNA damage. The increased mutation rate may result in the presence of more mutation-encoded neo-antigens in the tumors, which elicit stronger anti-tumor T cell responses.(27) Indeed, MMR-deficient CRC tumors are characterized by denser CD8^{+} T cell infiltration.(30) They also have higher expression levels of inhibitory checkpoint molecules, probably to resist immune-mediated tumor elimination.(31) Together, enhanced immune cell infiltration and upregulation of inhibitory immune checkpoints may render MMR-deficient CRC more sensitive to PD-1/PD-L1 blockade than MMR-proficient CRC.

In LM-CRC the incidence of MMR deficiency is low,(32) and it may therefore be expected that LM-CRC poorly respond to immune checkpoint inhibitors. Nevertheless, these tumors contain immune infiltrates, and increased numbers of tumor-infiltrating CD8^{+} T cells are positively associated with overall survival and response to chemotherapy,(33, 34) indicating

that intra-tumoral T cell immunity is an important determinant of LM-CRC progression. In addition, MMR-proficient LM-CRC are immunologically distinct from primary CRC in terms of immune infiltration.(35) Moreover, the unique immune environment in the liver(36) favors immunological tolerance,(36) and one of the mechanisms used by the liver to resist immune responses is the induction of expression of inhibitory receptors on hepatic T cells(37, 38) and their ligands on hepatocytes and other liver tissue cells.(39) Previously we have observed that intra-tumoral CD8^{+} cytotoxic T cells (CTL) and CD4^{+} T helper cells (Th) are functionally compromised in LM-CRC,(40) and we also demonstrated that the suppression mediated by intra-tumoral regulatory T cells (Treg) in LM-CRC can be alleviated by blocking the inhibitory receptor CTLA4 and activating the stimulatory receptor GITR.(41) However, the expression and functional roles of inhibitory receptor-ligand pathways in regulating tumor-infiltrating effector T cell responses have not been studied yet in LM-CRC.

Therefore, the aim of this study was to determine whether inhibitory immune checkpoint pathways can be targeted to enhance the functionality of tumor-infiltrating lymphocytes (TIL) in MMR-proficient LM-CRC. We measured the expression of inhibitory receptors and their ligands on leukocytes isolated from paired resected metastatic liver tumors, tumor-free liver tissues (TFL) and blood of patients with LM-CRC, and compared their expression levels with those on leukocytes isolated from peritoneal metastasis of CRC (PM-CRC) and primary CRC. In addition, we studied the effects of antibody blockade of inhibitory pathways on TIL responses of LM-CRC in *ex vivo* functional assays.

RESULTS

Comparison of immune infiltrates and expression of inhibitory molecules among MMR-proficient liver metastases, peritoneal metastases and primary CRC.
To speculate whether TIL in CRC tumors at different anatomical sites may differ in sensitivity to checkpoint inhibitors, we first compared frequencies of T cell and antigen-presenting cell (APC) subsets, as well as their expression of inhibitory molecules, between MMR-proficient LM-CRC, primary CRC, and metastases outside the liver. Two in all LM-CRC tumors and three out of twelve primary CRC tumors that we collected were MMR-deficient, whereas all eleven PM-CRC tumors were MMR-proficient (Table 1 and Supplementary Table S1). The data of the five patients with MMR-deficient tumors are shown in Supplementary Fig. S1.
We observed several interesting differences among MMR-proficient tumors from different anatomical locations. Firstly, both LM-CRC and PM-CRC contained significantly higher frequencies of CD8^{+} CTL and significantly lower frequencies of CD4^{+}Foxp3^{-} Th than primary CRC, while frequencies of Treg were similar in CRC tumors at all three sites (Fig. 1A).

Secondly, CD8^{+} CTL in LM-CRC displayed a higher frequency of PD1^{+} cells than those in primary CRC, and also contained higher frequencies of TIM3^{+} and LAG3^{+} cells than those in PM-CRC, while CD4^{+} Th in LM-CRC displayed a higher frequency of LAG3^{+} cells than those in PM-CRC (Fig. 1B). Thirdly, CD4^{+}Foxp3^{+} Treg in LM-CRC contained higher frequencies of PD-1^{+} and TIM3^{+} cells than those in primary CRC and PM-CRC, and also displayed a higher frequency of LAG3^{+} cells than those in PM-CRC (Fig. 1B). Finally, LM-CRC contained significantly higher frequencies of myeloid dendritic cells (mDC) and monocytes than primary CRC (Fig. 1C), which not only can present tumor antigens to T cells but also express the inhibitory ligands PD-L1 (for PD-1), galectin 9 (for TIM3), MHC class II molecules (for LAG3), CD86 and CD80 (for CTLA4) (Fig. 1D). Hierarchical clustering analysis showed that the immunological data of most LM-CRC patients clustered together as did the data of most primary CRC patients (Supplementary Fig. S2). Together, these data indicate that the CD8^{+} CTL:Treg ratio, which is critical for immunological tumor control in primary as well as metastasized CRC,(42) is more favorable in CRC metastases compared to primary CRC. In addition, the increased expression of PD-1 on TIL suggests that TIL of LM-CRC may be more sensitive to blockade of the PD-1/PD-L1 pathway than TIL of primary CRC.

Elevated expression of inhibitory receptors on CD8+ cytotoxic T cells, CD4+ T helper cells and regulatory T cells in MMR-proficient LM-CRC tumors.

We isolated leukocytes from surgically resected metastatic liver tumors, TFL and blood of LM-CRC patients, and compared the expression levels of five inhibitory receptors (PD-1, TIM3, LAG3, CTLA4 and BTLA) on CD8^{+} CTL, CD4^{+}Foxp3^{-} Th and CD4^{+}Foxp3^{+} Treg. When compared to TFL and blood, significantly higher proportions of CD8^{+} CTL, Th and Treg in TIL expressed PD-1 and TIM-3. In addition, TIL contained higher frequencies of CTLA4^{+} CTL and CTLA4^{+} Th, while LAG3 was overexpressed on CD8^{+} CTL in TIL when compared to TFL and blood (Fig. 2). Interestingly, the highest expression of CTLA4, which is functionally involved in the suppressive capacity of Treg,(43) and also of PD-1 and TIM3 was found on tumor-infiltrating Treg. In contrast, frequencies of BTLA^{+} cells in intra-tumoral T cells were low, and they did not differ significantly from those in TFL and blood (Supplementary Fig. S3). Therefore, we focused on the other four receptors in the rest of this study. To investigate whether the expression of inhibitory receptors on circulating T cells had a relation with the expression on intra-tumoral T cells, we performed correlation analysis, as illustrated in Supplementary Fig. S4. There were significant positive correlations between the frequencies of PD-1^{+} CTL and PD-1^{+} Treg in the tumor and those in the blood, between the frequency of LAG3^{+} Th in the tumor and that in the blood, and between the frequencies of CTLA4^{+} Th and CTLA4^{+} Treg in the tumor and those in the blood. These results indicate that the expression

of inhibitory receptors on circulating T cells partly reflects their expression on intra-tumoral T cells.

Intra-tumoral antigen-presenting cells express inhibitory ligands.

To study the expression of inhibitory ligands PD-L1, galectin 9, MHC-II molecules, CD86 and CD80 on APC in LM-CRC tissues, we measured these molecules by flow cytometry. Three major APC subsets BDCA-1$^+$CD19$^-$ mDC, CD14$^+$ monocytes and CD19$^+$ B cells were found in all tumors. The frequency of B cells was higher in tumors than in TFL, and the frequency of mDC was higher in tumors and TFL than in the blood, whereas the frequency of monocytes was lower in tumors than in the blood (Fig. 3A). The three different tumor-infiltrating APC populations expressed the five ligands at different levels and considerable variations between individual patients were observed (Fig. 3B, C). Intra-tumoral mDC and monocytes contained higher proportions of PD-L1$^+$ and MHC-II$^+$ cells than intra-tumoral B cells. The median fluorescence intensities of five ligands in APC subsets in the tumor, TFL and blood are presented in Fig. 3D, showing that the expression of inhibitory ligands is generally not increased on tumor-infiltrating APC compared to APC in TFL. Together, the abovementioned data suggest that inhibitory interactions between T cells and APC in MMR-proficient LM-CRC are possible.

Intra-tumoral T cells expressing inhibitory receptors show increased levels of activation markers.

Considering that increased expression of inhibitory receptors on T cells can be induced by recent activation, or by chronic stimulation that may lead to T cell dysfunctionality, we examined the *ex vivo* activation status and *in vitro* effector cytokine production of effector T cells derived from MMR-proficient LM-CRC. First we compared the expression of activation markers HLA-DR and CD69 on intra-tumoral T cells that do or do not express inhibitory receptors. Interestingly, PD-1$^+$, TIM3$^+$, LAG3$^+$ or CTLA4$^+$ CTL and Th showed a more activated status than PD-1$^-$, TIM3$^-$, LAG3$^-$ or CTLA4$^-$ CTL and Th, respectively (Fig. 4A, B). Subsequently, we assessed effector cytokine production of tumor-derived T cells after short-term PMA and ionomycin stimulation. Despite the activated status, the frequencies of inhibitory receptor positive CTL and Th cells that produced IFN-γ and TNF-α were reduced or similar to those in the respective receptor negative T cells (Fig. 4C, D). Interestingly, LAG3$^+$ CTL and Th cells did not show reduction in cytokine production. Because among all studied inhibitory receptors, tumor-infiltrating CTL and Th showed the highest expression of PD-1 (Fig. 2C, D), we analyzed co-expression of PD-1 and the other three receptors. Co-expression of PD-1 and either TIM3, LAG3 or CTLA4 was found, especially in CD8$^+$ CTL, but

expression of TIM3, LAG3 or CTLA4 without PD-1 was also observed (Supplementary Fig. S5). Similar to single receptor positive CTL and Th, double receptor positive CTL and Th showed reduced or comparable frequencies of IFN-γ and TNF-α producing cells to double receptor negative cells, while LAG3⁺PD-1⁺ CTL and Th did not show significant reduction in cytokine production (Fig. 4C, D). These data demonstrate that in general intra-tumoral T cells that express inhibitory receptors do not produce more effector cytokines, despite the activated status.

Antibody blockade of LAG3 or PD-L1 boosts ex vivo proliferation and effector cytokine production of T cells derived from MMR-proficient LM-CRC.

Because PD-1, TIM3, LAG3 and CTLA4 are upregulated on T cells in MMR-proficient LM-CRC tumors, we tested whether blockade of the PD-1/PD-L1, TIM3/galectin 9, LAG3/MHC-II or CTLA4/CD80/CD86 pathways could enhance the effector functions of tumor-derived T cells. We stimulated CFSE-labeled total tumor-infiltrating mononuclear leukocytes with CD3/CD28 beads, in the presence or absence of antagonistic antibodies against human PD-L1, TIM3, LAG3, CTLA4 or isotype controls (mIgG1 or mIgG2a). After four days of culture, T cell proliferation was measured by flow cytometry (Fig. 5A), and effector cytokine secretion in the culture supernatants was quantified by enzyme-linked immunosorbent assay. Fig. 5B illustrates that the baseline proliferation of CD8⁺ and CD4⁺ T cells derived from tumors was significantly lower than that of T cells from the blood of the same patients, indicating the proliferative function of intra-tumoral T cells is impaired compared to circulating T cells of patients with MMR-proficient LM-CRC. Interestingly, treatment with anti-LAG3 antibody or anti-PD-L1 antibody significantly increased the proliferation of both CD8⁺ and CD4⁺ TIL compared with the control condition without antagonistic antibody (Fig. 5C). These two antibodies also significantly increased IFN-γ and TNF-α secretion (Fig. 5D).

Antibody blockade of LAG3 or PD-L1 boosts ex vivo responses of T cells derived from MMR-proficient LM-CRC to autologous tumor antigens.

To investigate whether blockade of the aforementioned inhibitory pathways can enhance tumor-specific anti-tumor T cell responses, we stimulated CFSE-labeled total tumor-infiltrating mononuclear leukocytes with autologous blood-derived mDC preloaded with autologous tumor lysates, in the presence or absence of antagonistic antibodies, and measured CD8⁺ and CD4⁺ T cell proliferation after six days. Increased TIL proliferation against mDC loaded with tumor lysates compared with mDC without tissue lysates was observed in all five tested patients, while loading of mDC with normal liver lysates did not increase or minimally increased TIL proliferative responses (Fig. 6A, C). Addition of anti-PD-

L1 antibody enhanced proliferative responses of TIL in all four tested patients, while treatment with anti-LAG3 antibody increased both CD8$^+$ and CD4$^+$ TIL proliferation in four out of five patients. In three out of four patients anti-LAG3 antibody boosted CD8$^+$ and/or CD4$^+$ TIL responses to higher levels than anti-PD-L1 antibody (Fig. 6A, C). After five hours of restimulation, intracellular expression of IFN-γ and TNF-α in proliferating T cells was analyzed, and was found to be enhanced by both anti-LAG3 and anti-PD-L1 antibodies in most patients (Fig. 6B, D, E). Like in CD3/CD28 stimulations, anti-TIM3 and anti-CTLA4 antibodies boosted TIL responses less strongly and also in less patients.

Higher LAG3 expression on intra-tumoral CD8+ T cells is associated with longer progression-free survival of patients with MMR-proficient LM-CRC.

In a subset of patients, we could analyze associations between the frequencies of inhibitory receptor positive TIL and patient progression-free survival after the LM-CRC resection. In survival analysis higher expression of LAG3 on CD8$^+$ TIL, CD4$^+$ Th and Treg was associated with longer time to recurrence (Fig. 7), whereas higher expression of PD-1 or TIM3 on CD8$^+$ TIL was associated with shorter time to recurrence (data not shown). In multivariable analysis only LAG3 expression on CD8$^+$ TIL was demonstrated to be an independent predictor of progression-free survival (Table 2), which supports its functional relevance to anti-cancer immunity in TIL of LM-CRC. We hypothesize that LAG3$^+$CD8$^+$ TIL may be highly activated T cells (Fig. 4A) stimulated by tumor antigens, but subsequently inhibited by increased and continuous expression of LAG3 and interaction with its ligands on APC and tumor cells, yet with preserved effector functions (Fig. 4C), which may control tumor growth. Because the sample size is small, these results need conformation in an independent study. In one fourth of the patients we only have data of LAG3 expression on CD8$^+$ TIL but not on CD4$^+$ Th or Treg, so we did not include the latter T cell subsets in the multivariable analysis. The death events were too few to analyze overall survival of LM-CRC patients.

DISCUSSION

Checkpoint inhibitors have recently emerged as attractive treatments for several types of solid cancers. However, PD-1 and PD-L1 blocking antibodies were proven unsuccessful in CRC, with the exception of MMR-deficient CRC.(23-25, 27, 28) The first aim of this study was to investigate whether the composition of the immune infiltrates and the intra-tumoral expression levels of inhibitory molecules in CRC metastases in the liver environment differ from those in primary CRC tumors and metastases outside the liver, which would suggest potential differences in sensitivity to checkpoint inhibitors among CRC tumors at different anatomical locations. The second objective was to determine whether targeting of inhibitory

checkpoint pathways by antagonistic antibodies can enhance the functionality and anti-tumor responses of tumor-infiltrating T cells in LM-CRC. Because the incidence of MMR deficiency in LM-CRC is low, we focused on MMR-proficient tumors.

This study is the first to investigate the expression levels of inhibitory receptors on TIL in LM-CRC. Similar to what we reported in hepatocellular carcinoma,(44) intra-tumoral CD8$^+$ CTL and CD4$^+$ Th in MMR-proficient LM-CRC displayed increased expression of PD-1, TIM3, CTLA4 and/or LAG3 compared to their counterparts in TFL and blood. In addition, we found selectively enhanced expression of PD-1 and TIM3 on intra-tumoral Treg (Fig. 2C-E). The elevated frequencies of inhibitory receptor positive cells in TIL together with the expression of their ligands on tumor-infiltrating APC (Fig. 3B-D) suggest that these inhibitory checkpoint pathways may be involved in intra-tumoral suppression of T cells in MMR-proficient LM-CRC.

Interestingly, we observed higher expression of PD-1 and/or TIM3 on CD8$^+$ CTL and Treg in LM-CRC than in primary CRC, while expression of LAG3, TIM3 and/or PD-1 on CD8$^+$ CTL, Th and Treg was higher in LM-CRC than in PM-CRC (Fig. 1B). We hypothesize that these differences are due to the unique tolerogenic properties of the liver environment, which induces expression of inhibitory receptors on hepatic T cells both in diseased and healthy conditions.(37, 38) Furthermore, we found increased proportions of CD8$^+$ CTL in LM-CRC and PM-CRC compared with primary CRC (Fig. 1A). The observed differences between MMR-proficient LM-CRC and MMR-proficient primary CRC are to some extent reminiscent of those found between MMR-deficient primary CRC and MMR-proficient primary CRC by Llosa *et al.* (31) They demonstrated that MMR-deficient primary CRC displayed higher infiltration with CD8$^+$ CTL as well as upregulated expression of PD-1, PD-L1, CTLA4 and LAG3 compared to MMR-proficient primary CRC, and suggested that these differences contributed to the enhanced clinical responsiveness to anti-PD-1 therapy of microsatellite instable CRC compared with microsatellite stable CRC.(31) In addition, we found that LM-CRC contained increased frequencies of professional APC subsets (mDC and monocytes) (Fig. 1C), which may result in improved presentation of tumor antigens to intra-tumoral T cells as well as more PD-L1 and MHC-II expression in LM-CRC compared with primary CRC, because in LM-CRC mDC and monocytes expressed more PD-L1 and MHC-II than B cells (Fig. 3C). Hierarchical clustering analysis showed that the immune phenotypical data of most LM-CRC tumors clustered together as did the data of most primary CRC tumors (Supplementary Fig. S2). These data confirm those of Halama *et al.*, who demonstrated similar heterogeneity in composition of immune infiltrates between paired primary CRC tumors and liver metastases derived from the same patients.(35) We extracted and statistically analyzed their paired data

of primary CRC and LM-CRC from 16 patients and found a higher CD8$^+$ cell density in LM-CRC than in primary CRC (Supplementary Fig. S6).

Moreover, discrepancies in somatic mutations, copy number alterations, genetic and epigenetic molecular alterations between primary CRC tumors and matched liver metastases were revealed in up to a half of the cases, which may lead to higher mutational load and thereby more neo-epitopes in LM-CRC.(45-48) Together, these findings indicate major differences between liver metastases and primary CRC as well as peritoneal metastases, including differences in immune cell infiltration and inhibitory molecule expression, which may be at least partly induced by the liver environment. We therefore suggest that TIL of MMR-proficient LM-CRC may be more sensitive to PD-1/PD-L1 blockade and other checkpoint inhibitors than TIL of MMR-proficient primary CRC and CRC metastases at other anatomical locations. Nevertheless, to precisely compare the effects of checkpoint inhibitors on TIL of primary CRC and LM-CRC, experiments with TIL from paired tissues might be needed but were unfortunately not available in the current study.

To determine whether TIL expressing inhibitory receptors represent T cells that are recently activated upon recognition of tumor antigens, or are dysfunctional due to chronic antigenic stimulation, we studied their *ex vivo* activation status and *in vitro* effector cytokine production. Similar to what we reported in hepatocellular carcinoma,(44) intra-tumoral CD4$^+$ Th and CD8$^+$ CTL expressing any of the four inhibitory receptors showed a more activated status but produced reduced or similar levels of effector cytokines than their counterparts not expressing the corresponding inhibitory receptor (Fig. 4). However, in our *ex vivo* cultures, tumor cells that may express inhibitory ligands are lacking, so the TIL might be less functional *in vivo* and need checkpoint inhibitors. Nevertheless, proliferative responses of tumor-derived T cells to CD3/CD28 stimulation were lower than those of circulating T cells (Fig. 5B). Consistent with what others reported on IFN-γ production by CD8$^+$ TIL in primary CRC patients,(49, 50) our results demonstrate a certain degree of dysfunctionality of intra-tumoral CD4$^+$ Th and CD8$^+$ CTL in MMR-proficient LM-CRC, which may be at least partly due to inhibitory checkpoint interactions between T cells and APC subsets in the TIL cultures, but not complete dysfunctionality.

This study is also the first to investigate the effects of antibody blockade of four inhibitory checkpoint pathways on responses of TIL isolated from MMR-proficient LM-CRC. In both polyclonal T cell activation and tumor-specific TIL stimulation assays, increased proliferation of TIL and increased production of effector cytokines were observed upon the addition of anti-LAG3 antibody or anti-PD-L1 antibody (Fig. 5 and Fig. 6) In some patients *ex vivo* anti-

tumor responses of TIL were more robustly enhanced by anti-LAG3 antibody than by anti-PD-L1 antibody (Fig. 6), suggesting that LAG3 might be the most promising target for immunotherapy of LM-CRC among all four checkpoint pathways tested in this study. However, these data need confirmation using TIL from a larger number of patients. The superiority of LAG3 blockade compared to PD-L1 blockade was more seen in tumor antigen-specific stimulation than in polyclonal stimulation. We hypothesize that the small proportion of LAG3+ TIL is strongly enriched with tumor antigen-reactive T cells, which are known to constitute only a small proportion of all tumor-infiltrating T cells. In addition, we propose that PD-1 is expressed on a larger fraction of TIL which contains more non-tumor antigen-specific T cells. Although TIM3 blockade was reported to reduce T cell apoptosis and inhibit tumor growth in a mouse CT26 colon tumor model,(51) little effect was observed in our experiments using TIL derived from human LM-CRC. This result also contrasts to our recent observation that *ex vivo* responses of TIL isolated from hepatocellular carcinomas can be invigorated by TIM3 blockade.(44) This difference may relate to the lower expression of galectin 9 on APC subsets in LM-CRC compared to hepatocellular carcinomas.

Because we were interested in the net effects of checkpoint inhibitors on TIL responses in a context that reflected the LM-CRC tumor microenvironment as much as possible, we used total tumor-infiltrating mononuclear leukocytes in our functional assays, which contained both T cells expressing inhibitory receptors and APC expressing inhibitory ligands. As a consequence, tumor-infiltrating Treg,(40, 41) type 1 regulatory T cells(52) and probably other types of immune suppressor cells were also present in these assays. Therefore, the reported functional effects of checkpoint inhibitors on effector T cells in these assays may be partly indirect, mediated by effects of these antibodies on suppressor cells. The effects of checkpoint inhibitor on effector T cells in our assays might even be counteracted by its effects on suppressor cells. We found that half of Treg in LM-CRC tumors expressed PD-1, and blocking PD-1/PD-L1 interaction was shown to enhance the suppressive function of Treg isolated from liver tissues of patients with chronic hepatitis C infection.(53)

Interestingly, higher expression of LAG3 on CD8+ TIL was associated with longer time to recurrence of patients with LM-CRC. We hypothesize that LAG3+CD8+ TIL are cells which have recently been activated (Fig. 4A) by recognition of antigens in the tumor, and upregulate LAG3 expression in response to activation but still have functional capacity to exert effector functions and delay tumor growth (Fig. 4C). LAG3 expression is upregulated on T cells after activation and differentiation,(54, 55) and intra-tumoral T cells that recognize tumor antigens are characterized by expression of LAG3 and other inhibitory receptors.(56) Although chronic tumor antigen stimulation in the tumor microenvironment can induce T cell

exhaustion with simultaneous induction of high expression of multiple inhibitory receptors, this does not mean that all CD8^{+} TIL which express one or more inhibitory receptors at any level are functionally exhausted. Indeed, a recent mouse study showed that tumor antigen-specific TIL which expressed LAG3 or PD-1 produced IFN-γ in situ and had cytolytic potential.(57) Likewise, in the current study we observed that LAG3^{+}CD8^{+} TIL in LM-CRC were not functionally impaired (Fig. 4C). Nevertheless, they could be functionally invigorated upon antibody blockade of LAG3 (Fig. 5 and Fig. 6), indicating that interaction of LAG3 with its ligands serves as an extrinsic mechanism in the tumor microenvironment which inhibits their functionality.

Our study has several limitations: 1) Due to the finite numbers of isolated TIL, the tumor-specific stimulation assay could only be performed in a limited number of LM-CRC patients (Supplementary Table S1), neither could all the conditions be tested in every functional assay, nor could the relation between the expression of inhibitory molecules on TIL and the effects of checkpoint inhibitors on TIL responses be well analyzed. 2) We could not study paired LM-CRC, primary CRC and PM-CRC tumors from the same patients because primary and metastatic CRC tumors were resected at different time points and in different hospitals. 3) MMR-deficient tumors could not be studied well, because we received fresh tissues from only a few MMR-deficient tumors during our study.

In conclusion, increased frequencies of CD8^{+} CTL, mDC and monocytes as well as increased inhibitory receptor expression on intra-tumoral T cells in MMR-proficient LM-CRC suggest that TIL of MMR-proficient LM-CRC may be more sensitive to immune checkpoint inhibitors than TIL of MMR-proficient primary CRC. Blockade of LAG3 and PD-L1 can both enhance *ex vivo* functions of tumor-infiltrating T cells from MMR-proficient LM-CRC. Therefore, these two inhibitory pathways may be potential immunotherapeutic targets for the most prevalent metastatic liver cancer, despite the lack of MMR deficiency. Clinical studies focusing on responses of LM-CRC to anti-LAG3 and combination with anti-PD-L1 or anti-PD-1 antibodies(12, 58) are required to conclude whether this prediction based on our preclinical study is correct.

PATIENTS AND METHODS

Patients and specimens

Fifty three patients who were eligible for surgical resection of LM-CRC were enrolled in the study from November 2013 to March 2017. Another twelve patients who received surgical resection of primary CRC and another eleven patients whose PM-CRC were surgically

resected before hyperthermic intraperitoneal chemotherapy were enrolled in the study from February 2016 to December 2016. Fresh tissue samples from hepatic tumors, tumor-free liver tissues as distant as possible from the tumor (minimum 1cm distance), colorectal tumors and peritoneal tumors were obtained. Peripheral blood from LM-CRC patients was also collected on the day of resection. None of the patients received chemotherapy or immunosuppressive therapy at least three months before surgery. The clinical characteristics of the patients are summarized in Table 1. The study was approved by the local ethics committee, and signed informed consent from all patients was obtained before tissue and blood donation.

Cell preparation

Peripheral blood mononuclear cells (PBMC) were isolated by Ficoll density gradient centrifugation. Single cell suspensions from tumors and tumor-free liver were obtained by tissue digestion. Briefly, fresh tissues were first cut into small pieces and then digested with 0.125 mg/mL collagenase IV (Sigma-Aldrich, St. Louis, MO) and 0.2 mg/mL DNAse I (Roche, Indianapolis, IN) in Hanks' Balanced Salt solution with Ca^{2+} and Mg^{2+} (Sigma, Zwijndrecht, The Netherlands) for 30 minutes at 37 °C with interrupted gently swirling. Cell suspensions were filtered through 100 μm pore cell strainers (BD Biosciences, Erembodegem, Belgium) and mononuclear leukocytes were obtained by Ficoll density gradient centrifugation. Viability was determined by trypan blue exclusion.

Flow cytometric analysis

Fresh peripheral blood mononuclear cells (PBMC) and leukocytes isolated from tissues were analyzed for expression of surface and intracellular markers using specific antibodies (Supplementary Table S2). Cell surface staining with fluorochrome-conjugated antibodies was performed in the dark at 4°C for 30 minutes, then cells were washed and resuspended in phosphate buffered saline with 0.2 mM EDTA and 0.5% human serum. For Foxp3 and CTLA4 staining, cells were fixed and permeabilized using the Foxp3 staining buffer set (eBioscience, Vienna, Austria). For intracellular cytokine staining, cells were stimulated with 40 ng/mL PMA (Sigma, Zwijndrecht, The Netherlands) and 1 μg/mL ionomycin (Sigma) at 37°C for five hours in the presence of 5 μg/mL brefeldin (Sigma) for the last four hours, followed by staining of IFN-γ and TNF-α upon fixation and permeabilization using the Foxp3 staining buffer set. Dead cells were excluded by using a LIVE/DEAD fixable dead cell stain kit with aqua fluorescent reactive dye (Invitrogen, Paisley, UK). Cells were measured using a FACS Canto II flow cytometer (BD Biosciences, San Diego, USA) and analyzed using

FlowJo software (version 10.0, LLC). Appropriate isotype control antibodies were used for gating purposes (Supplementary Table S2).

Ex vivo polyclonal T cell activation assay

All LM-CRC cell cultures were performed in complete medium RPMI 1640 (Lonza, Breda, The Netherlands) supplemented with 10% human AB serum (Invitrogen), 2mM L-glutamine (Invitrogen), 50 mM Hepes Buffer (Lonza), 1% penicillin-streptomycin (Life Technologies), 5mM Sodium Pyruvate (Gibco) and 1% minimum essential medium non-essential amino acids), at 37°C. TIL and PBMC from LM-CRC were labeled with 0.1 μM carboxyfluorescein diacetate succinimidyl ester (CFSE, Invitrogen); afterwards 10^5 TIL or PBMC were cultured in 200 μl complete medium in each well of a 96-well round-bottom culture plate and stimulated with anti-human CD3/CD28 dynabeads (Gibco-Life Technologies AS, Norway) at a cell : bead ratio of 10:1, in the presence or absence of 10 μg/ml antagonistic monoclonal antibodies against human PD-L1 (clone 5H1, kindly provided by Dr. Haidong Dong, Mayo Clinic College of Medicine(59)), TIM3 (clone F38-2E2, Biolegend, San Diego, USA(60, 61)), LAG3 (clone 17B4, AdipoGen, Liestal, Switzerland(62)) or CTLA4 (clone BNI3, Beckman Coulter, Marseille, France(63)), or isotype-matched control antibodies (mIgG1 and mIgG2a, Biolegend, London, UK). In preliminary experiments a cell : bead ratio of 10:1 was established to provide sub-optimal stimulation of T cell proliferation. After four days, culture supernatant was collected and frozen at -20°C until secretion of IFN-γ and TNF-α was quantified by enzyme-linked immunosorbent assay (ELISA, Ready-SET-Go!, eBioscience). CFSE-labeled cells were harvested and stained with CD8, CD4 and CD3 antibodies. Dead cells were excluded by using the LIVE/DEAD fixable dead cell stain kit with aqua fluorescent reactive dye, and T cell proliferation was determined based on CFSE dilution by flow cytometric analysis.

Ex vivo tumor-specific T cell stimulation assay

Tumor lysates and normal liver lysates were generated from a small piece of freshly resected metastatic liver tumor or TFL by five cycles of freezing and thawing in phosphate buffered saline, followed by filtration (0.2 μm syringe filter), as previously described.(40, 41) Myeloid dendritic cells (mDC) were isolated from patient autologous PBMC by depletion of CD19$^+$ B cells followed by positive selection for BDCA-1 (BDCA-1 DC isolation kit, Miltenyi Biotec). mDC were cultured overnight with or without 20 μg/mL autologous tumor lysates or normal liver lysates, in the presence of 10 ng/mL granulocyte-macrophage colony-stimulating factor (Miltenyi Biotec) and 0.5 μg/mL polyinosinic : polycytidylic acid (InvivoGen, San Diego, CA). Simultaneously TIL isolated from LM-CRC were kept at 4°C in complete medium overnight.

Thereafter TIL were labeled with 0.1 μM carboxyfluorescein diacetate succinimidyl ester (CFSE, Invitrogen), and 10^5 TIL were co-cultured with autologous mDC preloaded with or without tumor lysates or normal liver lysates at an mDC : TIL ratio of 1:5, in the presence or absence of 10 μg/ml antagonistic monoclonal antibodies against human PD-L1 (clone 5H1, kindly provided by Dr. Haidong Dong, Mayo Clinic College of Medicine(59)), TIM3 (clone F38-2E2, Biolegend, San Diego, USA(44)), LAG3 (clone 17B4, AdipoGen, Liestal, Switzerland(44)) or CTLA4 (clone BNI3, Beckman Coulter, Marseille, France(63)), in 200 μl complete medium in each well of a 96-well round-bottom culture plate. After six days, cells were restimulated with PMA (40 ng/mL) and ionomycin (1 μg/mL) for five hours in the presence of 5 μg/mL brefeldin for the last four hours. Cells were then stained with CD8, CD4 and CD3 antibodies, followed by intracellular staining of IFN-γ and TNF-α upon fixation and permeabilization according to the manufacturer's instructions (eBioscience A&B fixation/permeabilization kit). Dead cells were excluded by using the LIVE/DEAD fixable dead cell stain kit with aqua fluorescent reactive dye, and T cell proliferation was determined based on CFSE dilution by flow cytometric analysis.

Determination of mismatch repair status by immunohistochemistry

Immunostainings were performed on formalin-fixed paraffin-embedded whole tissue sections (4 μm thick) using the Benchmark Ultra autoimmunostainer (Ventana Medical Systems Inc, Roche Group, Tucson, USA) according to the manufacturer's protocols and instructions. Briefly, deparaffinization was followed by heat-induced epitope retrieval in Ultra CC1 pre-diluted buffer for 48-60 minutes at 100°C. Primary antibodies anti-MLH1 (Novocastra; Leica Microsystems B.V., Amsterdam, The Netherlands; clone ES05; dilution 1:75), anti-PMS2 (Cell Marque, Rocklin, USA; clone EPR3947, ready to use), anti-MSH2 (Cell Marque, clone G219-1129; ready to use) and anti-MSH6 (Dako, Glosturp, Denmark; clone EP49; dilution 1:75) were applied and followed by incubation (from 40 minutes to 1 hour and 32 minutes). Upon antibody incubation Ventana standard signal amplification was performed, followed by ultraWash counter-staining with one drop of Hematoxylin (for 20 minutes) and one drop of bluing reagent (for 4 minutes). Then slides were removed from the stainer, washed in water with a drop of dishwashing detergent and mounted. These immunohistochemical stainings detected the presence or absence of the protein products of the MMR genes MLH1, PMS2, MSH2 and MSH6. The pattern of their loss provides information about which gene is not functioning properly. IHC staining was evaluated under a light microscope as follows: nuclear expression of all MMR proteins indicates an MMR-proficient tumor status, loss of nuclear expression of any of the proteins indicates an MMR-deficient tumor status.

Statistical analysis

The distributions of all continuous data set were analyzed for normality by the Shapiro-Wilk normality test. Differences between paired groups of data were analyzed by either paired t test or Wilcoxon matched pairs test according to their distribution. Differences between different groups of patients were analyzed by either unpaired t test or Mann-Whitney test according to their distributions. Correlation was analyzed by either Pearson or Spearman correlation test according to their distributions. These statistical analyses were performed using GraphPad Prism 5 (GraphPad Software). Hierarchical clustering was analyzed by one minus Pearson correlation using GENE-E (Broad Institute). Progression-free survival (time to recurrence) was calculated from the date of LM-CRC surgery to the date of event (LM-CRC recurrence), or the date of last follow-up. Patients lost to follow-up were censored as of the last day of follow-up. Survival curves were estimated by the Kaplan-Meier mothed. The Breslow test was used to assess differences between survival curves of different groups. For multivariable analysis, the Cox proportional Hazard regression analysis was used. These statistical analyses were performed using SPSS Statistics 21 (IBM). P values less than 0.05 were considered statistically significant (* $p < 0.05$; ** $p < 0.01$; *** $p < 0.001$).

Table 1. Patient characteristics

	LM-CRC (n=53)	PM-CRC (n=11)	primary CRC (n=12)
Gender (female/male)	16 / 37	4 / 7	5 / 7
Age (years)**	66.3 ± 3.3	56.9 ± 3.8	63.4 ± 3.4
Stage of disease (TNM)	Stage IV n=53	Stage IV n=11	Stage I n=3, Stage II n=4, Stage III n=4, Stage IV n=1
Tumor MMR status	MMR-deficient n=2, MMR-proficient n=51	MMR-deficient n=0, MMR-proficient n=11	MMR-deficient n=3, MMR-proficient n=9

Abbreviations: CRC, colorectal cancer; LM-CRC, liver metastasis of CRC; PM-CRC, peritoneal metastasis of CRC; TNM, tumor-node-metastasis; MMR, mismatch repair.

**Mean ± standard error of the mean.

Table 2. Multivariable Cox proportional Hazard regression analysis of progression-free survival of patients with MMR-proficient LM-CRC

| | P | | 95% CI for HR | |
Variables	value	HR	Lower	Upper
PD-1 on CD8$^+$ TIL	.160	2.418	.706	8.283
TIM3 on CD8$^+$ TIL	.774	1.183	.375	3.732
LAG3 on CD8$^+$ TIL	**.032**	**.351**	**.135**	**.912**

Abbreviations: TIL, tumor-infiltrating lymphocytes; HR, hazard ratio; CI, confidence interval.

The hazard ratio is interpreted as the chance of recurrence occurring in the "> median" group to the chance of recurrence occurring in the "< median" group.

Figure legends

Figure 1. Comparison of immune infiltrates and inhibitory molecule expression among MMR-proficient liver metastases (LM), peritoneal metastases (PM) and primary CRC. (A) The frequencies of CD8+ CTL, CD4+Foxp3- Th and CD4+Foxp3+ Treg within CD3+ TIL from LM-CRC, primary CRC and PM-CRC. (B) The frequencies of inhibitory receptor positive cells within CD8+ CTL, Th and Treg in LM-CRC, primary CRC and PM-CRC. (C) The frequencies of B cells, mDC and monocytes (Mono) within CD45+ cells from LM-CRC, primary CRC and PM-CRC. (D) The frequencies of inhibitory ligand positive cells within tumor-infiltrating B cells, mDC and monocytes from LM-CRC, primary CRC and PM-CRC. Values of individual patients are shown, and lines depict medians. Differences were analyzed by unpaired t test or Mann-Whitney test; * $p < 0.05$, ** $p < 0.01$, *** $p < 0.001$.

Figure 2. Expression of inhibitory receptors on CD8+ CTL, CD4+ Th and CD4+ Treg in the tumor, TFL and blood of MMR-proficient LM-CRC. PBMC and leukocytes isolated from LM-CRC tumors and TFL were stained with antibodies against PD-1, LAG3, TIM3 and CTLA4. (A) (B) Representative dot plots of inhibitory receptor expression on (A) CD3+CD8+ CTL and (B) CD3+CD4+Foxp3- Th in the tumor, TFL and blood; the gates were made according to appropriate isotype controls. (C) (D) (E) The frequencies of inhibitory receptor positive cells within (C) CD8+ CTL, (D) CD4+Foxp3- Th and (E) CD4+Foxp3+ Treg in the tumor, TFL and blood. Values of individual patients are shown, and lines depict medians. Differences were analyzed by paired t test or Wilcoxon matched pairs test; * $p < 0.05$, ** $p < 0.01$, *** $p < 0.001$.

Figure 3. Intra-tumoral antigen-presenting cells of MMR-proficient LM-CRC express inhibitory ligands. Expression of inhibitory ligands PD-L1, galectin 9 (GAL-9), MHC-II, CD86 and CD80 was measured by flow cytometry. (A) The frequencies of CD19+ B cells, BDCA1+CD19- mDC and CD14+ monocytes (Mono) within CD45+ cells derived from tumors, TFL and blood. Values of individual patients are presented, lines depict medians. (B) Representative histograms of inhibitory ligand stainings and isotype controls on tumor-infiltrating mDC, monocytes and B cells. (C) The frequencies of inhibitory ligand positive cells within tumor-infiltrating B cells, mDC and monocytes in individual patients are presented; lines depict medians. (D) The median fluorescence intensities (MFI) of inhibitory ligands on B cells, mDC and monocytes derived from tumors, TFL and blood of LM-CRC patients. Values of individual patients are shown, and lines depict medians. Differences were analyzed by paired t test or Wilcoxon matched pairs test; * $p < 0.05$, ** $p < 0.01$, *** $p < 0.001$.

Figure 4. Tumor-infiltrating T cells expressing inhibitory receptors show increased expression of activation markers. TIL from MMR-proficient LM-CRC were stained *ex vivo* with antibodies against surface activation markers HLA-DR and CD69. (A) (B) The frequencies of HLA-DR$^+$ or CD69$^+$ cells in (A) CD8$^+$ CTL and (B) CD4$^+$ Th that do or do not express PD-1, TIM3, LAG3, or CTLA4 are presented (n=9-11). Lines show medians, whiskers depict minimum to maximum. Differences were analyzed by paired t test or Wilcoxon matched pairs test. (C) (D) TIL from MMR-proficient LM-CRC were stimulated with PMA and ionomycin at 37°C for five hours, in the presence of protein transport inhibitor brefeldin for the last four hours, followed by intracellular cytokine staining. The frequencies of cytokine-producing cells in (C) CD8$^+$ CTL and (D) CD4$^+$ Th that do or do not express inhibitory receptors are presented (n=7-12). Lines show medians, whiskers depict Min to Max, boxes indicate the 25th to 75th percentiles. Differences were analyzed by paired t test or Wilcoxon matched pairs test; * $p < 0.05$, ** $p < 0.01$, *** $p < 0.001$.

Figure 5. Antibody blockade of LAG3 or PD-L1 boosts *ex vivo* proliferation and cytokine production of intra-tumoral T cells from MMR-proficient LM-CRC in response to polyclonal stimuli. CFSE-labeled TIL from LM-CRC patients were stimulated with CD3/CD28 beads for four days, in the presence or absence of 10 µg/ml antagonistic antibodies. (A) Representative dot plots of CD3$^+$CD8$^+$ and CD3$^+$CD4$^+$ TIL proliferation in response to CD3/CD28 beads (a-CD3/CD28) in the presence or absence of antagonistic antibodies (a-) or isotype controls (iso ctrl). Dotplots indicated by "TIL" show proliferative responses in the absence of CD3/CD28 beads. In all other conditions, CD3/CD28 beads were added. (B) The percentages of proliferating cells (CFSE-low) within CD8$^+$ and CD4$^+$ T cells derived from the tumor or blood in response to CD3/CD28 beads without addition of any antagonistic antibody. Values of individual patients are presented. (C) Effects of antibody blockade of inhibitory interactions on CD8$^+$ and CD4$^+$ TIL proliferation (n=7-9). Because the proliferative responses differed between patients, the results are reported as relative proliferation in the presence of antibodies compared to baseline proliferation, which was calculated by dividing the percentages of proliferating (CFSE-low) T cells in the presence of antagonistic antibody or isotype control antibody by the percentages in the control condition with only CD3/CD28 beads. Values are depicted as means with standard error of the mean. (D) IFN-γ and TNF-α accumulation in culture supernatants was quantified at day four by enzyme-linked immunosorbent assay. Values are depicted as medians with interquartile range (n=10-11). Differences were analyzed by paired t test or Wilcoxon matched pairs test; * $p < 0.05$, ** $p < 0.01$.

Figure 6. Antibody blockade of LAG3 or PD-L1 boosts *ex vivo* responses of intra-tumoral T cells from MMR-proficient LM-CRC to autologous tumor antigens. Blood mDC loaded with autologous tumor lysates were used to stimulate CFSE-labeled TIL, in the presence or absence of 10 µg/mL antagonistic antibodies. After six days T cell proliferation and intracellular cytokine production were analyzed after re-stimulation with PMA and ionomycin. (A) (B) Representative dot plots of T cell proliferation, IFN-γ and TNF-α expression in CD3$^+$CD8$^+$ and CD3$^+$CD4$^+$ TIL, in response to autologous mDC pre-loaded with tumor lysates (TIL+mDC+tumor lysate), in the presence or absence of antagonistic antibodies (a-). TIL responses to mDC that were not pre-loaded with tumor lysates (TIL+mDC) served as controls to determine non-antigen-specific TIL proliferation and cytokine production. (C) (D) (E) Collective data of five patients tested. Each line and each color represent one patient. The results are reported as net tumor-specific responses, calculated by subtracting the percentages of proliferating (CFSE-low) T cells or IFN-γ$^+$ or TNF-α$^+$ proliferating T cells in the control condition (mDC without tissue lysates) from the percentages in the conditions with tumor lysates (TL) in the absence or presence of antagonistic antibody. In two experiments an additional control was included, in which TIL were stimulated with blood mDC pre-loaded with normal liver lysates (NL), which did not lead to increased TIL responses.

Figure 7. Kaplan-Meier curves of progression-free survival (time to recurrence) in relation to LAG3 expression on intra-tumoral T cells in MMR-proficient LM-CRC. The cutoff values to divide the patients into two groups are the median percentages of LAG3$^+$ cells in tumor-infiltrating CD8$^+$ CTL, CD4$^+$Foxp3$^-$ Th or CD4$^+$Foxp3$^+$ Treg cells. For determination of the p values the Breslow test was used.

Figure 1.
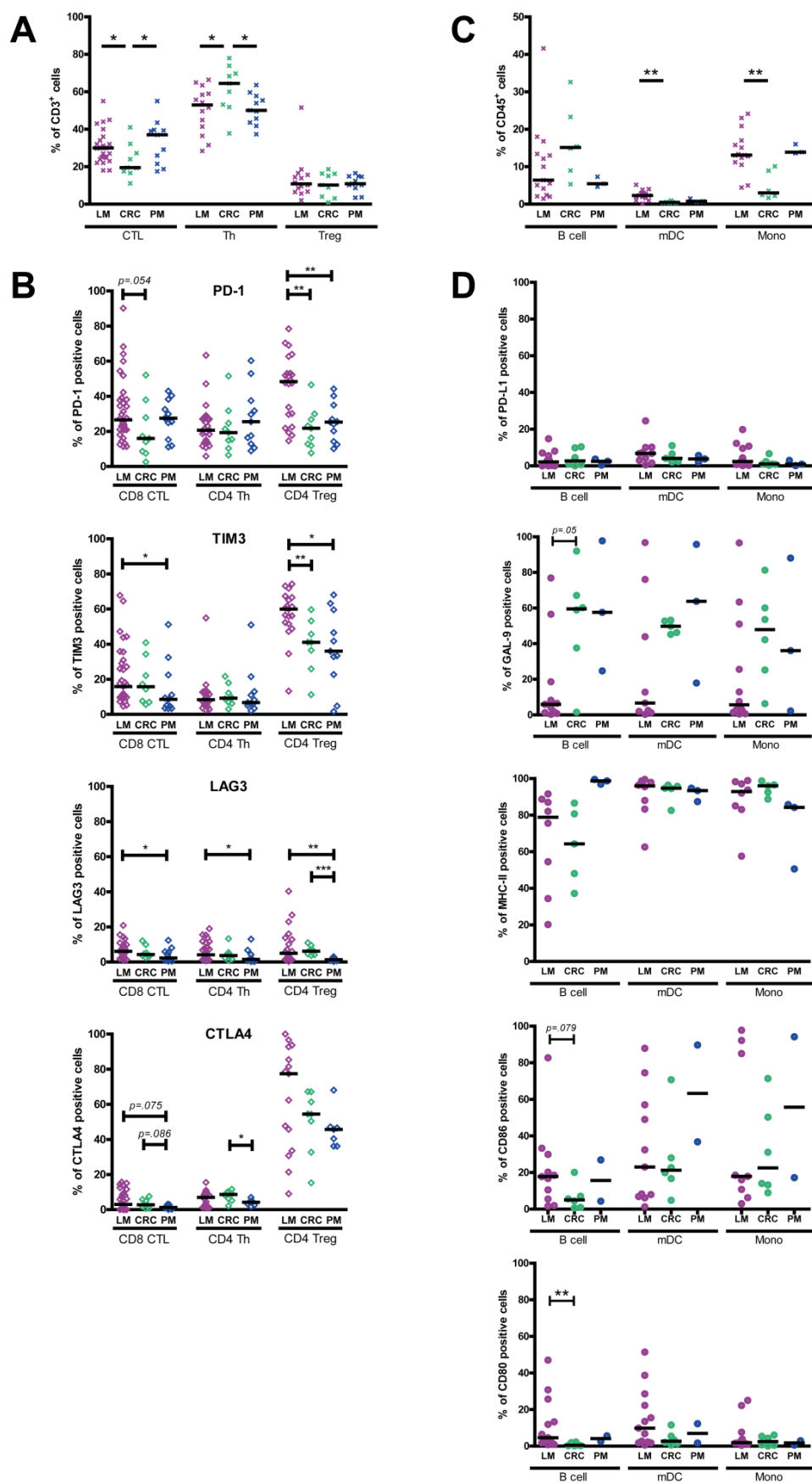
Figure 2.
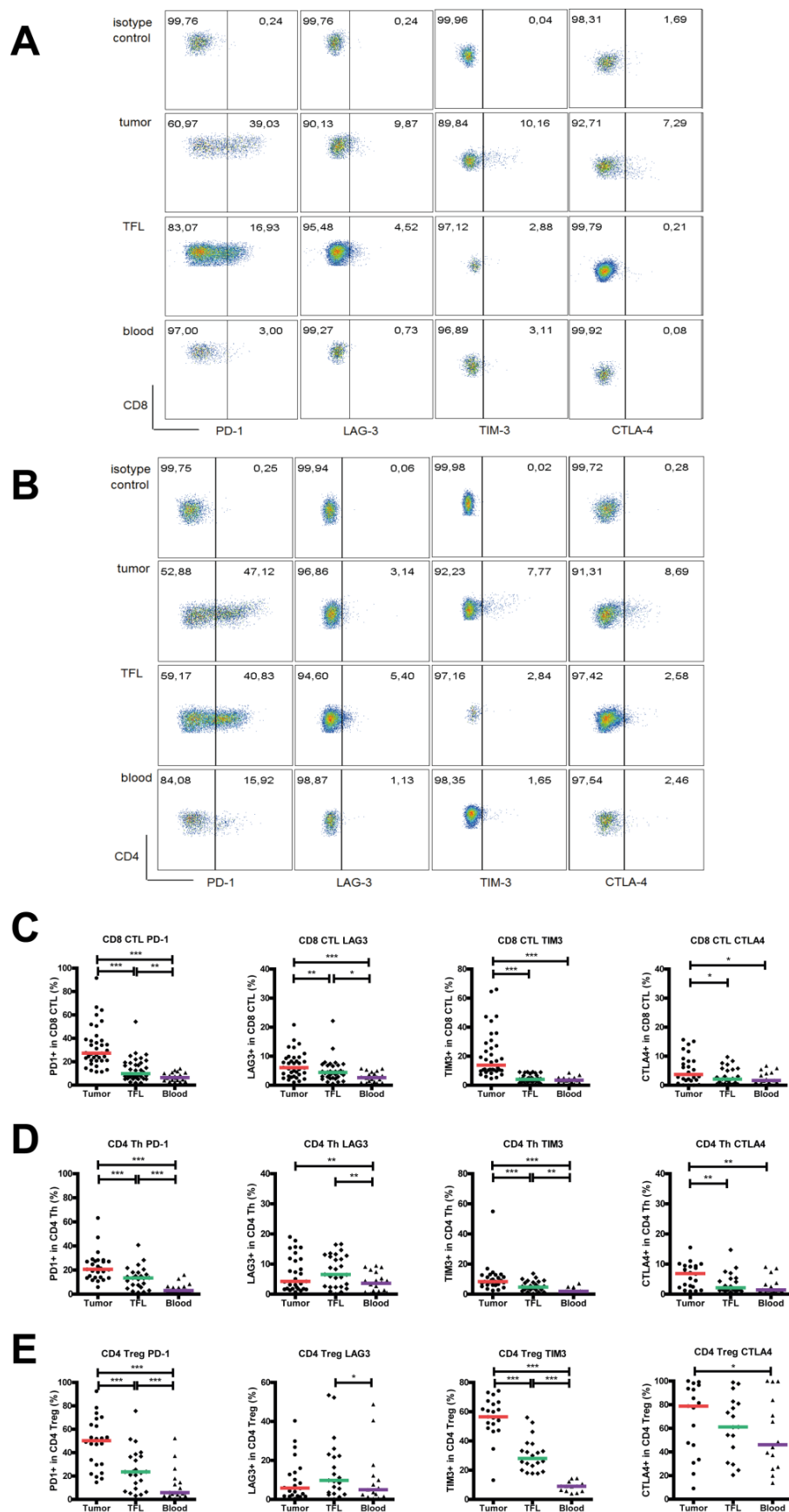
Figure 3.

Figure 4.

Figure 5.

Figure 6.

Figure 7.

LAG3 in CD8

LAG3 in CD4 Th

LAG3 in CD4 Treg
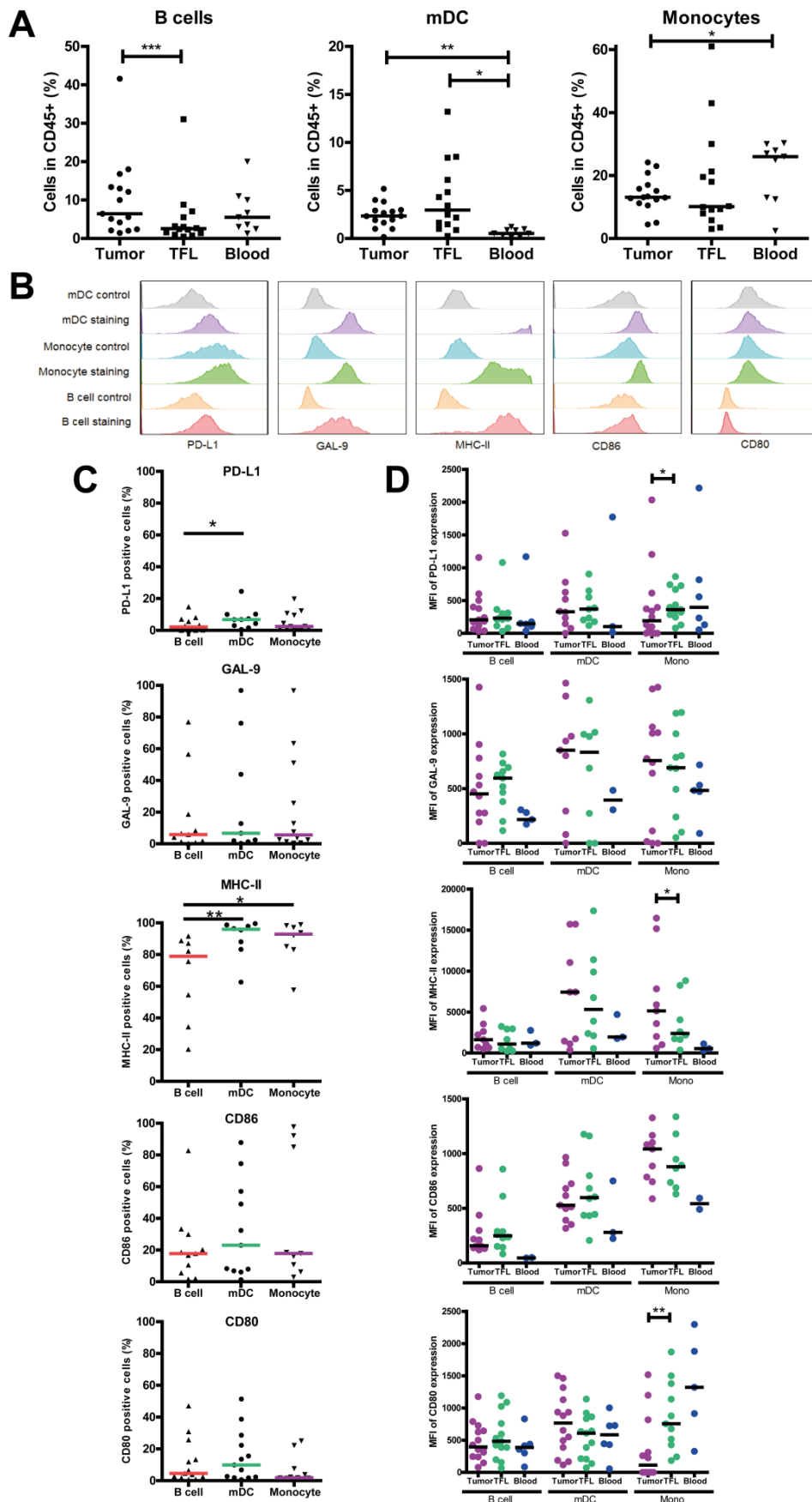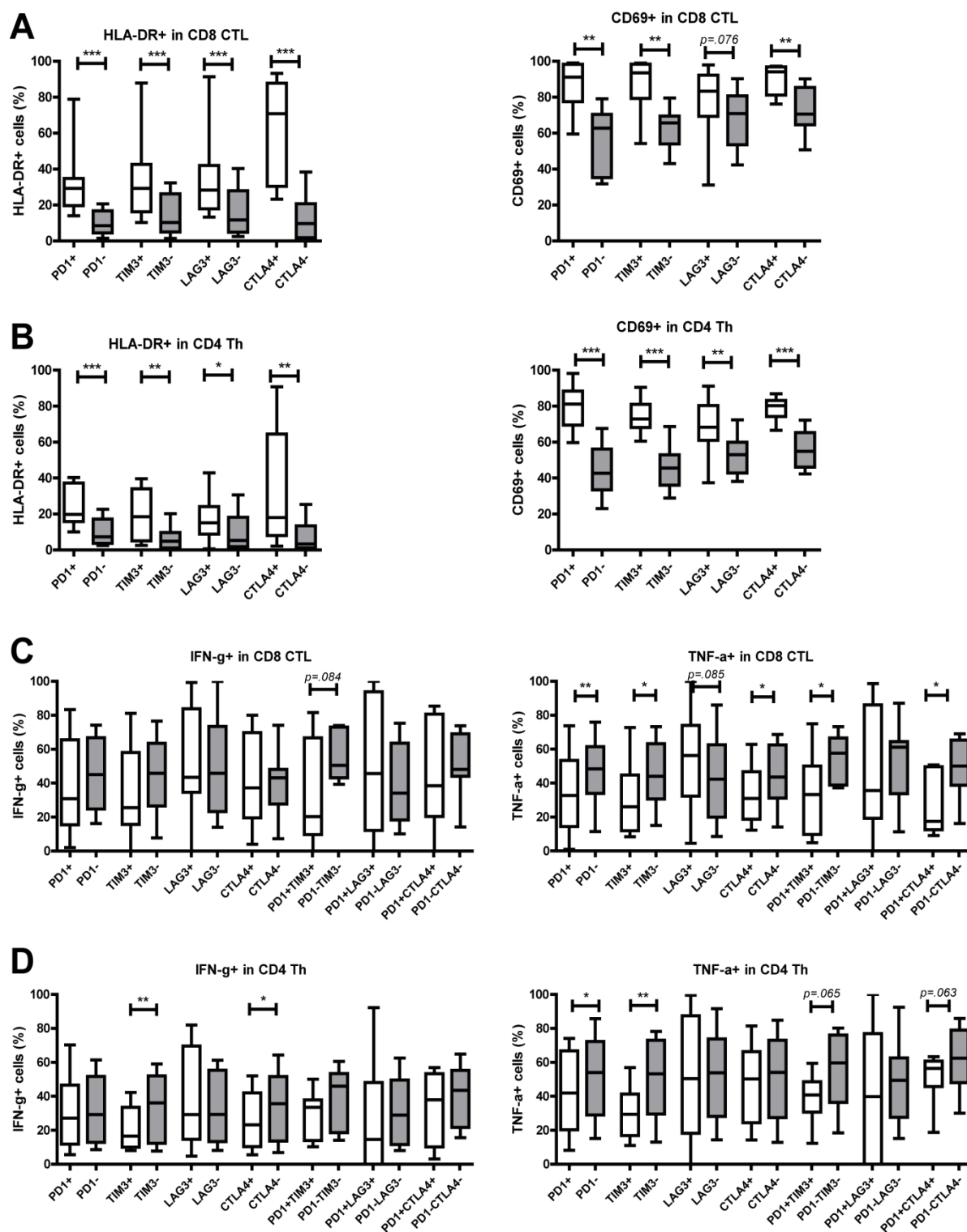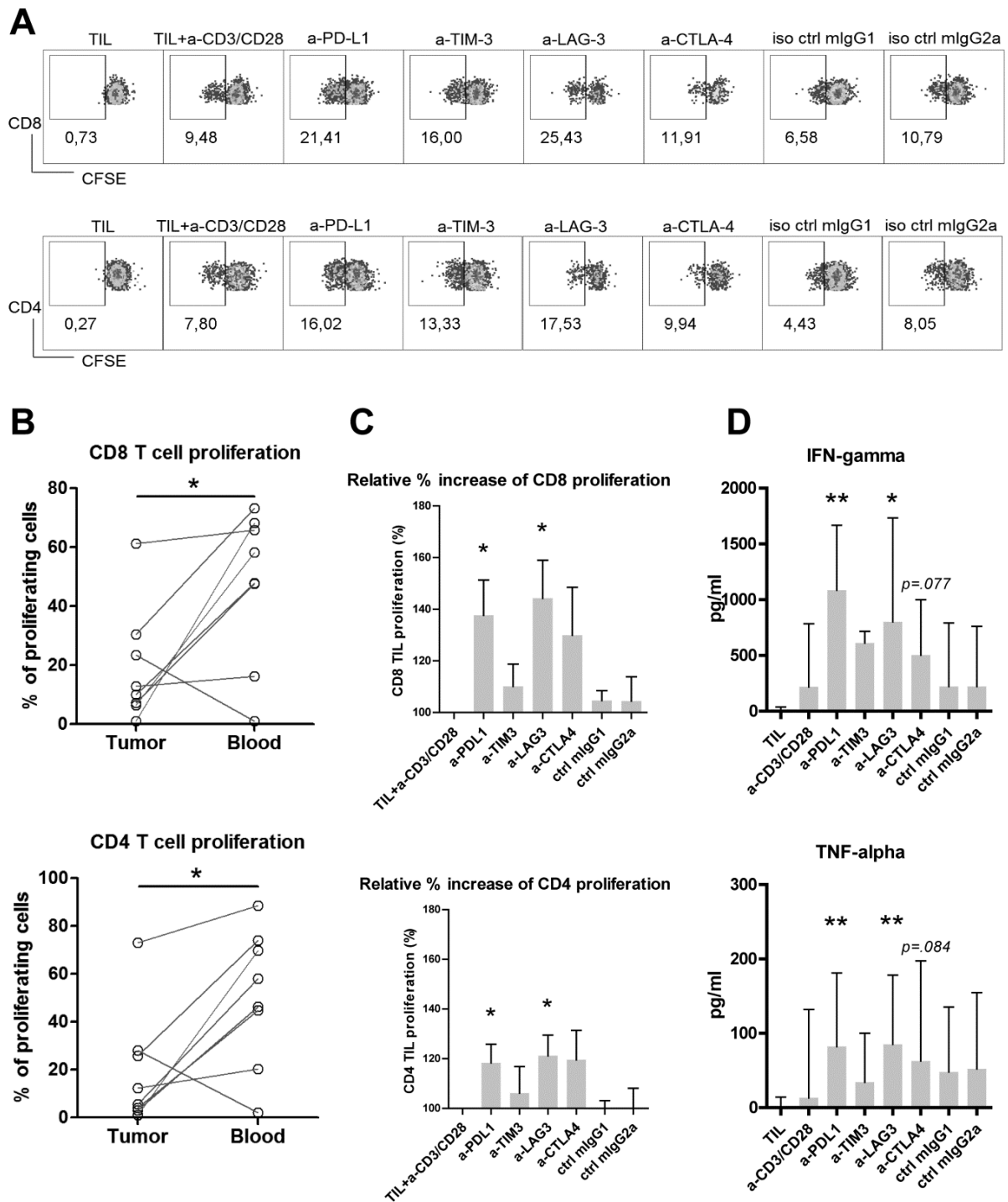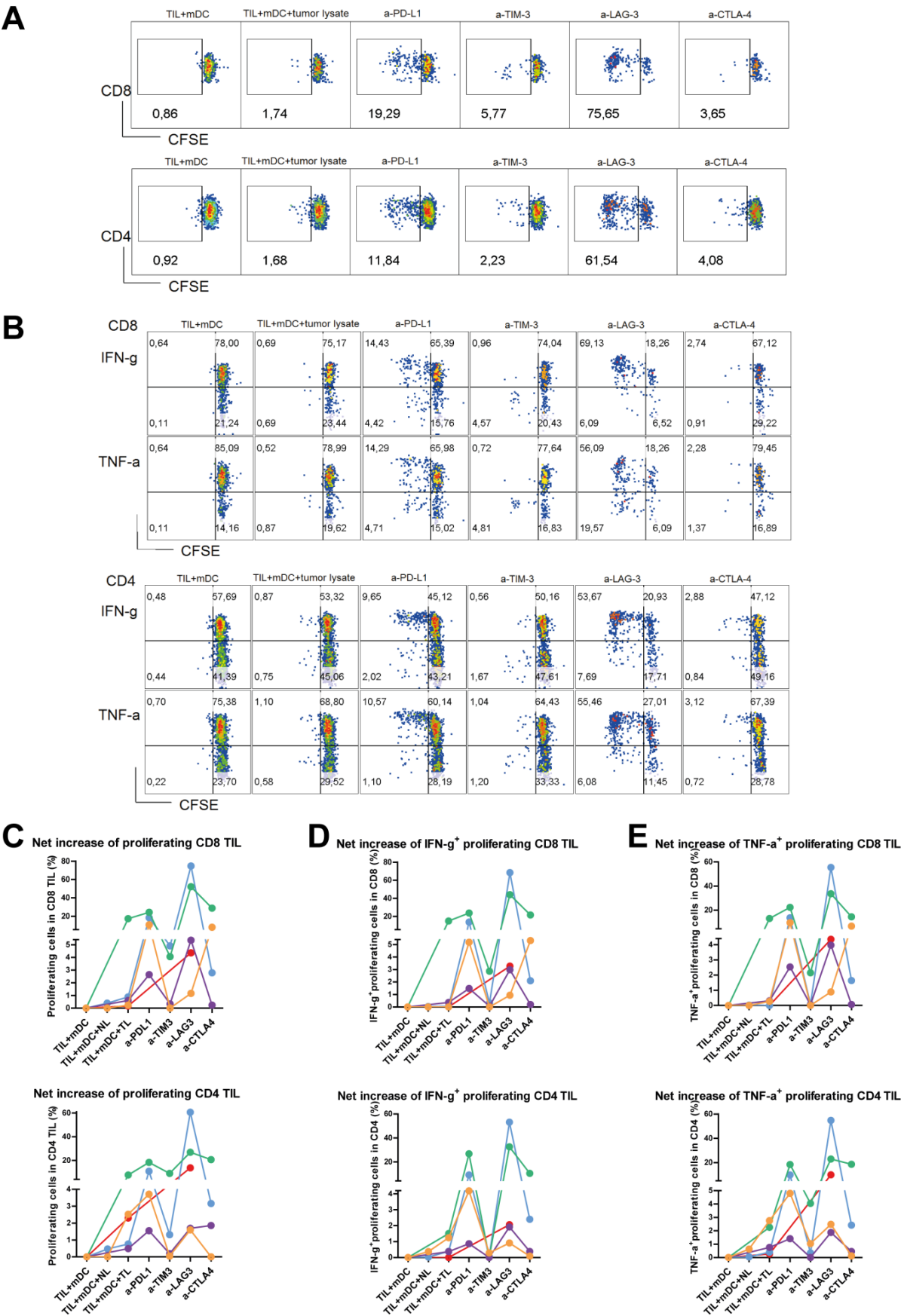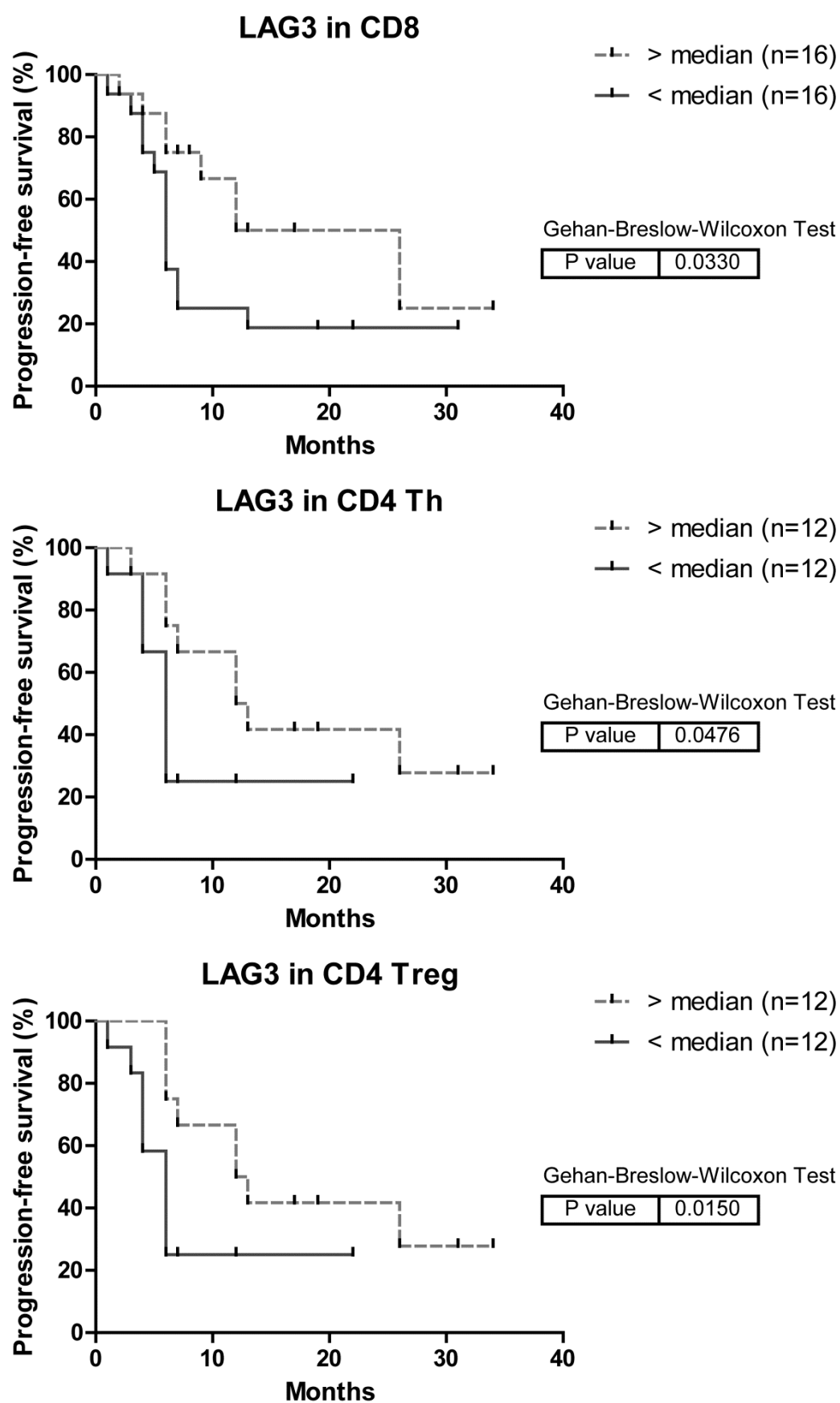
Supplementary figure legends

Supplementary Figure S1. Immune infiltrates and inhibitory molecule expression in MMR-deficient liver metastases (LM) and primary CRC. (A) The frequencies of CD8$^+$ CTL, CD4$^+$Foxp3$^-$ Th and CD4$^+$Foxp3$^+$ Treg within CD3$^+$ TIL from LM-CRC and primary CRC. (B) The frequencies of inhibitory receptor positive cells within CD8$^+$ CTL, Th and Treg in LM-CRC and primary CRC. (C) The frequencies of B cells, mDC and monocytes (Mono) within CD45$^+$ cells from primary CRC. (D) The frequencies of inhibitory ligand positive cells within tumor-infiltrating B cells, mDC and monocytes from primary CRC. Values of individual patients are shown, and lines depict medians.

Supplementary Figure S2. Hierarchical clustering analysis of MMR-proficient liver metastases, peritoneal metastases and primary CRC. Heatmap illustrating the frequencies of CD8$^+$ CTL, CD4$^+$ Th and CD4$^+$ Treg within CD3$^+$ TIL, the frequencies of inhibitory receptor positive cells within CD8$^+$ CTL, CD4$^+$ Th and CD4$^+$ Treg, the frequencies of B cells, mDC and monocytes within CD45$^+$ cells, and the frequencies of inhibitory ligand positive cells within tumor-infiltrating B cells, mDC and monocytes, across LM-CRC, PM-CRC and primary CRC tumors. Rows represent different parameters. Columns represent individual patients clustered by one minus pearson correlation (LM-CRC: n=5, primary CRC: n=6, PM-CRC: n=2). Due to limited numbers of TIL isolated from each tumor sample we could measure all the different phenotypic markers only in TIL isolated from limited numbers of tumors. (A) Absolute values: 0%-100%. (B) Relative values: row minimum (min) to row maximum (max). Grey: missing values.

Supplementary Figure S3. Expression of BTLA on CD8$^+$ CTL, CD4$^+$ Th and CD4$^+$ Treg in the tumor, TFL and blood of MMR-proficient LM-CRC. (A) (B) Representative dot plots of BTLA expression on CD3$^+$CD8$^+$ CTL and CD3$^+$CD4$^+$Foxp3$^-$ Th in the tumor, TFL and blood; the gates were made according to appropriate isotype controls. (C) (D) (E) The frequencies of BTLA positive cells within CD8$^+$ CTL, CD4$^+$ Foxp3$^-$ Th and CD4$^+$ Foxp3$^+$ Treg in the tumor, TFL and blood. Values of individual patients are shown, and lines depict medians. Differences were analyzed by paired t test or Wilcoxon matched pairs test; * p < 0.05.

Supplementary Figure S4. Correlation of inhibitory receptor expression on T cells between the tumor and the blood of patients with mismatch repair-proficient LM-CRC. Spearman correlation analysis demonstrates (A) positive correlation of the frequencies of PD-1$^+$ cells in CD8$^+$ CTL and CD4$^+$ Treg between tumors and blood, (B) positive correlations of the frequencies of LAG3$^+$ cells in CD4$^+$ Th between tumors and blood, and (C) positive

correlations of the frequencies of CTLA4^{+} cells in CD4^{+} Th and CD4^{+} Treg between tumors and blood. Correlations were analyzed by Spearman correlation test.
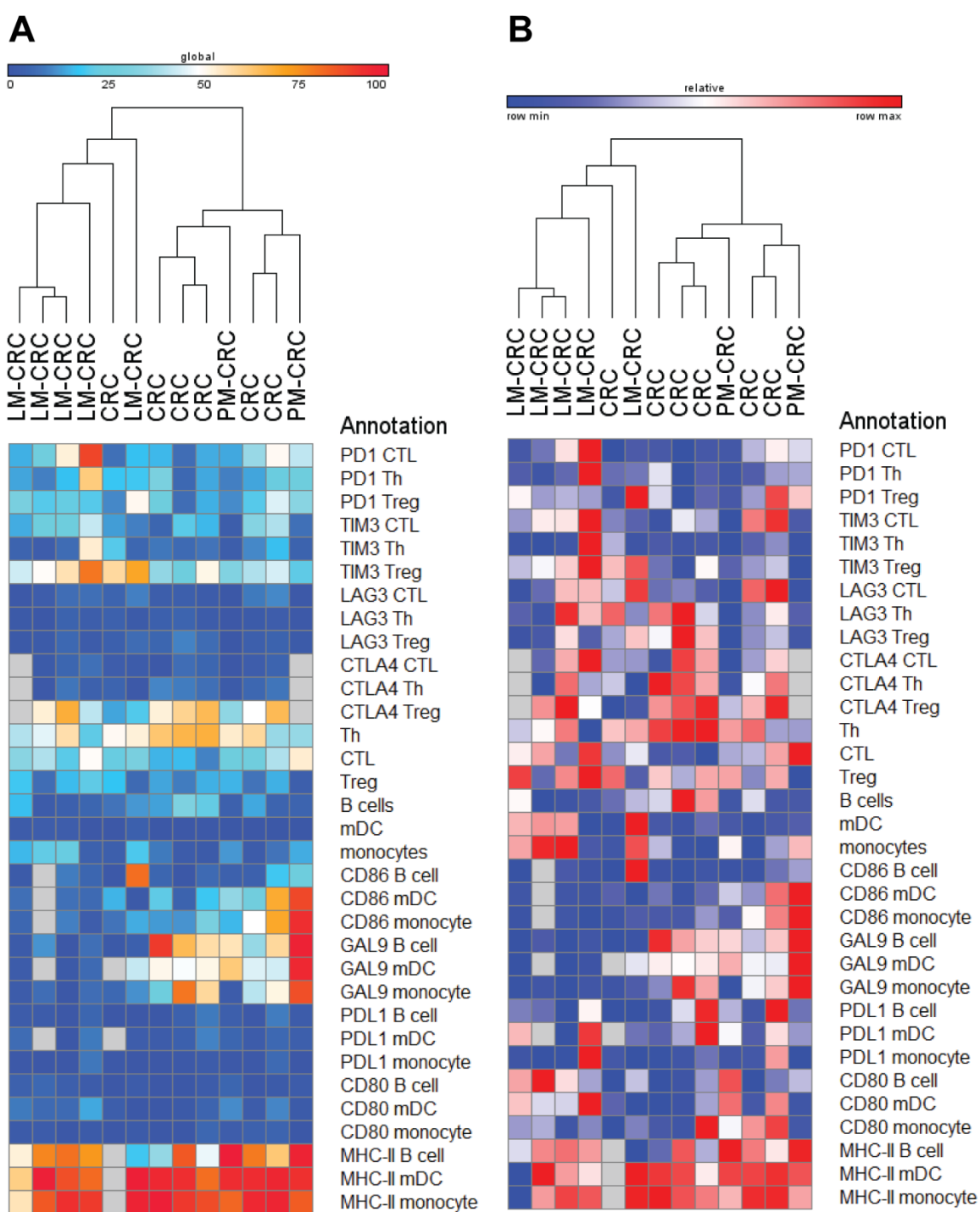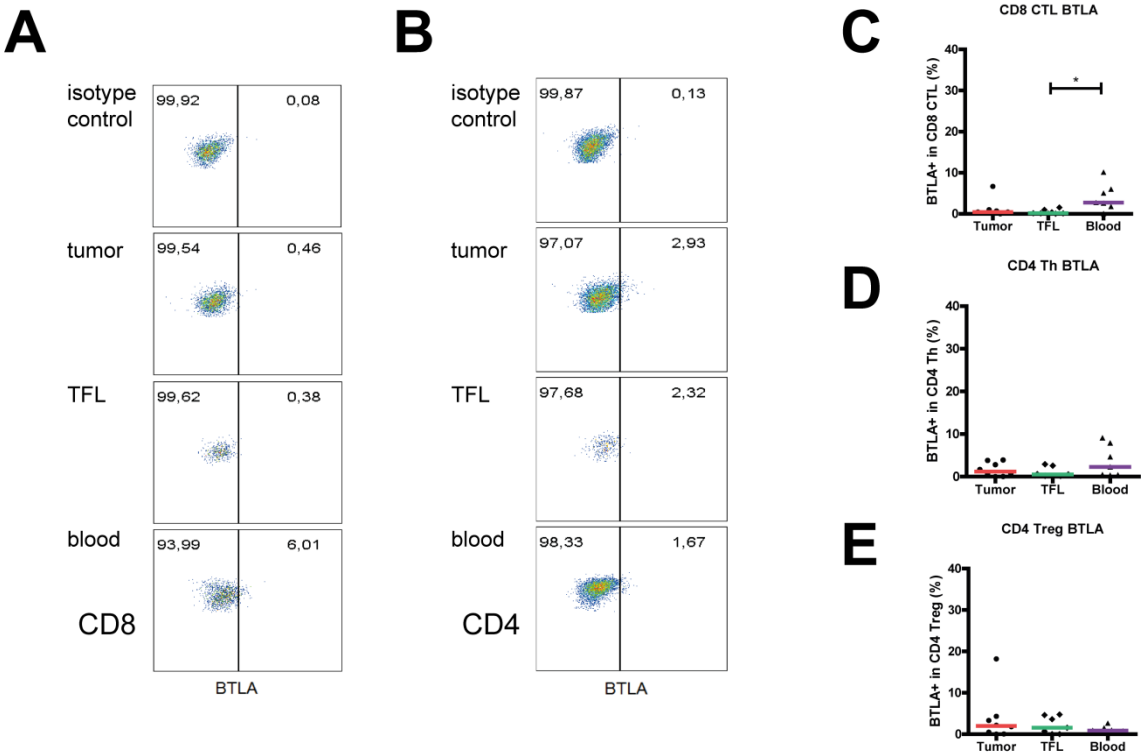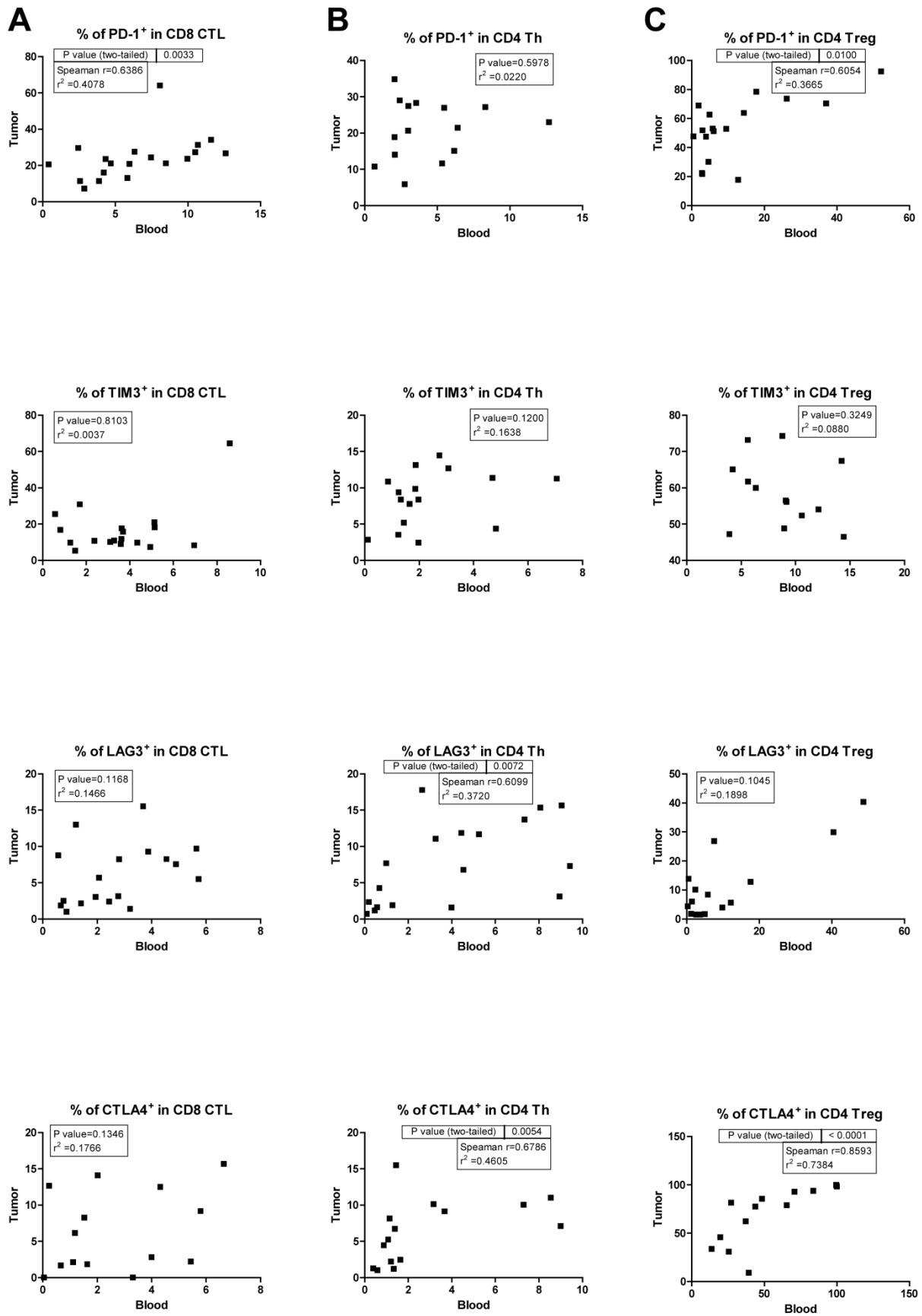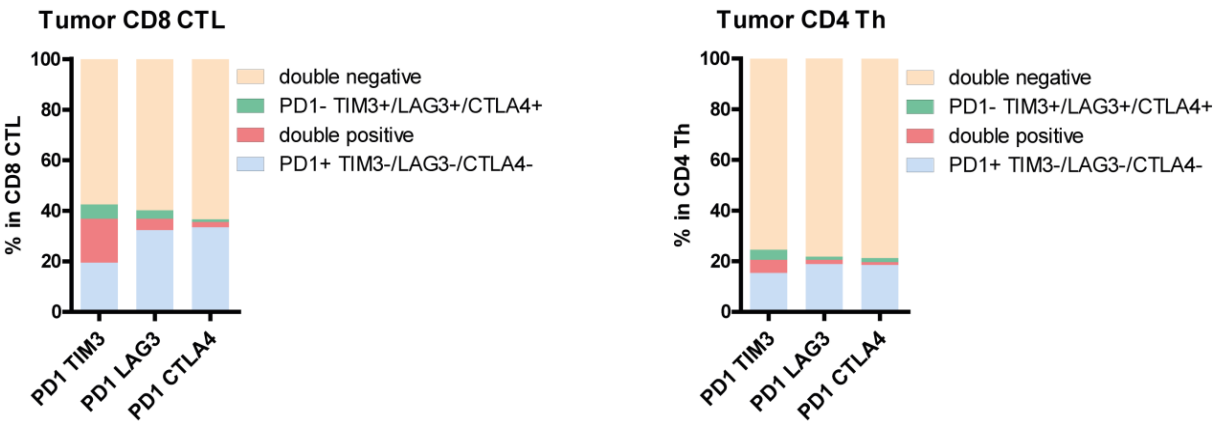
Supplementary Figure S5. Co-expression of inhibitory receptors on tumor-derived T cells in MMR-proficient LM-CRC. The mean frequencies of co-expression of PD-1 with TIM3, LAG3 or CTLA4 in CD8^{+} CTL (n=20) and CD4^{+} Th (n=10).

Supplementary Figure S6. T cell densities in primary CRC tumors and liver metastases. CD3^{+}, CD8^{+} and granzyme B^{+} cell densities in paired primary CRC and LM-CRC of 16 patients. The data were reanalyzed after being extracted from Halama *et al.* Table 1.(35) Values of individual patients are shown, and lines depict means. Differences were analyzed by paired t test or Wilcoxon matched pairs test; * p < 0.05.

Supplementary Figure S1.
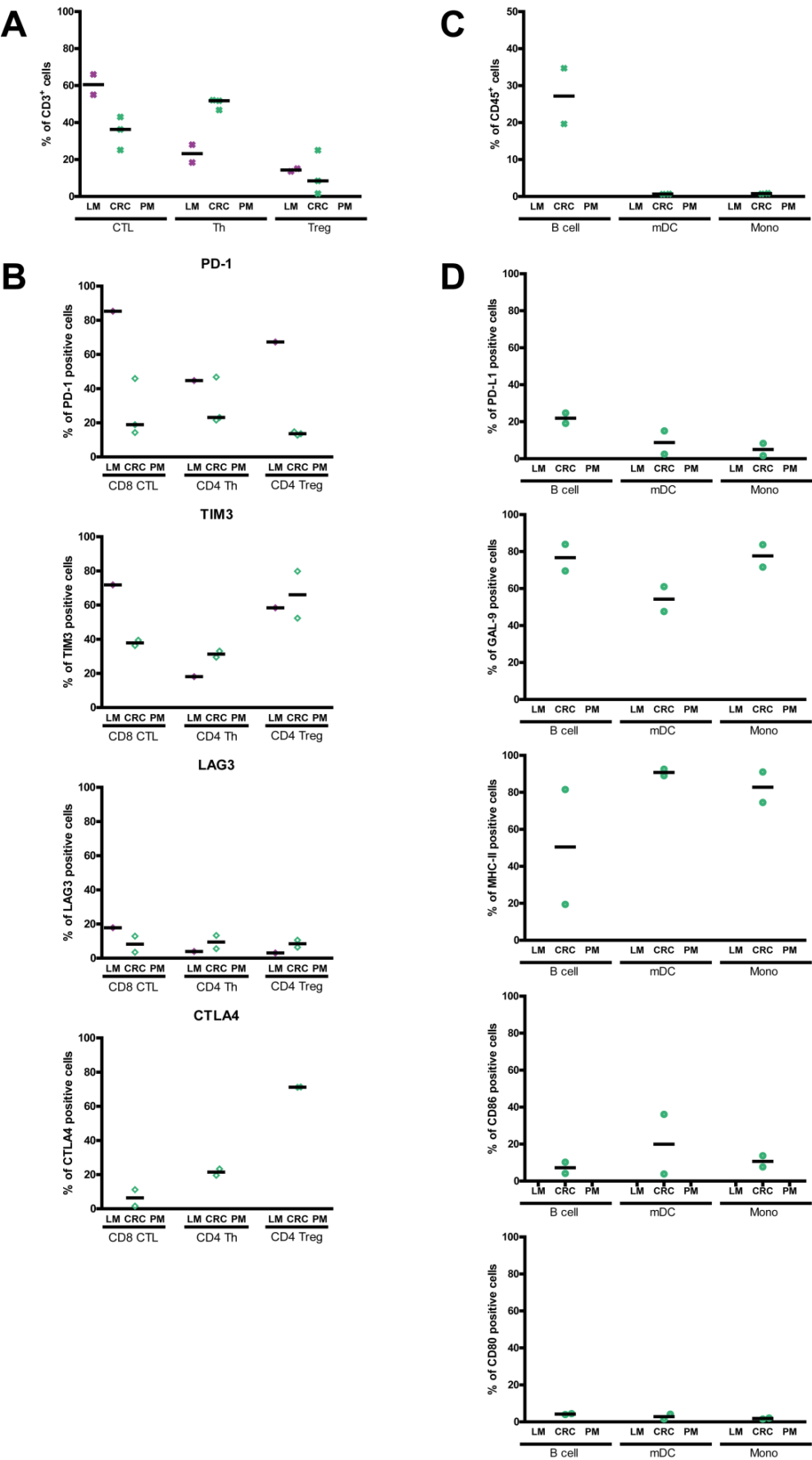
Supplementary Figure S2.

Supplementary Figure S3.

Supplementary Figure S4.

A

% of PD-1⁺ in CD8 CTL

P value (two-tailed) | 0.0033
Speaman r=0.6386
r² =0.4078

B

% of PD-1⁺ in CD4 Th

P value=0.5978
r² =0.0220

C

% of PD-1⁺ in CD4 Treg

P value (two-tailed) | 0.0100
Speaman r=0.6054
r² =0.3665

% of TIM3⁺ in CD8 CTL

P value=0.8103
r² =0.0037

% of TIM3⁺ in CD4 Th

P value=0.1200
r² =0.1638

% of TIM3⁺ in CD4 Treg

P value=0.3249
r² =0.0880

% of LAG3⁺ in CD8 CTL

P value=0.1168
r² =0.1466

% of LAG3⁺ in CD4 Th

P value (two-tailed) | 0.0072
Speaman r=0.6099
r² =0.3720

% of LAG3⁺ in CD4 Treg

P value=0.1045
r² =0.1898

% of CTLA4⁺ in CD8 CTL

P value=0.1346
r² =0.1766

% of CTLA4⁺ in CD4 Th

P value (two-tailed) | 0.0054
Speaman r=0.6786
r² =0.4605

% of CTLA4⁺ in CD4 Treg

P value (two-tailed) | < 0.0001
Speaman r=0.8593
r² =0.7384

Supplementary Figure S5.

Tumor CD8 CTL

Tumor CD4 Th

Supplementary Figure S6.

Supplementary Table S1. Numbers of patient samples used in each type of experiments in the study

Tumor type and number of samples	MMR status and number of samples	T cell or APC subsets Figure 1	Inhibitory receptors Figure 1, Figure 2	Inhibitory ligands Figure 1, Figure 3	Activation or cytokine Figure 4	Polyclonal T cell activation assay Figure 5	Tumor-specific T cell stimulation assay Figure 6
53 LM-CRC	1 deficient	X					
	1 deficient		X				
	1 proficient						X
	1 proficient			X	X		
	1 proficient	X	X			X	
	1 proficient	X	X	X			
	1 proficient	X	X	X			X
	1 proficient	X	X	X	X	X	X
	2 proficient	X	X	X			
	2 proficient	X	X				X
	4 proficient					X	
	5 proficient	X	X			X	
	6 proficient			X			
	11 proficient	X	X				
	15 proficient				X		
11 PM-CRC	2 proficient	X	X	X			
	9 proficient	X	X	X			
12 primary CRC	1 deficient	X	X	X			
	2 deficient	X	X				
	3 proficient	X	X				
	6 proficient	X	X	X			

Abbreviations: CRC, colorectal cancer; LM-CRC, liver metastasis of CRC; PM-CRC, peritoneal metastasis of CRC; MMR, mismatch repair.

Supplementary Table S2. Antibodies used in flow cytometry

Antibody	Clone	Supplier	Antibody	Clone	Supplier
CD69 APC	L78	BD Biosciences	CD8-PE	RPA-T8	eBioscience
IFN-gamma-FITC	25723.11	BD Biosciences	HLA-DR-APC	LN3	eBioscience
CD137 (4-1BB)-APC	4B4-1	BD Biosciences	HLA-DR-PE	LN3	eBioscience
CD14-PerCP	MOP9	BD Biosciences	HLA-DR-PerCP-Cy5.5	LN3	eBioscience
CD3 PerCP-Cy5.5	UCHT1	BD Biosciences	CD3 PE-Cy7	UCHT1	eBioscience
CD19 APC-H7	SJ25C1	BD Biosciences	CD8-APC	okt-08	eBioscience
mIgG2b-FITC	27-35	BD Biosciences	IFN-gamma-Pe-Cy7	4S.B3	eBioscience
mIgG1-PB	MOPC-21	BD Biosciences	HLA-DR-APC-eFluor780	LN3	eBioscience
mIgG2b-PE	27-35	BD Biosciences	CD279 (PD1)-PE-Cy7	J105	eBioscience

mIgG1-PerCP	X40	BD Biosciences	CD8-efluor450	RPA-T8	eBioscience
mIgG1-FITC	MOPC-21	BD Biosciences	CD274(B7-H1)-PE-Cy7	MIH1	eBioscience
mIgG1-pacific blue	MOPC-21	BD Biosciences	CD270 (HVEM)-PE	eBioHVEM-122	eBioscience
mIgG2a-PerCP	X39	BD Biosciences	CD4-APC-eFluor780	OKT4	eBioscience
CD69-PE	TP1.55.3	Beckman	CD3-APC-eFluor780	SK7	eBioscience
CD3 FITC	UCHT1	Beckman	FoxP3-eFluor450	236A/E7	eBioscience
CD45 FITC	J33	Beckman	CD45 efluor 450	HI30	eBioscience
mIgG2a-PE	U7.27	Beckman	CD8a-PerCp-Cy5.5	RPA-T8	eBioscience
CD272 (BTLA)-APC	MIH26	Biolegend	CD223(LAG3)-PE	3DS223H	eBioscience
CD3 PE	UCHT1	Biolegend	CD223(LAG3)-PerCP-eF710	3DS223H	eBioscience
CD86-PB	IT2.2	Biolegend	CD8-FITC	SK1	eBioscience
anti-TNF-α-PerCP-Cy5.5	Mab11	Biolegend	rat IgG2a-APC	eBR2a	eBioscience
Galectin-9 PE	9M1-3	Biolegend	mIgG1-FITC	P3	eBioscience
CD80-PE-Cy7	2D10	Biolegend	mIgG2a-APC	eBM2a	eBioscience
CD152 (CTLA4)-APC	L3D10	Biolegend	rat IgG2b-APC	eB149/10H5	eBioscience
HLA-DR, DP, DQ-FITC	Tü39	Biolegend	mIgG1-PE	P3.6.2.8.1	eBioscience
mIgG1-Pe-Cy7	MOPC-21	Biolegend	BDCA1-APC	AD5-8E7	Miltenyi
rat IgG2a-PE	RTK2758	Biolegend	TIM3-PE	344823	R&D systems
mIgG2a-FITC	MOPC-173	Biolegend			
mIgG1-APC	MOPC-21	Biolegend			

REFERENCES

1.   Torre LA, Bray F, Siegel RL, Ferlay J, Lortet-Tieulent J, Jemal A. Global cancer statistics, 2012. CA Cancer J Clin. 2015;65(2):87-108. Epub 2015/02/06. doi: 10.3322/caac.21262. PubMed PMID: 25651787.

2.   Jalili-Nik M, Soltani A, Moussavi S, Ghayour-Mobarhan M, Ferns GA, Hassanian SM, et al. Current status and future prospective of Curcumin as a potential therapeutic agent in the treatment of colorectal cancer. J Cell Physiol. 2017. Epub 2017/12/09. doi: 10.1002/jcp.26368. PubMed PMID: 29219177.

3.   Kallini JR, Gabr A, Abouchaleh N, Ali R, Riaz A, Lewandowski RJ, et al. New Developments in Interventional Oncology: Liver Metastases From Colorectal Cancer. Cancer J. 2016;22(6):373-80. Epub 2016/11/22. doi: 10.1097/PPO.0000000000000226
00130404-201611000-00003 [pii]. PubMed PMID: 27870679.

4.   Zarour LR, Anand S, Billingsley KG, Bisson WH, Cercek A, Clarke MF, et al. Colorectal Cancer Liver Metastasis: Evolving Paradigms and Future Directions. Cell Mol Gastroenterol Hepatol. 2017;3(2):163-73. Epub 2017/03/10. doi: 10.1016/j.jcmgh.2017.01.006
S2352-345X(17)30011-5 [pii]. PubMed PMID: 28275683; PubMed Central PMCID: PMC5331831.

5.   Kemeny N. The management of resectable and unresectable liver metastases from colorectal cancer. Curr Opin Oncol. 2010;22(4):364-73. Epub 2010/06/04. doi: 10.1097/CCO.0b013e32833a6c8a. PubMed PMID: 20520544.

6.   Fonseca GM, Herman P, Faraj SF, Kruger JAP, Coelho FF, Jeismann VB, et al. Pathological factors and prognosis of resected liver metastases of colorectal carcinoma: implications and proposal for a pathological reporting protocol. Histopathology. 2018;72(3):377-90. Epub 2017/09/01. doi: 10.1111/his.13378. PubMed PMID: 28858385.

7.   Engstrand J, Nilsson H, Stromberg C, Jonas E, Freedman J. Colorectal cancer liver metastases - a population-based study on incidence, management and survival. BMC Cancer. 2018;18(1):78. Epub 2018/01/18. doi: 10.1186/s12885-017-3925-x
10.1186/s12885-017-3925-x [pii]. PubMed PMID: 29334918; PubMed Central PMCID: PMC5769309.
8.   Bartlett EK, Simmons KD, Wachtel H, Roses RE, Fraker DL, Kelz RR, et al. The rise in metastasectomy across cancer types over the past decade. Cancer. 2015;121(5):747-57. Epub 2014/11/08. doi: 10.1002/cncr.29134. PubMed PMID: 25377689.
9.   Tomlinson JS, Jarnagin WR, DeMatteo RP, Fong Y, Kornprat P, Gonen M, et al. Actual 10-year survival after resection of colorectal liver metastases defines cure. J Clin Oncol. 2007;25(29):4575-80. Epub 2007/10/11. doi: 25/29/4575 [pii]
10.1200/JCO.2007.11.0833. PubMed PMID: 17925551.
10.   Nordlinger B, Sorbye H, Glimelius B, Poston GJ, Schlag PM, Rougier P, et al. Perioperative FOLFOX4 chemotherapy and surgery versus surgery alone for resectable liver metastases from colorectal cancer (EORTC 40983): long-term results of a randomised, controlled, phase 3 trial. Lancet Oncol. 2013;14(12):1208-15. Epub 2013/10/15. doi: S1470-2045(13)70447-9 [pii]
10.1016/S1470-2045(13)70447-9. PubMed PMID: 24120480.
11.   Van Cutsem E, Kohne CH, Hitre E, Zaluski J, Chang Chien CR, Makhson A, et al. Cetuximab and chemotherapy as initial treatment for metastatic colorectal cancer. N Engl J Med. 2009;360(14):1408-17. Epub 2009/04/03. doi: 360/14/1408 [pii]
10.1056/NEJMoa0805019. PubMed PMID: 19339720.
12.   Ascierto PA, McArthur GA. Checkpoint inhibitors in melanoma and early phase development in solid tumors: what's the future? J Transl Med. 2017;15(1):173. Epub 2017/08/10. doi: 10.1186/s12967-017-1278-5
10.1186/s12967-017-1278-5 [pii]. PubMed PMID: 28789707; PubMed Central PMCID: PMC5549368.
13.   Granier C, De Guillebon E, Blanc C, Roussel H, Badoual C, Colin E, et al. Mechanisms of action and rationale for the use of checkpoint inhibitors in cancer. ESMO Open. 2017;2(2):e000213. Epub 2017/08/02. doi: 10.1136/esmoopen-2017-000213
esmoopen-2017-000213 [pii]. PubMed PMID: 28761757; PubMed Central PMCID: PMC5518304.
14.   Rotte A, Jin JY, Lemaire V. Mechanistic overview of immune checkpoints to support the rational design of their combinations in cancer immunotherapy. Ann Oncol. 2018;29(1):71-83. Epub 2017/10/27. doi: 4563564 [pii]
10.1093/annonc/mdx686. PubMed PMID: 29069302.
15.   Anderson AC, Joller N, Kuchroo VK. Lag-3, Tim-3, and TIGIT: Co-inhibitory Receptors with Specialized Functions in Immune Regulation. Immunity. 2016;44(5):989-1004. Epub 2016/05/19. doi: S1074-7613(16)30155-8 [pii]
10.1016/j.immuni.2016.05.001. PubMed PMID: 27192565; PubMed Central PMCID: PMC4942846.
16.   Buchbinder EI, Desai A. CTLA-4 and PD-1 Pathways: Similarities, Differences, and Implications of Their Inhibition. Am J Clin Oncol. 2016;39(1):98-106. Epub 2015/11/13. doi: 10.1097/COC.0000000000000239. PubMed PMID: 26558876; PubMed Central PMCID: PMC4892769.
17.   Schachter J, Ribas A, Long GV, Arance A, Grob JJ, Mortier L, et al. Pembrolizumab versus ipilimumab for advanced melanoma: final overall survival results of a multicentre, randomised, open-label phase 3 study (KEYNOTE-006). Lancet. 2017;390(10105):1853-62. Epub 2017/08/22. doi: S0140-6736(17)31601-X [pii]
10.1016/S0140-6736(17)31601-X. PubMed PMID: 28822576.
18.   Kang YK, Boku N, Satoh T, Ryu MH, Chao Y, Kato K, et al. Nivolumab in patients with advanced gastric or gastro-oesophageal junction cancer refractory to, or intolerant of, at least two previous chemotherapy regimens (ONO-4538-12, ATTRACTION-2): a randomised, double-blind, placebo-controlled, phase 3 trial. Lancet. 2017;390(10111):2461-71. Epub 2017/10/11. doi: S0140-6736(17)31827-5 [pii]
10.1016/S0140-6736(17)31827-5. PubMed PMID: 28993052.
19.   Rittmeyer A, Barlesi F, Waterkamp D, Park K, Ciardiello F, von Pawel J, et al. Atezolizumab versus docetaxel in patients with previously treated non-small-cell lung cancer (OAK): a phase 3, open-label, multicentre randomised controlled trial. Lancet. 2017;389(10066):255-65. Epub 2016/12/17. doi: S0140-6736(16)32517-X [pii]
10.1016/S0140-6736(16)32517-X. PubMed PMID: 27979383.
20.   Bellmunt J, de Wit R, Vaughn DJ, Fradet Y, Lee JL, Fong L, et al. Pembrolizumab as Second-Line Therapy for Advanced Urothelial Carcinoma. N Engl J Med. 2017;376(11):1015-26. Epub 2017/02/18. doi: 10.1056/NEJMoa1613683. PubMed PMID: 28212060; PubMed Central PMCID: PMC5635424.

21.   Larkin J, Chiarion-Sileni V, Gonzalez R, Grob JJ, Cowey CL, Lao CD, et al. Combined Nivolumab and Ipilimumab or Monotherapy in Untreated Melanoma. N Engl J Med. 2015;373(1):23-34. Epub 2015/06/02. doi: 10.1056/NEJMoa1504030. PubMed PMID: 26027431; PubMed Central PMCID: PMC5698905.

22.   El-Khoueiry AB, Sangro B, Yau T, Crocenzi TS, Kudo M, Hsu C, et al. Nivolumab in patients with advanced hepatocellular carcinoma (CheckMate 040): an open-label, non-comparative, phase 1/2 dose escalation and expansion trial. Lancet. 2017;389(10088):2492-502. Epub 2017/04/25. doi: S0140-6736(17)31046-2 [pii]
10.1016/S0140-6736(17)31046-2. PubMed PMID: 28434648.

23.   Topalian SL, Hodi FS, Brahmer JR, Gettinger SN, Smith DC, McDermott DF, et al. Safety, activity, and immune correlates of anti-PD-1 antibody in cancer. N Engl J Med. 2012;366(26):2443-54. Epub 2012/06/05. doi: 10.1056/NEJMoa1200690. PubMed PMID: 22658127; PubMed Central PMCID: PMC3544539.

24.   Brahmer JR, Tykodi SS, Chow LQ, Hwu WJ, Topalian SL, Hwu P, et al. Safety and activity of anti-PD-L1 antibody in patients with advanced cancer. N Engl J Med. 2012;366(26):2455-65. Epub 2012/06/05. doi: 10.1056/NEJMoa1200694. PubMed PMID: 22658128; PubMed Central PMCID: PMC3563263.

25.   Brahmer JR, Drake CG, Wollner I, Powderly JD, Picus J, Sharfman WH, et al. Phase I study of single-agent anti-programmed death-1 (MDX-1106) in refractory solid tumors: safety, clinical activity, pharmacodynamics, and immunologic correlates. J Clin Oncol. 2010;28(19):3167-75. Epub 2010/06/03. doi: JCO.2009.26.7609 [pii]
10.1200/JCO.2009.26.7609. PubMed PMID: 20516446; PubMed Central PMCID: PMC4834717.

26.   O'Neil BH, Wallmark JM, Lorente D, Elez E, Raimbourg J, Gomez-Roca C, et al. Safety and antitumor activity of the anti-PD-1 antibody pembrolizumab in patients with advanced colorectal carcinoma. PLoS One. 2017;12(12):e0189848. Epub 2017/12/29. doi: 10.1371/journal.pone.0189848
PONE-D-17-23956 [pii]. PubMed PMID: 29284010; PubMed Central PMCID: PMC5746232.

27.   Le DT, Uram JN, Wang H, Bartlett BR, Kemberling H, Eyring AD, et al. PD-1 Blockade in Tumors with Mismatch-Repair Deficiency. N Engl J Med. 2015;372(26):2509-20. Epub 2015/06/02. doi: 10.1056/NEJMoa1500596. PubMed PMID: 26028255; PubMed Central PMCID: PMC4481136.

28.   Le DT, Durham JN, Smith KN, Wang H, Bartlett BR, Aulakh LK, et al. Mismatch repair deficiency predicts response of solid tumors to PD-1 blockade. Science. 2017;357(6349):409-13. Epub 2017/06/10. doi: science.aan6733 [pii]
10.1126/science.aan6733. PubMed PMID: 28596308.

29.   Grady WM, Carethers JM. Genomic and epigenetic instability in colorectal cancer pathogenesis. Gastroenterology. 2008;135(4):1079-99. Epub 2008/09/09. doi: S0016-5085(08)01451-0 [pii]
10.1053/j.gastro.2008.07.076. PubMed PMID: 18773902; PubMed Central PMCID: PMC2866182.

30.   Mlecnik B, Bindea G, Angell HK, Maby P, Angelova M, Tougeron D, et al. Integrative Analyses of Colorectal Cancer Show Immunoscore Is a Stronger Predictor of Patient Survival Than Microsatellite Instability. Immunity. 2016;44(3):698-711. Epub 2016/03/18. doi: S1074-7613(16)30064-4 [pii]
10.1016/j.immuni.2016.02.025. PubMed PMID: 26982367.

31.   Llosa NJ, Cruise M, Tam A, Wicks EC, Hechenbleikner EM, Taube JM, et al. The vigorous immune microenvironment of microsatellite instable colon cancer is balanced by multiple counter-inhibitory checkpoints. Cancer Discov. 2015;5(1):43-51. Epub 2014/11/02. doi: 2159-8290.CD-14-0863 [pii]
10.1158/2159-8290.CD-14-0863. PubMed PMID: 25358689; PubMed Central PMCID: PMC4293246.

32.   Alvarado-Bachmann R, Smith A, Gundara JS, Kuo SC, Gill AJ, Samra JS, et al. The incidence of mismatch repair gene defects in colorectal liver metastases. Mol Med Rep. 2014;10(2):1003-6. Epub 2014/05/27. doi: 10.3892/mmr.2014.2257. PubMed PMID: 24859327.

33.   Katz SC, Pillarisetty V, Bamboat ZM, Shia J, Hedvat C, Gonen M, et al. T cell infiltrate predicts long-term survival following resection of colorectal cancer liver metastases. Ann Surg Oncol. 2009;16(9):2524-30. Epub 2009/07/02. doi: 10.1245/s10434-009-0585-3. PubMed PMID: 19568816.

34.   Halama N, Michel S, Kloor M, Zoernig I, Benner A, Spille A, et al. Localization and density of immune cells in the invasive margin of human colorectal cancer liver metastases are prognostic for response to chemotherapy. Cancer Res. 2011;71(17):5670-7. Epub 2011/08/19. doi: 0008-5472.CAN-11-0268 [pii]
10.1158/0008-5472.CAN-11-0268. PubMed PMID: 21846824.

35.   Halama N, Spille A, Lerchl T, Brand K, Herpel E, Welte S, et al. Hepatic metastases of colorectal cancer are rather homogeneous but differ from primary lesions in terms of immune cell infiltration. Oncoimmunology. 2013;2(4):e24116. Epub 2013/06/05. doi: 10.4161/onci.24116
2012ONCOIMM0236R [pii]. PubMed PMID: 23734335; PubMed Central PMCID: PMC3654605.

36.   Crispe IN. Immune tolerance in liver disease. Hepatology. 2014;60(6):2109-17. Epub 2014/06/11. doi: 10.1002/hep.27254. PubMed PMID: 24913836; PubMed Central PMCID: PMC4274953.

37.   Kroy DC, Ciuffreda D, Cooperrider JH, Tomlinson M, Hauck GD, Aneja J, et al. Liver environment and HCV replication affect human T-cell phenotype and expression of inhibitory receptors. Gastroenterology. 2014;146(2):550-61. Epub 2013/10/24. doi: S0016-5085(13)01496-0 [pii]
10.1053/j.gastro.2013.10.022. PubMed PMID: 24148617; PubMed Central PMCID: PMC3946973.

38.   Shi XL, Mancham S, Hansen BE, de Knegt RJ, de Jonge J, van der Laan LJ, et al. Counter-regulation of rejection activity against human liver grafts by donor PD-L1 and recipient PD-1 interaction. J Hepatol. 2016;64(6):1274-82. Epub 2016/03/05. doi: S0168-8278(16)00172-0 [pii]
10.1016/j.jhep.2016.02.034. PubMed PMID: 26941095.

39.   Kassel R, Cruise MW, Iezzoni JC, Taylor NA, Pruett TL, Hahn YS. Chronically inflamed livers up-regulate expression of inhibitory B7 family members. Hepatology. 2009;50(5):1625-37. Epub 2009/09/10. doi: 10.1002/hep.23173. PubMed PMID: 19739236; PubMed Central PMCID: PMC2897253.

40.   Pedroza-Gonzalez A, Verhoef C, Ijzermans JN, Peppelenbosch MP, Kwekkeboom J, Verheij J, et al. Activated tumor-infiltrating CD4+ regulatory T cells restrain antitumor immunity in patients with primary or metastatic liver cancer. Hepatology. 2013;57(1):183-94. Epub 2012/08/23. doi: 10.1002/hep.26013. PubMed PMID: 22911397.

41.   Pedroza-Gonzalez A, Zhou G, Singh SP, Boor PP, Pan Q, Grunhagen D, et al. GITR engagement in combination with CTLA-4 blockade completely abrogates immunosuppression mediated by human liver tumor-derived regulatory T cells ex vivo. Oncoimmunology. 2015;4(12):e1051297. Epub 2015/11/21. doi: 10.1080/2162402X.2015.1051297
1051297 [pii]. PubMed PMID: 26587321; PubMed Central PMCID: PMC4635937.

42.   Katz SC, Bamboat ZM, Maker AV, Shia J, Pillarisetty VG, Yopp AC, et al. Regulatory T cell infiltration predicts outcome following resection of colorectal cancer liver metastases. Ann Surg Oncol. 2013;20(3):946-55. Epub 2012/09/27. doi: 10.1245/s10434-012-2668-9. PubMed PMID: 23010736; PubMed Central PMCID: PMC3740360.

43.   Zheng Y, Manzotti CN, Burke F, Dussably L, Qureshi O, Walker LS, et al. Acquisition of suppressive function by activated human CD4+ CD25- T cells is associated with the expression of CTLA-4 not FoxP3. J Immunol. 2008;181(3):1683-91. Epub 2008/07/22. doi: 181/3/1683 [pii]. PubMed PMID: 18641304; PubMed Central PMCID: PMC2758479.

44.   Zhou G, Sprengers D, Boor PPC, Doukas M, Schutz H, Mancham S, et al. Antibodies Against Immune Checkpoint Molecules Restore Functions of Tumor-infiltrating T cells in Hepatocellular Carcinomas. Gastroenterology. 2017. Epub 2017/06/27. doi: S0016-5085(17)35802-X [pii]
10.1053/j.gastro.2017.06.017. PubMed PMID: 28648905.

45.   Lee SY, Haq F, Kim D, Jun C, Jo HJ, Ahn SM, et al. Comparative genomic analysis of primary and synchronous metastatic colorectal cancers. PLoS One. 2014;9(3):e90459. Epub 2014/03/07. doi: 10.1371/journal.pone.0090459
PONE-D-13-40229 [pii]. PubMed PMID: 24599305; PubMed Central PMCID: PMC3944022.

46.   Munoz-Bellvis L, Fontanillo C, Gonzalez-Gonzalez M, Garcia E, Iglesias M, Esteban C, et al. Unique genetic profile of sporadic colorectal cancer liver metastasis versus primary tumors as defined by high-density single-nucleotide polymorphism arrays. Mod Pathol. 2012;25(4):590-601. Epub 2012/01/10. doi: modpathol2011195 [pii]
10.1038/modpathol.2011.195. PubMed PMID: 22222638.

47.   Kawamata H, Yamashita K, Kojo K, Ushiku H, Ooki A, Watanabe M. Discrepancies between the K-ras mutational status of primary colorectal cancers and corresponding liver metastases are found in codon 13. Genomics. 2015;106(2):71-5. Epub 2015/06/01. doi: S0888-7543(15)30003-3 [pii]
10.1016/j.ygeno.2015.05.007. PubMed PMID: 26026309.

48.   Miranda E, Bianchi P, Destro A, Morenghi E, Malesci A, Santoro A, et al. Genetic and epigenetic alterations in primary colorectal cancers and related lymph node and liver metastases. Cancer. 2013;119(2):266-76. Epub 2012/07/13. doi: 10.1002/cncr.27722. PubMed PMID: 22786759.

49.   Wu X, Zhang H, Xing Q, Cui J, Li J, Li Y, et al. PD-1(+) CD8(+) T cells are exhausted in tumours and functional in draining lymph nodes of colorectal cancer patients. Br J Cancer. 2014;111(7):1391-9. Epub 2014/08/06. doi: bjc2014416 [pii]
10.1038/bjc.2014.416. PubMed PMID: 25093496; PubMed Central PMCID: PMC4183848.

50.   Xu B, Yuan L, Gao Q, Yuan P, Zhao P, Yuan H, et al. Circulating and tumor-infiltrating Tim-3 in patients with colorectal cancer. Oncotarget. 2015;6(24):20592-603. Epub 2015/05/27. doi: 4112 [pii]

10.18632/oncotarget.4112. PubMed PMID: 26008981; PubMed Central PMCID: PMC4653028.

51.   Kang CW, Dutta A, Chang LY, Mahalingam J, Lin YC, Chiang JM, et al. Apoptosis of tumor infiltrating effector TIM-3+CD8+ T cells in colon cancer. Sci Rep. 2015;5:15659. Epub 2015/10/27. doi: srep15659 [pii] 10.1038/srep15659. PubMed PMID: 26493689; PubMed Central PMCID: PMC4616166.

52.   Pedroza-Gonzalez A, Zhou G, Vargas-Mendez E, Boor PP, Mancham S, Verhoef C, et al. Tumor-infiltrating plasmacytoid dendritic cells promote immunosuppression by Tr1 cells in human liver tumors. Oncoimmunology. 2015;4(6):e1008355. Epub 2015/07/15. doi: 10.1080/2162402X.2015.1008355 1008355 [pii]. PubMed PMID: 26155417; PubMed Central PMCID: PMC4485712.

53.   Franceschini D, Paroli M, Francavilla V, Videtta M, Morrone S, Labbadia G, et al. PD-L1 negatively regulates CD4+CD25+Foxp3+ Tregs by limiting STAT-5 phosphorylation in patients chronically infected with HCV. J Clin Invest. 2009;119(3):551-64. Epub 2009/02/21. doi: 36604 [pii] 10.1172/JCI36604. PubMed PMID: 19229109; PubMed Central PMCID: PMC2648671.

54.   Baitsch L, Legat A, Barba L, Fuertes Marraco SA, Rivals JP, Baumgaertner P, et al. Extended co-expression of inhibitory receptors by human CD8 T-cells depending on differentiation, antigen-specificity and anatomical localization. PLoS One. 2012;7(2):e30852. Epub 2012/02/22. doi: 10.1371/journal.pone.0030852 PONE-D-11-20364 [pii]. PubMed PMID: 22347406; PubMed Central PMCID: PMC3275569.

55.   Legat A, Speiser DE, Pircher H, Zehn D, Fuertes Marraco SA. Inhibitory Receptor Expression Depends More Dominantly on Differentiation and Activation than "Exhaustion" of Human CD8 T Cells. Front Immunol. 2013;4:455. Epub 2014/01/07. doi: 10.3389/fimmu.2013.00455. PubMed PMID: 24391639; PubMed Central PMCID: PMC3867683.

56.   Gros A, Robbins PF, Yao X, Li YF, Turcotte S, Tran E, et al. PD-1 identifies the patient-specific CD8(+) tumor-reactive repertoire infiltrating human tumors. J Clin Invest. 2014;124(5):2246-59. Epub 2014/03/29. doi: 73639 [pii] 10.1172/JCI73639. PubMed PMID: 24667641; PubMed Central PMCID: PMC4001555.

57.   Williams JB, Horton BL, Zheng Y, Duan Y, Powell JD, Gajewski TF. The EGR2 targets LAG-3 and 4-1BB describe and regulate dysfunctional antigen-specific CD8+ T cells in the tumor microenvironment. J Exp Med. 2017;214(2):381-400. Epub 2017/01/25. doi: jem.20160485 [pii] 10.1084/jem.20160485. PubMed PMID: 28115575; PubMed Central PMCID: PMC5294847.

58.   Paolo Antonio A, Ignacio M, Shailender B, Petri B, Rachel ES, Evan JL, et al. Initial efficacy of anti-lymphocyte activation gene-3 (anti–LAG-3; BMS-986016) in combination with nivolumab (nivo) in pts with melanoma (MEL) previously treated with anti–PD-1/PD-L1 therapy. Journal of Clinical Oncology. 2017;35(15_suppl):9520-. doi: 10.1200/JCO.2017.35.15_suppl.9520.

59.   Dong H, Strome SE, Salomao DR, Tamura H, Hirano F, Flies DB, et al. Tumor-associated B7-H1 promotes T-cell apoptosis: a potential mechanism of immune evasion. Nat Med. 2002;8(8):793-800. Epub 2002/07/02. doi: 10.1038/nm730 nm730 [pii]. PubMed PMID: 12091876.

60.   da Silva IP, Gallois A, Jimenez-Baranda S, Khan S, Anderson AC, Kuchroo VK, et al. Reversal of NK-cell exhaustion in advanced melanoma by Tim-3 blockade. Cancer Immunol Res. 2014;2(5):410-22. Epub 2014/05/06. doi: 2326-6066.CIR-13-0171 [pii] 10.1158/2326-6066.CIR-13-0171. PubMed PMID: 24795354; PubMed Central PMCID: PMC4046278.

61.   Fourcade J, Sun Z, Benallaoua M, Guillaume P, Luescher IF, Sander C, et al. Upregulation of Tim-3 and PD-1 expression is associated with tumor antigen-specific CD8+ T cell dysfunction in melanoma patients. J Exp Med. 2010;207(10):2175-86. Epub 2010/09/08. doi: jem.20100637 [pii] 10.1084/jem.20100637. PubMed PMID: 20819923; PubMed Central PMCID: PMC2947081.

62.   Matsuzaki J, Gnjatic S, Mhawech-Fauceglia P, Beck A, Miller A, Tsuji T, et al. Tumor-infiltrating NY-ESO-1-specific CD8+ T cells are negatively regulated by LAG-3 and PD-1 in human ovarian cancer. Proc Natl Acad Sci U S A. 2010;107(17):7875-80. Epub 2010/04/14. doi: 1003345107 [pii] 10.1073/pnas.1003345107. PubMed PMID: 20385810; PubMed Central PMCID: PMC2867907.

63.   Boor PP, Metselaar HJ, Jonge S, Mancham S, van der Laan LJ, Kwekkeboom J. Human plasmacytoid dendritic cells induce CD8(+) LAG-3(+) Foxp3(+) CTLA-4(+) regulatory T cells that suppress allo-reactive memory T cells. Eur J Immunol. 2011;41(6):1663-74. Epub 2011/04/07. doi: 10.1002/eji.201041229. PubMed PMID: 21469126.

CHAPTER 7

Abrogation of the immunosuppressive tumor microenvironment in cholangiocarcinoma by targeting PD-1 or GITR

Guoying Zhou[1], Dave Sprengers[1], Remco Erkens[1], Shanta Mancham[1], Michail Doukas[2], Lisanne Noordam[1], Patrick P. C. Boor[1], Roelof W. F. van Leeuwen[3], Bas Groot Koerkamp[4], Wojciech G. Polak[4], Jeroen de Jonge[4], Jan N. M. IJzermans[4], Marco J. Bruno[1], Jaap Kwekkeboom[1]

Departments of [1]Gastroenterology and Hepatology, [2]Pathology, [3]Hospital Pharmacy and Medical Oncology, and [4]Surgery, Erasmus MC-University Medical Center, Rotterdam, the Netherlands.

ABSTRACT

Background and aims: Cholangiocarcinoma (CCA) is an aggressive hepatobiliary malignancy originating from the biliary tract epithelium. More effective therapies for CCA are urgently needed. Whether CCA is responsive to immune checkpoint antibody therapy is unknown, and knowledge of immune microenvironment in CCA tumors is very limited. We aimed to: 1) characterize tumor-infiltrating lymphocytes (TIL) in resected CCA tumors by comparison to lymphocytes in paired tumor-free liver tissues (TFL) of the same patients; 2) determine the expression of co-stimulatory and co-inhibitory molecules on TIL and assess the functional effects of targeting these molecules on TIL *ex vivo*.

Results: Compared with TFL, proportions of CD8⁺ T cells, NKT cells and NK cells were decreased, whereas CD4⁺Foxp3⁺ regulatory T cells were increased in tumors. While regulatory T cells accumulated in the tumors, the majority of CD8⁺ and CD4⁺ helper T cells were sequestered at the tumor margin. Tumor-infiltrating CD8⁺ T cells showed reduced expression of the cytotoxic molecules perforin and granzyme compared to those in TFL and blood. Co-stimulatory receptor GITR as well as co-inhibitory receptors PD-1 and CTLA4 were over-expressed on tumor-infiltrating T cells compared with T cells in TFL and blood. PD-L1, CD86 and CD80 were expressed on antigen-presenting cells in tumors, but GITR ligand not. Antagonistic targeting of PD-1 or agonistic targeting of GITR enhanced granzyme B, effector cytokine production and/or T cell proliferation in *ex vivo* stimulations of TIL from CCA patients.

Conclusions: Decreased numbers of cytotoxic immune cells and increased numbers of regulatory T cells together with the expression of co-inhibitory receptors on tumor-infiltrating T cells and their ligands in the tumors suggest that the tumor microenvironment in CCA is immunosuppressive. Targeting PD-1 or GITR enhances the effector functions of tumor-infiltrating T cells from CCA patients *ex vivo*, indicating that these molecules are potential targets for immunotherapy of CCA patients.

Keywords: cholangiocarcinoma; co-stimulatory; co-inhibitory; lymphocyte; T cell

Introduction

Liver cancer is the second most common cause of cancer-related mortality worldwide.(1) Cholangiocarcinoma (CCA) accounts for 10% of primary liver cancers and the incidence is significantly increasing. Mixed hepatocellular cholangiocarcinoma has emerged as a distinct subtype of primary liver cancers.(2) CCA is an aggressive hepatobiliary malignancy originating from the biliary tract epithelium with features of cholangiocyte differentiation.(3, 4) It is classified as the following types according to its anatomic location along the biliary tree: intrahepatic (iCCA), perihilar (pCCA) and distal (dCCA).(2, 4, 5) The median overall survival after diagnosis is 24 months and 5-year survival rate is around 10%.(6) The current treatment options for CCA are very limited. Surgical resection is potentially curative, but it can only be achieved in 10% of the patients and is associated with a high recurrence rate (>50%).(4) Liver transplantation is a curative option for selected patients with pCCA but not with iCCA or dCCA.(2) The therapeutic efficacy of chemotherapy for advanced CCA is disappointing.(4) Therefore, more effective therapies for curing CCA and preventing recurrence are urgently needed.

Cancer immunotherapy aims at stimulating the immune system to combat cancer. T cells are critical immune cells in immune responses against cancer. CD8$^+$ cytotoxic T lymphocytes (CTL) that recognize tumor antigens, can kill tumor cells. CD4$^+$ T helper lymphocytes (Th) that recognize tumor antigens, can provide help to CD8$^+$ T cells, to macrophages to phagocytose tumor cells, and to B cells to produce antibodies against tumor cells. Upon antigen recognition, T cell activation is tightly regulated by two types of co-signalling receptor-ligand interactions which are also called 'immune checkpoint pathways', which either co-stimulate or co-inhibit T cells. T cells infiltrating into tumors generally express high levels of co-inhibitory receptors, while tumor cells and intra-tumoral antigen-presenting cells can express ligands for these co-inhibitory receptors.(7)**[Zhou 2018 Oncoimmunology]** Blocking co-inhibitory PD-1/PD-L1 immune checkpoint interaction by specific antibodies has recently shown unprecedented and durable therapeutic effects, resulting in long-term patient survival in several types of advanced cancer, amongst which hepatocellular carcinoma (HCC).(8) In early phase trials the safety and preliminary efficacy of agonistic targeting of co-stimulatory receptors, amongst which GITR, for cancer immunotherapy are addressed.(9) However, whether CCA is responsive to immune checkpoint antibody therapy is as yet unknown.

Recent studies have revealed variable numbers of PD-1$^+$ lymphocytes and variable PD-L1 expression in CCA tissues,(10, 11) and both are associated with the clinical course of the disease,(12-14), suggesting that the PD-1/PD-L1 pathway may be an interesting

immunotherapeutic target for CCA. In order for immune checkpoint antibody therapy to be effective, T cells must recognize epitopes of tumor antigens on tumor cells and infiltration of T cells into the tumor is needed.(15, 16) While the majority of CCA tumors contain a limited number of mutations and are therefore expected to express few neoantigens,(17) a recent study has demonstrated that TIL in CCA contain tumor antigen-reactive T cells and that adoptive transfer of enriched populations of tumor-reactive T cells induced tumor regression.(18)

In addition, the limited number of studies available have shown CD8^{+} and CD4^{+} T cell as well as dendritic cell infiltrations in CCA tumors.(12, 19, 20) However, PD-L1 expression and defective HLA class I antigen expression by iCCA tumor cells, as well as the presence of regulatory T cells (Treg) and alternatively activated (M2) macrophages in CCA tumors have been identified as immune escape mechanisms.(12, 21-23) Altogether, these data indicate that the CCA tumor microenvironment contains immune infiltrates with T cells that can recognize the tumor cells, but is probably immunosuppressive. All these data are based on immunohistochemistry staining of CCA tissues. However, knowledge of the phenotypic and functional characteristics of intra-tumoral lymphocytes of CCA patients, their expression of immune checkpoint molecules, and whether targeting immune checkpoint molecules can improve the functions of CCA tumor-infiltrating lymphocytes (TIL) is lacking.

Therefore, the objectives of this study were: 1) to investigate the composition of TIL from CCA patients and to characterize TIL at phenotypic and functional levels in comparison with their counterparts in tumor-free liver (TFL) tissues and blood from the same patients; 2) to identify which co-stimulatory and co-inhibitory molecules are over-expressed on TIL compared with their counterparts in TFL and blood, and to determine whether targeting of these immune checkpoint molecules can improve *ex vivo* functions of tumor-infiltrating T cells of CCA patients.

Materials and Methods

Study population

In this study, we focused on intrahepatic and perihilar CCA. Twenty-one patients who underwent surgical resection of iCCA or pCCA, and three patients who underwent surgical resection of mixed hepatocellular cholangiocarcinoma in Erasmus Medical Center from September 2015 to February 2018, were included in the study. Fresh tissue samples from tumor and tumor-free liver as distant as possible from the tumor (minimum 1cm distance) were collected. Peripheral blood of CCA patients was also obtained just before surgery. None of the patients received chemotherapy or immunosuppressive therapy at least three

months prior to surgery. The study was approved by the local ethics committee, and signed informed consent from all patients was obtained before tissue and blood donation. The clinical characteristics of the patients are summarized in Table 1.

Tissue dissociation and cell preparation

Peripheral blood mononuclear cells (PBMC) were isolated by Ficoll density gradient centrifugation. Single cell suspensions from tumors and tumor-free liver tissues were obtained by tissue digestion. Briefly, fresh tissues were first cut into small pieces and then digested with 0.125 mg/mL collagenase IV (Sigma-Aldrich, St. Louis, MO) and 0.2 mg/mL DNAse I (Roche, Indianapolis, IN) in Hanks' Balanced Salt solution with Ca^{2+} and Mg^{2+} (Sigma, Zwijndrecht, The Netherlands) for 30-60 minutes at 37 °C with interrupted gently swirling. Cell suspensions were filtered through 100 µm pore cell strainers (BD Biosciences, Erembodegem, Belgium) and mononuclear immune cells were obtained by Ficoll density gradient centrifugation. Viability was determined by trypan blue exclusion.

Flow cytometry

Fresh PBMC and immune cells isolated from tissues were analyzed for expression of surface and intracellular markers using specific antibodies (Supplementary Table 1). Cell surface staining with fluorochrome-conjugated antibodies was performed in the dark at 4°C for 30 minutes, then cells were washed and resuspended in phosphate buffered saline (PBS) with 0.2 mM EDTA and 0.5% human serum. For Foxp3, CTLA4, Ki-67, perforin and granzyme B staining, cells were fixed and permeabilized using the Foxp3 staining buffer set (eBioscience, Vienna, Austria). Dead cells were excluded by using a LIVE/DEAD fixable dead cell stain kit with aqua fluorescent reactive dye (Invitrogen, Paisley, UK). Cells were measured using a FACSCanto II flow cytometer (BD Biosciences, San Diego, USA) and analyzed using FlowJo software (version 10.0, LLC). Appropriate isotype control antibodies were used for gating purposes (Supplementary Table 1).

Ex vivo polyclonal T cell stimulation assay

All cell cultures were performed in complete medium (RPMI 1640 (Lonza, Breda, The Netherlands) supplemented with 10% human AB serum (Invitrogen), 2mM L-glutamine (Invitrogen), 50 mM Hepes Buffer (Lonza), 1% penicillin-streptomycin (Life Technologies), 5mM Sodium Pyruvate (Gibco) and 1% minimum essential medium non-essential amino acids (Gibco), at 37°C. TIL from CCA were labeled with 0.1 µM carboxyfluorescein diacetate succinimidyl ester (CFSE, Invitrogen). Afterwards 10^5 TIL were cultured in 200 µl complete medium in each well of a 96-well round-bottom culture plate, and stimulated with anti-human

CD3/CD28 dynabeads (Gibco-Life Technologies AS, Norway) at a cell : bead ratio of 10:1. In some conditions 1 µg/ml azide-free and low endotoxin soluble GITR ligand (GITRL, R&D systems) crosslinked with 2.5 µg/ml anti-hemagglutinin antibody (R&D systems), or human monoclonal antibodies against human PD-1 (nivolumab, human IgG4, Bristol-Myers Squibb, New York, USA), CTLA4 (ipilimumab, human IgG1, Bristol-Myers Squibb) which were both obtained from the Erasmus MC hospital pharmacy, or isotype-matched human control antibodies (hIgG4 and hIgG1, Biolegend, London, UK) were added. After four days, culture supernatant was collected and frozen at -20°C until production of IFN-γ, TNF-α and granzyme B was quantified by LegendPlex assay (BioLegend, San Diego, USA). CFSE-labeled cells were harvested and stained with CD8, CD4 and CD3 antibodies. Dead cells were excluded by using the LIVE/DEAD fixable dead cell stain kit with aqua fluorescent reactive dye, and T cell proliferation was determined based on CFSE dilution by flow cytometry.

Immunohistochemistry

Formalin fixed, paraffin embedded tissue samples from 12 patients with iCCA or pCCA and 2 patients with mixed hepatocellular cholangiocarcinoma, who underwent surgical resection in the period from 2011 to 2016, were retrieved from the archive of the Department of Pathology, Erasmus Medical Center. The clinical characteristics of the patients are summarized in Table 2.

Tissue sections of 4 micrometer thickness were cut and mounted on glass slides. After deparaffination the slides were treated for antigen retrieval. For CD8 staining antigen retrieval was performed in 10mM citric acid monohydrate buffers (pH 6.0) and for PD-L1 in 1 mM EDTA buffer with a pH of 8.0. The slides were boiled for 10 minutes in a microwave at 200 W in the buffers and afterwards cooled down for 1 hour. Endogenous peroxidase was blocked by incubation for 15 minutes in 0.075% H_2O_2 in citric acid phosphate buffer (pH 5.8). Immunohistochemistry was done in Shandon cover plates (Thermo Scientific). To prevent non-specific antibody binding, the slides were first incubated at room temperature for 30 minutes in 100 µL PBS supplemented with 10% human serum, 10% goat serum and 10% BSA. Then 100 µL of the primary mouse antibody CD8 (clone C8/144B, Dako) in a 1:100 dilution, NKp46 (polyclonal Goat IgG, R&D systems) in a 1:100 dilution, or PD-L1 (clone 405.1.9A11; a kind gift of Dr. Gordon J. Freeman, Dana-Farber Cancer Institute, Boston, MA, USA) in a 1:50 dilution in PBS 1% human serum was added and incubated overnight at 4°C. The slides were then washed with two times with PBS 0.1% Tween, and incubated with 100 µL of EnVision system HRP labelled polymer goat-anti-mouse antibody (Dako, Glostrup,

Denmark) for 1 hour at room temperature. After washing antibody binding was visualized by incubation with DAB and 0.03% H_2O_2 in TRIS HCL buffer (pH 7.6) until the positive control tissues (tonsil for CD8, lymph node for NKp46 and placenta for PD-L1) showed clear staining. The slides were counterstained for 10 seconds in Hematoxylin, dehydrated and covered with Pertex and a cover slide.

Immunohistochemistry for Foxp3 (clone 236A/E7, eBioscience) and CD4 (clone SP35, Ventana) was done by automated staining using the ultraView DAB (v1.02.0018) BenchMark ULTRA IHC/ISH Staining Module (Ventana Medical Systems).

We counted stained cells in 10 random high power fields (400 times magnification) in each of the three representative areas: inside tumors, in adjacent tumor-free liver, and at the tumor margins. We defined the tumor margin as the border between the tumor and tumor-free liver, and we counted the cells in the visible area (400 times high power field) with the border in the middle. Of each slide 10 high power fields (400 times magnification) were randomly selected per tumor, tumor-free liver and tumor margin area. Of every high power field a picture was taken using a Zeiss Axioskop 20 microscope with a Nikon digital sight DS-U1 camera and the program NIS-Elements D3.0. For CD8 and NKp46 brown-stained cells with a round nucleus and for Foxp3 brown nuclei on every picture were counted by two researchers independently.

Statistical analysis

The distributions of all continuous data set were analyzed for normality by the Shapiro-Wilk normality test. Differences between paired groups of data were analyzed by either paired t test or Wilcoxon matched pairs test according to their distribution. The statistical analysis was performed using GraphPad Prism 5 (GraphPad Software). P values less than 0.05 were considered statistically significant (*$P < 0.05$; ** $P < 0.01$; *** $P < 0.001$*).

Results

Poor infiltration of cytotoxic immune cells but accumulation of regulatory T cells in cholangiocarcinoma

To compare the composition of immune cells in the tumor, TFL and blood of CCA patients, we analyzed the proportions of $CD19^+$ B cells, $BDCA1^+CD19^-$ myeloid dendritic cells (mDC) and $CD14^+$ monocytes/macrophages, $CD3^+CD56^-$ T cells, $CD3^+CD56^+$ natural killer T (NKT) cells, and natural killer (NK) cells within $CD45^+$ leukocytes freshly isolated from these three compartments by flow cytometry (Fig. 1). Data derived from mixed hepatocellular

cholangiocarcinoma did not differ from those of CCA patients. Therefore, we included these data in the analyses. Proportions of mDC were increased in the solid tissues, while proportions of CD14$^+$ cells were decreased in solid tissues, compared with the blood, but no differences were found between the tumor and TFL (Fig. 1B). However, proportions of NKT cells and NK cells were decreased in the tumor compared with TFL, whereas proportions of CD3$^+$CD56$^-$ T cells in tumors were increased (Fig. 1D). In TFL about half of the T cells were CD8$^+$ T cells. However, T cells in the tumor contained significantly less CD8$^+$ T cells, but more CD4$^+$Foxp3$^+$ Treg and CD4$^+$Foxp3$^-$ Th than T cells in TFL. These data demonstrate that the CCA tumors show characteristics of an immunosuppressive microenvironment with reduced proportions of cytotoxic immune effector cells but increased proportions of regulatory T cells compared to surrounding non-tumorous liver tissues.

Cytotoxic and helper T cells are sequestered around the tumors but regulatory T cells infiltrate into the tumors

To assess the localization of immune cell populations in CCA tissues, we did immunohistochemistry stains for Foxp3 (a marker of Treg), CD8, CD4 and NKp46 (a marker of NK cells) and we counted the numbers of stained cells (Fig. 2A). Foxp3$^+$ cells were observed both within the tumor and at the tumor margin (Fig. 2A and E), but the vast majority of CD8$^+$ T cells was sequestered at the tumor margin (Fig. 2B and E). Consequently, in the tumor the ratio of Foxp3$^+$ cell density to CD8$^+$ cell density was highest (Fig. 2E) compared to that at the tumor margin and in TFL. Since the CD4 antibody also stained sinusoidal cells it was difficult to count CD4$^+$ lymphocytes, but from the distributions observed in the tissue sections it became clear that CD4$^+$ lymphocytes were also sequestered at the tumor margin (Fig. 2C). However, there is no significant difference in numbers of NKp46$^+$ cells among tumor inside, tumor margin and tumor-free liver areas (Fig. 2D). These data demonstrate that the majority of CD8$^+$ CTL and CD4$^+$ Th are sequestered at the tumor margin, but Treg can infiltrate into the tumors of CCA patients.

Activation status and cytotoxic molecule expression of lymphocytes in cholangiocarcinoma patients

To characterize TIL and compare them with lymphocytes from paired TFL and blood of CCA patients, we measured the expression of several activation and functional markers on the anti-tumor Th, CD8$^+$ CTL, NK cells and NKT cells (Fig. 3). The percentages of CD4$^+$ Th and CD8$^+$ CTL expressing the proliferation marker Ki-67, as well as those expressing the IL-2 receptor alpha chain (CD25), were slightly higher in the tumor than in TFL, but this difference was not observed for the activation marker HLA-DR. The percentages of CD69$^+$ T cells were

all higher in the solid tissue compartments than in the blood, as CD69 is also a tissue-resident marker.(24-26) Although CD4$^+$Foxp3$^+$ Treg accumulated in tumors and showed some signs of a higher activation status (CD25, CD69) compared to Treg in TFL, they did not show higher expression of the proliferation marker Ki-67, suggesting that their accumulation in the tumor bed is not due to local proliferation. Interestingly, in the tumor lower percentages of CD8$^+$ CTL expressed the cytotoxic effector molecules granzyme B and perforin than in TFL. In addition, in the tumor lower proportions of NK cells and NKT cells expressed perforin than in TFL and blood. This suggests that the tumor-infiltrating cytotoxic lymphocytes may be dysfunctional in cholangiocarcinoma.

Expression of co-stimulatory and co-inhibitory receptors on T cells in cholangiocarcinoma patients

To study the relevance and significance of immune checkpoint interactions in CCA, we first measured the expression of co-stimulatory receptors GITR and ICOS, as well as co-inhibitory receptors PD-1, CTLA4, LAG3, BTLA, CD160 and CD224 on Treg, Th and CD8$^+$ CTL (Fig. 4A). In all three compartments, Treg displayed significantly higher expression of GITR, ICOS, CTLA4 and PD-1 than Th and CD8$^+$ T cells. Interestingly, Treg from the tumors showed higher frequencies of positive cells and enhanced expression levels of co-stimulatory receptors GITR and ICOS as well as co-inhibitory receptors PD-1 and CTLA4 than those from paired TFL and blood (Fig. 4B, C). Th and CD8$^+$ CTL also showed higher frequencies of cells expressing GITR, PD-1 and CTLA4 than those from paired TFL and blood, but only PD-1 displayed enhanced expression levels on individual Th and CD8+ CTL. Furthermore, no or minimal upregulation of co-inhibitory receptors BTLA, LAG3, CD160 or CD244 was observed in the tumor. These data suggest that GITR, PD-1 and CTLA4 may be involved in regulating T cell functions in the CCA tumor microenvironm*ent.*

Expression of co-stimulatory and co-inhibitory ligands in cholangiocarcinoma

Because GITR, PD-1 and CTLA4 were upregulated in cholangiocarcinoma, we measured the expression of their respective ligands GITR ligand, PD-L1, CD86 and CD80 on three subsets of antigen-presenting cells: B cells, mDC and CD14$^+$ monocytes/macrophages (Fig. 5A). CD86 and CD80 were expressed on mDC and CD14$^+$ cells in all compartments, while CD80 was also expressed on B cells. However, PD-L1 was expressed at relatively low level, also on tumor-infiltrating antigen-presenting cells (Fig. 5B, C). GITR ligand was almost absent. For co-inhibitory pathways to suppress T cells, both the receptor and the ligand are needed. CD86 and CD80 are known to be mainly expressed on antigen-presenting cells, while PD-L1 can also be expressed on tumor cells. Therefore we performed immunohistochemical

staining for PD-L1 on CCA tissues. Immunohistochemistry showed that in tumors PD-L1 was not only expressed on stromal cells, such as leukocytes, but also on tumor cells, while in TFL weak expression was observed on hepatocytes. We observed PD-L1 expression on tumor cells in CCA tumors in 10 out of 14 patients and on hepatocytes in TFL in 12 out of 14 patients, in either a diffuse or a patchy pattern (Fig. 5D).

Effector functions of tumor-infiltrating T cells are enhanced by targeting GITR or PD-1

Given that tumor-infiltrating CD8$^+$ CTL might be dysfunctional and GITR, PD-1 and CTLA4 may play an important role in regulating T cell functions, we evaluated the effects of stimulating GITR by soluble GITRL, blocking PD-1 by nivolumab and blocking CTLA4 by ipilimumab on *ex vivo* functional responses of tumor-infiltrating T cells (Fig. 6). CFSE-labeled total tumor-infiltrating immune cells, including T cells expressing immune checkpoint receptors and antigen-presenting cells expressing their ligands, were stimulated with anti-CD3/CD28 beads. After four days, proliferation of CD4$^+$ and CD8$^+$ TIL as well as secretion of granzyme B were significantly increased in the presence of GITRL. Nivolumab significantly increased CD8$^+$ TIL proliferation as well as production of granzyme B, IFN-γ and TNF-α. Ipilimumab significantly increased production of granzyme B and IFN-γ, but with lower effects than nivolumab and GITRL. Together, these data indicate that the effector functions of tumor-infiltrating T cells of CCA patients can be best enhanced by targeting GITR or PD-1.

Discussion

Previously, it has been shown that there are CD8$^+$, CD4$^+$ and Foxp3$^+$ cell infiltrations in iCCA,(12, 13, 19, 22, 27). Our immunohistochemistry findings confirm previous reports(12, 21) showing that CD8$^+$ and CD4$^+$ cells are predominantly sequestered at the tumor margin, while Foxp3$^+$ cells are present both inside the tumor and at the tumor margin (Fig. 2). Since Foxp3$^+$ cells most probably represent CD4$^+$Foxp3$^+$ Treg (as shown by flow cytometry that all the Foxp3$^+$ cells are CD4$^+$), we believe that most CD4$^+$ cells accumulating at the tumor margin are T helper cells that are unable to enter the tumor. Because our CD56 antibodies failed to stain specific NK cells by immunohistochemistry, we used an NKp46 antibody, and the infiltration of NKp46$^+$ cells seem not to differ among tumor inside, tumor margin and tumor-free liver. Using mononuclear immune cells isolated from blood and tissues of CCA patients and flow cytometry, we found that in accordance with the immunohistochemistry data, the proportion of CD8$^+$ CTL within the isolated TIL was decreased while the proportion of CD4$^+$Foxp3$^+$ Treg in TIL was increased compared with TFL (Fig. 1D). In addition, we observed that percentages of NKT cells and NK cells within CD45$^+$ cells were lower in tumors than in TFL using CD56 marker. The observed reduction of the three main types of cytotoxic

immune cells and the increase of suppressive Treg in the tumors, are similar to our previous data in HCC patients(28, 29) and demonstrate that the CCA tumor microenvironment has immunosuppressive characteristics.

We are the first to study the *ex vivo* status of TIL in CCA patients. Th and CD8^{+} CTL in CCA tumors showed a slightly more activated and proliferative status than those in TFL according to their CD25, CD69 and Ki-67 expression (Fig. 3A, C, D). Nevertheless, less CD8^{+} CTL expressed cytolytic proteins perforin and granzyme B, similar to what we observed in HCC tumors,(28). In addition, less NK cells and NKT cells expressed perforin in the tumor compared with TFL (Fig. 3E, F). Treg in tumors also displayed a slightly more activated status than those in TFL. Together, TIL have an at least partly distinct profile in terms of activation and function from TFL-resident lymphocytes and circulating lymphocytes and may be dysfunctional in cytotoxicity.

There is immunohistochemical evidence that co-inhibitory molecules PD-1, CTLA4 and PD-L1 are expressed in CCA tumor tissues,(13, 14, 30) and that PD-L1 can be expressed by both tumor cells and tumor-infiltrating immune cells.(10, 31) However, which types of immune cells in CCA tumors express these co-inhibitory molecules was unknown, and data on expression of other immune checkpoint molecules in CCA were lacking. Therefore, using mononuclear immune cells isolated from tissues and blood of CCA patients we determined the expression of multiple co-stimulatory and co-inhibitory molecules on different immune cell subsets by flow cytometry. Similar to and in addition to our previous data in HCC patients,(7, 28, 29) we observed higher expression of GITR, PD-1 and CTLA4 on Treg, Th and CD8^{+} CTL in CCA tumors than in TFL and blood (Fig. 4B, C), but in contrast to our observation in HCC(7) LAG3 was not upregulated on tumor-infiltrating T cells in CCA tumors. Tumor-infiltrating Treg displayed the highest expression of the immune checkpoint receptors, and both tumor-infiltrating Th and CD8^{+} cells upregulated PD1 to a larger extent than CTLA4 and GITR. The ligands of co-inhibitory receptors were variably expressed on B cells, mDC and monocytes/macrophages (Fig. 5B, C), and we confirmed that PD-L1 can be expressed on CCA tumor cells (Fig. 5D), like in HCC tumors.(7, 32) The over-expression of PD-1 and CTLA4 on tumor-infiltrating T cells and their respective ligands in the tumors suggested that these co-inhibitory pathways can potentially be targeted to invigorate intra-tumoral immunity in CCA patients. In addition, the over-expression of the co-stimulatory receptor GITR on tumor-infiltrating T cells whereas GITR ligand is virtually not expressed in the tumors, suggested that agonistic targeting of GITR may offer another possibility to revitalize intra-tumoral immunity in CCA.

Functional effects of targeting co-stimulatory or co-inhibitory receptors on tumor-infiltrating T cells of CCA patients have not been studied before. Our previous data have demonstrated that soluble GITRL as well as CTLA4 blockade partially abrogate suppression mediated by tumor-infiltrating Treg of HCC,(28, 29) while PD-L1 blockade enhances functional responses of CD8$^+$ and CD4$^+$ TIL from HCC patients in *ex vivo* assays.(7) Here we used soluble ligand GITRL in *ex vivo* stimulations of CCA-derived TIL to stimulate T cells via their co-stimulatory receptor GITR, and the therapeutic human antibodies nivolumab and ipilimumab to block co-inhibitory receptors PD-1 and CTLA4 on T cells, respectively. Our data reveal that the secretion of cytotoxic granzyme and effector cytokines and/or T cell proliferation of TIL were increased by the three reagents, but most robustly by nivolumab and GITRL (Fig. 6). Therefore, GITR and PD-1 seem to be the most promising targets for immunotherapy of CCA patients among all the immune checkpoint molecules tested in this study. There are some limitations in the study. 1) Due to limited numbers of isolated TIL, not all types of experiments could be performed for every CCA patient. 2) The patient cohort was recent and small, so we were unable to associate immunological data with patient survival.

In summary, decreased numbers of cytotoxic immune cells and increased numbers of regulatory T cells together with the expression of two co-inhibitory receptors PD-1 and CTLA4 on tumor-infiltrating T cells and their ligands in the tumors indicate that the tumor microenvironment in CCA is immunosuppressive. Blockade of PD-1 or stimulation of GITR enhances the *ex vivo* effector functions of tumor-infiltrating T cells from CCA patients, suggesting that these two molecules may be potential targets for immunotherapy of CCA patients. Targeting PD-1 and GITR might be clinically applicable to eradicate CCA tumors and prevent cancer recurrence.

Table 1. Characteristics of patients for flow cytometry data

	iCCA or pCCA (n=21)	HCC-CCA (n=3)
Sex (female/male)	10 / 11	2 / 1
Age (years)**	62.2 ± 4.0	67.7 ± 5.5

Abbreviations: iCCA, intrahepatic cholangiocarcinoma; pCCA, perihilar cholangiocarcinoma; HCC-CCA, mixed hepatocellular cholangiocarcinoma.

**Mean ± standard error of the mean.

Table 2. Characteristics of patients for immunohistochemistry data

	iCCA or pCCA (n=12)	HCC-CCA (n=2)
Sex (female/male)	8 / 4	1 / 1
Age (years)**	59.8 ± 2.4	69.0 ± 2.0

Abbreviations: iCCA, intrahepatic cholangiocarcinoma; pCCA, perihilar cholangiocarcinoma; HCC-CCA, mixed hepatocellular cholangiocarcinoma.

**Mean ± standard error of the mean.

Figure legends

Figure 1. Proportions of lymphocyte subpopulations and antigen-presenting cell subpopulations in immune cells from tumors, TFL and blood of CCA patients. (A) Representative FACS contour plots show the gating strategies for $CD19^+$ B cells, $CD14^+$ monocytes/macrophages and $BDCA1^+CD19^-$ mDC within live $CD45^+$ cells. (B) The frequencies of $CD19^+$ B cells, $BDCA1^+CD19^-$ mDC and $CD14^+$ monocytes/macrophages

within CD45$^+$ cells in tumors, TFL and blood. (C) Representative FACS zebra plots show the gating strategies for CD3$^-$CD56$^+$ NK cells, CD3$^+$CD56$^+$ NKT cells, CD3$^+$CD8$^+$ CTL, CD4$^+$Foxp3$^-$ Th and CD3$^+$CD4$^+$Foxp3$^+$ Treg within live CD45$^+$ cells. (D) The frequencies of CD3$^+$CD56$^-$ T cells, NKT cells, NK cells, CD8$^+$ CTL, CD4$^+$Foxp3$^-$ Th and CD4$^+$Foxp3$^+$ Treg within CD45$^+$ cells in tumors, TFL and blood. Values of individual patients are presented, lines depict medians. Red symbols are values of patients with mixed HCC-CCA. Differences were analyzed by paired t test or Wilcoxon matched pairs test; * p < 0.05, ** p < 0.01, *** p < 0.001.

Figure 2. Lymphocyte infiltration in the tumor, tumor margin and TFL of CCA patients. Formalin fixed, paraffin embedded tissue slides were stained with antibodies against Foxp3, CD8, CD4 and NKp46 by immunohistochemistry. Representative high power fields (400 times magnification) show the staining of (A) Foxp3, (B) CD8, (C) CD4, (D) NKp46 in the CCA tumor, tumor margin and TFL areas. Brown color (in some pictures indicated by red arrows) indicates positive staining. (E) Numbers of positive cells per 10 high power fields (400 times magnification) in the tumor, tumor margin or TFL areas, which are the average numbers counted by two independent researchers. Values of individual patients are presented, lines depict medians. Red symbols are values of patients with mixed HCC-CCA. Differences were analyzed by paired t test or Wilcoxon matched pairs test; * p < 0.05, ** p < 0.01, *** p < 0.001.

Figure 3. Expression of activation markers and cytotoxic molecules on lymphocytes. PBMC and mononuclear immune cells isolated from CCA tumors and TFL were stained *ex vivo* with antibodies against surface molecules HLA-DR, CD69 and CD25, and intracellular molecules of Ki-67, perforin and granzyme B. The frequencies of (A) Ki-67$^+$, (B) HLA-DR$^+$, (C) CD69$^+$, (D) CD25$^+$ cells within CD4$^+$Foxp3$^+$ Treg, CD4$^+$Foxp3$^-$ Th and CD8$^+$ CTL, as well as (E) perforin$^+$ and (F) granzyme B$^+$ cells within CD8$^+$ CTL, NK cells and NKT cells in the tumor, TFL and blood of CCA patients. Values of individual patients are shown, and lines depict medians. Red symbols are values of patients with mixed HCC-CCA. Differences were analyzed by paired t test or Wilcoxon matched pairs test; * p < 0.05, ** p < 0.01, *** p < 0.001.

Figure 4. Expression of co-stimulatory and co-inhibitory receptors on T cells in tumors, TFL and blood. Expression of immune checkpoint receptors GITR, ICOS, PD-1, CTLA4, LAG3, BTLA, CD160 and CD244 was measured by flow cytometry. (A) Representative histograms of co-stimulatory and co-inhibitory receptor expression on CD3$^+$CD4$^+$Foxp3$^+$ Treg, CD3$^+$CD4$^+$Foxp3$^-$ Th and CD3$^+$CD8$^+$ CTL as well as fluorescence

minus one control isolated from the tumor. (B) The frequencies of receptor positive cells within Treg, Th and CTL in the tumor, TFL and blood. (C) Median fluorescence intensity (MFI) of receptors on Treg, Th and CTL in the tumor, TFL and blood of CCA patients. Values of individual patients are shown, and lines depict medians. Red symbols are values of patients with mixed HCC-CCA. Differences were analyzed by paired t test or Wilcoxon matched pairs test; * p < 0.05, ** p < 0.01, *** p < 0.001.

Figure 5. Expression of co-stimulatory and co-inhibitory ligands on antigen-presenting cells in tumors, TFL and blood. Expression of immune checkpoint ligands GITRL, PD-L1, CD86 and CD80 was measured by flow cytometry. (A) Representative histograms of ligand staining and fluorescence minus one control on CD19$^+$ B cells, BDCA1$^+$CD19$^-$ mDC and CD14$^+$ monocytes/macrophages isolated from the tumor. (B) The frequencies of ligand positive cells within B cells, mDC and monocytes/macrophages in the tumor, TFL and blood. (C) Median fluorescence intensity (MFI) of ligands on B cells, mDC and monocytes/macrophages in the tumor, TFL and blood of CCA patients. Values of individual patients are shown, and lines depict medians. Red symbols are values of patients with mixed HCC-CCA. Differences were analyzed by paired t test or Wilcoxon matched pairs test; * p < 0.05, ** p < 0.01, *** p < 0.001. (D) Representative pictures show the positive and negative controls of PD-L1 in placenta as well as PD-L1 staining in the CCA tumor, tumor margin and TFL areas (100 times magnification).

Figure 6. Tumor-infiltrating T cell functions are enhanced by targeting GITR or PD-1. CFSE-labeled TIL from CCA patients were stimulated with CD3/CD28 beads, in the presence or absence of nivolumab (anti-PD-1; human IgG4), ipilimumab (anti-CTLA4; human IgG1), soluble GITRL, or human isotype control antibodies. (A) (B) Representative FACS dot plots of CD3$^+$CD4$^+$ and CD3$^+$CD8$^+$ TIL proliferation in response to CD3/CD28 stimulations in the presence or absence of the antibodies or GITRL. The relative percentages of (C) proliferating cells (CFSE-low) within CD4$^+$ TIL and CD8$^+$ TIL are shown. The results are reported as relative percentage calculated by dividing the percentage of proliferating T cells in the presence of the antibody, by the percentage in the baseline condition with only anti-CD3/CD28 beads. Values are depicted as means with standard error of the mean (n=11 independent experiments with TIL from 10 different CCA patients, with detectable suboptimal proliferations). (D) Accumulation of IFN-γ, TNF-α and granzyme B in culture supernatant was quantified by LegendPlex assay. Values are depicted as medians with interquartile range (n=9-12, with detectable cytokine concentrations). Differences were analyzed by paired t test or Wilcoxon matched pairs test; * p < 0.05, ** p < 0.01.
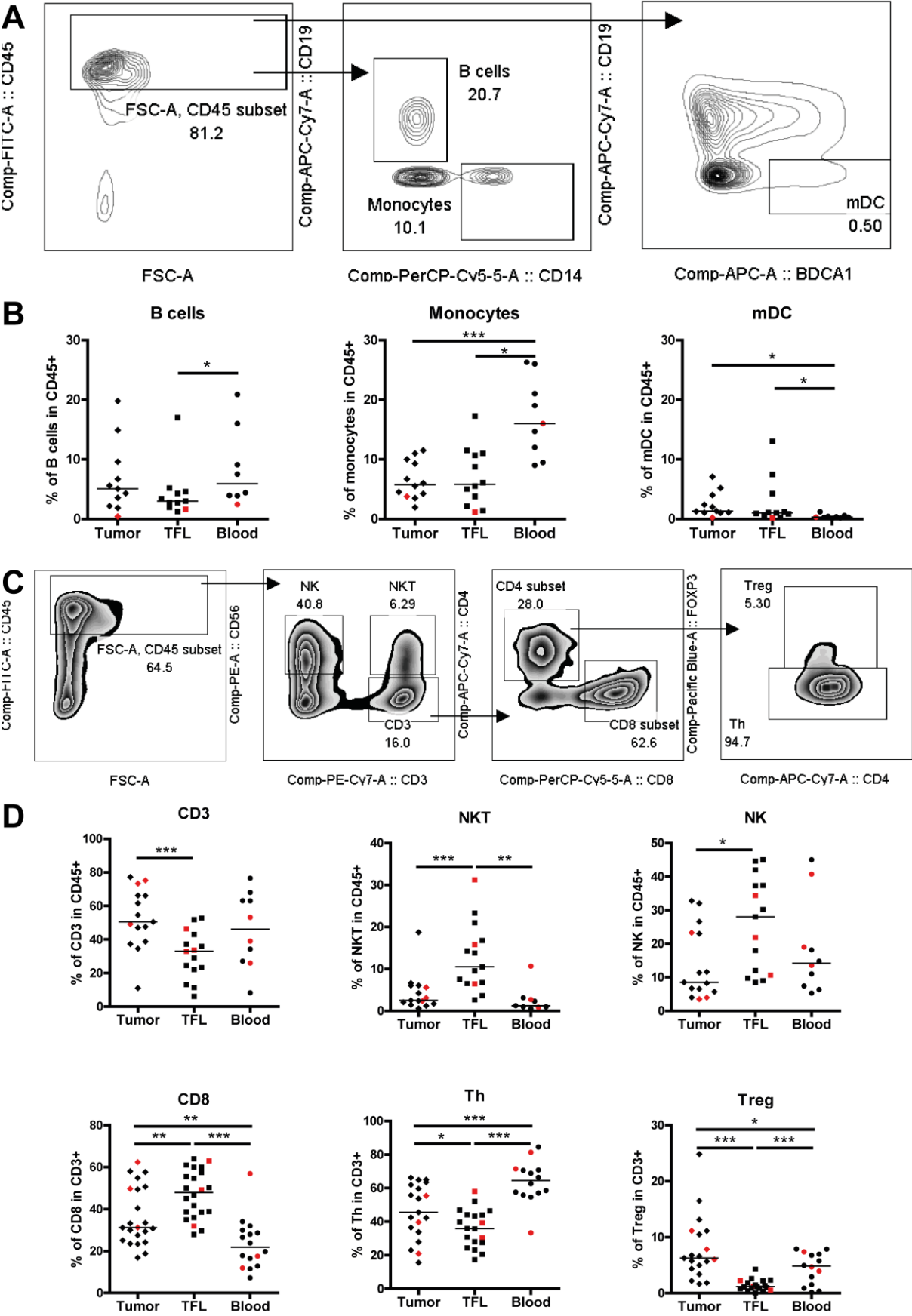
Figure 1.

Figure 2.
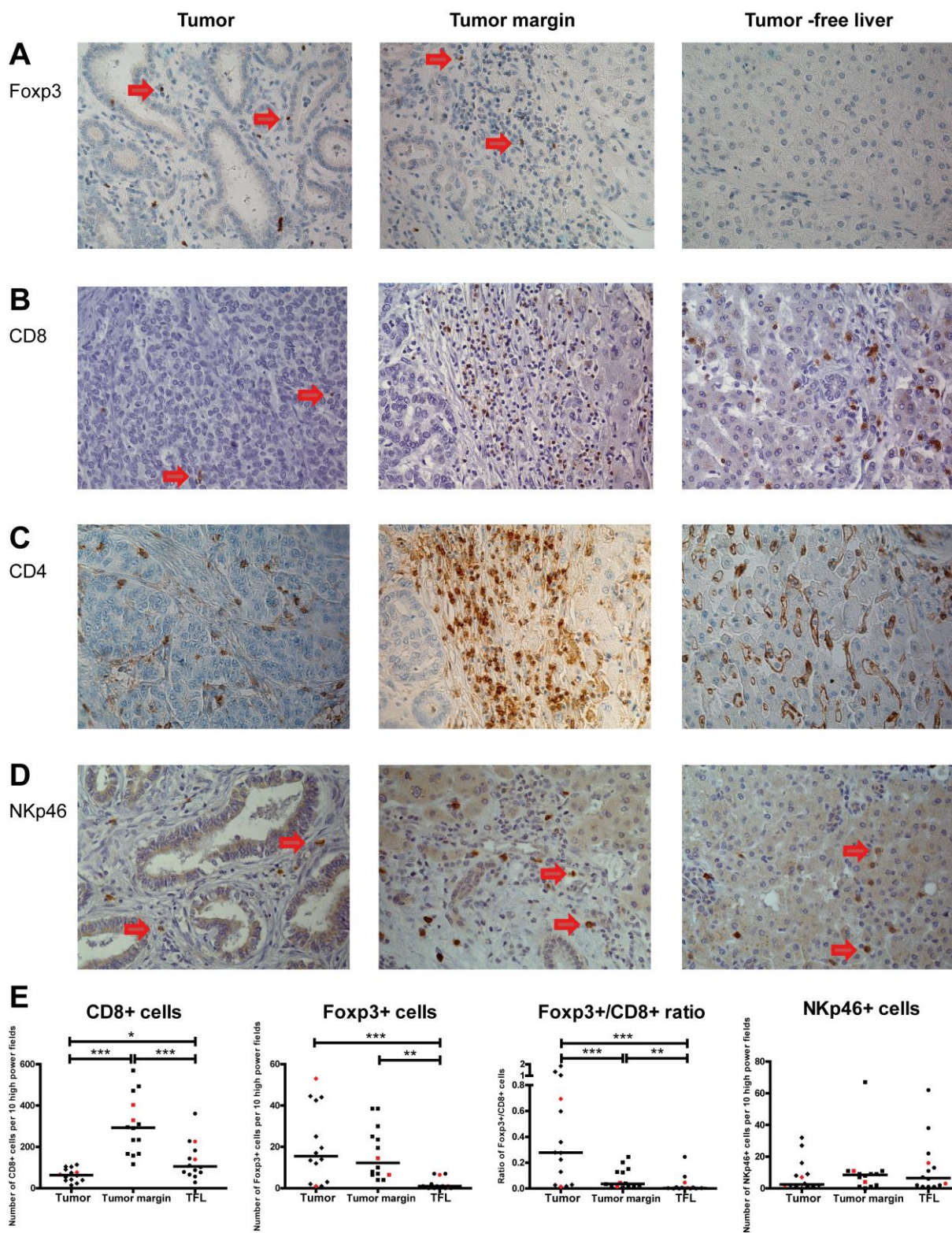
Figure 3.
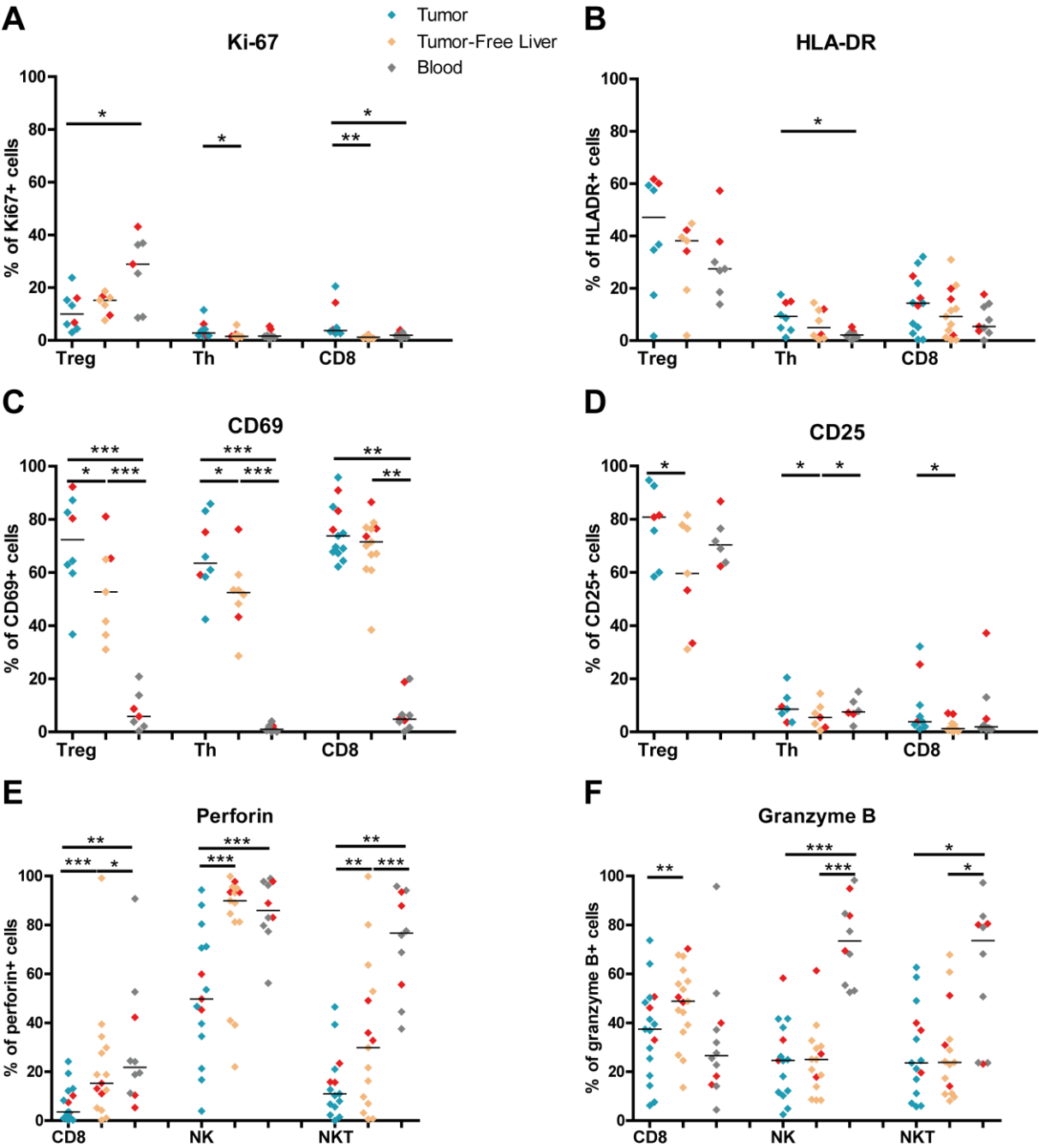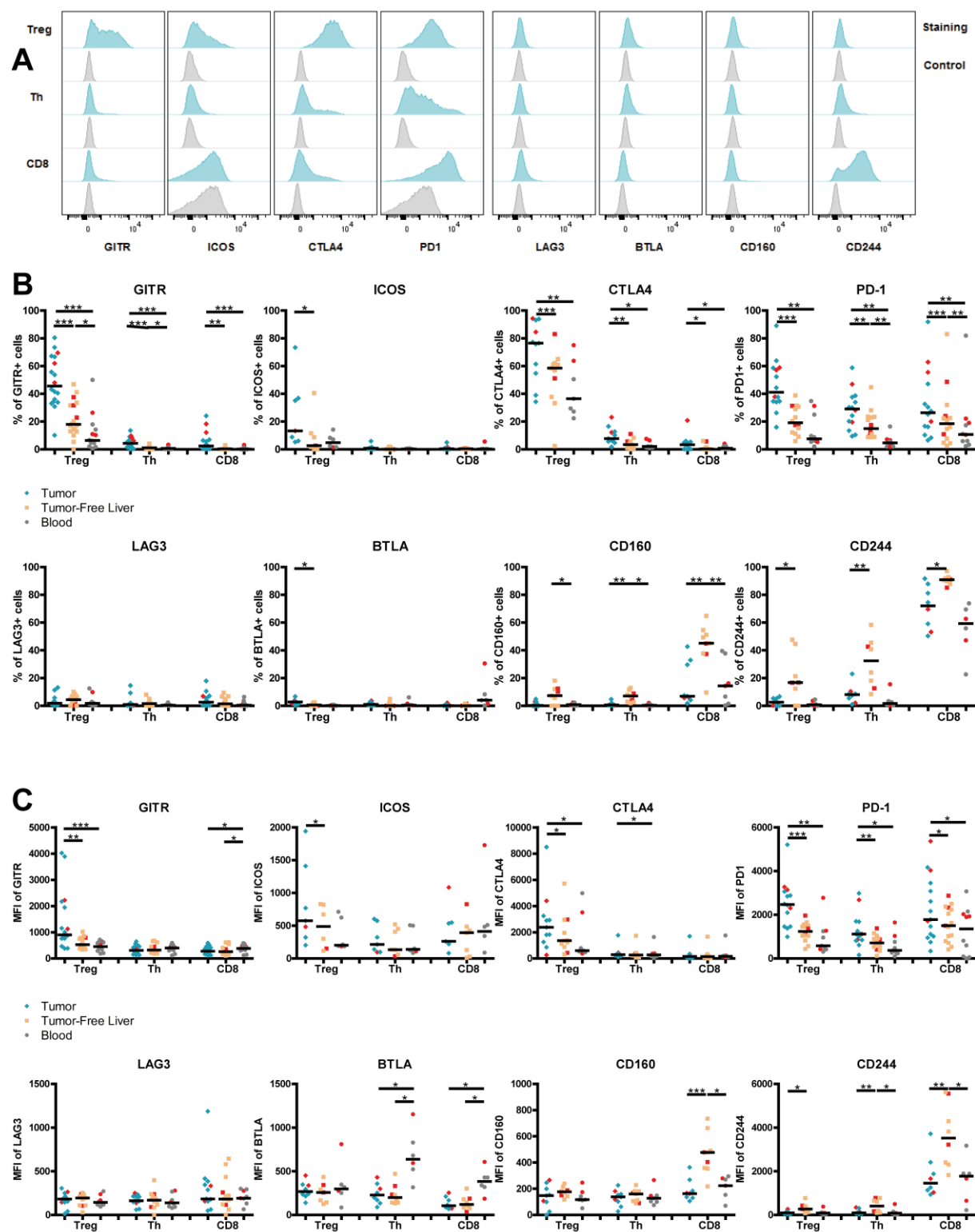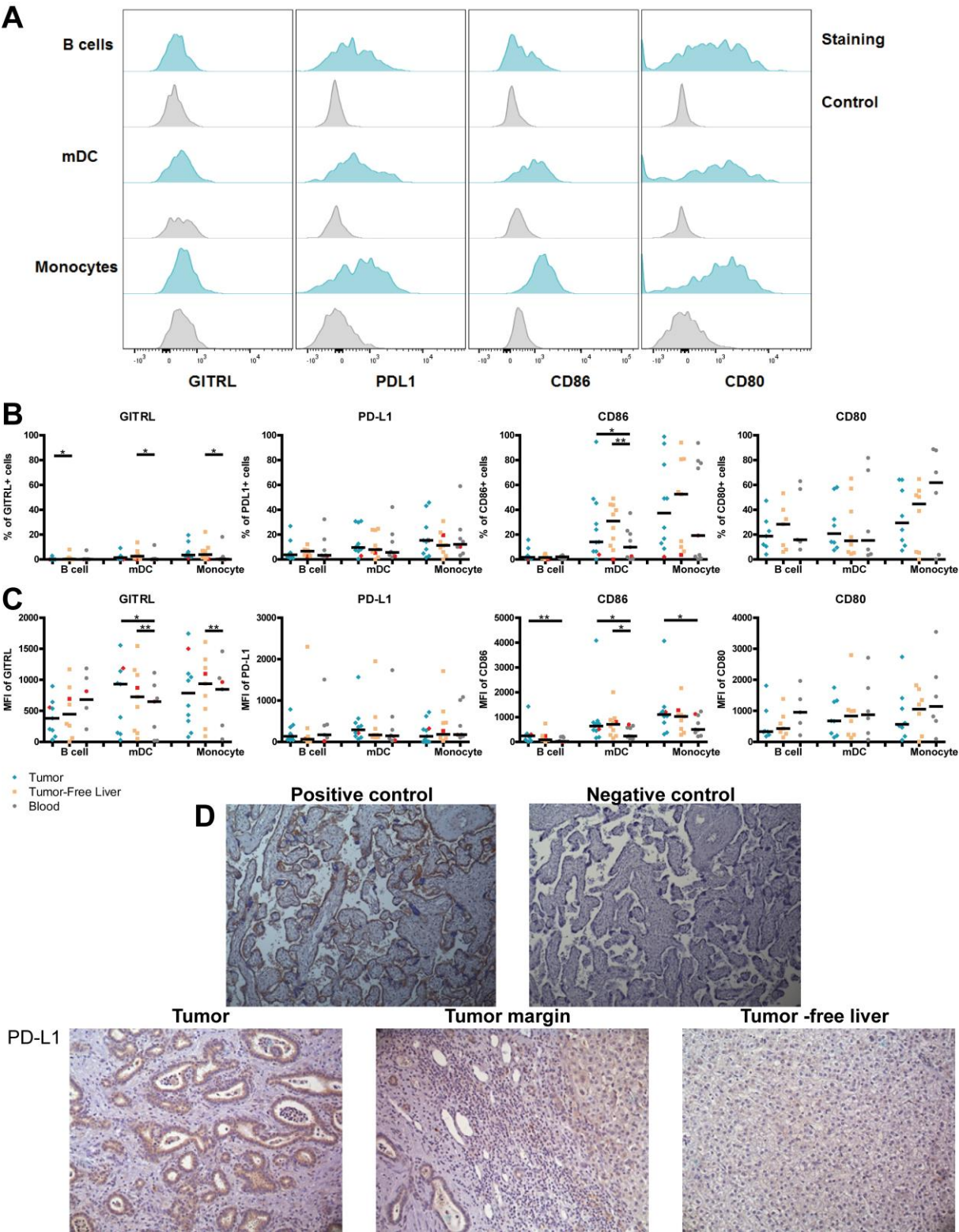
Figure 4.

Figure 5.

Figure 6.
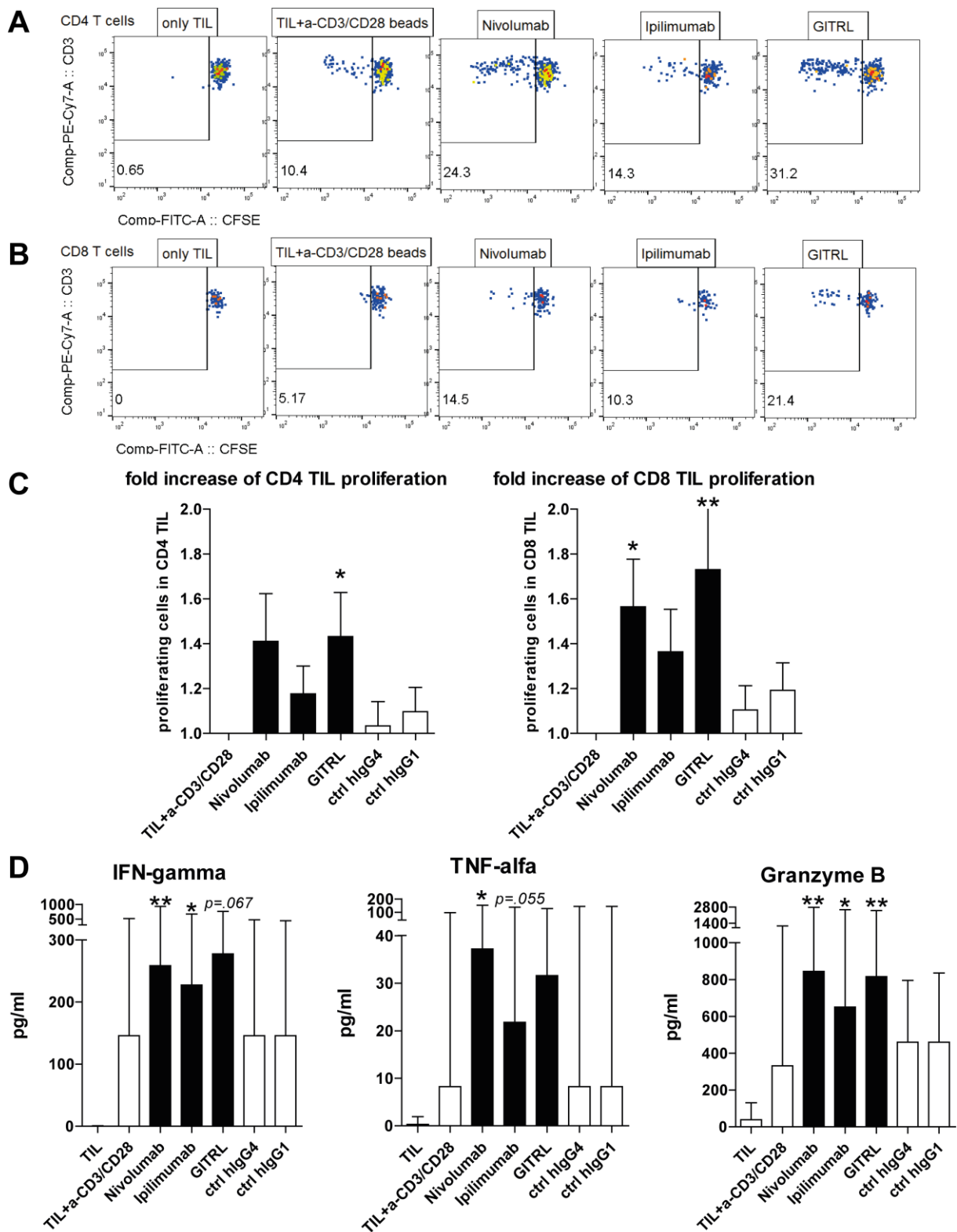
Supplementary Table 1. Antibodies used for flow cytometry

Antibody	Clone	Supplier	Antibody	Clone	Supplier
CD69 APC	L78	BD Biosciences	CD8-PE	RPA-T8	eBioscience
Ki67-FITC	B56	BD Biosciences	HLA-DR-APC	LN3	eBioscience
CD137 (4-1BB)-APC	4B4-1	BD Biosciences	CD56 PE	TULY56	eBioscience
CD14-PerCP	MOP9	BD Biosciences	HLA-DR-PerCP-Cy5.5	LN3	eBioscience
CD3 PerCP-Cy5.5	UCHT1	BD Biosciences	CD3 PE-Cy7	UCHT1	eBioscience
CD19 APC-H7	SJ25C1	BD Biosciences	CD8-APC	okt-08	eBioscience
mIgG2b-FITC	27-35	BD Biosciences	CD244 (2B4)-APC	eBioDM244	eBioscience
mIgG1-PB	MOPC-21	BD Biosciences	HLA-DR-APC-eFluor780	LN3	eBioscience
mIgG2b-PE	27-35	BD Biosciences	CD279 (PD1)-PE-Cy7	J105	eBioscience
mIgG1-PerCP	X40	BD Biosciences	CD8-efluor450	RPA-T8	eBioscience
mIgG1-FITC	MOPC-21	BD Biosciences	CD274(B7-H1)-PE-Cy7	MIH1	eBioscience
mIgG1-pacific blue	MOPC-21	BD Biosciences	CD278 (ICOS)-PE-Cy7	ISA-3	eBioscience
mIgG2a-PerCP	X39	BD Biosciences	CD4-APC-eFluor780	OKT4	eBioscience
GranzymeB-V450	GB11	BD Biosciences	CD3-APC-eFluor780	SK7	eBioscience
mIgG2b-FITC	27-35	BD Biosciences	FoxP3-eFluor450	236A/E7	eBioscience
mIgG1-FITC	MOPC-21	BD Biosciences	CD45 efluor 450	HI30	eBioscience
CD25 APC	2A3	BD Biosciences	CD8a-PerCp-Cy5.5	RPA-T8	eBioscience
CD272 (BTLA)-APC	MIH26	Biolegend	CD223(LAG3)-PE	3DS223H	eBioscience
CD3 PE	UCHT1	Biolegend	CD223(LAG3)-PerCP-eF710	3DS223H	eBioscience
CD86-PB	IT2.2	Biolegend	CD8-FITC	SK1	eBioscience
mIgG2a-FITC	MOPC-173	Biolegend	rat IgG2a-APC	eBR2a	eBioscience
mIgG1-APC	MOPC-21	Biolegend	mIgG1-FITC	P3	eBioscience
CD80-PE-Cy7	2D10	Biolegend	mIgG2a-APC	eBM2a	eBioscience
rat IgG2a-PE	RTK2758	Biolegend	rat IgG2b-APC	eB149/10H5	eBioscience

mIgG1-Pe-Cy7	MOPC-21	Biolegend	mIgG1-PE	P3.6.2.8.1	eBioscience
CD152 (CTLA4)-APC	L3D10	Biolegend	mIgG1-FITC	P3	eBioscience
CD69-PE	TP1.55.3	Beckman	CD160-PE	688327	R&D systems
CD3 FITC	UCHT1	Beckman	GITR-FITC	apr-02	R&D systems
CD45 FITC	J33	Beckman	GITR-Ligand-PE	109101	R&D systems
mIgG2a-PE	U7.27	Beckman	BDCA1-APC	AD5-8E7	Miltenyi

REFERENCES

1.   Torre LA, Bray F, Siegel RL, Ferlay J, Lortet-Tieulent J, Jemal A. Global cancer statistics, 2012. CA Cancer J Clin 2015;65:87-108.

2.   Razumilava N, Gores GJ. Cholangiocarcinoma. Lancet 2014;383:2168-2179.

3.   Patel T. Cholangiocarcinoma--controversies and challenges. Nat Rev Gastroenterol Hepatol 2011;8:189-200.

4.   Rizvi S, Gores GJ. Pathogenesis, diagnosis, and management of cholangiocarcinoma. Gastroenterology 2013;145:1215-1229.

5.   Blechacz B, Komuta M, Roskams T, Gores GJ. Clinical diagnosis and staging of cholangiocarcinoma. Nat Rev Gastroenterol Hepatol 2011;8:512-522.

6.   Bergquist A, von Seth E. Epidemiology of cholangiocarcinoma. Best Pract Res Clin Gastroenterol 2015;29:221-232.

7.   Zhou G, Sprengers D, Boor PPC, Doukas M, Schutz H, Mancham S, Pedroza-Gonzalez A, et al. Antibodies Against Immune Checkpoint Molecules Restore Functions of Tumor-infiltrating T cells in Hepatocellular Carcinomas. Gastroenterology 2017.

8.   El-Khoueiry AB, Sangro B, Yau T, Crocenzi TS, Kudo M, Hsu C, Kim TY, et al. Nivolumab in patients with advanced hepatocellular carcinoma (CheckMate 040): an open-label, non-comparative, phase 1/2 dose escalation and expansion trial. Lancet 2017;389:2492-2502.

9.   Cabo M, Offringa R, Zitvogel L, Kroemer G, Muntasell A, Galluzzi L. Trial Watch: Immunostimulatory monoclonal antibodies for oncological indications. Oncoimmunology 2017;6:e1371896.

10.   Fontugne J, Augustin J, Pujals A, Compagnon P, Rousseau B, Luciani A, Tournigand C, et al. PD-L1 expression in perihilar and intrahepatic cholangiocarcinoma. Oncotarget 2017;8:24644-24651.

11.   Walter D, Herrmann E, Schnitzbauer AA, Zeuzem S, Hansmann ML, Peveling-Oberhag J, Hartmann S. PD-L1 expression in extrahepatic cholangiocarcinoma. Histopathology 2017;71:383-392.

12.   Sabbatino F, Villani V, Yearley JH, Deshpande V, Cai L, Konstantinidis IT, Moon C, et al. PD-L1 and HLA Class I Antigen Expression and Clinical Course of the Disease in Intrahepatic Cholangiocarcinoma. Clin Cancer Res 2016;22:470-478.

13.   Ye Y, Zhou L, Xie X, Jiang G, Xie H, Zheng S. Interaction of B7-H1 on intrahepatic cholangiocarcinoma cells with PD-1 on tumor-infiltrating T cells as a mechanism of immune evasion. J Surg Oncol 2009;100:500-504.

14.   Ma K, Wei X, Dong D, Wu Y, Geng Q, Li E. PD-L1 and PD-1 expression correlate with prognosis in extrahepatic cholangiocarcinoma. Oncol Lett 2017;14:250-256.

15.   Taube JM, Anders RA, Young GD, Xu H, Sharma R, McMiller TL, Chen S, et al. Colocalization of inflammatory response with B7-h1 expression in human melanocytic lesions supports an adaptive resistance mechanism of immune escape. Sci Transl Med 2012;4:127ra137.

16.   Tumeh PC, Harview CL, Yearley JH, Shintaku IP, Taylor EJ, Robert L, Chmielowski B, et al. PD-1 blockade induces responses by inhibiting adaptive immune resistance. Nature 2014;515:568-571.

17.   Nakamura H, Arai Y, Totoki Y, Shirota T, Elzawahry A, Kato M, Hama N, et al. Genomic spectra of biliary tract cancer. Nat Genet 2015;47:1003-1010.

18.   Tran E, Turcotte S, Gros A, Robbins PF, Lu YC, Dudley ME, Wunderlich JR, et al. Cancer immunotherapy based on mutation-specific CD4+ T cells in a patient with epithelial cancer. Science 2014;344:641-645.
19.   Takagi S, Miyagawa S, Ichikawa E, Soeda J, Miwa S, Miyagawa Y, Iijima S, et al. Dendritic cells, T-cell infiltration, and Grp94 expression in cholangiocellular carcinoma. Hum Pathol 2004;35:881-886.
20.   Goeppert B, Frauenschuh L, Zucknick M, Stenzinger A, Andrulis M, Klauschen F, Joehrens K, et al. Prognostic impact of tumour-infiltrating immune cells on biliary tract cancer. Br J Cancer 2013;109:2665-2674.
21.   Gu FM, Gao Q, Shi GM, Zhang X, Wang J, Jiang JH, Wang XY, et al. Intratumoral IL-17(+) cells and neutrophils show strong prognostic significance in intrahepatic cholangiocarcinoma. Ann Surg Oncol 2012;19:2506-2514.
22.   Hasita H, Komohara Y, Okabe H, Masuda T, Ohnishi K, Lei XF, Beppu T, et al. Significance of alternatively activated macrophages in patients with intrahepatic cholangiocarcinoma. Cancer Sci 2010;101:1913-1919.
23.   Goeppert B, Frauenschuh L, Zucknick M, Roessler S, Mehrabi A, Hafezi M, Stenzinger A, et al. Major histocompatibility complex class I expression impacts on patient survival and type and density of immune cells in biliary tract cancer. Br J Cancer 2015;113:1343-1349.
24.   McCully ML, Ladell K, Andrews R, Jones RE, Miners KL, Roger L, Baird DM, et al. CCR8 Expression Defines Tissue-Resident Memory T Cells in Human Skin. J Immunol 2018.
25.   Turner DL, Bickham KL, Thome JJ, Kim CY, D'Ovidio F, Wherry EJ, Farber DL. Lung niches for the generation and maintenance of tissue-resident memory T cells. Mucosal Immunol 2014;7:501-510.
26.   Sathaliyawala T, Kubota M, Yudanin N, Turner D, Camp P, Thome JJ, Bickham KL, et al. Distribution and compartmentalization of human circulating and tissue-resident memory T cell subsets. Immunity 2013;38:187-197.
27.   Zhao X, Guo F, Li Z, Jiang P, Deng X, Tian F, Li X, et al. Aberrant expression of B7-H4 correlates with poor prognosis and suppresses tumor-infiltration of CD8+ T lymphocytes in human cholangiocarcinoma. Oncol Rep 2016;36:419-427.
28.   Pedroza-Gonzalez A, Verhoef C, Ijzermans JN, Peppelenbosch MP, Kwekkeboom J, Verheij J, Janssen HL, et al. Activated tumor-infiltrating CD4+ regulatory T cells restrain antitumor immunity in patients with primary or metastatic liver cancer. Hepatology 2013;57:183-194.
29.   Pedroza-Gonzalez A, Zhou G, Singh SP, Boor PP, Pan Q, Grunhagen D, de Jonge J, et al. GITR engagement in combination with CTLA-4 blockade completely abrogates immunosuppression mediated by human liver tumor-derived regulatory T cells ex vivo. Oncoimmunology 2015;4:e1051297.
30.   Lim YJ, Koh J, Kim K, Chie EK, Kim S, Lee KB, Jang JY, et al. Clinical Implications of Cytotoxic T Lymphocyte Antigen-4 Expression on Tumor Cells and Tumor-Infiltrating Lymphocytes in Extrahepatic Bile Duct Cancer Patients Undergoing Surgery Plus Adjuvant Chemoradiotherapy. Target Oncol 2017;12:211-218.
31.   Wang L, Dong H, Ni S, Huang D, Tan C, Chang B, Sheng W. Programmed death-ligand 1 is upregulated in intrahepatic lymphoepithelioma-like cholangiocarcinoma. Oncotarget 2016;7:69749-69759.
32.   Sideras K, Biermann K, Verheij J, Takkenberg BR, Mancham S, Hansen BE, Schutz HM, et al. PD-L1, Galectin-9 and CD8(+) tumor-infiltrating lymphocytes are associated with survival in hepatocellular carcinoma. Oncoimmunology 2017;6:e1273309.

CHAPTER 8

GITR ligation enhances functionality of tumor-infiltrating T cells in hepatocellular carcinoma

Guoying Zhou[*][1], Adriaan A. van Beek[*][1], Michail Doukas[2], Patrick P.C. Boor[1], Lisanne Noordam[1], Shanta Mancham[1], Lucia Campos Carrascosa[1], Marieke van der Heide-Mulder[1], Wojciech G. Polak[3], Jan N.M. IJzermans[3], Qiuwei Pan[1], Carlo Heirman[4], Ashley Mahne[5], Samantha L. Bucktrout[5], Marco J. Bruno[1], Dave Sprengers[#][1], Jaap Kwekkeboom[#][1]

Departments of [1]Gastroenterology and Hepatology, [2]Pathology, and [3]Surgery, Erasmus MC-University Medical Center, Rotterdam, the Netherlands; [4]Laboratory of Molecular and Cellular Therapy, Vrije Universiteit Brussel, Brussels, Belgium; [5]Rinat Laboratories, Pfizer Inc., South San Francisco, USA.

*Shared first authorship, #Shared last authorship.

ABSTRACT

No curative treatment options are available for advanced hepatocellular carcinoma (HCC). A recent study demonstrated that anti-PD1 antibody therapy can induce tumor regression in advanced HCC, although in a minority of patients, thereby revealing that co-inhibitory immune checkpoint blockade may have therapeutic potential for this type of cancer. However, whether agonistic antibodies against co-stimulatory receptors might be able to stimulate anti-tumor immunity in HCC is as yet unknown.

In a proof-of-concept pre-clinical study, we investigated whether agonistic targeting of the co-stimulatory receptor GITR could reinvigorate *ex vivo* functional responses of tumor-infiltrating lymphocytes (TIL) freshly isolated from resected tumors of HCC patients. In addition, we compared GITR expression between TIL and paired samples of leukocytes isolated from peripheral blood and tumor-free liver tissues and studied the effects of combined GITR and PD1 targeting on *ex vivo* TIL responses.

In all three tissue compartments, CD4$^+$FoxP3$^+$ regulatory T cells (Treg) showed higher GITR-expression than effector T-cell subsets, while the highest expression of GITR was observed on CD4$^+$FoxP3^{hi}CD45RA$^-$ activated Treg in tumors. To determine the effect of GITR ligation, we performed *ex vivo* proliferation assays with TIL from HCC. Addition of recombinant GITR ligand or a humanized agonistic antibody against GITR (10H2#13, Pfizer) to *ex vivo* cultures of TIL derived from HCC patients increased proliferation of CD8$^+$ T cells and enhanced granzyme B production upon stimulation with anti-CD3/CD28 antibodies. In addition, GITR ligation enhanced proliferative responses of HCC-derived CD4$^+$ and CD8$^+$ TIL to the tumor antigens glypican 3 and MAGEC2 presented by mRNA-transfected autologous B cell blasts.

Combining GITR ligation with anti-PD1 antibody further enhanced tumor antigen-specific proliferative responses of CD4$^+$ and CD8$^+$ TIL from some, but not all, HCC patients, compared to either single treatment.

In conclusion, agonistic targeting of GITR may be a promising strategy for single or combinatorial immunotherapy in HCC.

Keywords: GITR, CD357, TNFRSF18, Treg, HCC, Cancer Immunotherapy, PD1

Introduction

Liver cancer is the second most common cause of cancer-related mortality worldwide, killing approximately 750,000 people each year. The most common primary liver cancer is hepatocellular carcinoma (HCC), an aggressive malignancy derived from hepatocytes.[1, 2] Surgical resection and liver transplantation are curative therapies for patients with early stage disease. However, about 80% of HCC patients present with advanced disease at diagnosis and can only be offered systemic sorafenib therapy which provides a survival advantage of <3 months.[3] Therefore, novel therapies for HCC are urgently needed.

Immune checkpoint antibodies are a new class of cancer immune therapeutics. T cells are activated upon antigen recognition via their T cell receptor and engagement of their co-stimulatory immune checkpoint receptors with corresponding ligands on other cells, while they are suppressed upon interaction of their co-inhibitory immune checkpoint receptors with their ligands. Therapeutic antibodies that block interaction of the co-inhibitory receptor PD1 with its ligands can unleash pre-existing anti-cancer T cell responses within tumors, and have resulted in recent breakthroughs in clinical treatment of several types of advanced cancer.[4-12] In HCC, a recent trial showed significant tumor load reduction in response to anti-PD1 antibody (nivolumab) therapy in about 20% of advanced HCC patients.[13] Nevertheless, at least 80% of advanced HCC patients did not respond to nivolumab. Therefore, more effective immunotherapies are still required for HCC.

Besides blockade of co-inhibitory receptors, agonistic targeting of co-stimulatory receptors has the potential to boost intra-tumoral T cell immunity to combat cancer growth and evoke cancer regression. Importantly, in addition to activating intra-tumoral T cell responses, co-stimulatory receptors can stimulate systemic anti-tumor immunity which may protect against tumor recurrence.[14, 15] Currently, antibodies targeting different co-stimulatory receptors are being evaluated in clinical trials for several types of solid cancer, including for HCC.[16, 17]

One of the important co-stimulatory receptors is CD357, TNF receptor superfamily member 18 (TNFRSF18), or glucocorticoid-induced TNFR-related protein (GITR). Previously we have revealed that tumor-infiltrating T cells in HCC are functionally compromised, which is partly due to co-inhibitory interactions,[18-20] and because liver tumors contain high numbers of conventional CD4$^+$FoxP3$^+$CD25$^+$ regulatory T cells (Treg)[19] and type 1 regulatory T cells[21] which inhibit functions of effector T cells. We also demonstrated that agonistic targeting of GITR can alleviate the suppressive capacity of liver tumor-derived CD4$^+$CD25$^+$ regulatory T cells.[22] However, the expression of GITR on tumor-infiltrating CD8$^+$ cytotoxic T cells and CD4$^+$FoxP3$^-$ T helper cells (Th) in HCC patients is unknown. Whether agonistic targeting of

GITR can boost anti-tumor responses of HCC patient-derived tumor-infiltrating lymphocytes (TIL) has not been studied, nor is it known whether combining GITR ligation with PD1 blockade may have synergistic effects on HCC patient-derived TIL proliferation and activation.

Therefore, in a proof-of-concept preclinical study, we investigated whether agonistic targeting of the co-stimulatory receptor GITR could reinvigorate *ex vivo* functional responses of TIL from HCC patients. In addition, we compared GITR expression between TIL and paired samples of leukocytes isolated from peripheral blood and tumor-free liver (TFL) tissues, and studied the effects of combined GITR and PD1 targeting on *ex vivo* TIL responses.

Patients and Methods

Patients

Thirty-seven patients who were eligible for surgical resection of HCC and two HCC patients who were eligible for liver transplantation were enrolled in the study from January 2014 to December 2017. Paired fresh tissue samples from tumors and surrounding (minimum 1cm distance from the tumor) tumor-free liver tissues were obtained, and tumor-infiltrating leukocytes and intra-hepatic leukocytes were isolated, respectively. Peripheral blood from the same patients was also collected on the day of resection. None of the patients received chemotherapy or immunosuppressive treatment within three months prior to the surgery. The study was approved by the local ethics committee, and all the patients signed the informed consent before tissue and blood donation.

Cell preparation

Peripheral blood mononuclear cells (PBMC) were isolated by Ficoll density gradient centrifugation. Single cell suspensions from tumors and TFL were obtained by tissue digestion. Briefly, fresh tissues were cut into small pieces and digested with 0.125 mg/mL of collagenase IV (Sigma-Aldrich, St. Louis, MO) and 0.2 mg/mL of DNAse I (Roche, Indianapolis, IN) in Hanks' Balanced Salt solution with Ca^{2+} and Mg^{2+} (Sigma, Zwijndrecht, The Netherlands) for 30-60 minutes under continuous stirring at 37 °C. Cell suspensions were filtered through 100 μm pore cell strainers (BD Biosciences, Erembodegem, Belgium) and mononuclear leukocytes were obtained by Ficoll density gradient centrifugation. Viability was determined by trypan blue exclusion.

Flow cytometric analysis

Fresh PBMC and mononuclear leukocytes isolated from tumors and TFL were analyzed for expression of surface and intracellular markers using specific antibodies (Supplementary

Table 1). Dead cells were excluded by using a LIVE/DEAD fixable dead cell stain kit with aqua fluorescent reactive dye (Invitrogen, Paisley, UK) or Live/dead stain eFluor506 (eBioscience, Vienna, Austria). Cell surface staining with fluorochrome-conjugated antibodies was *performed* in the dark at 4°C for 30 minutes, after which cells were fixed and permeabilized using the FoxP3 staining buffer set (eBioscience) and stained for intracellular antigens. Cells were measured by a FACSCanto II or a FACSAria SORP II flow cytometer (BD Biosciences, San Diego, USA) and analyzed using FlowJo software version X.0.7 (TreeStar Inc.). Appropriate isotype control antibodies were used for gating purposes.

Ex vivo polyclonal T cell activation assay

All TIL cultures were performed in RPMI 1640 (Lonza, Breda, The Netherlands) supplemented with 10% human AB serum (Sigma), 2mM L-glutamine (Invitrogen), 50 mM Hepes Buffer (Lonza), 1% penicillin-streptomycin (Life Technologies), 5mM Sodium Pyruvate (Gibco) and 1% minimum essential medium non-essential amino acids (MEM NEAA) at 37°C. TIL were cultured in 96-well round-bottom culture plates (10^6 cells/mL) and typically stimulated with anti-human CD3/CD28 Dynabeads (Gibco-Life Technologies AS, Norway) at a cell:bead ratio of 10:1. This ratio provides suboptimal T cell stimulation.[18] To test the effects of GITR stimulation or PD1 blockade, 1 μg/ml azide-free and low endotoxin soluble GITR ligand (GITRL, RnD systems), crosslinked with 2.5 μg/ml anti-HA antibody (RnD systems), or 10 μg/mL humanized agonistic antibody against GITR (10H2#13, Pfizer), or 10 μg/mL nivolumab (BMS, obtained from Erasmus MC hospital pharmacy), or corresponding isotype control antibodies (anti-HA hIgG1 clone 4FNL and anti-BHV hIgG4 clone 26H6, Pfizer) were added. After 4-5 days, culture supernatant was collected and production of IFN-γ and granzyme B was quantified by LegendPlex (BioLegend, San Diego, USA). Cells were harvested and stained with anti-CD8, anti-CD4, and anti-CD3 antibodies (surface staining) and anti-Ki-67 antibody (intracellular staining). Dead cells were excluded by using the LIVE/DEAD fixable dead cell stain kit with aqua fluorescent reactive dye, and T cell proliferation was determined based on Ki-67 positivity by flow cytometry analysis.

Ex vivo mRNA-encoded full length tumor antigen-specific T cell stimulation assay

Expansion of patient B cells from PBMC by stimulation with trimeric CD40 ligand and IL-4, *in vitro* generation of eGFP, glypican 3 (GPC3) and MAGEC2 mRNA, and mRNA electroporation were performed as previously described.[18]

Tumor-infiltrating leukocytes of HCC patients were labeled with 0.1 μM carboxyfluorescein diacetate succinimidyl ester (CFSE, Invitrogen), after which 10^5 cells in RPMI medium

supplemented with 10% human AB serum, 2mM L-glutamine, 50 mM Hepes Buffer, 1% penicillin-streptomycin, 5mM Sodium Pyruvate and 1% MEM NEAA were transferred to each well of 96-well round-bottom culture plates. GPC3 mRNA-, MAGEC2 mRNA- or (as a negative control) eGFP mRNA-transfected autologous CD40-activated B cells (B cell blasts) in the same medium were added at a TIL:B cell ratio of 1:1. TIL were co-cultured with B cell blasts in the presence or absence of 1 µg/ml GITRL, crosslinked with 2.5 µg/ml anti-HA antibody, or 10 µg/mL humanized agonistic antibody against GITR (10H2#13, Pfizer), or 10 µg/mL nivolumab, or corresponding isotype control antibodies (hIgG1 and hIgG4 respectively). After 6 days, supernatants were stored for later cytokine analysis, whilst cells were harvested, and stained with CD3, CD4, and CD8 antibodies. Dead cells were excluded by using the LIVE/DEAD fixable dead cell stain kit with aqua fluorescent reactive dye, and T cell proliferation was determined based on CFSE dilution by flow cytometry analysis.

Statistical analysis

All data set distributions were analyzed for normality by the Shapiro-Wilk normality test. Differences between paired groups of data were analyzed according to their distribution by either paired t test or Wilcoxon matched pairs test. The statistical analysis was performed using GraphPad Prism Software (version 5.0). P-values less than 0.05 were considered statistically significant (*=p<0.05; **=p<0.01; ***=p<0.001).

Results

Intra-tumoral CD4$^+$FoxP3$^+$ T cells show high GITR expression

First, we determined frequencies of CD3$^-$CD56$^+$ NK cells, CD3$^+$CD56$^+$ NKT cells, CD8$^+$ T cells, total CD4$^+$ T cells, CD4$^+$FoxP3$^-$ T cells, and CD4$^+$FoxP3$^+$ T cells isolated from blood, TFL tissues, and tumors of HCC patients. While tumors contained lower frequencies of NK cells and NKT cells, they contained more T cells within total CD45$^+$ cells than TFL (Supplementary Figure 1A). The distribution of T cell subsets further showed that CD4$^+$FoxP3$^+$ T cells accumulated within tumors, rather than CD8$^+$ T cells or CD4$^+$FoxP3$^-$ T cells (Supplementary Figure 1B). Then, we analyzed GITR expression within these immune cell subsets. No differences in proportions of NK cells and CD8$^+$ T cells expressing GITR were found among blood, TFL, and tumor, with on average 12% of NK cells and 5% of CD8$^+$ T cells expressing GITR in the tumor (Figure 1A-B). In contrast, GITR expression was increased on tumor NKT cells compared with NKT cells in TFL, and was increased on CD4$^+$FoxP3$^-$ T cells in TFL and tumor as compared with blood, with on average 7% of intra-tumoral CD4$^+$FoxP3$^-$ T cells expressing GITR (Figure 1A-B). The highest expression of GITR

was observed on intra-tumoral CD4$^+$FoxP3$^+$ T cells, with an average of 45% of cells expressing GITR, which was significantly higher than CD4$^+$FoxP3$^+$GITR$^+$ T cell proportions in blood and TFL (Figure 1A-B).

CD4$^+$FoxP3^{hi}CD45RA$^-$ activated Treg are highly abundant in the tumor and display highest GITR expression

Because FoxP3 alone is insufficient to define *bona fide* Treg,[23] we included CD45RA to further define FoxP3-expressing CD4$^+$ T cells. The combination of FoxP3 and CD45RA leads to the identification of five CD4$^+$ T cell subsets: FoxP3^{lo}CD45RA$^+$ resting Treg (fraction I), FoxP3^{hi}CD45RA$^-$ activated Treg (fraction II), FoxP3^{lo}CD45RA$^-$ activated Th (fraction III), FoxP3$^-$CD45RA$^-$ Th (fraction IV), and FoxP3$^-$CD45RA$^+$ Th (fraction V; Figure 2A). We evaluated the CD4$^+$FoxP3$^+$ subset distributions in blood, TFL, and tumor. The frequencies of activated Th (fraction III) were significantly higher in blood and tumor than in TFL (Figure 2B). Resting Treg (fraction I) were significantly reduced in liver tissues compared with blood, whereas activated Treg (fraction II) were about 9-fold more abundant in tumors than in TFL or blood (Figure 2B).

We then set out to analyze GITR expression on FoxP3-expressing CD4$^+$ T cell subsets (fraction I, II, and III). All fractions expressed GITR, but significantly more GITR expression was found on intra-tumoral activated Treg (fraction II), with on average nearly 70% of cells expressing GITR (Figure 2C-D). This percentage was significantly higher than in any other fraction in tumor, TFL, and blood (Figure 2C). Combining the increased proportion of activated Treg in tumors (Figure 2B) with the increased GITR expression on these cells (Figure 2C), we observed an approximately 30-fold increase of GITR-expressing activated Treg in the tumor over TFL and an approximately 50-fold increase of GITR-expressing activated Treg in the tumor over blood (Figure 2E).

GITR is co-expressed with activation markers CD25 and 4-1BB

Subsequently, we aimed to identify whether GITR expression coincided with expression of the activation markers CD25 and 4-1BB. We found that GITR$^+$ activated Th and activated Treg in liver tissues expressed significantly higher levels of CD25 than GITR$^-$ activated Th and Treg (Figure 3A). Similarly, GITR$^+$CD4$^+$FoxP3$^-$ cells expressed higher levels of CD25 than GITR$^-$CD4$^+$FoxP3$^-$ cells (data not shown).

We further found that GITR was co-expressed with 4-1BB in on average 60% of activated Treg in tumors. Proportions of activated Treg that co-expressed GITR and 4-1BB were significantly higher in tumors than in TFL and blood (Figure 3B-C), which was also observed

for CD8^{+} T cells, CD4^{+}FoxP3^{-} T cell subsets, and activated Th (data not shown). GITR-expressing CD8^{+} T cells, CD4^{+}FoxP3^{-}CD45RA^{+}, CD4^{+}FoxP3^{-}CD45RA^{-}, and activated Th cells in liver tissues and blood showed a more activated phenotype than GITR^{-} T cell subsets, whereas GITR-expressing activated Treg in liver tissues, but not in blood, showed a more activated phenotype, as marked by increased 4-1BB expression on GITR^{+} cells (Figure 3D), which is in line with enhanced CD25 expression on GITR^{+} cells.

GITR ligation enhances tumor-infiltrating CD4^{+} and CD8^{+} T cell proliferation

We previously showed that engagement of GITR by GITRL reduced the suppression of Treg purified from HCC tumors on blood-derived CD4^{+}CD25^{-} T cells.[19, 22] We now evaluated the effect of GITR ligation on HCC-derived CD4^{+} and CD8^{+} TIL responses. Because monoclonal antibodies are more amenable to therapeutic development than recombinant proteins, we also assessed the effect of a humanized agonistic antibody against GITR (10H2#13, Pfizer). To test the effect of GITR ligation, we used two T cell stimulation assays.

First, we analyzed TIL proliferation and cytokine secretion after 4- to 5-day culture with anti-CD3/anti-CD28 beads in the absence or presence of GITRL or anti-GITR agonistic antibody (10H2#13, Pfizer). GITRL significantly enhanced CD4^{+} T cell proliferation, CD8^{+} T cell proliferation and granzyme B production, whereas anti-GITR antibody significantly enhanced CD8^{+} T cell proliferation, granzyme B and IFN-γ production (Figure 4). No enhanced proliferation or cytokine secretion was observed in the presence of the corresponding hIgG1 isotype control (Figure 4A-B).

For the second (tumor antigen-specific) assay, we expanded autologous B cell blasts from patient PBMC by a 2- to 3-week culture in the presence of trimeric CD40 ligand and IL-4. These B cell blasts were then transfected with mRNA encoding the tumor antigens GPC3 or MAGEC2, or eGFP as a negative control, and co-cultured with CFSE-labelled TIL for 6 days, as previously described.[18] Proliferation of tumor-derived CD4^{+} T cells and CD8^{+} T cells was significantly enhanced after engagement of GITR by GITRL or anti-GITR antibody (Figure 5A-B), in contrast to the corresponding hIgG1 isotype control.

PD1 blockade and combination with GITR ligation

Because PD1 blockade with the humanized anti-PD1 antagonistic antibody nivolumab resulted in tumor regression in about 20% of patients with advanced HCC,[13] we assessed the co-expression of GITR and PD1 on CD8^{+} T cells, FoxP3^{-}CD45RA^{+} Th, FoxP3^{-}CD45RA^{-} Th, activated Th, resting Treg and activated Treg in blood, TFL, and tumor (Figure 6A-B).

Addition of nivolumab significantly enhanced *ex vivo* proliferative responses of tumor-derived CD4$^+$ T and CD8$^+$ T cells to tumor antigens (Figure 7A-B).

Next, we combined nivolumab with GITRL in the tumor antigen-specific *ex vivo* T cell assay. Although the combination of nivolumab with GITRL did not significantly enhance proliferation of tumor antigen-specific CD4$^+$ or CD8$^+$ T cells compared to single nivolumab or GITRL treatment, individual patients' T cell responses (HCC-001, HCC-004, HCC-005, HCC-006) benefited from the combination of nivolumab and GITRL (Figure 7A-B). In addition, we observed that the average proliferative response to the combination of nivolumab and GITRL was 19-20% higher in CD4$^+$ T cells and 27-34% higher in CD8$^+$ T cells, compared with nivolumab alone or GITRL alone, respectively (Supplementary Figure 2).

Discussion

We have previously shown that GITR ligation decreases the suppressive capacity of conventional regulatory T cells.[19] In this study, we are the first to test the proof of concept that the application of GITR ligation may be promising for immunotherapy of HCC patients. As monoclonal antibodies are more amenable to therapeutic development than recombinant proteins, we not only assessed the effect of GITRL, but also a humanized agonistic antibody against GITR.

In addition to our earlier studies,[19, 22] we evaluated GITR expression on more lymphocyte subsets (Figure 1), showing that CD4$^+$FoxP3$^+$ T cells express particularly high levels of GITR, in contrast to other T cell subsets or NK and NKT cells. The increased proportion of CD4$^+$FoxP3$^+$ T cells in HCC tumors (Supplementary Figure 1) suggests that this immune subset is of particular interest for GITR targeting.

Because FoxP3 alone is insufficient to characterize human Treg,[24] we included CD45RA as a marker to further characterize different subsets within CD4$^+$FoxP3$^+$ T cells. As recommended by Miyara et al., we included CD45RA to distinguish CD45RA$^-$FoxP3^{hi} activated Treg from CD45RA$^-$FoxP3^{lo} activated T helper cells and CD45RA$^+$FoxP3^{lo} resting Treg.[23] The need to distinguish these subsets is highlighted by a recent study by Saito et al. They showed that the distinction between activated T helper cells and activated Treg is necessary to interpret the correlation with the prognostic value of activated T helper cells versus activated Treg in CRC studies.[25] We evaluated the distribution of these more defined subsets, showing that activated Treg are highly enriched in HCC tumors (Figure 2). Furthermore, we found that GITR$^+$ activated Treg are 30- to 50-fold more abundant in tumors than in blood and TFL (Figure 2), indicating that GITR is a highly selective tumor target. In addition, GITR$^+$ activated

Treg show a more activated phenotype, as evidenced by elevated CD25 and 4-1BB expression. These data indicate that GITR is highly expressed on the abundantly present intra-tumoral activated Treg, and that GITR expression marks the most activated cells within this subset and all other T cell subsets. Recently, a similar co-expression pattern was reported in TIL from patients with non-small cell lung carcinoma, showing higher GITR expression on CD4$^+$CD25$^+$ T cells than on CD4$^+$CD25$^-$ T cells.[26]

We show that GITR ligation enhances *ex vivo* TIL proliferation in polyclonal and tumor antigen-specific stimulations of unfractionated mononuclear leukocytes from HCC tumors (Figure 4-5). GITRL and anti-GITR antibody resulted in similar enhancement of *ex vivo* TIL proliferation and effector cytokine production, showing that a fully humanized anti-GITR antibody in our setup is as effective as the natural ligand. In addition, we evaluated the combination of GITR ligation and PD1 blockade (Figure 7 and Supplementary Figure 2) because there is a need for combination therapies. Our results suggest that combined targeting of GITR and PD1 may be considered as an effective combination strategy to enhance anti-tumor immune responses in some HCC patients. In mouse tumor models, the combination of GITR ligation and PD1 blockade induced potent antitumor immunity and tumor regression.[27] Some clinical studies already target both the GITR and the PD1/PDL1 pathway,[17] indicating the potential benefit of these combinations.

Importantly, we used an anti-GITR antibody which prevents binding of GITRL to GITR. After engagement of GITR by soluble GITRL, reverse signaling through GITRL induced indoleamine 2,3-dioxygenase expression in antigen-presenting cells, leading to T cell suppression.[28] The use of an anti-GITR antibody that prevents binding of the natural ligand to GITR and thereby prevents reverse signaling in antigen-presenting cells, might further attenuate immunosuppression.[17]

Our study has some limitations: 1) as patient samples are often limited and the required numbers of TIL in the assays are large, we could include only a fraction of patients for functional assays; 2) because most of our patients underwent resection, and a few underwent liver transplantation, they do not represent the whole HCC patient population; 3) most patients in our cohort have no underlying liver disease, in contrast to many other studies in e.g. Asia.

On the other hand, our study has several strengths: 1) the use of the total tumor-infiltrating leukocytes enabled us to study both co-stimulatory and co-inhibitory pathways; 2) we were able to use an antigen-specific assay that included two prevalent HCC tumor-associated

antigens (GPC3 and MAGEC2); 3) we directly compared GITRL with an agonistic anti-GITR antibody.

In sum, our study demonstrates that GITR ligation enhances the functionality of tumor-infiltrating T cells in hepatocellular carcinoma, and therefore may be a new immunotherapeutic option for patients with hepatocellular carcinoma.

Supplementary Table 1. Anti-human antibodies used for flow cytometry

Target	Format	Clone	Company
CD3	APC-R700	UCHT1	BD Biosciences
CD3	PE-Cy7	UCHT1	eBioscience
CD4	APC-eFluor780	OKT4	eBioscience
CD4	eVolve605	SK3	eBioscience
CD8	APC-eFluor780	OKT8	eBioscience
CD8	PE	RPA-T8	eBioscience
CD25	PE-Cy7	M-A251	BD Biosciences
CD45	APC-Cy7	HI30	eBioscience
CD45	PE-CF594	HI30	BD Biosciences
CD45RA	PE-CF594	HI100	BD Biosciences
CD56	PE	TULY56	eBioscience
CD137 (4-1BB)	BV421	4B4-1	BD Biosciences
CD279 (PD1)	APC	J105	eBioscience
CD357 (GITR)	FITC	apr-02	R&D systems
FoxP3	PE	236A/E7	eBioscience
Ki-67	APC	20Raj1	eBioscience
Human Fc block	Purified		BD Biosciences

Figure legends

Figure 1. Intra-tumoral CD4⁺FoxP3⁺ cells from HCC patients show highest GITR expression. (A) GITR⁺ cell frequencies within NK cells, NKT cells, and T cell subsets in mononuclear leukocytes isolated from blood, tumor-free liver (TFL), and tumor tissues from HCC patients. (B) As in (A), showing median fluorescence intensities (MFI) of GITR expression on the indicated immune cell subsets. Dots represent individual patients and lines present means. N=19-27 patients. *=$p<0.05$; **=$p<0.01$; ***=$p<0.001$.

Figure 2. Activated regulatory T cells are highly enriched in HCC tumors and express high levels of GITR. (A) Representative example of flow cytometric analysis of CD4⁺ T cell subsets by FoxP3 and CD45RA, identifying five fractions: FoxP3ˡᵒCD45RA⁺ resting Treg (fraction I), FoxP3ʰⁱCD45RA⁻ activated Treg (fraction II), FoxP3ˡᵒCD45RA⁻ activated Th (fraction III), FoxP3⁻CD45RA⁻ Th (fraction IV), and FoxP3⁻CD45RA⁺ Th (fraction V). (B) Percentages of fractions I-III within CD45⁺ mononuclear leukocytes. (C) GITR⁺ frequencies within fractions I-III. (D) Median fluorescence intensities (MFI) of GITR expression on cells within fractions I-III. (E) Percentages of total activated Treg (left) and GITR⁺ activated Treg (right) within CD45⁺ mononuclear leukocytes. Dots represent individual patients and lines present means. N=12 patients. *=$p<0.05$; **=$p<0.01$; ***=$p<0.001$.

Figure 3. GITR expression on activated regulatory T cells is accompanied by increased CD25 and 4-1BB expression. (A) GITR⁺ activated T helper (aTh) and regulatory T cells (aTreg)express higher levels of CD25 than GITR⁻ cells. (B) Representative example of flow cytometric analysis, showing co-expression of GITR and 4-1BB on intra-tumoral FoxP3ʰⁱCD45RA⁻ activated regulatory T cells (fraction II). (C) Percentages of GITR⁺4-1BB⁺ activated regulatory T cells in blood, TFL, and tumor. Dots represent individual patients and lines present means. (D) 4-1BB⁺ frequencies within GITR⁻ versus GITR⁺ of five CD4⁺ T cell subsets in blood, TFL, and tumor. N=12 patients. *=$p<0.05$; **=$p<0.01$; ***=$p<0.001$.

Figure 4. GITR ligation enhances *ex vivo* proliferation of tumor-infiltrating CD4⁺ and CD8⁺ T cells. Effects of soluble GITRL (1 µg/mL crosslinked with anti-HA antibody) or 10 µg/mL humanized agonistic anti-GITR antibody on proliferation of (A) tumor-derived CD4⁺ T cells, and (B) tumor-derived CD8⁺ T cells upon 4 to 5 days' culture of tumor-derived mononuclear cells with a suboptimal amount of anti-CD3/CD28 beads. Proliferation was measured by determination of percentages of CD4⁺ or CD8⁺ T cells expressing Ki-67 at the end of the culture. Baseline proliferation (= % of Ki-67⁺ T cells in the absence of GITRL or antibodies) was normalized to 100% for each tested patient. Bars show mean percentages of Ki-67⁺ CD4⁺ or CD8⁺ T cells in cultures relative to baseline proliferation in cultures derived

from n=9 patients with SEM. An irrelevant human IgG1 antibody served as an isotype-matched control antibody for the anti-GITR antibody. (C) Production of IFN-γ and (D) granzyme B in culture supernatant was quantified. Data of patients with detectable amounts are shown, each line represents one patient. *=p<0.05; **=p<0.01.

Figure 5. GITR ligation increases *ex vivo* proliferation of CD4$^+$ and CD8$^+$ TIL in response to tumor antigens presented by mRNA-transfected autologous B cells. Effects of soluble GITRL (1 µg/mL crosslinked with anti-HA antibody) or 10 µg/mL humanized agonistic anti-GITR antibody on proliferation of (A) tumor-derived CD4$^+$ T cells, and (B) tumor-derived CD8$^+$ T cells upon 6 days' culture of CFSE-labeled tumor-derived mononuclear cells with B cell blasts electroporated with mRNA encoding tumor antigens GPC3 or MAGEC2 (or eGFP as a control). Proliferation was measured by determination of percentages of CD4$^+$ or CD8$^+$ T cells with CFSE dilution at the end of the culture. Baseline proliferation (= % of CFSE^{low} T cells in the presence of eGFP-electroporated B cells) was normalized to 100% for each tested patient. For those patients whose TIL responded to both tumor antigens, the average response to GPC3- and MAGEC2-electroporated B cells was depicted. Each line represents one patient. An irrelevant human IgG1 antibody served as an isotype-matched control antibody for the anti-GITR antibody. Data show responses in cultures of n=8 patients. *=p<0.05; **=p<0.01.

Figure 6. Co-expression of GITR and PD1 by activated regulatory T cells. (A) Representative example of flow cytometric analysis of GITR and PD1 expression on activated regulatory T cells. (B) Mean frequencies of GITR$^-$PD1$^-$, GITR$^-$PD1$^+$, GITR$^+$PD1$^-$ and GITR$^+$PD1$^+$ within CD8$^+$ T cells, FoxP3$^-$CD45RA$^+$ Th, FoxP3$^-$CD45RA$^-$ Th, activated Th, resting Treg and activated Treg in blood, TFL, and tumor with SEM. N=12 patients.

Figure 7. Combined targeting of GITR and PD1 increases *ex vivo* proliferation of CD4$^+$ and CD8$^+$ TIL in response to tumor antigens presented by mRNA-transfected autologous B cells. Effects of 10 µg/mL antagonistic anti-PD1 antibody (nivolumab) or anti-PD1 antibody combined with soluble GITRL (1 µg/mL crosslinked with anti-HA antibody) on proliferation of (A) tumor-derived CD4$^+$ T cells, and (B) tumor-derived CD8$^+$ T cells upon 6 days' culture of CFSE-labeled tumor-derived mononuclear cells with B cell blasts electroporated with mRNA encoding tumor antigens GPC3 or MAGEC2 (or eGFP as a control). Proliferation was measured by determination of percentages of CD4$^+$ or CD8$^+$ T cells with CFSE dilution at the end of the culture. Baseline proliferation (= % of CFSE^{low} T cells in the presence of eGFP-electroporated B cells) was normalized to 100% for each tested patient. For those patients whose TIL responded to both tumor antigens, the average

response to GPC3- and MAGEC2-electroporated B cells was depicted. Each line represents one patient. An irrelevant human IgG4 antibody served as an isotype-matched control antibody for the anti-PD1 antibody. Data show responses in cultures of n=8 patients. *=p<0.05; **=p<0.01.

Figure 1 A/B
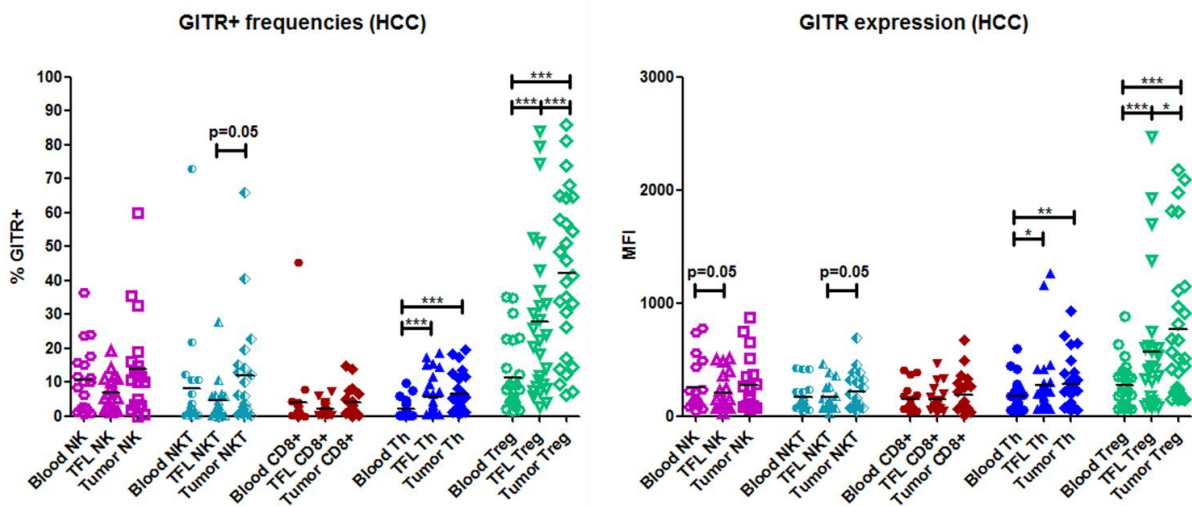
Figure 2 A
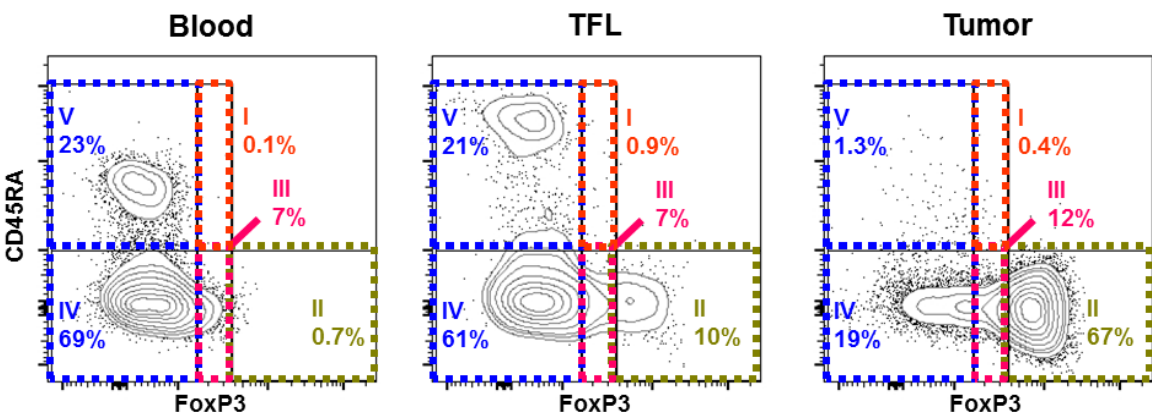
Figure 2 B
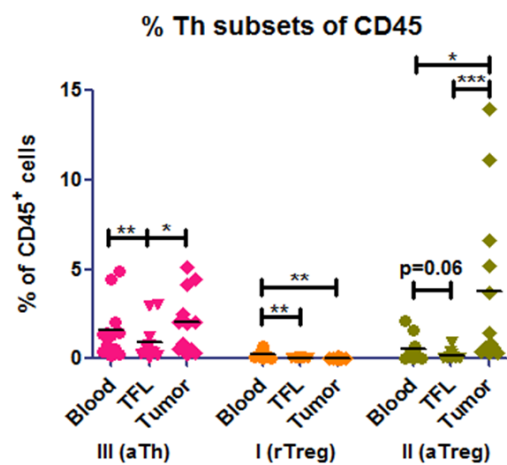
Figure 2 C/D
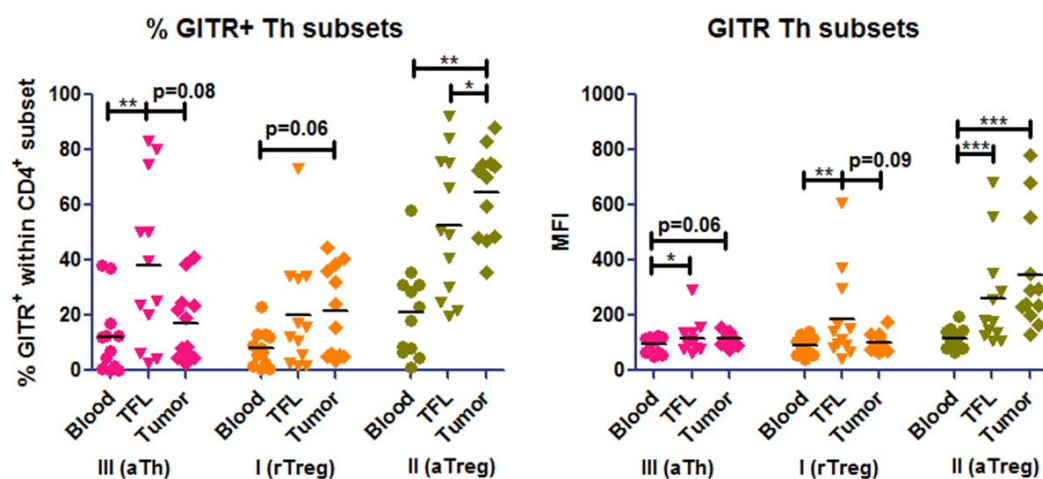
Figure 2 E
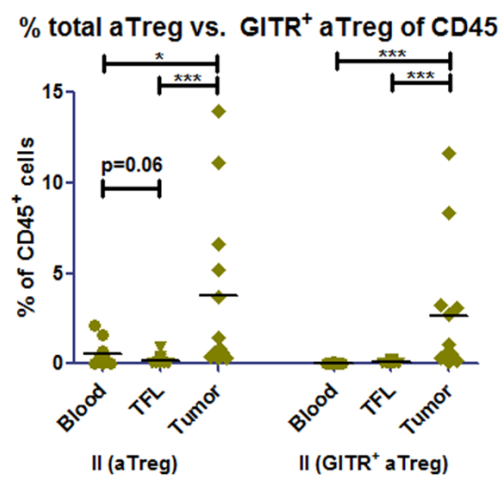
Figure 3 A
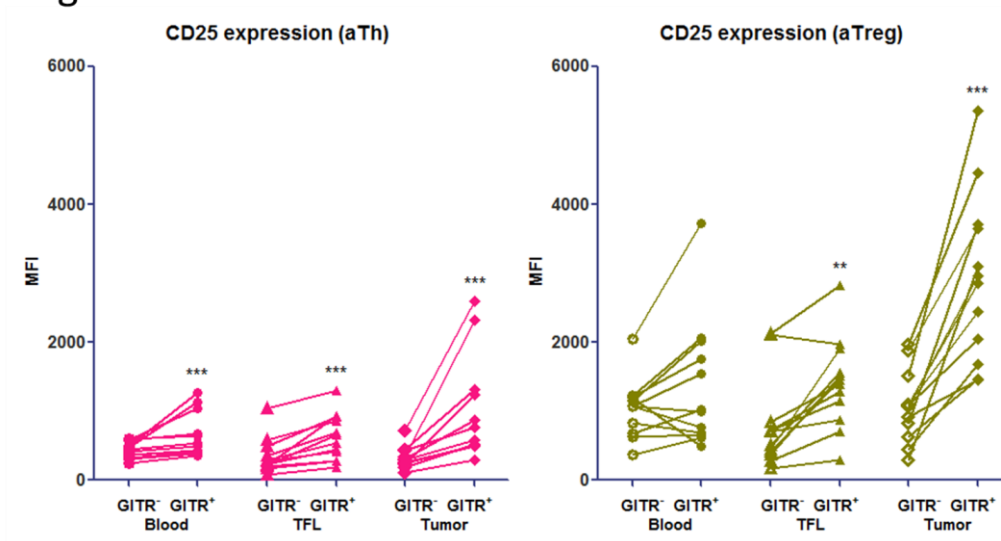
Figure 3 B/C
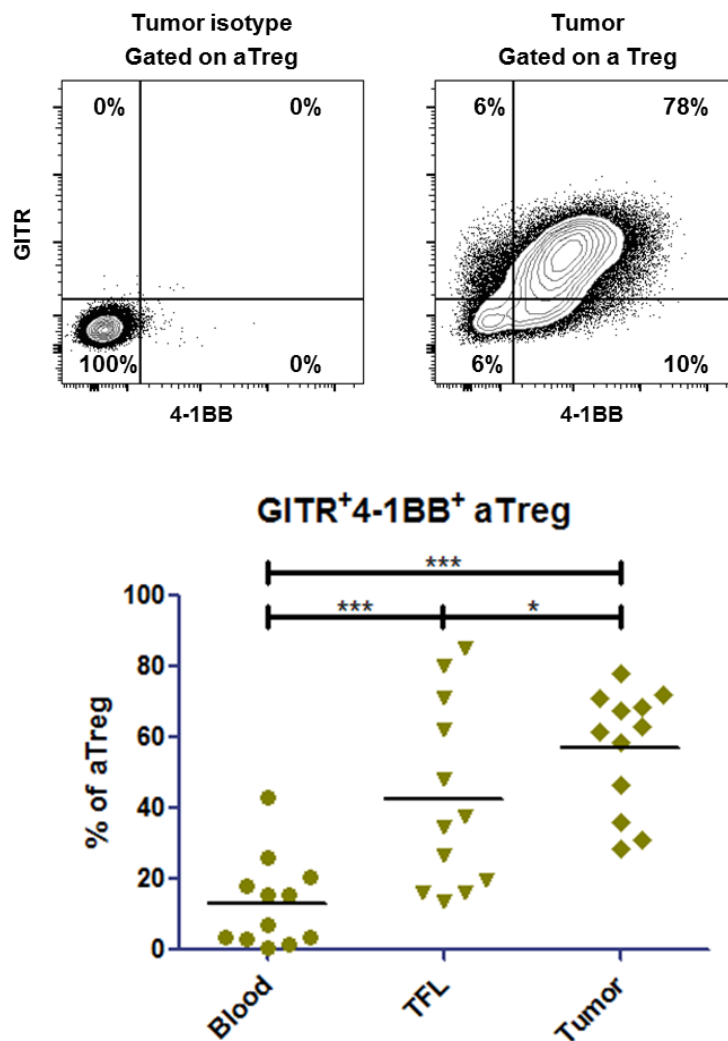
Figure 3 D
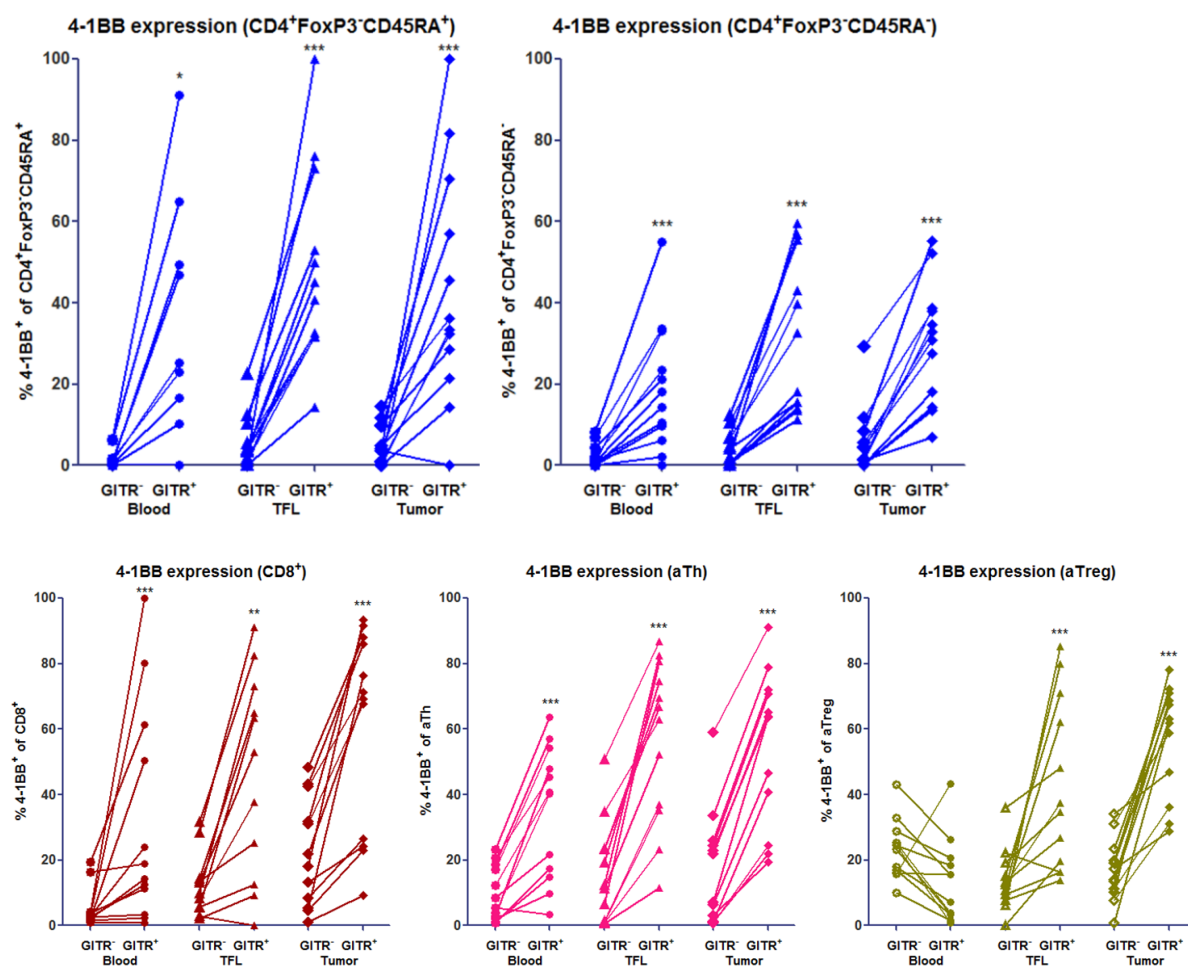
Figure 4 A/B
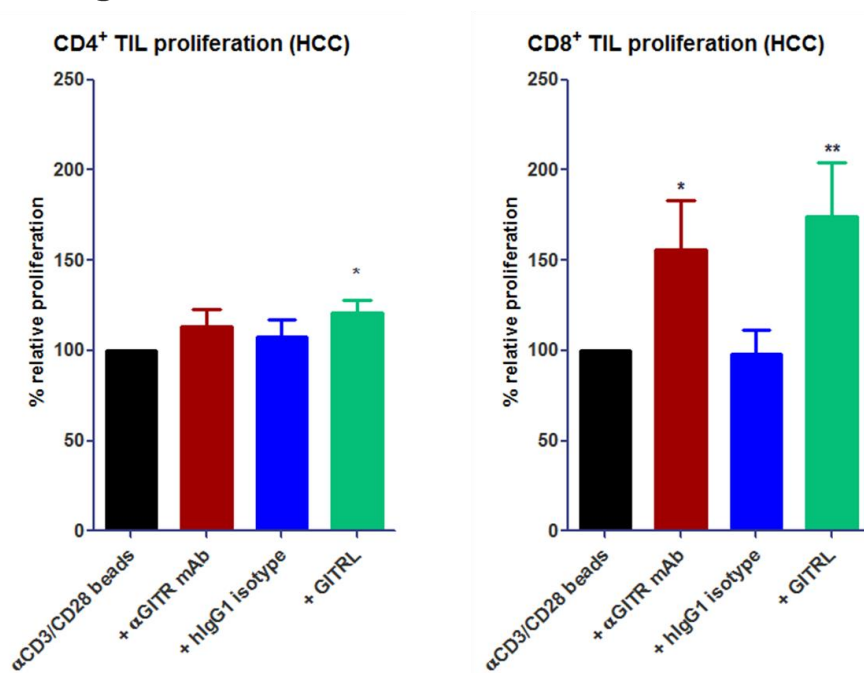
Figure 4 C/D

Figure 5 A/B

Figure 6 A

Tumor isotype
Gated on aTreg

GITR

| 0% | 0% |
| 100% | 0% |

PD1

Tumor
Gated on aTreg

| 17% | 63% |
| 9% | 11% |

PD1

Figure 6 B

Blood PD1 GITR

% of subset

CD8+ FoxP3-CD45RA+ FoxP3-CD45RA- aTh rTreg aTreg

XTitle

TFL PD1 GITR

% of subset

CD8+ FoxP3-CD45RA+ FoxP3-CD45RA- aTh rTreg aTreg

XTitle

Tumor PD1 GITR

% of subset

CD8+ FoxP3-CD45RA+ FoxP3-CD45RA- aTh rTreg aTreg

XTitle

- □ PD1-GITR-
- ■ PD1+GITR- (grey)
- ■ PD1-GITR+ (blue)
- ■ PD1+GITR+ (red)
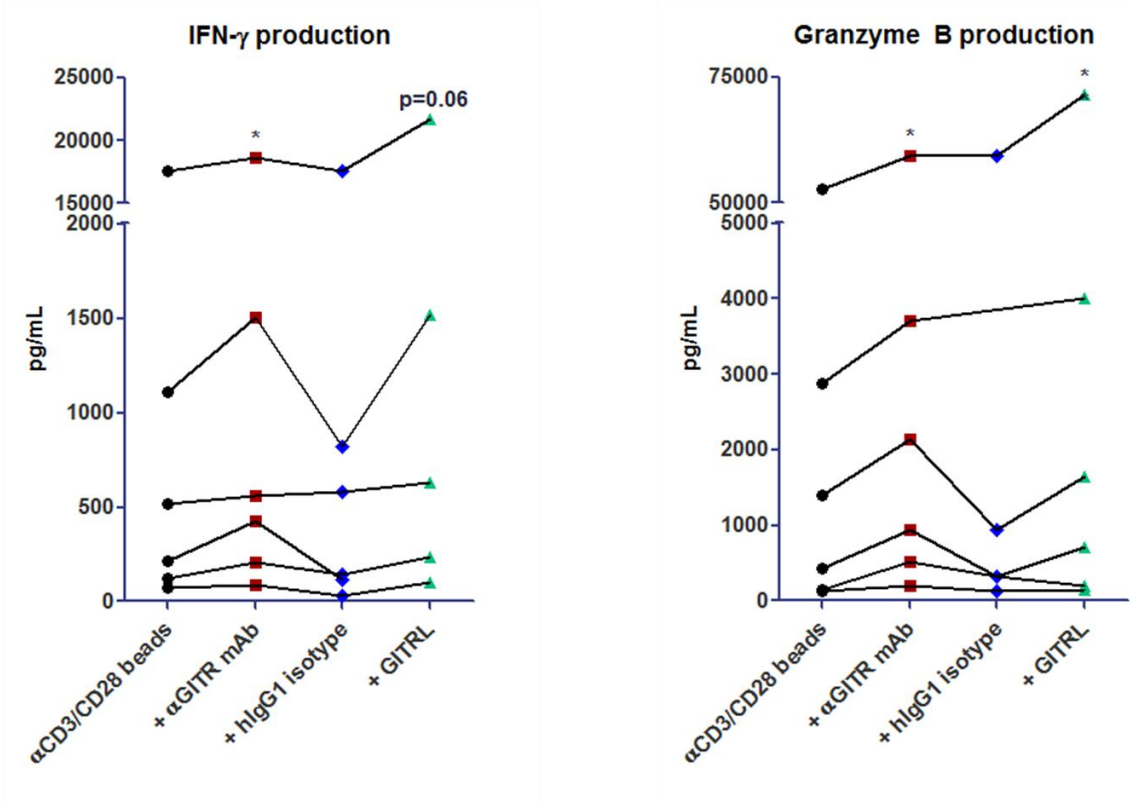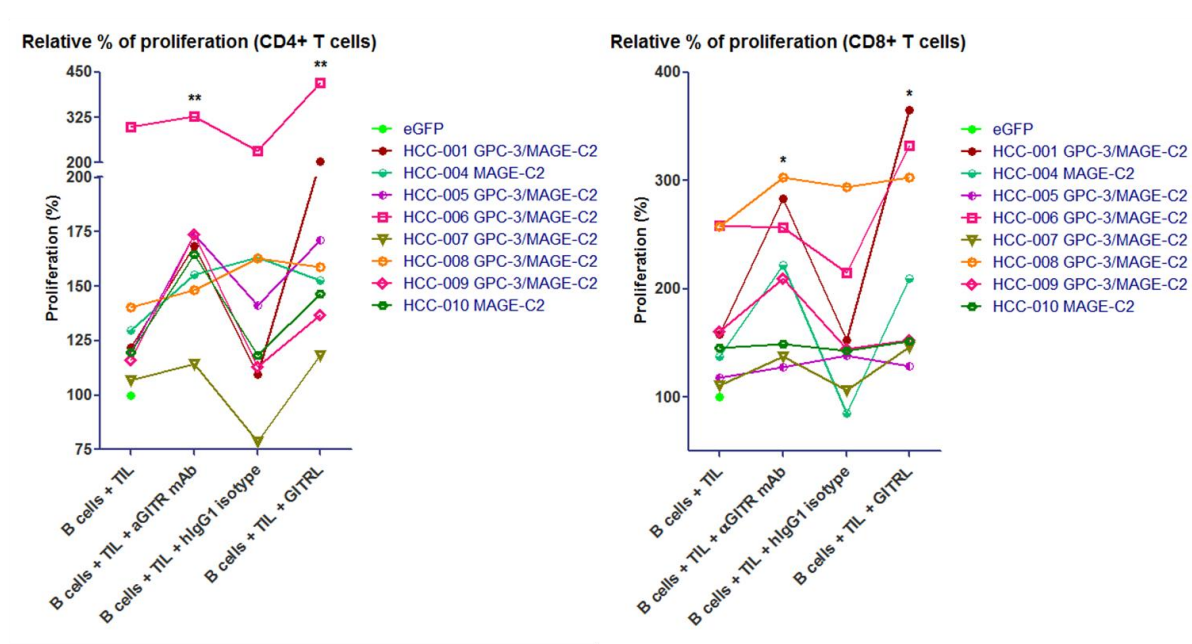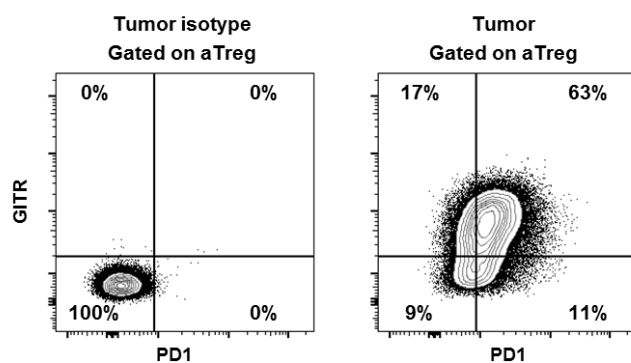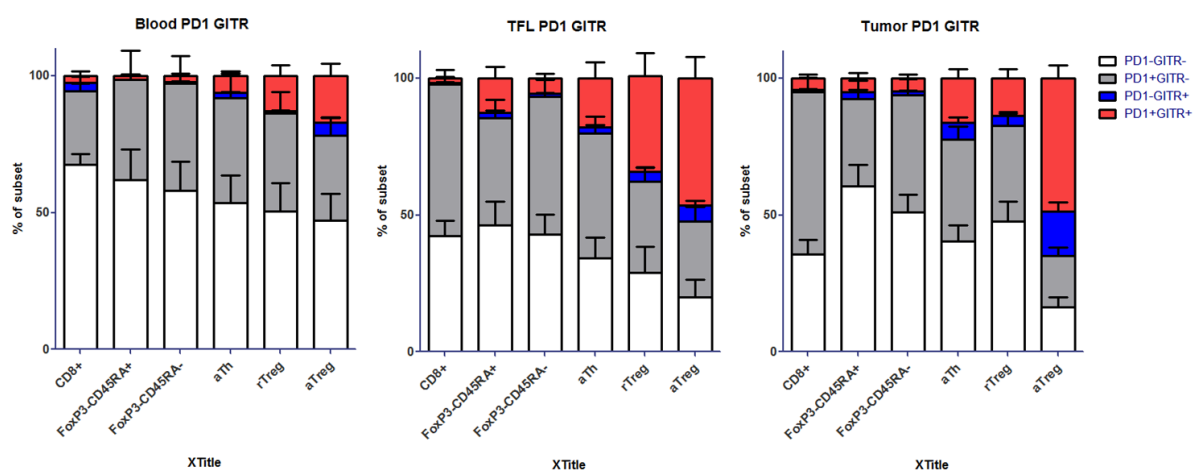
Figure 7 A/B

Relative % of proliferation (CD4+ T cells)

Proliferation (%)

** **

B cells + TIL   B cells + TIL + αPD1 mAb   B cells + TIL + hIgG4 isotype   B cells + TIL + αPD1+GITRL

- eGFP
- HCC-001 GPC-3/MAGE-C2
- HCC-004 MAGE-C2
- HCC-005 GPC-3/MAGE-C2
- HCC-006 GPC-3/MAGE-C2
- HCC-007 GPC-3/MAGE-C2
- HCC-008 GPC-3/MAGE-C2
- HCC-009 GCP-3/MAGE-C2
- HCC-010 MAGE-C2

Relative % of proliferation (CD8+ T cells)

Proliferation (%)

$p = 0.05$

$p = 0.05$

B cells + TIL   B cells + TIL + αPD1 mAb   B cells + TIL + hIgG4 isotype   B cells + TIL + αPD1+GITRL

- eGFP
- HCC-001 GPC-3/MAGE-C2
- HCC-004 MAGE-C2
- HCC-005 GPC-3/MAGE-C2
- HCC-006 GPC-3/MAGE-C2
- HCC-007 GPC-3/MAGE-C2
- HCC-008 GPC-3/MAGE-C2
- HCC-009 GCP-3/MAGE-C2
- HCC-010 MAGE-C2

Supplementary Figure 1 A/B

Supplementary Figure 2
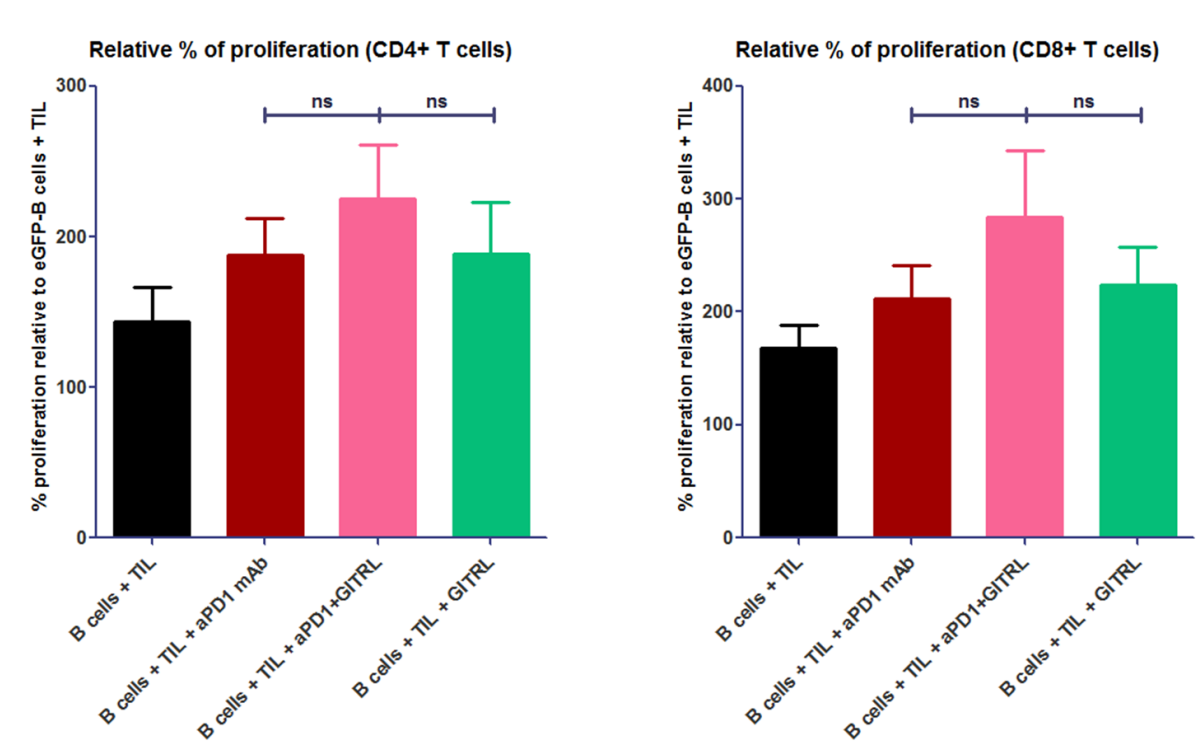
Supplementary figure legends

Supplementary Figure 1. Distribution of NK, NKT, and T cell subsets in blood, tumor-free liver, and HCC tumor tissues. (A) Frequencies of $CD3^-CD56^+$ NK cells, $CD3^+CD56^+$ NKT cells, and $CD3^+CD56^-$ T cells within $CD45^+$ mononuclear leukocytes. N=11-12 patients. (B) Frequencies of $CD8^+$ T cells, $CD4^+FoxP3^-$ T cells (Th), and $CD4^+FoxP3^+$ T cells (Treg) within $CD3^+$ cells. N=16-20 patients. Dots represent individual patients and lines present means. *=p<0.05; **=p<0.01; ***=p<0.001.

Supplementary Figure 2. Effects of single targeting of PD1 or GITRL and **combined targeting of PD1 and GITR on TIL proliferation in response to tumor antigens presented by mRNA-transfected autologous B cells.** Effects of 10 µg/mL antagonistic anti-PD1 antibody (nivolumab), soluble GITRL (1 µg/mL crosslinked with anti-HA antibody), or anti-PD1 antibody combined with soluble GITRL on proliferation of (A) tumor-derived $CD4^+$ T cells, and (B) tumor-derived $CD8^+$ T cells upon 6 days' culture of CFSE-labeled tumor-derived mononuclear cells with B cell blasts electroporated with mRNA encoding tumor antigens GPC3 or MAGEC2 (or eGFP as a control). Proliferation was measured by determination of percentages of $CD4^+$ or $CD8^+$ T cells with CFSE dilution at the end of the culture. Baseline proliferation (= % of $CFSE^{low}$ T cells in the presence of eGFP-electroporated B cells) was normalized to 100% for each tested patient. For those patients whose TIL responded to both tumor antigens, the average response to GPC3- and MAGEC2-electroporated B cells was depicted. Bars show mean percentages in cultures derived from n=8 patients with SEM.

REFERENCES

1.   Torre LA, Bray F, Siegel RL, et al. Global cancer statistics, 2012. CA Cancer J Clin 2015;65:87-108.
2.   Mazzanti R, Gramantieri L, Bolondi L. Hepatocellular carcinoma: epidemiology and clinical aspects. Mol Aspects Med 2008;29:130-43.
3.   El-Serag HB, Marrero JA, Rudolph L, et al. Diagnosis and treatment of hepatocellular carcinoma. Gastroenterology 2008;134:1752-63.
4.   Schachter J, Ribas A, Long GV, et al. Pembrolizumab versus ipilimumab for advanced melanoma: final overall survival results of a multicentre, randomised, open-label phase 3 study (KEYNOTE-006). Lancet 2017;390:1853-1862.
5.   Kang YK, Boku N, Satoh T, et al. Nivolumab in patients with advanced gastric or gastro-oesophageal junction cancer refractory to, or intolerant of, at least two previous chemotherapy regimens (ONO-4538-12, ATTRACTION-2): a randomised, double-blind, placebo-controlled, phase 3 trial. Lancet 2017;390:2461-2471.
6.   Rittmeyer A, Barlesi F, Waterkamp D, et al. Atezolizumab versus docetaxel in patients with previously treated non-small-cell lung cancer (OAK): a phase 3, open-label, multicentre randomised controlled trial. Lancet 2017;389:255-265.

7.   Bellmunt J, de Wit R, Vaughn DJ, et al. Pembrolizumab as Second-Line Therapy for Advanced Urothelial Carcinoma. N Engl J Med 2017;376:1015-1026.

8.   Larkin J, Chiarion-Sileni V, Gonzalez R, et al. Combined Nivolumab and Ipilimumab or Monotherapy in Untreated Melanoma. N Engl J Med 2015;373:23-34.

9.   McDermott DF, Drake CG, Sznol M, et al. Survival, Durable Response, and Long-Term Safety in Patients With Previously Treated Advanced Renal Cell Carcinoma Receiving Nivolumab. J Clin Oncol 2015;33:2013-20.

10.   Topalian SL, Sznol M, McDermott DF, et al. Survival, durable tumor remission, and long-term safety in patients with advanced melanoma receiving nivolumab. J Clin Oncol 2014;32:1020-30.

11.   Borghaei H, Paz-Ares L, Horn L, et al. Nivolumab versus Docetaxel in Advanced Nonsquamous Non-Small-Cell Lung Cancer. N Engl J Med 2015;373:1627-39.

12.   Hamid O, Robert C, Daud A, et al. Safety and tumor responses with lambrolizumab (anti-PD-1) in melanoma. N Engl J Med 2013;369:134-44.

13.   El-Khoueiry AB, Sangro B, Yau T, et al. Nivolumab in patients with advanced hepatocellular carcinoma (CheckMate 040): an open-label, non-comparative, phase 1/2 dose escalation and expansion trial. Lancet 2017;389:2492-2502.

14.   Sagiv-Barfi I, Czerwinski DK, Levy S, et al. Eradication of spontaneous malignancy by local immunotherapy. Sci Transl Med 2018;10.

15.   Kvistborg P, Philips D, Kelderman S, et al. Anti-CTLA-4 therapy broadens the melanoma-reactive CD8+ T cell response. Sci Transl Med 2014;6:254ra128.

16.   Knee DA, Hewes B, Brogdon JL. Rationale for anti-GITR cancer immunotherapy. Eur J Cancer 2016;67:1-10.

17.   Waight JD, Gombos RB, Wilson NS. Harnessing co-stimulatory TNF receptors for cancer immunotherapy: Current approaches and future opportunities. Hum Antibodies 2017;25:87-109.

18.   Zhou G, Sprengers D, Boor PPC, et al. Antibodies Against Immune Checkpoint Molecules Restore Functions of Tumor-Infiltrating T Cells in Hepatocellular Carcinomas. Gastroenterology 2017;153:1107-1119 e10.

19.   Pedroza-Gonzalez A, Verhoef C, Ijzermans JN, et al. Activated tumor-infiltrating CD4+ regulatory T cells restrain antitumor immunity in patients with primary or metastatic liver cancer. Hepatology 2013;57:183-94.

20.   Flecken T, Schmidt N, Hild S, et al. Immunodominance and functional alterations of tumor-associated antigen-specific CD8+ T-cell responses in hepatocellular carcinoma. Hepatology 2014;59:1415-26.

21.   Pedroza-Gonzalez A, Zhou G, Vargas-Mendez E, et al. Tumor-infiltrating plasmacytoid dendritic cells promote immunosuppression by Tr1 cells in human liver tumors. Oncoimmunology 2015;4:e1008355.

22.   Pedroza-Gonzalez A, Zhou G, Singh SP, et al. GITR engagement in combination with CTLA-4 blockade completely abrogates immunosuppression mediated by human liver tumor-derived regulatory T cells ex vivo. Oncoimmunology 2015;4:e1051297.

23.   Miyara M, Yoshioka Y, Kitoh A, et al. Functional delineation and differentiation dynamics of human CD4+ T cells expressing the FoxP3 transcription factor. Immunity 2009;30:899-911.

24.   Liu W, Putnam AL, Xu-Yu Z, et al. CD127 expression inversely correlates with FoxP3 and suppressive function of human CD4+ T reg cells. J Exp Med 2006;203:1701-11.

25.   Saito T, Nishikawa H, Wada H, et al. Two FOXP3(+)CD4(+) T cell subpopulations distinctly control the prognosis of colorectal cancers. Nat Med 2016;22:679-84.

26.   Sukumar S, Wilson DC, Yu Y, et al. Characterization of MK-4166, a Clinical Agonistic Antibody That Targets Human GITR and Inhibits the Generation and Suppressive Effects of T Regulatory Cells. Cancer Res 2017;77:4378-4388.

27.   Lu L, Xu X, Zhang B, et al. Combined PD-1 blockade and GITR triggering induce a potent antitumor immunity in murine cancer models and synergizes with chemotherapeutic drugs. J Transl Med 2014;12:36.

28.   Grohmann U, Volpi C, Fallarino F, et al. Reverse signaling through GITR ligand enables dexamethasone to activate IDO in allergy. Nat Med 2007;13:579-86.

CHAPTER 9

General discussion and summary

Liver cancer represents the second most common cause of cancer-related mortality worldwide. Hepatocellular carcinoma (HCC) is the most prevalent primary liver cancer, cholangiocarcinoma (CCA) second. Liver metastasis of colorectal cancer (LM-CRC) is the most common secondary liver cancer and a leading cause of death from CRC. The current therapeutic options for all three types of liver cancer are very limited. Hence, there is a pressing need for novel and effective treatments. The goals of this thesis are: 1) to determine whether regulatory T cells and co-inhibitory immune checkpoint pathways contribute to the immunosuppression within the tumor microenvironment in liver cancers, 2) and to identify potential promising targets to alleviate these immune suppressive mechanisms, thereby enhancing anti-tumor functions of tumor-infiltrating T cells in patients with liver cancer. In this chapter we will summarize and discuss the main findings in this thesis and propose suggestions for future research.

In **Chapter 1,** we review the current knowledge on immune suppressive mechanisms in the tumor microenvironment of HCC, CCA and LM-CRC, summarize the results of clinical studies to overcome these immune suppressive mechanisms, suggest alternative therapeutic approaches to abrogate these mechanisms based on the described novel insights from preclinical studies, and point out the current gaps in our knowledge on immune suppressive mechanisms in the tumor microenvironment of liver cancer. We discuss 1) suppressive immune cell subsets such as conventional regulatory T cells and type 1 regulatory T cells that can supress effector T cell functions, 2) co-inhibitory pathways between T cells expressing co-inhibitory receptors and other immune cells and tumor cells expressing the ligands for these receptors, 3) intra-tumoral enzymes generating immune suppressive metabolites, 4) inhibition of migration of immune effector cells into the tumors, which leads to a paucity of immune cells inside liver cancers.

Regulation of intra-tumoral suppressor T cells in liver cancers

Part I focuses on conventional regulatory T cells (Treg) and type 1 regulatory T cells (Tr1). We have studied how to abrogate the immune suppression exerted by these cells in the tumor microenvironment (Figure 1).

In **Chapter 2**, we show that treatment with a soluble form of the natural ligand of the co-stimulatory receptor GITR, or a blocking antibody to co-inhibitory receptor CTLA4, reduced *ex vivo* suppression of effector $CD4^+$ T cells mediated by $CD4^+Foxp3^+$ Treg isolated from HCC and LM-CRC tumors, thereby restoring effector T cell proliferation and cytokine production. Importantly, a combination of low doses of both treatments exhibited a stronger recovery of effector T cell function in the presence of tumor-derived Treg compared with

either treatment alone. Our data suggest that in patients with HCC or LM-CRC both GITR-ligation and anti-CTLA-4 antibody can improve antigen-specific T cell responses in the tumors by decreasing tumor-infiltrating Treg-mediated suppression. However, as part of an immunotherapeutic strategy, combining low doses of both drugs may be at least as effective as monotherapy with higher doses of either drug.

In **Chapter 3**, we identified a population of tumor-infiltrating Tr1 cells that contributes to local immune suppression in an IL-10 dependent manner in HCC and LM-CRC. Importantly, the presence of tumor-infiltrating Tr1 cells is correlated with tumor infiltration of plasmacytoid dendritic cells. Plasmacytoid dendritic cells may drive intra-tumoral immunosuppression by Tr1 cells through stimulating IL-10 production by Tr1 cells via ICOS/ICOS-ligand signaling. Therefore, Tr1 cells may inhibit anti-tumor immunity in HCC and LM-CRC and thereby foster tumor progression. Blockade of the engagement of ICOS on Tr1 cells and ICOS-ligand on plasmacytoid dendritic cells may provide alleviation of this intra-tumoral immunosuppressive mechanism, and provide a new potential immunotherapeutic approach for patients with solid cancers in which IL-10-producing CD4$^+$ T cells are present, .

In **Chapter 4**, we propose that CD25 is a less attractive target for cancer immunotherapy in humans than originally suggested by Arce Vargas et al.,(1) because CD25 is not solely expressed on conventional Treg, but also on CD4$^+$Foxp3^{low}CD45RA$^-$ non-Treg in tumors, tumor-free tissues, lymph nodes and peripheral blood of HCC and CRC patients. CD25 antibody-mediated depletion of these cells may counteract the enhancement of anti-tumor immunity by Treg depletion. In addition, based on the observed reduction of CD16 (FcγR III) expression on intra-tumoral NK cells in cancer patients, the capacity of antibody-dependent cell-mediated cytotoxicity (ADCC) to deplete immune cells in human tumors may be more limited than previously expected. Therefore, CD25-depleting antibodies might not be appropriate for intra-tumoral Treg depletion in humans. Future research to develop Treg-depleting antibody therapies should focus on other targets than CD25.

Higher frequencies of Treg have been observed in HCC and LM-CRC tumors compared to paired tumor-free liver tissues and blood in Part I, and the same finding is also described for CCA tumors in Part II of this thesis. In addition, lower frequencies of CD8$^+$ cytotoxic T cells, natural killer T cells and natural killer cells as well as lower expression of the cytotoxic effector molecules perforin and granzyme B in CD8$^+$ T cells in HCC and LM-CRC tumors have previously been reported by us,(2) and are reported in Part II of this thesis for CCA tumors. These data indicate that the composition of immune infiltrates in liver tumors has immunosuppressive properties. It has been reported that the composition of tumor-infiltrating

lymphocytes is associated with the prognosis of liver cancers, for instance increased numbers of intra-tumoral Treg are associated with disease progression and recurrence.(3-8) Moreover, higher number of intra-tumoral Treg has been associated with increased numbers of intra-tumoral macrophages, circulating myeloid-derived suppressor cells, and with a compromised intra-tumoral CD8^{+} T cell response.(9-13) Altogether these observations suggest that depletion or inhibition of intra-tumoral Treg and concomitant stimulation of immune effector cells may be effective to reduce tumor growth and recurrence as well as prolong survival of patients with liver cancer.

Until recently direct evidence for a role of Tr1 cells in human solid tumors was lacking. The recent description of co-expression of CD49b and LAG3 as markers that can specifically identify this population of cells,(14) enabled us to show that the majority of liver tumor-infiltrating IL-10-producing CD4^{+} T cells consists of Tr1 cells and only a minor proportion corresponds to Th2 cells or Foxp3^{+} Treg. Our data demonstrate a possible interaction between Tr1 cells and plasmacytoid dendritic cells by which tumor-infiltrating Tr1 cells may be activated by plasmacytoid dendritic cells present in the tumor microenvironment. The main population expressing ICOS-ligand in tumor tissues are CD123^{+} plasmacytoid dendritic cells. There is substantial evidence indicating that plasmacytoid dendritic cells have a specialized role in the induction of peripheral tolerance by inducing IL-10 production by conventional Treg through ICOS-ICOS-ligand signaling.(15, 16) Stimulation of conventional Treg to produce IL-10 by plasmacytoid dendritic cells has been described in breast cancer and ovarian cancer.(17, 18) Our results are consistent with a role for plasmacytoid dendritic cells to stimulate IL-10 production by Tr1 cells in the tumor microenvironment of patients with liver cancer. Altogether these data suggest that ICOS co-stimulation represents a potential target for immunotherapeutic intervention, affecting tumor-specific immunosuppression mediated by both Treg and Tr1 cells.

In addition, other issues have already been discussed in the previous chapters.

Regulation of intra-tumoral effector T cells in liver cancers

Part II focuses on CD8^{+} cytotoxic T cells (CTL) and CD4^{+} T helper cells (Th). Here, we have studied how to invigorate effector functions of tumor-infiltrating T cells by targeting co-inhibitory and co-stimulatory immune checkpoint pathways (Figure 1).

In **Chapter 5**, we conclude that co-inhibitory receptors PD-1, TIM3 and LAG3 are upregulated on tumor antigen-specific CD8^{+} T cells isolated from patient HCC tumor tissues. Myeloid dendritic cells, monocytes and B cells in HCC tumors express ligands for these

receptors. Compared with tumor-infiltrating CD8^{+} CTL and CD4^{+} Th that did not express these co-inhibitory receptors, tumor-infiltrating CTL and Th that did express these receptors showed higher levels of activation markers, but similar or decreased levels of granzyme B and effector cytokines. While blocking a single co-inhibitory pathway had variable effects on *ex vivo* functional responses of HCC-derived T cells, combining antibody against PD-L1 with antibodies against TIM3, LAG3 or CTLA4 revitalized *ex vivo* tumor-specific responses of HCC-derived CD8^{+} and CD4^{+} T cells in most patients and additively enhanced these effects compared to single PD-L1 blockade. Overall, the aforementioned combined targeting of co-inhibitory checkpoints is a promising immunotherapeutic strategy for HCC, and may result in superior clinical responses in more patients than targeting a single co-inhibitory checkpoint.

In **Chapter 6**, we demonstrate higher proportions of CD8^{+} T cells, myeloid dendritic cells and monocytes within immune cells isolated from mismatch repair (MMR)-proficient LM-CRC compared to immune cells derived from MMR-proficient primary CRC, suggesting an increased cytotoxic and antigen-presenting capacity of immune infiltrates in LM-CRC. In addition, we observed increased expression of co-inhibitory receptors on intra-tumoral T cells in MMR-proficient LM-CRC, which suggests that tumor-infiltrating T cells in MMR-proficient LM-CRC may be more sensitive to immune checkpoint inhibitors than tumor-infiltrating T cells in MMR-proficient primary CRC. Antibody blockade of LAG3 or PD-L1 enhanced *ex vivo* effector functions of CD8^{+} and CD4^{+} T cells derived from MMR-proficient LM-CRC, with LAG3 blockade showing the most robust effects on tumor-specific responses. In addition, higher LAG3 expression on intra-tumoral CD8^{+} T cells associated with longer progression-free survival of LM-CRC patients. Overall, LAG3 may be a new promising immunotherapeutic target for LM-CRC, even for MMR-proficient tumor type. Clinical studies focusing on responses of LM-CRC to anti-LAG3 antibody treatment are recommended.

In **Chapter 7**, we analyzed the composition and characteristics of intra-tumoral immune infiltrates in CCA. We found decreased numbers of cytotoxic lymphocytes and increased numbers of Treg in CCA tumors compared with paired tumor-free liver tissues. While Treg infiltrate into the tumors, the majority of CD8^{+} CTL and CD4^{+} Th are sequestered at the tumor margin. Furthermore, intra-tumoral CD8^{+} T cells show reduced expression of cytotoxic molecules compared with T cells in tumor-free liver tissues and blood. Expression of co-inhibitory receptors PD-1 and CTLA4 as well as co-stimulatory receptor GITR are upregulated on tumor-infiltrating T cells compared to T cells in tumor-free liver tissues and blood. Stimulation of GITR by the soluble ligand or blocking PD-1 by a therapeutic human antibody enhanced the effector functions of CCA-derived CD8^{+} and CD4^{+} T cells *ex vivo*,

which indicates that these two molecules are potential targets for immunotherapy of CCA patients.

In **Chapter 8**, we evaluated a proof of concept that agonists of co-stimulatory molecules may be effective for HCC immune therapy. We observed the highest GITR expression on CD4$^+$Foxp3^{hi}CD45RA$^-$ activated Treg in HCC tumors, although GITR expression on activated Treg in tumor-free liver tissues and blood was also higher than on CD4$^+$ Th and CD8$^+$ CTL in the same compartments. Furthermore, addition of recombinant GITR-ligand or humanized agonistic antibody to GITR to CD8$^+$ and CD4$^+$ T cells isolated from HCC tumors invigorated their responses to stimulations with polyclonal antigens and tumor antigens. Agonistic targeting of GITR may therefore be a potential strategy for single or combinatorial immunotherapy in HCC.

Interestingly, PD-1-expressing cells are increased in CD8$^+$ CTL, Th and Treg in HCC, LM-CRC and CCA tumors, while TIM3-expressing cells are increased in CD8$^+$ CTL and Treg, while CTLA4-expressing cells are increased in CD8$^+$ CTL and Th, and GITR-expressing cells are increased in Treg in all liver tumors compared with paired tumor-free liver tissues and blood, but LAG3 is not upregulated in CCA tumors (some data are not shown in the thesis).

In HCC, co-inhibitory receptors PD-1, TIM3 and LAG3 are selectively upregulated on intra-tumoral tumor antigen-specific CD8$^+$ T cells. The selective increased expression of these co-inhibitory receptors on tumor antigen-specific T cells together with the expression of their respective ligands on antigen-presenting cells in HCC tumors suggests that these co-inhibitory pathways may be involved in the regulation of tumor antigen-specific responsiveness of intra-tumoral T cells.

In both HCC and LM-CRC, tumor-infiltrating CD8$^+$ CTL and CD4$^+$ Th that expressed PD-1, TIM3, LAG3 or CTLA4 displayed higher levels of activation markers, compared with their counterparts that did not express the corresponding co-inhibitory receptor, except for CD69 expression on LAG3$^+$CD8$^+$ versus LAG3$^-$CD8$^+$ T cells. However, the tumor-infiltrating T cells expressing either co-inhibitory receptor displayed comparable or lower levels of effector cytokines and/or cytotoxic molecules. Expression of co-inhibitory receptors on T cells can be induced by recent T cell activation upon recognition of tumor antigens,(19, 20) but continuous expression of increasing numbers of co-inhibitory receptors often coincides with gradual loss of effector T cell functions due to chronic antigenic stimulation.(21-23) Our findings indicate that, in accordance with recent studies in other human cancers,(23-25) tumor-infiltrating T cells that express co-inhibitory receptors are probably tumor-reactive T cells, which continue to upregulate the expression of these receptors in response to chronic

stimulation by tumor antigens to prevent further over activation, and thereby are subsequently inhibited by the interactions of these receptors with their ligands on tumor cells or antigen-presenting cells.

In all the *in vitro* functional assays of HCC, LM-CRC and CCA, we used total tumor-infiltrating mononuclear leukocytes which contained both T cells expressing co-inhibitory receptors and antigen-presenting cells expressing their ligands, because we were interested in the net effects of antibody interventions on intra-tumoral T cell responses in a context that resembled the tumor microenvironment as much as possible. Consequently, intra-tumoral Treg, Tr1 cells and probably other types of immune suppressor cells were also present. Therefore, the reported functional effects of antibodies on effector T cells in these assays may be partly indirect, mediated by the effects of these antibodies on immune suppressor cells. A limitation of our *in vitro* assays is the lack of tumor cells which can also express ligands for co-inhibitory receptors and exert other unknown immunosuppressive effects. Therefore tumor-infiltrating T cells might be more suppressed *in vivo* than in our *ex vivo* culture models.

In HCC, targeting either CTLA4 or GITR has been shown to both reduce the immunosuppression mediated by tumor-infiltrating Treg (Part I) and restore anti-tumor functions of tumor-infiltrating effector T cells (Part II). Although the mechanisms by which these molecules exert their immunomodulatory effects are still elusive, our results suggest that they can act either by abrogating the suppressive function of Treg or by rendering effector T cells resistant to Treg-mediated suppression.

Additionally, other issues have already been discussed in the previous chapters.

Overall conclusions and future perspectives

The ultimate aim of this thesis is to provide new immunotherapeutic approaches to treat patients with primary liver cancer or CRC liver metastasis. Our studies show that, increased proportions of Treg and Tr1 cells and decreased proportions of cytotoxic lymphocytes in immune infiltrates within liver tumors, as well as elevated expression of several co-inhibitory receptors on tumor-infiltrating T cells and the presence of their ligands in human liver tumors, both contribute to an immunosuppressive tumor microenvironment in liver cancers. Co-inhibitory pathways CTLA4-CD80/CD86, PD-1-PD-L1, TIM3-galectin 9, LAG3-MHC class II and co-stimulatory pathways GITR-GITR-ligand and ICOS-ICOS-ligand play an important role in regulating intra-tumor T cell immunity in patients with HCC, CCA or LM-CRC. This thesis provides new clues for immunotherapeutic interventions to overcome the abovementioned immune suppressive mechanisms and to reinforce the anti-tumor reactivity,

by demonstrating that combined blockade of PD-1/PD-L1 and TIM3, LAG3 or CTLA4 as well as stimulation of GITR are effective in reinvigorating tumor-derived T cells in HCC, antibody against LAG3 has similar potential for LM-CRC, while agonistic antibody of GITR and blocking antibody of PD-1/PD-L1 are suggested for CCA.

Currently, several clinical trials exploring the effects of anti-PD-1 antibodies in CCA patients are ongoing. Clinical trials investigating whether combination treatments of anti-PD-1/PD-L1 antibodies and anti-CTLA4 antibodies result in improved clinical efficacy are also ongoing in HCC and CCA patients. In addition, GITR agonistic antibody combined with PD-1 and/or CTLA4 antagonistic antibody, CD134 agonistic antibody combined with PD-1 and/or CTLA4 antagonistic antibody, CD134 agonistic antibody in combination with CD137 agonistic antibody are being tested in HCC patients.(26)[ClinicalTrials.gov] However, clinical trials on immunotherapy with anti-TIM3 and anti-LAG3 antibodies have not been initiated in patients with liver cancer. Moreover, clinical studies on LAG3 antagonistic antibody for patients with LM-CRC and clinical studies on GITR agonistic antibody for patients with CCA are lacking. Further research on co-expression of different immune checkpoints and clinical efficacy of combinatorial immunotherapies in patients with liver cancer is definitely needed to improve the clinical outcome.
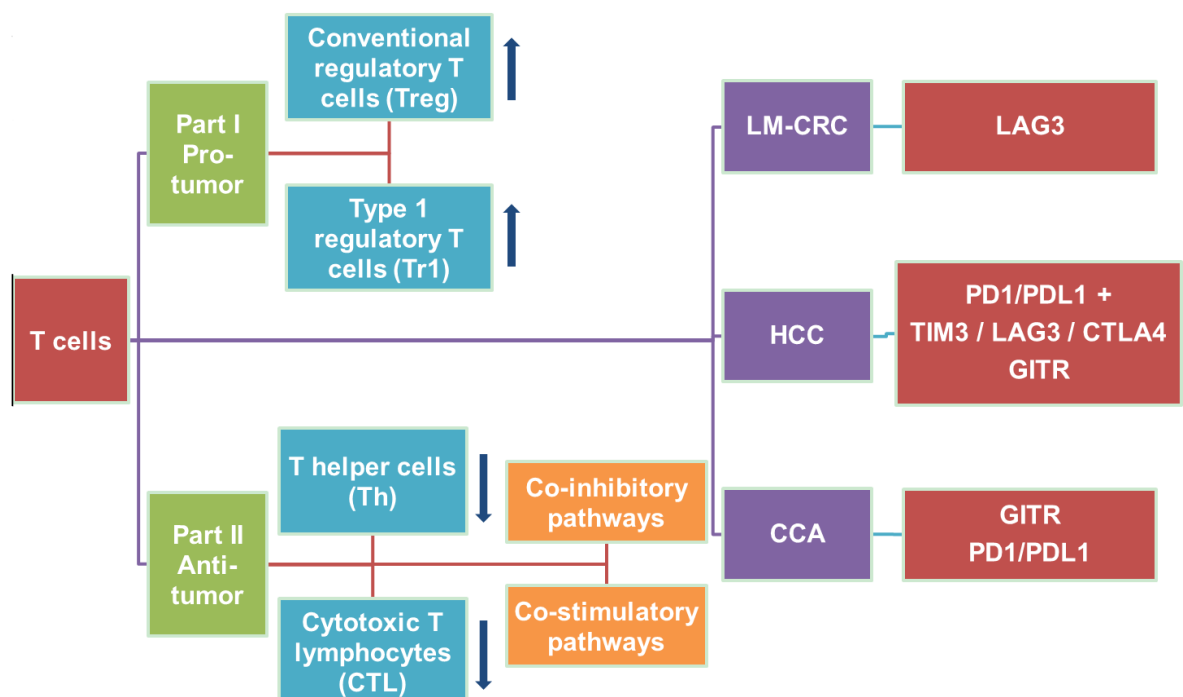

Figure 1. Summary of the main findings of the thesis

REFERENCES

1.   Arce Vargas F, Furness AJS, Solomon I, Joshi K, Mekkaoui L, Lesko MH, et al. Fc-Optimized Anti-CD25 Depletes Tumor-Infiltrating Regulatory T Cells and Synergizes with PD-1 Blockade to Eradicate Established Tumors. Immunity. 2017;46(4):577-86.

2.   Pedroza-Gonzalez A, Verhoef C, Ijzermans JN, Peppelenbosch MP, Kwekkeboom J, Verheij J, et al. Activated tumor-infiltrating CD4+ regulatory T cells restrain antitumor immunity in patients with primary or metastatic liver cancer. Hepatology. 2013;57(1):183-94.

3.   Kobayashi N, Hiraoka N, Yamagami W, Ojima H, Kanai Y, Kosuge T, et al. FOXP3+ regulatory T cells affect the development and progression of hepatocarcinogenesis. Clin Cancer Res. 2007;13(3):902-11.

4.   Chen KJ, Lin SZ, Zhou L, Xie HY, Zhou WH, Taki-Eldin A, et al. Selective recruitment of regulatory T cell through CCR6-CCL20 in hepatocellular carcinoma fosters tumor progression and predicts poor prognosis. PLoS One. 2011;6(9):e24671.

5.   Shen X, Li N, Li H, Zhang T, Wang F, Li Q. Increased prevalence of regulatory T cells in the tumor microenvironment and its correlation with TNM stage of hepatocellular carcinoma. J Cancer Res Clin Oncol. 2010;136(11):1745-54.

6.   Ling KL, Pratap SE, Bates GJ, Singh B, Mortensen NJ, George BD, et al. Increased frequency of regulatory T cells in peripheral blood and tumour infiltrating lymphocytes in colorectal cancer patients. Cancer Immun. 2007;7:7.

7.   Brudvik KW, Henjum K, Aandahl EM, Bjornbeth BA, Tasken K. Regulatory T-cell-mediated inhibition of antitumor immune responses is associated with clinical outcome in patients with liver metastasis from colorectal cancer. Cancer Immunol Immunother. 2012;61(7):1045-53.

8.   Sasaki A, Tanaka F, Mimori K, Inoue H, Kai S, Shibata K, et al. Prognostic value of tumor-infiltrating FOXP3+ regulatory T cells in patients with hepatocellular carcinoma. Eur J Surg Oncol. 2008;34(2):173-9.

9.   Zhou J, Ding T, Pan W, Zhu LY, Li L, Zheng L. Increased intratumoral regulatory T cells are related to intratumoral macrophages and poor prognosis in hepatocellular carcinoma patients. Int J Cancer. 2009;125(7):1640-8.

10.   Liu J, Zhang N, Li Q, Zhang W, Ke F, Leng Q, et al. Tumor-associated macrophages recruit CCR6+ regulatory T cells and promote the development of colorectal cancer via enhancing CCL20 production in mice. PLoS One. 2011;6(4):e19495.

11.   Hoechst B, Ormandy LA, Ballmaier M, Lehner F, Kruger C, Manns MP, et al. A new population of myeloid-derived suppressor cells in hepatocellular carcinoma patients induces CD4(+)CD25(+)Foxp3(+) T cells. Gastroenterology. 2008;135(1):234-43.

12.   Fu J, Xu D, Liu Z, Shi M, Zhao P, Fu B, et al. Increased regulatory T cells correlate with CD8 T-cell impairment and poor survival in hepatocellular carcinoma patients. Gastroenterology. 2007;132(7):2328-39.

13.   Unitt E, Rushbrook SM, Marshall A, Davies S, Gibbs P, Morris LS, et al. Compromised lymphocytes infiltrate hepatocellular carcinoma: the role of T-regulatory cells. Hepatology. 2005;41(4):722-30.

14.   Gagliani N, Magnani CF, Huber S, Gianolini ME, Pala M, Licona-Limon P, et al. Coexpression of CD49b and LAG-3 identifies human and mouse T regulatory type 1 cells. Nat Med. 2013;19(6):739-46.

15.   Ito T, Yang M, Wang YH, Lande R, Gregorio J, Perng OA, et al. Plasmacytoid dendritic cells prime IL-10-producing T regulatory cells by inducible costimulator ligand. J Exp Med. 2007;204(1):105-15.

16.   Akbari O, Freeman GJ, Meyer EH, Greenfield EA, Chang TT, Sharpe AH, et al. Antigen-specific regulatory T cells develop via the ICOS-ICOS-ligand pathway and inhibit allergen-induced airway hyperreactivity. Nat Med. 2002;8(9):1024-32.

17.   Conrad C, Gregorio J, Wang YH, Ito T, Meller S, Hanabuchi S, et al. Plasmacytoid dendritic cells promote immunosuppression in ovarian cancer via ICOS costimulation of Foxp3(+) T-regulatory cells. Cancer Res. 2012;72(20):5240-9.

18.   Sisirak V, Faget J, Gobert M, Goutagny N, Vey N, Treilleux I, et al. Impaired IFN-alpha production by plasmacytoid dendritic cells favors regulatory T-cell expansion that may contribute to breast cancer progression. Cancer Res. 2012;72(20):5188-97.

19.   Baitsch L, Legat A, Barba L, Fuertes Marraco SA, Rivals JP, Baumgaertner P, et al. Extended co-expression of inhibitory receptors by human CD8 T-cells depending on differentiation, antigen-specificity and anatomical localization. PLoS One. 2012;7(2):e30852.

20.		Legat A, Speiser DE, Pircher H, Zehn D, Fuertes Marraco SA. Inhibitory Receptor Expression Depends More Dominantly on Differentiation and Activation than "Exhaustion" of Human CD8 T Cells. Front Immunol. 2013;4:455.

21.		Fourcade J, Sun Z, Benallaoua M, Guillaume P, Luescher IF, Sander C, et al. Upregulation of Tim-3 and PD-1 expression is associated with tumor antigen-specific CD8+ T cell dysfunction in melanoma patients. J Exp Med. 2010;207(10):2175-86.

22.		Fourcade J, Sun Z, Pagliano O, Guillaume P, Luescher IF, Sander C, et al. CD8(+) T cells specific for tumor antigens can be rendered dysfunctional by the tumor microenvironment through upregulation of the inhibitory receptors BTLA and PD-1. Cancer Res. 2012;72(4):887-96.

23.		Matsuzaki J, Gnjatic S, Mhawech-Fauceglia P, Beck A, Miller A, Tsuji T, et al. Tumor-infiltrating NY-ESO-1-specific CD8+ T cells are negatively regulated by LAG-3 and PD-1 in human ovarian cancer. Proc Natl Acad Sci U S A. 2010;107(17):7875-80.

24.		Baitsch L, Baumgaertner P, Devevre E, Raghav SK, Legat A, Barba L, et al. Exhaustion of tumor-specific CD8(+) T cells in metastases from melanoma patients. J Clin Invest. 2011;121(6):2350-60.

25.		Gros A, Robbins PF, Yao X, Li YF, Turcotte S, Tran E, et al. PD-1 identifies the patient-specific CD8(+) tumor-reactive repertoire infiltrating human tumors. J Clin Invest. 2014;124(5):2246-59.

26.		ClinicalTrials.gov.

CHAPTER 10

Dutch Summary

Nederlandse samenvatting

Leverkanker is de op één na meest voorkomende oorzaak van kanker gerelateerde mortaliteit in de wereld. Hepatocellulair carcinoom (HCC) is de meest frequent voorkomende primaire leverkanker, cholangiocarcinoom (CCA) de tweede. In de lever gemetastaseerde colorectaal kanker (LM-CRC) is de meest voorkomende secundaire leverkanker, en de voornaamste doodsoorzaak van patiënten met colorectaal kanker (CRC). De huidige therapeutische mogelijkheden voor alle drie deze typen van leverkanker zijn heel beperkt. Vandaar dat er een dringende behoefte bestaat aan nieuwe en effectieve behandelmethoden. De doelen van dit proefschrift zijn: 1) om te bepalen of regulatoire T-cellen en co-inhibitoire immuun checkpoint routes bijdragen aan het immunosuppressieve micromilieu in levertumoren, en 2) om potentiël veelbelovende factoren te identificeren die deze immuun suppressieve mechanismen onderdrukken en daardoor de anti-tumor functie van de in de tumor infiltrerende T-cellen in patiënten met leverkanker versterken. In dit hoofdstuk zullen we de belangrijkste bevindingen samenvatten en bediscussiëren en suggesties geven voor toekomstig onderzoek.

In **hoofdstuk 1** geven we een overzicht van de actuele kennis over immunosuppressieve mechanismen in het tumor micromilieu van HCC, CCA en LM-CRC. We vatten de resultaten van klinische studies samen die proberen deze immunosuppressieve mechanismen te onderdrukken, we stellen alternatieve therapeutische benaderingen voor om deze mechanismen op te heffen gebaseerd op beschreven nieuwe inzichten van preklinische studies en we wijzen op actuele hiaten in onze kennis over immunosuppressieve mechanismen in het tumor micromilieu van leverkanker. We bediscussiëren 1) suppressieve immuun cel subsets zoals conventionele regulatoire T-cellen en type 1 regulatoire T-cellen die de functie van effector T-cellen kunnen onderdrukken, 2) co-inhibitoire interacties tussen T-cellen die co-inhibitoire receptoren tot expressie brengen en andere immuun cellen en tumor cellen, die de liganden voor deze receptoren tot expressie brengen, 3) enzymen in tumoren die metabolieten genereren die het immuunsysteem onderdrukken, 4) het verhinderen van de migratie van immuun effector cellen naar de tumor, wat leidt tot een te kort aan immuun cellen in leverkanker.

Regulatie van intra-tumorale suppressieve T-cellen in leverkanker

Deel I focust op conventionele regulatoire T-cellen (Treg) en type 1 regulatoire T-cellen (Tr1). We hebben bestudeerd hoe de immuun suppressie die wordt uitgeoefend door deze cellen kan worden onderdrukt in het tumor micromilieu (figuur 1).

In **hoofdstuk 2** laten we zien dat een oplosbare vorm van het natuurlijke ligand van de co-stimulatoire receptor GITR en/of een blokkerende antistof tegen de co-inhibitoire receptor

CTLA4 de *ex vivo* suppressie van effector CD4^{+} T-cellen door CD4^{+}Foxp3^{+} Treg uit HCC en LM-CRC tumoren vermindert, waardoor de celdeling en cytokine productie van deze effector T-cellen wordt hersteld. Belangrijk is hierbij dat een combinatie van lage doses van beide behandelingen een sterker herstel van de functie van effector T cellen laat zien in aanwezigheid van uit de tumor geïsoleerde Treg dan iedere behandeling afzonderlijk. Onze data suggereren dat behandeling van HCC en LM-CRC patiënten met GITR-ligatie of antistoffen tegen CTLA4 de antigen specifieke T-cel responsen kan verbeteren in tumoren door vermindering van de suppressie door in de tumor geïnfiltreerde Treg. Echter, als immunotherapeutische strategie kan een combinatie van een lage dosis van beiden medicijnen even effectief zijn als een monotherapie met een hoge dosis van één van deze medicijnen.

In **hoofdstuk 3** hebben we een populatie van in de tumor geïnfiltreerde Tr1 cellen geïdentificeerd die bijdraagt aan lokale immuun suppressie op een IL-10 afhankelijke manier in HCC en LM-CRC. De aantallen van Tr1 cellen in deze tumoren zijn positief gecorreleerd aan de aantallen in de tumor geïnfiltreerde plasmacytoïde dendritische cellen. We hebben aanwijzingen gevonden die erop wijzen dat plasmacytoïde dendritische cellen via ICOS/ICOS-ligand interacties de IL-10 productie van Tr1 cellen stimuleren en hierdoor bijdragen aan de door de Tr1 veroorzaakte intra-tumorale immuun suppressie. Dus Tr1 cellen kunnen mogelijk anti-tumor immuniteit onderdrukken in HCC en LM-CRC en daardoor de tumorprogressie bevorderen. Het blokkeren van de interactie van ICOS op de Tr1 cel en ICOS-ligand op de plasmacytoïde dendritische cel kan dit intra-tumorale immunosuppressieve mechanisme verminderen en een nieuwe potentiële immunotherapeutische benadering bieden voor patiënten met solide tumoren waarin IL-10-producerende CD4^{+} T-cellen aanwezig zijn.

In **hoofdstuk 4** suggereren we dat CD25 een minder aantrekkelijk doelwit is voor immunotherapie bij kanker bij mensen dan oorspronkelijk werd gesuggereerd door Arce Vargas et al., omdat CD25 niet alleen tot expressie komt op conventionele Treg, maar ook op CD4^{+}Foxp3[laag]CD45RA[-]non-Treg die voorkomen in tumoren, tumorvrije weefsels, lymfeklieren en perifeer bloed van HCC en CRC patiënten. CD25 antistof-gemedieerde depletie van deze cellen kan de verhoging van anti-tumor immuniteit door Treg-depletie tegengaan. Doordat intra-tumorale NK-cellen in kankerpatiënten minder CD16 (FcγR III) tot expressie brengen, kan bovendien het vermogen om immuun cellen in menselijke tumoren te depleteren door antistof-afhankelijke celgemedieerde cytotoxiciteit (ADCC), beperkter zijn dan eerder was verwacht. Daarom zijn CD25-depleterende antistoffen mogelijk niet geschikt voor intra-tumorale Treg-depletie bij mensen. Toekomstig onderzoek met betrekking tot

Treg-depletie met behulp van antistoffen zou zich moeten richten op andere doelwitten dan CD25.

Regulatie van intra-tumorale effector T cellen in levertumoren

Deel II focust op CD8⁺ cytotoxische T lymfocyten (CTL) en CD4⁺ T helper cellen (Th). In dit gedeelte hebben we bestudeerd hoe effector functies van tumor-infiltrerende T cellen kunnen worden versterkt door targeting van co-inhibitoire en co-stimulerende immuun checkpoint pathways (Figuur 1).

In **Hoofdstuk 5** concluderen we dat de co-inhibitoire receptoren PD-1, TIM3 en LAG3 verhoogd tot expressie komen op tumor antigen-specifieke CD8⁺ CTL geïsoleerd uit humane HCC-tumor weefsels. Myeloïde dendritische cellen, monocyten en B cellen in HCC tumoren brengen de liganden van deze receptoren tot expressie. Vergeleken met tumor-infiltrerende CD8+ CTL en CD4+ Th zonder co-inhibitoire receptoren, brengen de tumor-infiltrerende CTL en Th met deze receptoren, meer activatie markers tot expressie, maar is de hoeveelheid granzyme B en effector cytokines die ze tot expressie brengen, is vergelijkbaar of verminderd. Het blokkeren van één co-inhibitoire pathway had variabele effecten op *ex vivo* functionele responsen van HCC tumor infiltrerende lymphocyten, maar het combineren van een antagonistisch PD-L1 antistof met een antagonistisch TIM3, LAG3 of CTLA4 antilistof, versterkte *ex vivo* tumor-specifieke responsen van CD8+ en CD4+ T cellen geïsoleerd uit HCC in de meeste patiënten, en dit effect ervan was groter in vergelijking met alleen blokkering van PD-L1. We concluderen dat de eerdergenoemde combinatie therapie van co-inhibitoire checkpoint antistoffen een veelbelovende immunotherapeutische strategie is voor HCC, die zou kunnen resulteren in een superieure klinische respons in een groter percentage van de patiënten vergeleken met monotherapie met één co-inhibitoire checkpoint antistof.

In **Hoofdstuk 6** laten we zien dat immuun cellen geïsoleerd uit DNA mismatch repair (MMR)-proficiënte LM-CRC tumoren hogere proporties CD8⁺ T cellen, myeloïde dendritische cellen en monocyten bevatten dan immuun cellen geïsoleerd uit MMR-proficiënte primaire CRC tumoren. Dit suggereert een verhoogde cytotoxische en antigen-presenterende capaciteit van immuun infiltraten in LM-CRC. Daarnaast zagen we verhoogde expressie van co-inhibitoire receptoren op intra-tumorale T cellen in MMR-proficiënte LM-CRC, wat suggereert dat de tumor-infiltrerende T cellen in MMR-proficiënte LM-CRC gevoeliger zijn voor immuun checkpoint antagonisten dan tumor-infiltrerende T cellen in MMR-proficiënte primaire CRC. Blokkade van LAG3 of PD1 door antistoffen verbeterde *ex vivo* de effector functies van CD8⁺ en CD4⁺ T cellen verkregen uit MMR-proficiënte LM-CRC tumoren.Van deze twee liet

blokkade van LAG3 de meest robuuste effecten zien op tumor-specifieke T-cel responsen. Bovendien was hogere LAG3 expressie op intra-tumorale CD8$^+$ T cellen geassocieerd met langere progressie-vrije overleving in LM-CRC patiënten. Alles bijeengenomen zou LAG3 een nieuwe en veelbelovende immunotherapeutische target kunnen zijn voor LM-CRC, zelfs voor het MMR-proficiënte tumor type. Klinische studies naarhet effect van anti-LAG3 antilistof behandeling op LM-CRC wordt aangeraden om deze bevindingen te bevestigen.

In **Hoofdstuk 7** hebben we de samenstelling en karakteristieken van intra-tumorale immuun cel infiltraten in CCA geanalyseerd. In de CCA tumoren vonden we verlaagde aantallen cytotoxische lymfocyten en verhoogde aantallen Treg in vergelijking met de gepaarde tumorvrije leverweefsels. Waar Treg in de tumoren infiltreren, is het merendeel van de CD8$^+$ CTL en CD4$^+$ Th juist te vinden in het overgangsgebied tussen tumorvrij leverweefsel en de tumor. Daarnaast laten de intra-tumorale CD8$^+$ T cellen verminderde expressie van cytotoxische moleculen zien vergeleken met T cellen in het tumorvrije leverweefsel en bloed, en is zowel de expressie van de co-inhibitoire receptoren PD-1 en CTLA4 als de co-stimulerende receptor GITR hoger in de tumor-infiltrerende T cellen dan op de T cellen uit het tumorvrije leverweefsel en bloed. Stimulatie van GITR door het oplosbare ligand of het blokkeren van PD-1 door een therapeutische humane antistof, verbeterden de effector functies *ex vivo* van CD8$^+$ en CD4$^+$ T cellen verkregen uit CCA tumoren, wat aangeeft dat deze twee moleculen potentiële targets zijn voor immunotherapeutische behandeling van CCA patiënten.

In **Hoofdstuk 8** onderzochten we het concept dat agonisten van co-stimulerende moleculen een effectieve immunotherapeutische behandeling kunnen bieden voor HCC. Geactiveerde CD4$^+$FoxP3^{hoog}CD45RA$^-$ Treg hadden de hoogste GITR expressie van alle immuuncellen in HCC tumoren. Ook in tumorvrij leverweefsel en bloed was de expressie van GITR hogerop geactiveerde Treg dan op CD4$^+$ Th en CD8$^+$ CTL in dezelfde compartimenten. Toevoeging van recombinant GITR-ligand of een gehumaniseerde agonistische antistof tegen GITR aan CD8+ en CD4+ T cellen geïsoleerd uit HCC tumoren verhoogde hun responsen op polyclonale of tumorantigen-specifieke stimulatie. Dus agonistische targeting van GITR zou een potentiële strategie zijn voor mono- of combinatie immunotherapie van HCC.

Algemene conclusies en toekomstperspectieven

Het uiteindelijke doel van dit proefschrift is om nieuwe immunotherapeutische methoden te identificeren voor de behandeling van patiënten met primaire leverkanker of CRC levermetastasen. Onze studies tonen aan dat verhoogde aantallen Treg- en Tr1-cellen en verlaagde aantallen cytotoxische lymfocyten in immuun-infiltraten in tumoren bijdragen aan

een immunosuppressief tumor-micromilieu in levertumoren, evenals een verhoogde expressie van verschillende co-inhiberende receptoren op in de tumor geïnfiltreerde T-cellen en de aanwezigheid van hun liganden in de levertumoren. Beide factoren dragen bij aan een immunosuppressief tumor-micromilieu in leverkanker. De co-inhiberende routes CTLA4-CD80/CD86, PD-1-PD-L1, TIM3-galectine 9, LAG3-MHC klasse II en de co-stimulerende routes GITR-GITR-ligand en ICOS-ICOS-ligand spelen een belangrijke rol in de regulatie van intra-tumorale T-cel immuniteit bij patiënten met HCC, CCA of LM-CRC. Dit proefschrift biedt nieuwe suggesties voor immunotherapeutische interventies om de bovengenoemde immunosuppressieve mechanismen te onderdrukken en om de anti-tumor reactiviteit van in de tumoren geïnfiltreerde T cellen te verbeteren. Er wordt aangetoond dat gecombineerde blokkade van PD-1/PD-L1 en TIM3, LAG3 of CTLA4, evenals stimulatie van GITR, effectief zijn in het stimuleren van T-cellen afkomstig uit HCC tumoren. Antistoffen tegen LAG3 bieden een vergelijkbare mogelijkheid voor LM-CRC, terwijl agonistische antistoffen tegen GITR en antistoffen die de interactie tussen PD-1/PD-L1 blokkeren worden voorgesteld voor CCA.

Momenteel lopen er verschillende klinische onderzoeken naar de effecten van anti-PD-1-antistoffen bij CCA-patiënten. Klinische studies bij HCC en CCA patiënten die onderzoeken of een combinatie van een anti-PD-1/PD-L1-antistof met eenanti-CTLA4-antistof leidt tot verbeterde klinische werkzaamheid zijn ook lopend. Bovendien worden in HCC patiënten de combinatie van een GITR-agonistische antistof met een PD-1 en/of CTLA4-antagonistische antistof, evenals een CD134-agonistische antistof gecombineerd met een PD-1 en/of CTLA4-antagonistische antistof, en een CD134-agonistische antistof in combinatie met een CD137-agonistische antistof getest. Echter, klinische trials met anti-TIM3 en anti-LAG3-antistoffen zijn niet gestart bij patiënten met leverkanker. Bovendien ontbreken in patiënten met LM-CRC klinische studies naar antagonistische antistoffen tegen LAG3, en in patiënten met CCA ontbreken klinische studies met GITR-agonistische antistoffen. Verder onderzoek bij patiënten met leverkanker naar co-expressie van verschillende immuun checkpoints en klinische werkzaamheid van gecombineerde immunotherapieën is absoluut noodzakelijk om de klinische uitkomst te verbeteren.

Vertaald door Patrick Boor en Lisanne Noordam

APPENDIX

Acknowledgements

PhD portfolio

List of publications

About the author

Acknowledgements

Reno Noordam Lisanne Verhoef VanDerBoor Bruno Rosalie Katsikis Ijzermans Luiten Debets Kwekkeboom VanDerBurg Jaap Marco Sjoerd Jan Dave Peter Patrick Sprengers Cornelis

Boris Smits Doukas Nadine PanGaljart Boonstra Gwenny Berrevoets VanDerLaan Erler Cor Peppelenbosch Woltman Kunert Wojtek PronkVanMontfoort Luc FuhlerPedrozaGonzalezAndre Alexander Verstegen Grünhagen DeJonge Monique Buschow Lamers NicoleDirk Qiuwei Jeroen Sonja Polak Anand Menon Andrea MaikelRon Michael

Monique Pengyu Pieter Renee Hester Buyun ShanLi Aniek Paula Janine Wenhui Rutger Gertine Kim Petra Anthonie Gulce Amy Jan Jesse Emmeloes Eline KanChen Ishaku WenDang Jiaye DeBeijer Eelke Wenshi

Marcia Hanneke Ksenia Michiel Sunrui Yik Jorke Noel Lei Xun Rachid Yijin Changbo Cynthia JuanLi Manzhi SukYee Floris Kairong Ruby Xinying Yuebang JunHou Menggang Gijs Lauk Henk Aukes Marcele Thijmen Jasmijn

Alessandra Bernadette
Sharida Thomas
Kateryna Pratika Frances
Leonie LingWang Kelly
Shaojun
Zhijiang Sergey
Andrea YangLi
Hakim Buddy Peifa Rattana
Shihao Marla Ester
Pauline Janet Marieke
Xumin
Greta Shaoshi Hugo
Carla Junhong Ilknur Yunlong
Martine Natascha Raymond
Wouter QinYang
Diahann

ZhuSha
Xiaona
LuoNan
YaoYao
GaoYa Xiaolu
Danli Xiaofei
Guannan
Changbin
Yongkang
Chaoping
PingZhen
HuangLing
TongWei Changjiang WenBei
Wenhao Zhangling ZhihaoYuXue
Hongbo LiuJun Zongye
Kuikui WangLu Ruoyu
Hengyu

WuBin
LiuFan
GaoWen
Liejen LuTao
ChenSi
Kaiyin Baoyue
Zhongli
Jinluan Haibo
Jiangtao Yifan
ZhangKai
Zhanmin
Zhouqiao

　　致我的爸爸妈妈，您们绝对是最最重要的两位，没有人比您们更爱我了。我有时候在想，上了中学我全寄宿，每星期回家一次；上大学我去了另一个省，每半年回家一次；读博士我出了国，每年最多回家一次…我不能说自己有错，但实在对不起您们，原来我们的长期相处生活结束于我小学毕业时…往后几年我也不在您们身边，但我说过以后一定会回广东生活工作，期待还能和您们再相处二三十年，所以您们要身体健康。谢谢您们，我爱您们。

　　致爷爷嫲嫲公公婆婆，时常记挂您们！不忘点滴，感谢您们。

　　致大伯父大伯娘，二伯父，大舅父大舅母，三舅父三舅母，姨姨，大哥大嫂，二哥二嫂，表哥表嫂，表弟表妹们表妹夫们，洛奇和洛乐，有家人才有爱才有我，感谢您们。

　　致唐颖的爸爸妈妈，谢谢您们对我的关心，照顾，包容，支持，祝您们身体健康。

　　致我的侄仔们和外甥们，祝福你们有美好的童年和美好的未来，我愿意随时提供帮助。

　　致我的卤友们，祝你们拥有所爱所想，幸福快乐，我们友谊长存。

　　致唐颖 Ying Tang, We have spent eleven years together, I hope you don't get bored yet.^^ We are at the same age, so we always have our special events happen and have to make important choices in the same years. I feel very grateful and lucky that we have been able to walk every step side by side, make progress together and support each other. 我们最美好的二字头的时光，前一半在武汉度过，后一半留在了荷兰。2007, 2013, 2018, let's remember these numbers. And of course, we will have more and more years…… Looking forward to the bungee jump before our wedding.^^

PhD portfolio

Name of PhD student   Guoying Zhou

Department   Gastroenterology and Hepatology, Erasmus MC
University Medical Center Rotterdam

PhD period   October 2013 - April 2018

Promotor   Prof. Dr. Marco J. Bruno

Co-promotor   Dr. Jaap Kwekkeboom

General courses

Biomedical Research Techniques course

Annual Course on Molecular Medicine

Workshop on Microsoft Excel 2010: Advanced

Basic Introduction Course on SPSS

Biomedical English Writing Course for MSc and PhD-students

Advanced Immunology course

Workshop Presenting Skills for junior researchers

Basic and Translational Oncology course

Workshop on Photoshop and Illustrator CS6 for PhD-students and other researchers

Course on Scientific Integrity

Advanced course on Applications in flow cytometry

Daniel den Hoed Day (Erasmus MC Cancer Institute Research Day)

Erasmus MC PhD Day

Erasmus MC Liver Day

Erasmus MC Molecular Medicine Day

<u>Conferences – Oral presentations</u>

2015 European Congress of Immunology (ECI), Vienna, Austria

2016 The Erasmus Medical Center Molecular Medicine Day, Rotterdam, the Netherlands

2016 Dutch Association for Gastroenterology (NVGE) meeting, Veldhoven, the Netherlands

2016 Cancer Immunotherapy (CIMT) Annual Meeting, Mainz, Germany

2016 International Liver Cancer Association (ILCA) Annual Conference, Vancouver, Canada

2017 Dutch Association for Gastroenterology (NVGE) meeting, Veldhoven, the Netherlands

2017 Dutch Tumor Immunology Meeting (DTIM), Breukelen, the Netherlands

2017 The Erasmus Medical Center Cancer Institute Research Day, Rotterdam, the Netherlands

<u>Conferences – Invited talks</u>

2017 Liver Metastases Research Network (LMRN) Congress, Rotterdam, the Netherlands

2017 Hong Kong Society for Immunology (HKSI) Annual General Meeting and Scientific Meeting, Hong Kong, China

2018 Best Publication Award of the Erasmus Medical Center Molecular Medicine Day, Rotterdam, the Netherlands

2018 Top 3 Battle of NVH (Dutch Association for Hepatology) Young Hepatologist Award, Veldhoven, the Netherlands

<u>Conferences – Poster presentations</u>

2014 Dutch Society for Immunology (NVVI) Anniversary Congress, Efteling, the Netherlands

2015 Cancer Immunotherapy (CIMT) Annual Meeting, Mainz, Germany

2016 Cancer Immunotherapy (CIMT) Annual Meeting, Mainz, Germany

2016 International Liver Cancer Association (ILCA) Annual Conference, Vancouver, Canada

2017 The Erasmus Medical Center Molecular Medicine Day, Rotterdam, the Netherlands

2017 The annual meeting of the Federation of Clinical Immunology Societies (FOCIS), Chicago, USA

2017 Dutch Tumor Immunology Meeting (DTIM), Breukelen, the Netherlands

2017 CRI-CIMT-EATI-AACR International Cancer Immunotherapy Conference, Mainz, Germany

2018 Cancer Immunotherapy (CIMT) Annual Meeting, Mainz, Germany

Scientific grants and awards

2015 Association for Cancer Immunotherapy (CIMT) travel grant and free conference admission

2015 Erasmus Trustfonds travel grant

2016 Dutch Society for Immunology (NVVI) travel grant

2016 Erasmus Trustfonds travel grant

2017 Dutch Association for Hepatology (NVH) travel grant

2018 Best Publication Award of the Erasmus Medical Center Molecular Medicine Day

2018 NVH (Dutch Association for Hepatology) Young Hepatologist Award and free conference admission

Teaching activities

2015 Supervising master thesis: Hannah Schutz

2016 Supervising master thesis: Remco Erkens

Other activities

Reviewer of articles for *Medicine* and *Canadian Journal of Gastroenterology and Hepatology*

2016 Selected for United European Gastroenterology (UEG) basic science course, *Hot topics in experimental gastrointestinal cancer*, Munich, Germany

List of publications

1. **<u>Guoying Zhou,</u>** L Noordam, D Sprengers, M Doukas, P Boor, A van Beek, R Erkens, S Mancham, D Grünhagen, A Menon, J Lange, P Burger, A Brandt, B Galjart, C Verhoef, J Kwekkeboom, M Bruno. Blockade of LAG3 enhances responses of tumor-infiltrating T cells in mismatch repair-proficient liver metastasis of colorectal cancer. ***Oncoimmunology.*** *2018 in press.*

2. **<u>Guoying Zhou</u>**, D Sprengers, P Boor, M Doukas, H Schutz, S Mancham, A Pedroza-Gonzalez, W Polak, J de Jonge, M Gaspersz, H Dong, K Thielemans, Q Pan, J IJzermans, M Bruno, J Kwekkeboom. Antibodies Against Immune Checkpoint Molecules Restore Functions of Tumor-infiltrating T cells in Hepatocellular Carcinomas. ***Gastroenterology.*** *2017 Oct;153(4):1107-1119.*

3. **<u>Guoying Zhou,</u>** D Sprengers, R Erkens, S Mancham, M Doukas, L Noordam, P Boor, R van Leeuwen, B Groot Koerkamp, W Polak, J de Jonge, J IJzermans, M Bruno, J Kwekkeboom. Abrogation of the immunosuppressive tumor microenvironment in cholangiocarcinoma by targeting PD-1 or GITR. *In submission.*

4. A Pedroza-Gonzalez, **<u>Guoying Zhou</u>**, S Pal Singh, P Boor, Q Pan, D Grunhagen, J de Jonge, T Khe Tran, C Verhoef, J IJzermans, H Janssen, K Biermann, J Kwekkeboom, D Sprengers. GITR engagement in combination with CTLA-4 blockade completely abrogates immunosuppression mediated by human liver tumor-derived regulatory T cells ex vivo. ***Oncoimmunology.*** *2015 May 29;4(12).*

5. A Pedroza-Gonzalez, **<u>Guoying Zhou</u>**, E Vargas-Mendez, P Boor, S Mancham, C Verhoef, W Polak, D Grunhagen, Q pan, H Janssen, G Garcia-Romo, K Biermann, E Tjwa, J IJzermans, J Kwekkeboom, D Sprengers. Tumor-infiltrating plasmacytoid dendritic cells promote immunosuppression by Tr1 cells in human liver tumors. ***Oncoimmunology.*** *2015 Mar 19;4(6).*

6. A van Beek, **<u>Guoying Zhou*,</u>** L Noordam*, P Boor, S Bucktrout, S ter Borg, P Doornebosch, M Doukas, D Sprengers, J Kwekkeboom. Concerns about targeting tumor-infiltrating regulatory T cells with Fc-optimized anti-CD25 antibodies in humans. *In submission.*

7. K Sideras, A Pedroza-Gonzalez, A Vasaturo, K Biermann, S Mancham, A Nigg, H Stoop, **<u>Guoying Zhou</u>**, C Verhoef, S Sleijfer, D Sprengers, J Kwekkeboom, M Bruno. Prognostic value of intra-tumoral $CD8^+$/$FoxP3^+$ lymphocyte ratio in patients with resected colorectal cancer liver metastasis. ***Journal of Surgical Oncology.*** *2018 in press.*

8. K Sideras, R de Man, S Harrington, **<u>Guoying Zhou</u>**, H Schutz, A Pedroza-Gonzalez, K Biermann, S Mancham, B Hansen, B Takkenberg, Q Pan, J Ijzermans, S Sleijfer, D Sprengers, H Dong, J Kwekkeboom, M Bruno. Circulating levels of PD-L1 and Galectin-9 are associated with patient survival in Hepatocellular Carcinoma independent of their intra-tumoral expression levels. *In submission.*

9. **<u>Guoying Zhou*</u>**, H Wang*, L Luo*, A Yuan, J Kou, G Yang, M Wang, J Wu, B von Blomberg, J Crusius, S Morré, A Peña, B Xia. Serological Screening for Celiac Disease in Adult Chinese Patients with Diarrhea Predominant Irritable Bowel Syndrome. ***Medicine (Baltimore).*** *2015 Oct;94(42).*

About the author

Guoying Zhou was born on January 6th 1988, in Shunde, Foshan, Guangdong Province, China. She was raised by her beloved parents Huabi Wu and Guanlun Zhou in her hometown.

In 2006, she graduated from high school and started to study medicine (seven-year program) in Wuhan University, Hubei Province. During her medical training, she conducted clinical rotations in Zhongnan Hospital, and performed her master research under supervision of Prof. Dr. Bing Xia at the department of Gastroenterology and Hepatology. In 2007 she also started to learn French, and in 2010 and 2012 she was twice selected for a half-year exchange internship with a scholarship in Brabois Hospital, Lorraine University, Nancy, France.

After obtaining her medical degree and passing the National Medical Licensing Examination in China in 2013, she started her PhD research on tumor immunology at the department of Gastroenterology and Hepatology, Erasmus University Medical Center, Rotterdam, the Netherlands. Under supervision of Prof. Dr. Marco Bruno and Dr. Jaap Kwekkeboom, she completed several translational studies on immunotherapy for hepatocellular carcinoma, cholangiocarcinoma and liver metastasis of colorectal cancer.